ANÁLISIS ESTRUCTURA-FUNCIÓN DE LA ATPASA PCH2 Y SU IMPLICACIÓN EN EL *CHECKPOINT* DE RECOMBINACIÓN MEIÓTICA

Structure-function analysis of the Pch2 ATPase and its implication in the meiotic recombination checkpoint

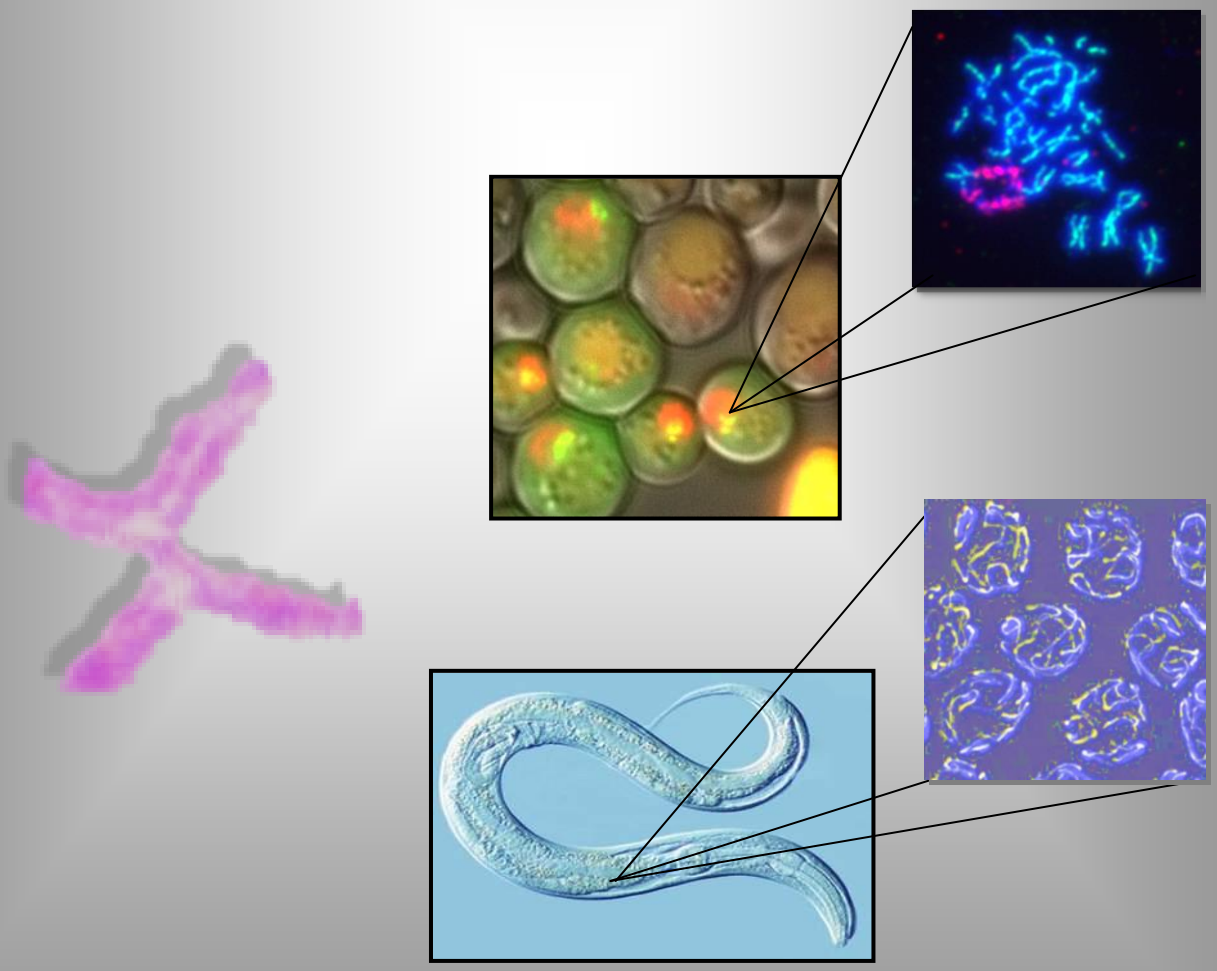

Esther Herruzo de la Fuente

Salamanca 2020

Instituto de Biología Funcional y Genómica
(CSIC / USAL)

Análisis estructura-función de la ATPasa Pch2 y su implicación en el *checkpoint* de recombinación meiótica

---

Structure-function analysis of the Pch2 ATPase and its implication in the meiotic recombination checkpoint.

Tesis doctoral

Esther Herruzo de la Fuente

Salamanca, marzo 2020.

La presente memoria, titulada "Análisis estructura-función de la ATPasa Pch2 y su implicación en el *checkpoint* de recombinación meiótica", elaborada por la graduada Esther Herruzo de la Fuente y que constituye su Tesis Doctoral para optar al grado de Doctora en Biología con Mención Internacional, ha sido redactada en el formato de compendio de artículos originales de investigación publicados en revistas científicas de prestigio internacional e indexadas en la edición científica del *Journal Citation Reports*.

Y para que así conste se recogen a continuación los tres artículos originales de investigación, su título, autores y afiliación de los mismos, junto la referencia completa de la revista científica donde fueron publicados:

"The Pch2 AAA+ ATPase promotes phosphorylation of the Hop1 meiotic checkpoint adaptor in response to synaptonemal complex defects"

Esther Herruzo[1], David Ontoso[1], Sara González-Arranz[1], Santiago Cavero[1], Ana Lechuga[1] and Pedro A. San-Segundo[1,*]

[1] Instituto de Biología Funcional y Genómica. Consejo Superior de Investigaciones Científicas and University of Salamanca, 37007 Salamanca, Spain

Nucleic Acids Res. Volumen 44, Número 16, Septiembre 2016.

DOI: 10.1093/nar/gkw506

ISSN: 0305-1048

https://doi.org/10.1093/nar/gkw506

Impact of histone H4K16 acetylation on the meiotic recombination checkpoint in *Saccharomyces cerevisiae*

Santiago Cavero[1, 2], **Esther Herruzo[1]**, David Ontoso[1, 3] and Pedro A. San-Segundo[1]

[1] Instituto de Biología Funcional y Genómica. Consejo Superior de Investigaciones Científicas and University of Salamanca, 37007 Salamanca, Spain.

[2] Present address: Department of Experimental and Health Sciences, Pompeu Fabra University, 08003-Barcelona, Spain.

[3] Present address: Molecular Biology Program, Memorial Sloan Kettering Cancer Center, New York, New York 10065, USA.

Microbial Cell, Volumen 3, número 12, pp. 606 – 620.Diciembre 2016.

DOI: 10.15698/mic2016.12.548

ISSN (online): 2311-2638

https://doi.org/10.15698/mic2016.12.548

Characterization of Pch2 localization determinants reveals a nucleolar-independent role in the meiotic recombination checkpoint

Esther Herruzo[1], Beatriz Santos[1, 2], Raimundo Freire[3], Jesús A. Carballo[4] and Pedro A. San-Segundo[1].

[1] Instituto de Biología Funcional y Genómica (IBFG) Consejo Superior de Investigaciones Científicas (CSIC) and University of Salamanca, Salamanca, Spain.

[2] Departamento de Microbiología y Genética. University of Salamanca, Salamanca, Spain.

[3] Instituto de Tecnologías Biomédicas, Hospital Universitario de Canarias, La Laguna, Spain

[4] Department of Cellular and Molecular Biology, Centro de Investigaciones Biológicas, Consejo Superior de Investigaciones Científicas (CSIC), Madrid, Spain

Chromosoma, Volumen 128, número 3, pp. 297–316**.** Septiembre 2019.

DOI: 10.1007/s00412-019-00696-7

ISSN: 0009-5915

https://doi.org/10.1007/s00412-019-00696-7

DR. D. FRANCISCO DEL REY IGLESIAS, CATEDRÁTICO del DEPARTAMENTO DE MICROBIOLOGÍA Y GENÉTICA de la UNIVERSIDAD DE SALAMANCA,

CERTIFICA:

Que la graduada **Esther Herruzo de la Fuente** ha realizado el trabajo titulado "***Análisis estructura-función de la ATPasa Pch2 y su implicación en el checkpoint de recombinación meiótica***", bajo la dirección del Dr. Pedro A. San Segundo Nieto en el Instituto de Biología Funcional y Genómica, centro mixto de la Universidad de Salamanca y el Consejo Superior de Investigaciones Científicas, para optar al grado de Doctor. Además, certifico que el autor de dicho trabajo cumple con los requisitos necesarios para optar a la mención de "*Doctor Internacional*".

Que autorizo a la presentación de dicho trabajo en la modalidad de compendio de artículos científicos.

Y para autorizar su presentación y evaluación por el tribunal correspondiente, expide el presente certificado en Salamanca, a 29 de enero de 2020.

CSIC
CONSEJO SUPERIOR DE INVESTIGACIONES CIENTÍFICAS

ibfg Instituto de Biología Funcional y Genómica

DR. PEDRO ANTONIO SAN SEGUNDO NIETO, CIENTÍFICO TITULAR del CONSEJO SUPERIOR DE INVESTIGACIONES CIENTÍFICAS en el INSTITUTO DE BIOLOGÍA FUNCIONAL Y GENÓMICA,

CERTIFICA:

Que la graduada **Esther Herruzo de la Fuente** ha realizado el trabajo titulado "***Análisis estructura-función de la ATPasa Pch2 y su implicación en el checkpoint de recombinación meiótica***", bajo mi dirección en el Instituto de Biología Funcional y Genómica, centro mixto de la Universidad de Salamanca y el Consejo Superior de Investigaciones Científicas, para optar al grado de Doctor. Además, certifico que el autor de dicho trabajo cumple con los requisitos necesarios para optar a la mención de "*Doctor Internacional*".

Que autorizo a la presentación de dicho trabajo en la modalidad de compendio de artículos científicos.

Y para autorizar su presentación y evaluación por el tribunal correspondiente, expide el presente certificado en Salamanca, a 29 de enero de 2020.

VNiVERSiDAD D SALAMANCA
CAMPUS DE EXCELENCIA INTERNACIONAL

ibfg Instituto de Biología Funcional y Genómica

DRA. BEATRIZ SANTOS ROMERO, PROFESORA TITULAR del DEPARTAMENTO DE MICROBIOLOGÍA Y GENÉTICA de la UNIVERSIDAD DE SALAMANCA,

CERTIFICA:

Que la graduada **Esther Herruzo de la Fuente** ha realizado el trabajo titulado "***Análisis estructura-función de la ATPasa Pch2 y su implicación en el checkpoint de recombinación meiótica***", con mi tutoría y bajo la dirección del Dr. Pedro A. San Segundo Nieto, en el Instituto de Biología Funcional y Genómica, centro mixto de la Universidad de Salamanca y el Consejo Superior de Investigaciones Científicas, para optar al grado de Doctor. Además, certifico que el autor de dicho trabajo cumple con los requisitos necesarios para optar a la mención de "*Doctor Internacional*".

Que autorizo a la presentación de dicho trabajo en la modalidad de compendio de artículos científicos.

Y para autorizar su presentación y evaluación por el tribunal correspondiente, expide el presente certificado en Salamanca, a 29 de enero de 2020.

AGRADECIMIENTOS

Llega el momento de poner punto y final a otra etapa, el temido doctorado. Ni que decir tiene que solo el nombre asusta. Pero no todo iban a ser frustraciones y comeduras de coco. Muchos son los aspectos aprendidos que merece la pena valorar de este largo camino repleto de subidas y bajadas, destacando el trabajo minucioso y la perseverancia, en definitiva, el desarrollar un buen proyecto, en ciencia y en la vida en general. Por todo ello quiero agradecer a esas personas que han estado continuamente presentes en esta etapa que sin duda dejará huella.

En primer lugar a Pedro, el guía fundamental de este trabajo. Gracias por enseñarme que nada es blanco o negro, que hasta el más mínimo detalle es importante, por tu inagotable paciencia y por tirar de mí siempre que lo he necesitado. A mis compañeros del PSS: Sara, mi pareja de batalla, un placer compartir horas de trabajo de contigo y aprender de tu experiencia, Isa, por contagiarnos tu alegría en tus apariciones intermitentes, Bea, por esos consejos fuera de la poyata, y todos los estudiantes que habéis ido pasando por el lab, por dejarme enseñaros lo que hacemos.

Quiero agradecer también al C-lab por haber hecho de mi estancia en el Harvard Medical School una experiencia inigualable. Monica, por enseñarme que se puede ser excelente científica y familiar a la vez. Laura, por ayudarme a comprender a los gusanos y estar atenta a todo a cualquier hora. Un placer seguir colaborando con vosotras. Y por supuesto Marina, más que una suerte haber coincidido.

A mi segundo lab, los PPM por adoptarme a mí y a mis bichos. Qué bien sienta un cambio de aires! Y a todos los compañeros del IBFG por vuestro talento y disponibilidad.

Y por último y no menos importante a mis familiares y amigos. Gracias a la familia que Salamanca unió y a mis pucelanos por ser mi vía de escape. En especial a Marta, gracias por esos viajes, planes de viajes y más viajes, cafés, paseos e inyecciones de vitamina. A los de casa por vuestro apoyo diario e incondicional y recordarme que hay mucha vida fuera del laboratorio, con mención especial a mi mejor amigo y compañero de piso. Todo es mucho más fácil con vosotros.

Gracias por vuestras aportaciones a este proyecto!

ÍNDICE

Sinopsis

General

RESUMEN

Durante la meiosis existe un mecanismo de vigilancia denominado *checkpoint* de recombinación meiótica que asegura la correcta segregación del material genético a los gametos, siendo de vital importancia para el mantenimiento de la integridad genómica en los organismos con reproducción sexual. Por ello, nos propusimos como objetivo profundizar en el papel de Pch2, una ATPasa específica de meiosis de la familia AAA+, en el *checkpoint* de recombinación meiótica de *Saccharomyces cerevisiae*. En esta tesis hemos determinado que el papel principal de Pch2 en el *checkpoint* inducido por defectos en la sinapsis es promover la fosforilación de Hop1 en T318 y su incorporación en los cromosomas. También hemos estudiado la relevancia funcional de diversos motivos de la proteína Pch2, como el sitio catalítico (actividad ATPasa) y el dominio N-terminal, analizando su efecto en el *checkpoint* así como en la localización de Pch2. Por otro lado, hemos contribuido al conocimiento de los factores que determinan la correcta localización de Pch2 en levaduras. Así, hemos desvelado que, junto a la metilación de la histona H3K79, la acetilación de la histona H4K16 también regula el mecanismo del *checkpoint* meiótico de *S. cerevisiae*, presumiblemente controlando la localización de Pch2. Además, hemos analizado la interacción Orc1-Pch2 en el DNA ribosómico (rDNA), concluyendo que, en contra de hipótesis previas, la localización de Pch2 en el nucleolo no es necesaria para el *checkpoint*. De hecho, nuestros últimos resultados indican que una población citoplásmica de Pch2 es capaz de llevar a cabo la función en el *checkpoint*. Por último, hemos expandido nuestra investigación a otro sistema modelo, como *Caenorhabditis elegans*, estudiando el papel de H3K79me en la meiosis de este nematodo, analizando su implicación en el *checkpoint*, y explorando su efecto sobre PCH-2. En conclusión, la ATPasa conservada evolutivamente Pch2 desempeña un papel fundamental en el *checkpoint* meiótico inducido por fallos en sinapsis, y el control de su localización subcelular es importante para ello, la cual viene determinada por diversos factores entre los que se incluyen determinadas modificaciones post-traduccionales de histonas.

SUMMARY

During meiosis there is a surveillance mechanism, the meiotic recombination checkpoint, which monitors the correct distribution of genetic material to gametes, being crucial for the maintenance of genomic integrity in sexually reproducing organisms. We aimed to further explore the role of Pch2, a meiosis-specific AAA+ ATPase, in the meiotic recombination checkpoint of *Saccharomyces cerevisiae*. In this thesis, we have determined that the critical role of Pch2 in the checkpoint induced by synapsis defects is to promote Hop1 phosphorylation at T318 and Hop1 association to unsynapsed meiotic chromosomes. We have also studied the functional relevance of critical residues of the Pch2 protein, such as the catalytic site (ATPase activity) and the N-terminal domain, by analyzing its impact on Pch2 localization and checkpoint function. On the other hand, we have contributed to discover several factors that determine Pch2 proper localization in yeast. Thus, we have revealed that, together with H3K79 methylation, proper levels of H4K16 acetylation regulate the meiotic recombination checkpoint, likely by controlling Pch2 distribution. Moreover, we have analyzed Orc1-Pch2 interaction at the ribosomal DNA (rDNA), concluding that, in contrast to previous hypotheses, Pch2 nucleolar localization is not required for the meiotic checkpoint. Indeed, we provide evidence indicating that a cytoplasmic pool of Pch2 sustains checkpoint function. Finally, we have expanded our investigation to another model system such as *Caenorhabditis elegans*. We have studied the meiotic role of H3K79 methylation in this nematode, analyzing its checkpoint implication and exploring its impact on PCH-2 regulation. In conclusion, the evolutionarily conserved Pch2 ATPase plays a critical role in the meiotic checkpoint induced by synapsis defects. The control of Pch2 subcellular localization orchestrated by several factors, including histone post-translational modifications, is vital for its checkpoint function.

1. ANTECEDENTES

El genoma de los organismos está constantemente expuesto a agentes exógenos y endógenos que producen daño de forma accidental. También existen procesos fisiológicos que introducen roturas en el genoma de manera natural como es el caso de la meiosis.

La meiosis es un proceso especial de división celular que genera células haploides (esporas en levaduras o gametos en metazoos) a partir de células parentales diploides, resultando esencial para los organismos con reproducción sexual. Durante la profase meiótica tiene lugar la recombinación entre cromosomas homólogos, la cual se inicia con la introducción de dobles roturas en el DNA (DSBs, *Double-Strand Breaks*) inducidas por la proteína conservada Spo11, relacionada con las topoisomerasas, y sus proteínas asociadas (keeney 2001; Keeney et al., 2014). Estas roturas son procesadas por nucleasas para generar DNA de cadena sencilla (ssDNA, *Single-Strand* DNA) con extremos 3´OH libres (Neale et al., 2005, García et al., 2011) que sirven de sustrato a las recombinasas Dmc1 y Rad51. Estas recombinasas catalizan la invasión de la hebra de ssDNA para buscar la región de homología con la que reparar el daño, preferentemente en la cadena de la cromátida homóloga (Bishop et al., 1992; Schwacha and Kleckner, 1997), formándose una estructura conocida como *D-loop*. Posteriormente se sintetiza nuevo DNA utilizando como molde la hebra de la cromatida homóloga y se liga, dando lugar a una estructura denominada unión de *Holliday* doble (dHJ, *double Holliday Junction*) (Schwacha and Kleckner, 1995). Una fracción de estos intermediarios se resuelven como entrecruzamientos recíprocos (COs, *Crossovers*) (Allers and Litchen, 2001), que permiten establecer uniones físicas entre los cromosomas denominados quiasmas y que son esenciales para que la segregación de los cromosomas hacia polos opuestos durante la primera división meiótica se produzca correctamente. Además, la recombinación meiótica también es importante para promover la variabilidad genética de los gametos que se originan (Gray and Cohen, 2016, San-Segundo and Clemente-Blanco, 2020).

El proceso de recombinación ocurre de manera paralela a la formación del complejo sinaptonémico (SC, *Synaptonemal Complex*) una estructura proteica altamente conservada que mantiene unidos a los cromosomas homólogos y facilita la recombinación entre ellos (Cahoon and Hawley, 2016; Gao and Colaiacovo, 2017). El SC de *S. cerevisiae* está formado por una región central cuyo componente principal es Zip1 (Sym et al., 1993) y por dos elementos laterales (LEs, *Lateral Elements*) formados principalmente por las proteínas meióticas Hop1, Red1 y la cohesina meiótica Rec8 (Smith and Roeder, 1997; Klein et al., 1999; Tovah et al., 2017) (Figura 1). Además, dentro de la región central se puede distinguir el denominado elemento central formado por las proteínas Ecm11 y Gmc2 (Voelkel-Meiman 2013; Humphryes 2013). Los LEs también sirven como punto de anclaje para otras proteínas que participan en la recombinación y en el control del ciclo celular. Además, también interaccionan con los anillos de cohesina que mantienen unidas las cromátidas hermanas y participan en la organización de los bucles de cromatina. El ensamblaje del SC comienza en el estadio de leptonene de la profase meiótica, cuando se introducen las DSBs y

progresa durante el zigotene a medida que se produce la recombinación. La sinapsis de los cromosomas se completa en paquitene, coincidiendo con la formación de intermediarios de recombinación maduros que se resuelven al salir de paquitene y entrar en diplotene. En este estadio, el SC comienza a desensamblarse y desaparece en diaquinesis, cuando los cromosomas homólogos ya están unidos por los COs que se manifiestan citológicamente formado los quiasmas. En la mayoría de los casos, como ocurre en *S. cerevisiae* y mamíferos, la formación del SC depende de que se inicie la recombinación, y es necesario para que esta ocurra adecuadamente. Pero existen excepciones; por ejemplo, en *S. pombe* no se forma un SC maduro, tan solo los denominados elementos lineales (Bähler et al., 1993) y en las hembras de *Drosophila* y en *C. elegans* la sinapsis es independiente de la introducción de DSBs (Lake and Hawley, 2012; Lui and Colaiacovo, 2013).

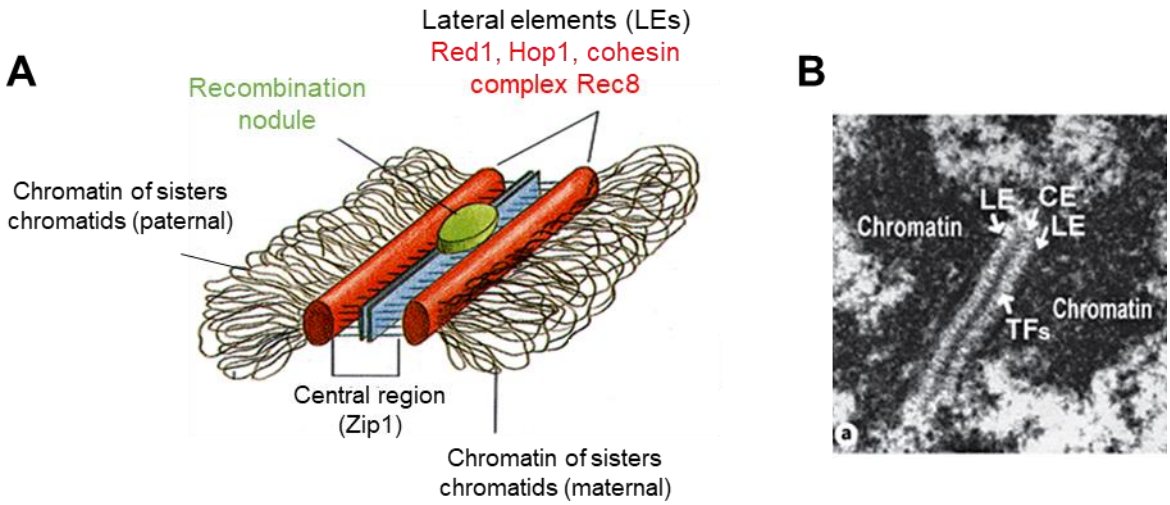

Figura 1. **El complejo sinaptonémico en *S. cerevisiae*. A)** Representación esquemática del SC. La región central del SC está formada mayoritariamente por filamentos transversales de la proteína Zip1, mientras que los elementos laterales están formados por las proteínas Hop1, Red1 y el complejo cohesina con Rec8. La cromatina de cada cromosoma homólogo se dispone a modo de bucles a ambos lados de los elementos laterales. Se representa un nódulo de recombinación. **(B)** Imagen de microscopía electrónica del SC. Se muestra la región central (CE), los elementos laterales (LE), los filamentos transversales (TFs) y la cromatina. Las imágenes han sido obtenidas de: **A)** Alberts B et al., 2002 y **B)** Geisinger and Benavente, 2016.

Para asegurar que la transmisión de la información genética a las células hijas se produzca de manera adecuada existe un mecanismo de vigilancia denominado *checkpoint* de recombinación meiótica o de paquitene que reconoce errores en sinapsis y/o recombinación y bloquea el ciclo celular en profase hasta que se eliminen los defectos, previniendo la segregación incorrecta de cromosomas y la consiguiente formación de gametos defectivos (Subramanian and Hochwagen, 2014). En humanos, fallos en estos procesos son la principal causa de enfermedades genéticas (como la trisomía del cromosoma 21), abortos espontáneos e infertilidad (Hassold and Hunt, 2001; Nagaoka et al., 2012).

Este *checkpoint* consiste en una ruta de señalización muy compleja y finamente regulada que se encuentra muy conservada en la evolución, existiendo en levaduras (Nyberg et al., 2002; Perez-Hidalgo et al., 2003), *C. elegans* (Bhalla and Dernburg, 2005), *Drosophila* (Joyce and McKim, 2009) y mamíferos (de Rooij and de Boer, 2003; Pacheco et al., 2015). En *S. cerevisiae* las proteínas sensor Mec1-Ddc2 detectan los errores en sinapsis y recombinación, transmiten la señal a los adaptadores como Hop1 y Red1 (Carballo et al., 2008; Eichinger and Jentsch 2010), que forman parte de los LEs, y estos la transmiten hasta la quinasa efectora Mek1 para producir el bloqueo del ciclo celular en profase (Acosta et al., 2011; Prugar et al., 2017). Concretamente la fosforilación de Hop1 en la T318 por las quinasas Mec1-Tel1 es necesaria para que Mek1 se reclute a los ejes de los cromosomas y se active (Carballo et al., 2008; Penedos et al., 2015). Además, para que la activación de Mek1 sea completa es también necesaria su dimerización y autofosforilación en *trans* en los residuos T327 y T331. (Niu et al., 2007) (Ontoso et al., 2013). Adicionalmente se requieren otras proteínas como Pch2, Sir2 y Dot1 que pueden modular la acción de los adaptadores (San Segundo and Roeder, 1999, 2000; Ontoso et al., 2013). La activación completa de Mek1 produce dos eventos bien diferenciados. Por un lado, bloquea la recombinación entre cromátidas hermanas, ya que impide que se forme el complejo Rad51-Rad54, necesario para la recombinación entre cromátidas hermanas. Mek1 ejecuta esta acción mediante dos vías: (1) fosfo-rila a Rad54 en la T132 disminuyendo su afinidad por Rad51 (Niu et al., 2009) y (2) fosforila a la proteína específica de meiosis Hed1 en la T40 que se une a Rad51, excluyendo a Rad54 (Callender et al., 2016). Por otro lado, Mek1 produce el bloqueo del ciclo celular en profase actuando de manera directa sobre Ndt80 (Chen et al., 2018) y, quizás, sobre Swe1. Así, la activación del *checkpoint* dependiente de Mek1 da lugar a que se mantengan niveles altos de Swe1, que inhibe a Cdc28, la principal CDK (*Cyclin-Dependent Kinase*) de *S. cerevisiae*, mediante su fosforilación en la Y19 (Leu and Roeder, 1999). Al mismo tiempo Mek1 fosforila e inhibe al factor de transcripción Ndt80, necesario para la transcripción de genes requeridos para la salida de paquitene, como la polo-quinasa *CDC5* (Sourirajan and Lichten, 2008) o para que se produzcan las divisiones nucleares, como la ciclina *CLB1* (Chu and Herskowitz, 1998). En otros organismos como *C. elegans, Drosophila* y mamíferos, la activación del *checkpoint* meiótico también induce la muerte celular por apoptosis (Edelmann et al., 1996; Yoshida et al., 1998; Gartner et al., 2000; Xu et al., 2001; Bhalla and Dernburg, 2005, Pacheco et al., 2015).

Para el estudio de este *checkpoint* en *S. cerevisiae* se emplean mutantes que inducen su activación, como *zip1Δ*, que presenta defectos en la formación del SC, o *dmc1Δ* que es defectivo en la reparación de DSBs meióticas (Figura 2).

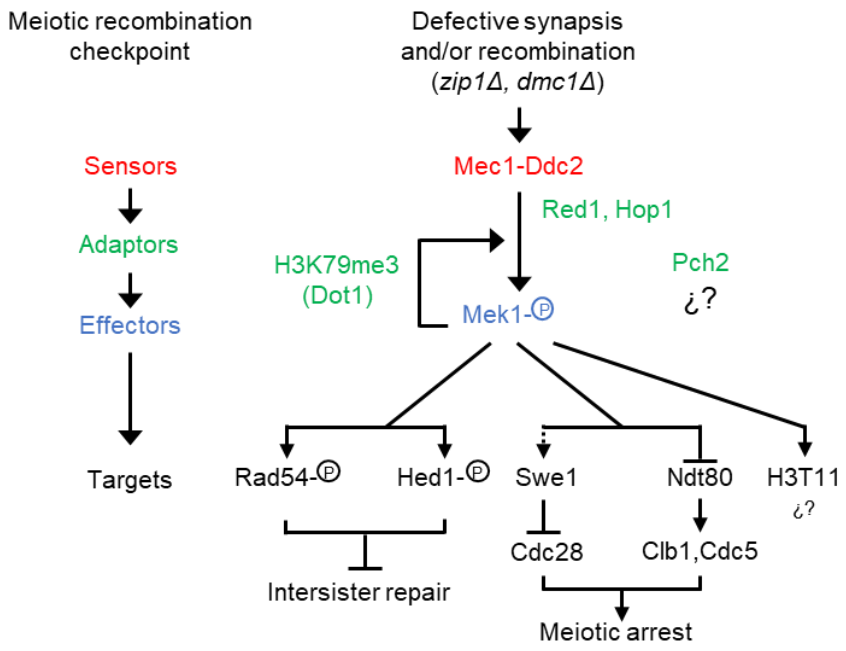

Figura 2. El *checkpoint* de recombinación meiótica. Representación esquemática de los componentes generales de la ruta de los *checkpoints*. Componentes principales de la ruta del *checkpoint* de recombinación meiótica en *S. cerevisiae*.

Pch2^{TRIP13} es una ATPasa de la familia AAA+ muy conservada en la evolución desde levaduras hasta humanos que forma complejos hexaméricos (Chen et al., 2014). La proteína homóloga en mamíferos se denomina TRIP13. Aunque inicialmente Pch2 se descubrió en *S. cerevisiae* como una proteína específica de meiosis implicada en el *checkpoint* de paquitene, actualmente se sabe que actúa en muchos otros eventos meióticos como son: la formación de DSBs (Farmer et al., 2012; Joshi et al., 2015), la distribución de las DSBs (Subramanian et al., 2019), la configuración de los ejes de los cromosomas (Börner et al., 2008; Joshi et al., 2009), la regulación de los COs (Zanders and Alani, 2009; Medhi et al., 2016; Chakraborty et al., 2017), la recombinación entre homólogos (Zanders et al., 2011; Subramanian et al., 2016) y la supresión de recombinación en el DNA ribosómico (rDNA) (San-Segundo and Roeder, 1999; Vader et al., 2011). Pch2 se engloba dentro de la familia de ATPasas AAA+ (ATPasas Asociadas a diversas Actividades celulares) que se caracterizan por utilizar la energía generada en la hidrólisis del ATP para producir cambios conformacionales en sus sustratos (Hanson and Whiteheart, 2005, Puchades et al., 2019). En el caso de Pch2^{TRIP13} los sustratos conocidos son las proteínas con dominios HORMA como Hop1^{HORMAD1,2} y MAD2 (Ye et al., 2017). Así, está descrito que en células meióticas Pch2 regula negativamente la acumulación de Hop1^{HORMAD1,2} en los cromosomas a medida que la sinapsis se va completando (Roig et al., 2010; Herruzo et al., 2016; Subramanian et al., 2016). Por su parte, en *C. elegans* y mamíferos PCH-2/TRIP13 también actúa sobre Mad2 en el

checkpoint de ensamblaje del huso en células somáticas (Nelson et al., 2015; Ye et al., 2015; West et al., 2017; Alfieri et al., 2018), aunque en levaduras no parece realizar esta función (Lago, Herruzo and San Segundo, Trabajo de Fin de Grado en realización). Además, se ha descrito recientemente que, en células somáticas de mamífero, TRIP13 regula la reparación del DNA a través del cambio conformacional de la proteína REV7 que también posee un dominio HORMA (Clairmont et al., 2020). Dentro de su papel en el *checkpoint* meiótico, Pch2 puede llevar a cabo diversas funciones según el estímulo que desencadene la activación del mismo. Así, en respuesta a DSBs sin procesar (como las que se acumulan en un mutante *sae2Δ* o *rad50S*) que son detectadas por la quinasa sensor Tel1, Pch2 actúa en conjunto con Xrs2 (un componente del complejo MRX) para regular la recombinación y la respuesta del *checkpoint* (Ho and Burgess, 2011). Por su parte, en respuesta a fallos en sinapsis, como ocurre en un mutante *zip1Δ* carente de la región central del SC, la quinasa Mec1 dispara la activación del *checkpoint* donde Pch2 estaría actuando por un mecanismo desconocido. Para conocer mejor los mecanismos moleculares del funcionamiento de Pch2 llevamos a cabo los experimentos publicados en el primer artículo que compone esta tesis doctoral: "*The Pch2 AAA+ ATPase promotes phosphorylation of the Hop1 meiotic checkpoint adaptor in response to synaptonemal complex defects*" (Herruzo et al., 2016).

La recombinación ocurre en el contexto de la cromatina por lo que factores que influencian la estructura de la cromatina como la histona metil-transferasa Dot1 y la histona deacetilasa Sir2 desempeñan papeles importantes en estos procesos. Dot1 cataliza la mono-, di- y tri- metilación de la histona H3 en la K79 (Frederiks et al., 2008) y no se conoce ninguna demetilasa que revierta su acción. Dot1 se encuentra muy conservada en la evolución (en mamíferos se denomina DOT1L) y regula un gran número de procesos celulares implicados en el mantenimiento de la integridad genómica (Jones et al., 2008; Mohan et al., 2010; Cecere et al., 2013; Kim et al., 2014; Ontoso et al., 2014). También se sabe que defectos en la función de DOT1L están relacionados con leucemias agudas con reordenamiento MLL (*Mixed Lineage Leukemia*) (Nguyen and Zhang, 2011). Actualmente, se están probando inhibidores de DOT1L como posible diana terapéutica (Daigle et al., 2011; Shukla et al., 2016; Stein et al., 2018). Más concretamente, dentro de su papel en el *checkpoint* meiótico de *S. cerevisiae,* Dot1 promueve la activación de Mek1 dependiente de Hop1 y su reclutamiento en los ejes de los cromosomas. Se ha propuesto que Dot1 ejerce esta función, mediante el control de la distribución cromosómica/nucleolar de Pch2 (San Segundo and Roeder, 2000; Ontoso et al., 2013). Por su parte, Sir2 también participa en el *checkpoint* meiótico regulando la localización de Pch2 en la cromatina (San-Segundo and Roeder, 1999). A pesar de la importancia de Sir2 en el *checkpoint* meiótico, poco se ha profundizado en su mecanismo de acción. Por ello, estudiar la contribución de los niveles de H4K16ac modulados por la histona-deacetilasa Sir2 y la histona acetil-transferasa Sas2 (Dang et al., 2009) fue otro de los objetivos de esta tesis. Estos resultados se encuentran recogidos en el segundo artículo de la memoria: "*Impact of histone H4K16 acetylation on the meiotic*

recombination checkpoint in Saccharomyces cerevisiae" (Cavero et al., 2016).

Pch2 se localiza mayoritariamente en la región del cromosoma XII que contiene el rDNA (nucleolo); también se puede encontrar una fracción más minoritaria de Pch2 en los cromosomas que establecen sinapsis interaccionando con proteínas del SC. Por el contrario, en un mutante *zip1Δ*, Pch2 solo se encuentra en el nucleolo, indicando que la fracción nucleolar de Pch2 puede ser importante para su función en el *checkpoint* (San-Segundo and Roeder, 1999). Además, existían otras evidencias que apuntaban a la relevancia de la localización de Pch2 en el rDNA, ya que su deslocalización del nucleolo se correlaciona con la pérdida de función del *checkpoint*, como ocurre en los mutantes *dot1Δ* y *sir2Δ* (San-segundo and Roeder, 1999, 2000). Estas observaciones nos han llevado a investigar los factores que determinan la localización de Pch2 y cómo esa localización afecta a la funcionalidad del *checkpoint*. Los resultados obtenidos se han publicado en el tercer artículo presentado en esta memoria: "*Characterization of Pch2 localization determinants reveals a nucleolar-independent role in the meiotic recombination checkpoint*" (Herruzo et al., 2019).

Los resultados de este artículo originaron la idea de que debe existir una población de Pch2 adicional, que no se localiza ni en los cromosomas ni en el nucleolo, que sería importante para su función en el *checkpoint*. Para explorar más en detalle dónde se localiza la fracción de Pch2 relevante para su función en el *checkpoint* se han llevado a cabo los experimentos incorporados en el Anexo que son los últimos resultados obtenidos como continuación del Artículo 3: "*The meiosis-specific AAA+ ATPase Pch2 implements the chromosome-synapsis checkpoint response from outside the nucleus".*

El mecanismo del *checkpoint* meiótico así como sus componentes principales se encuentran muy conservados en la evolución. Así, Pch2^{TRIP13} también responde a defectos en sinapsis o recombinación en *C. elegans* (Bhalla and Dernburg, 2005), *Drosophila* (Joyce and McKim, 2009, 2010) y, posiblemente, en hembras de ratón (Martinez-Marchal and Roig, Abstract Red Española de Meiosis). Además, se ha descrito que la localización de DOT1L, y de las distintas formas de metilación de H3K79 resultantes de su actividad, varía a lo largo de la espermatogénesis en ratón (Ontoso et al., 2014). Sin embargo, la función meiótica de Dot1 y su posible contribución al control de Pch2 no está descrito en nematodos, por lo que también nos propusimos como objetivo de esta tesis doctoral estudiar el papel de la H3K79me, mediada por DOT-1.1, en la meiosis de *C. elegans*. Los resultados obtenidos se describen en el Artículo 4 de esta tesis que se encuentra actualmente en preparación. Esta parte del trabajo se ha llevado a cabo en colaboración con el grupo de la Dra. Monica Colaiacovo (Harvard Medical School, USA): "*Role of DOT-1.1-dependent H3K79 methylation during meiosis in C. elegans*" (Lascarez-Lagunas, Herruzo, et al., 2020, en preparación).

Por tanto, la presente memoria de tesis titulada "Análisis estructura-función de la ATPasa Pch2 y su implicación en el *checkpoint* de recombinación meiótica", elaborada por compendio de artículos, queda estructurada en los siguientes apartados: tres artículos publicados, un Anexo que recoge los últimos resultados obtenidos aún sin publicar y un artículo en preparación:

ARTÍCULO 1: "*The Pch2 AAA+ ATPase promotes phosphorylation of the Hop1 meiotic checkpoint adaptor in response to synaptonemal complex defects*" (Herruzo et al., 2016).

ARTÍCULO 2: "*Impact of histone H4K16 acetylation on the meiotic recombination checkpoint in Saccharomyces cerevisiae"* (Cavero et al., 2016).

ARTÍCULO 3: "*Characterization of Pch2 localization determinants reveals a nucleolar-independent role in the meiotic recombination checkpoint*" (Herruzo et al., 2019).

ANEXO: *"The meiosis-specific AAA+ ATPase Pch2 implements the chromosome-synapsis checkpoint response from outside the nucleus"* (Herruzo and San Segundo, resultados sin publicar).

ARTÍCULO 4: "*Role of DOT-1.1-dependent H3K79 methylation during meiosis in C. elegans*" (Lascarez-Lagunas, Herruzo, et al., 2020, en preparación).

2. HIPÓTESIS DE TRABAJO

Pch2 es una ATPasa sobre la que se había descrito un papel en el *checkpoint* meiótico de varios organismos. Era muy bien conocida su función como regulador negativo de la localización de Hop1, excluyéndolo de los cromosomas a medida que progresa la sinapsis, pero no el mecanismo por el que actúa en el *checkpoint* inducido por fallos en sinapsis. Además, se sabía que, en levaduras, en condiciones en las que el *checkpoint* está activo, Pch2 se localiza únicamente en el nucleolo, por lo que cabía esperar un papel relevante en el *checkpoint* para esa población nucleolar de Pch2. Por otro lado, puesto que los mecanismos del *checkpoint* meiótico se encuentran muy conservados en la evolución, era lógico pensar que la H3K79me también podría ser importante en la meiosis de *C.elegans*, dada la importancia que tiene esta modificación post-traduccional en la localización de Pch2 y en el *checkpoint* de levaduras.

3. OBJETIVOS GENERALES

El objetivo principal de esta tesis es el estudio del mecanismo molecular por el que la ATPasa Pch2 actúa en el *checkpoint* de recombinación meiótica.

Los objetivos específicos son los siguientes:

- Estudiar la función de Pch2 en la ruta del *checkpoint* de recombinación meiótica en *S. cerevisiae* inducido por fallos en sinapsis (mutante *zip1Δ*).
- Determinar la contribución funcional de H4K16ac, controlada por la deacetilasa Sir2 y la acetil-transferasa Sas2, en la regulación del *checkpoint* meiótico.
- Analizar los factores que determinan la localización subcelular de Pch2 y su efecto en el *checkpoint*.
- Estudiar la contribución funcional de H3K79me, mediada por DOT-1, a la meiosis de *C. elegans* así como su papel en el *checkpoint* meiótico.

4. CONCLUSIONES GENERALES

1. La función principal de Pch2 en el *checkpoint* meiótico inducido por defectos en sinapsis es promover la fosforilación de Hop1 en la T318.
2. La actividad ATPasa de Pch2 se requiere para su función en el *checkpoint*. Además, la unión del ATP a Pch2 también

es necesaria para la formación o estabilidad del complejo hexamérico así como para la correcta localización de la proteína.

3. La regulación de los niveles de acetilación de H4K16 mediante la acción de Sir2 y Sas2, contribuye al funcionamiento correcto del *checkpoint*, posiblemente mediante la regulación de la localización de Pch2.

4. La localización nucleolar de Pch2 no se requiere para el *checkpoint* meiótico, puesto que cuando Pch2 no se recluta al rDNA en ausencia de Orc1, el *checkpoint* sigue siendo completamente funcional.

5. Además de la localización cromosómica y nucleolar de Pch2, existe una población de Pch2 en el citoplasma que parece ser la más relevante para su función en el *checkpoint*.

6. La metilación de H3K79 mediada por DOT-1 es importante para la meiosis en *C. elegans* puesto que niveles reducidos de dicha metilación producen defectos en apareamiento, sinapsis y recombinación, que incrementan la tasa de esterilidad de los gusanos.

4. GENERAL CONCLUSIONS

1. The critical role of Pch2 in the synapsis checkpoint is to promote Hop1 phosphorylation at T318.

2. The ATPase activity of Pch2 is required for its checkpoint function. Moreover, ATP binding is necessary for hexameric complex formation and proper Pch2 localization.

3. H4K16ac levels, controlled by Sir2 and Sas2, contribute to proper checkpoint function, likely due to regulation of Pch2 localization.

4. Pch2 nucleolar localization is not required for the meiotic checkpoint because, in the absence of nucleolar Pch2 (Orc1 depletion), the checkpoint is completely functional.

5. Besides the chromosomal and nucleolar localization of Pch2, there is a cytoplasmic pool of the protein that appears to be the most relevant for checkpoint function.

6. DOT-1.1-dependent H3K79me is important for *C. elegans* meiosis, since reduced levels of this methylation lead to pairing, synapsis and recombination defects that increase worm sterility rates.

Artículo

1

ARTÍCULO 1: "*The Pch2 AAA+ ATPase promotes phosphorylation of the Hop1 meiotic checkpoint adaptor in response to synaptonemal complex defects*"

RESUMEN

Las células meióticas poseen mecanismos de vigilancia que monitorizan eventos cruciales como la sinapsis y la recombinación de los cromosomas. Defectos meióticos resultantes de la ausencia de la proteína del complejo sinaptonémico Zip1 activan el *checkpoint* específico de meiosis, provocando el bloqueo o retraso de la progresión meiótica. Pch2 es una ATPasa AAA+ conservada en la evolución que se requiere para el bloqueo meiótico inducido por el *checkpoint* en el mutante *zip1Δ*, donde Pch2 sólo se detecta en el DNA ribosómico (nucleolo). Aquí describimos que niveles altos de la proteína Hop1, un adaptador del *checkpoint* que se localiza en los ejes de los cromosomas, suprime el defecto del *checkpoint* en el mutante *zip1Δ pch2Δ*, restaurando la actividad de Mek1 y el retraso del ciclo celular meiótico. Demostramos que el papel principal de Pch2 en este *checkpoint* de sinapsis es promover la fosforilación de Hop1, dependiente de Mec1, en la treonina 318. Además, mostramos que la actividad ATPasa de Pch2 es esencial para su función en el *checkpoint* y que la unión del ATP por Pch2 se requiere para su localización. Trabajos previos han mostrado que Pch2 regula negativamente la acumulación de Hop1 en los cromosomas durante una meiosis normal. Basándonos en nuestros resultados, proponemos que, en condiciones de activación del *checkpoint*, Pch2 también desempeña un papel positivo sobre Hop1 promoviendo su fosforilación y su distribución adecuada en los ejes de los cromosomas sin sinapsis.

GRAPHICAL ABSTRACT

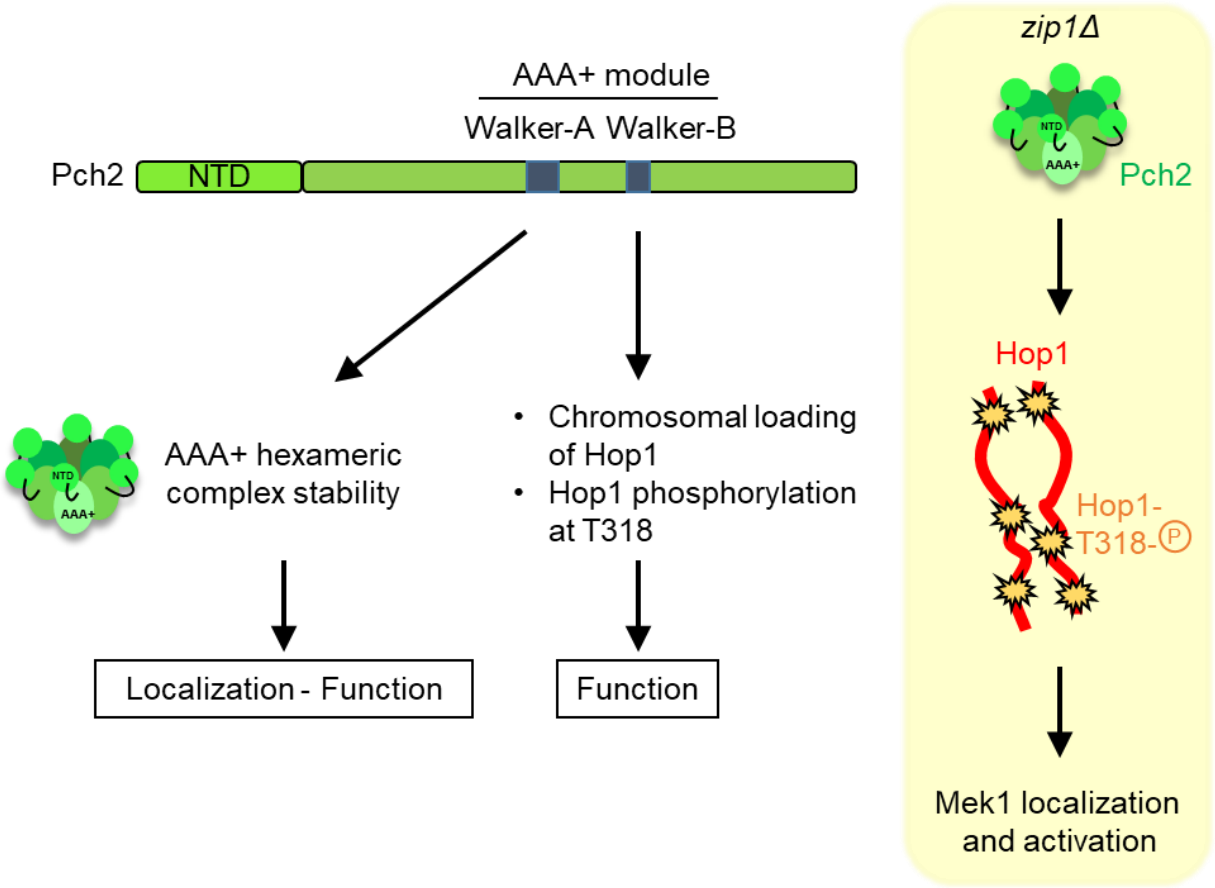

7722–7741 *Nucleic Acids Research, 2016, Vol. 44, No. 16* *Published online 2 June 2016*
doi: 10.1093/nar/gkw506

The Pch2 AAA+ ATPase promotes phosphorylation of the Hop1 meiotic checkpoint adaptor in response to synaptonemal complex defects

Esther Herruzo, David Ontoso, Sara González-Arranz, Santiago Cavero, Ana Lechuga and Pedro A. San-Segundo*

Instituto de Biología Funcional y Genómica. Consejo Superior de Investigaciones Científicas and University of Salamanca, 37007 Salamanca, Spain

Received December 22, 2015; Revised May 13, 2016; Accepted May 26, 2016

ABSTRACT

Meiotic cells possess surveillance mechanisms that monitor critical events such as recombination and chromosome synapsis. Meiotic defects resulting from the absence of the synaptonemal complex component Zip1 activate a meiosis-specific checkpoint network resulting in delayed or arrested meiotic progression. Pch2 is an evolutionarily conserved AAA+ ATPase required for the checkpoint-induced meiotic block in the *zip1* mutant, where Pch2 is only detectable at the ribosomal DNA array (nucleolus). We describe here that high levels of the Hop1 protein, a checkpoint adaptor that localizes to chromosome axes, suppress the checkpoint defect of a *zip1 pch2* mutant restoring Mek1 activity and meiotic cell cycle delay. We demonstrate that the critical role of Pch2 in this synapsis checkpoint is to sustain Mec1-dependent phosphorylation of Hop1 at threonine 318. We also show that the ATPase activity of Pch2 is essential for its checkpoint function and that ATP binding to Pch2 is required for its localization. Previous work has shown that Pch2 negatively regulates Hop1 chromosome abundance during unchallenged meiosis. Based on our results, we propose that, under checkpoint-inducing conditions, Pch2 also possesses a positive action on Hop1 promoting its phosphorylation and its proper distribution on unsynapsed chromosome axes.

INTRODUCTION

During meiosis, accurate distribution of chromosomes to the gametes is ensured by the action of meiosis-specific surveillance mechanisms commonly known as the meiotic recombination checkpoint or pachytene checkpoint (1,2) and, more recently, broadly referred to as the meiotic checkpoint network (3). This checkpoint monitors those meiotic events, such as chromosome synapsis and meiotic recombination, which are important to establish the adequate number and distribution of interhomolog connections essential for proper chromosome segregation. The meiotic checkpoint network reinforces the adequate order of events during normal meiotic prophase and, in addition, it is crucial to react to meiotic failures. In response to defects in synapsis and/or recombination, the pachytene checkpoint blocks or delays entry into meiosis I, thus preventing the formation of gametes harboring aneuploidy and other kinds of genetic abnormalities.

Chromosome synapsis is mediated by the synaptonemal complex (SC), an evolutionarily-conserved tripartite structure that holds homologous chromosomes together during the pachytene stage of meiotic prophase I. Meiotic recombination initiates with the generation of programmed DNA double-strand breaks (DSBs), which undergo strictly regulated repair during prophase, preferentially with a non-sister chromatid (4). A fraction of DSBs are repaired to yield crossovers that, together with sister chromatid cohesion, give rise to physical links between homologs – chiasmata– promoting proper chromosome distribution. In some organisms, including budding yeast and mouse, chromosome synapsis is tightly linked to and depends on meiotic recombination.

In *Saccharomyces cerevisiae*, the coiled-coil Zip1 protein is the major component of the central region of the SC. Mutants lacking Zip1 fail to synapse and undergo pachytene checkpoint-dependent meiotic arrest or delay in prophase (5). Importantly, the Red1 and Hop1 structural components of the SC lateral elements (LEs) are also involved in the checkpoint; they function as adaptors to support

*To whom correspondence should be addressed. Tel: +34 923294902; Fax: +34 923224876; Email: pedross@usal.es
Present addresses:
David Ontoso, Molecular Biology Program, Memorial Sloan Kettering Cancer Center, New York, NY 10065, USA.
Santiago Cavero, Department of Experimental and Health Sciences, Pompeu Fabra University, 08003 Barcelona, Spain.

activation of the meiosis-specific Mek1 effector kinase. In particular, phosphorylation of Hop1 at Thr318 by the upstream sensor kinases Mec1/Tel1 is necessary for Mek1 activation by phosphorylation (6,7). Full Mek1 activation involves sequential phosphorylation events that can be genetically separated and biochemically differentiated in phos-tag gels (8). Mec1/Tel1 dependent phosphorylation of Mek1 is followed by *in-trans* autophosphorylation at particular sites in its activation loop (Thr327 and Thr331) (9). Active Mek1 promotes two major meiotic responses: it reinforces interhomolog (IH) recombination bias (10,11), at least in part, through the inhibitory phosphorylation of Rad54 at Thr132 (12) and, on the other hand, it prevents exit from prophase and entry into meiosis I. Several crucial cell-cycle regulators, such as Swe1, Ndt80 and Cdc5, are targeted by the checkpoint to impose the cell cycle delay in response to defective recombination/synapsis; whether they are direct targets of Mek1 activity remains to be determined. The Swe1 kinase carries out the inhibitory phosphorylation of the main budding yeast cyclin-dependent kinase Cdc28 at Tyr19. In addition, inhibition and nuclear exclusion of the meiosis-specific transcription factor Ndt80 results in transcriptional down-regulation of a number of genes including those encoding B-type cyclins and the Cdc5 polo-like kinase that, together with inactive Cdc28, lead to meiotic cell cycle arrest (13–16).

Besides the Mec1-Ddc2/Tel1 sensors, the meiotic recombination checkpoint also shares other upstream components with the canonical DNA damage checkpoint, including Rad24 and the '9-1-1' (Rad17-Mec3-Ddc1) module, which interacts with Red1 (17). In addition, epigenetic regulators, such as the Sir2 histone deacetylase and the Dot1 histone methyltransferase, also operate in the meiotic checkpoint response, at least in part, by regulating the chromosomal distribution of the meiosis-specific Pch2 protein (8,18,19).

Pch2 (also known as TRIP13 in mammals) is an evolutionarily conserved AAA+ ATPase involved in various aspects of meiotic chromosome metabolism in an ample range of organisms, including budding yeast, plants, worms, flies and mice. Pch2 was initially discovered in *S. cerevisiae* as a component of the checkpoint responding to the meiotic defects of the synapsis-deficient *zip1* mutant lacking the central region of the SC (18,20). On the other hand, functional analyses of Pch2 in wild-type meiosis, has revealed that this ATPase negatively regulates the accumulation of the Hop1 protein at chromosome axes (18,21–23); in addition, functions for $Pch2^{Trip13}$ in DSB generation, crossover interference, IH recombination bias, and regulation of rDNA recombination have been also described in both yeast and mouse (24–28). Intriguingly, whereas the absence of Pch2 bypasses the meiotic delay of the synapsis-deficient *zip1* mutant, it has little effect on the checkpoint response to unrepaired resected DSBs in *dmc1*. In contrast, Pch2 acting through Xrs2 and Tel1 (but not Mec1) signals unprocessed DSBs in *sae2* strains; however, Tel1 is not required for the *zip1*-induced synapsis checkpoint (29). All these pieces of evidence suggest that, depending on the initiating event, Pch2 may perform specific functions in relaying the checkpoint signal generated by different meiotic perturbations.

Whereas in budding yeast Pch2 appears to be dedicated exclusively to meiotic functions, the $Trip13^{Pch2}$ homolog in metazoa is also involved in the mitotic spindle assembly checkpoint regulating the Mad2 protein, which, like Hop1, contains a HORMA domain (30–32). Underscoring the relevance of $Trip13^{Pch2}$ function in somatic cells, the expression levels of $Trip13^{Pch2}$ in certain types of cancer define the chemotherapy resistance and prognosis (33,34). Recent work has revealed the structural properties of this conserved ATPase and the conformational changes induced in some of its substrates (35).

In order to gain further insight into the functional impact of Pch2 during SC-deficient meiosis, we first describe here a genetic overexpression screen aimed to discover factors involved in the checkpoint role of Pch2. Despite the fact that Pch2 somehow promotes the turnover of Hop1 from meiotic chromosome axes; that is, Hop1 is more abundant and more continuous on *pch2* chromosomes, we surprisingly found that Hop1 overproduction suppresses the checkpoint defect of the *zip1 pch2* mutant. Then, we show that, in the *zip1* mutant, Pch2 is required for Mek1 autophosphorylation and formation of chromosomal Mek1 foci, and that *HOP1* overexpression restores full Mek1 activation in *zip1 pch2*. We also demonstrate that, in contrast with the *pch2* single mutant, Hop1 is not more abundant on *zip1 pch2* chromosomes; furthermore, in response to *zip1* defects, Pch2 specifically promotes high levels of Hop1 phosphorylation at Thr318 required to sustain checkpoint function. Finally, we show that *pch2* mutants carrying mutations in the Walker A or Walker B motifs phenocopy the defects of the *pch2* null-mutant, indicating that the ATPase activity of Pch2 is essential for its synapsis checkpoint function. Moreover, the Walker A-deficient Pch2 version fails to localize to the chromosomes and to form a stable complex suggesting that adenosine triphosphate (ATP) binding is required for formation or integrity of the Pch2 hexameric complex. We conclude that the critical function of the Pch2 ATPase in a *zip1*-deficient situation is to facilitate Mec1-dependent phosphorylation of Hop1 at Thr318.

MATERIALS AND METHODS

Yeast strains and meiotic time courses

The genotypes of yeast strains are listed in Supplementary Table S1. All strains are in the BR2495 or the BR1919 background (5,36). The *zip1::LEU2*, *zip1::LYS2*, *zip1::URA3*, *zip3::URA3*, *ecm11::kanMX6*, *ndt80::LEU2*, *ddc1::ADE2*, *rad17::LEU2*, *rad24::TRP1*, *dot1::TRP1*, *pch2::TRP1*, *sir2::LEU2*, *hop1::hphMX4* and *rad54::LEU2* gene deletions were previously described (5,8,15,18,19,37–39). The *rad51::natMX4* deletion was made following a PCR (polymerase chain reaction)-based approach (40). The *ndt80::kanMX3* construct was generated by marker swapping in *ndt80::LEU2* strains using the M3926 plasmid (41). The *pph3::kanMX6* cassette was amplified from genomic DNA of a W303-based strain containing that deletion (a gift from R. Bermejo; CIB-CSIC) and used to transform the appropriate BR1919 strains. For substitution of the *PCH2* gene for the *pch2Δ-lacZ::TRP1* construct, strains were transformed with the pSS67 plasmid (see below) digested with XhoI-SphI. N-terminal tagging of *PCH2* with

three copies of the HA epitope was previously described (18). *PCH2* was also tagged with three copies of the MYC epitope at the same position using identical procedures (42). The *MEK1-GFP* and *DDC2-GFP* constructs were also previously described (8,43). The *pch2-K320A* and *pch2-E399Q* mutations were introduced at the *PCH2* genomic locus using the *delitto perfetto* technique (44); they generate a NarI and a BstNI site, respectively, utilized for genotyping purposes during genetic crosses. The sequences of the primers used are available upon request. All strains were made by direct transformation or by genetic crosses always in an isogenic background. Sporulation conditions for meiotic time courses have been described (8). To score meiotic nuclear divisions, samples were taken at different time points, fixed in 70% Ethanol, washed in phosphate buffered saline (PBS) and stained with 1 μg/μl DAPI for 15 min. At least 300 cells were counted at each time point. Meiotic time courses were repeated several times; representative experiments are shown.

Plasmids

The plasmids used are listed in Supplementary Table S2. The pSS51 plasmid expressing a *pch2-lacZ* fusion was constructed by cloning a 1.3-kb XhoI-BamHI fragment containing the *PCH2* promoter and the N-terminal ORF region encoding the first 90 amino acids into the SalI-BamHI sites of the YCp50-derivative R1566 plasmid harboring the *E. coli lacZ* gene with a BamHI site at the 5′ end to generate an in-frame fusion. pSS67 contains a 4.3-kb BglII-NheI fragment from pSS51 harboring *pch2-lacZ* cloned into BglII-SphI of pSS53 (18). The R1692 plasmid overexpressing *HOP1* has been previously described (45). pSS54 contains a 3.2-kb KpnI-PstI *PCH2* fragment in the high-copy YEp352 vector. The pSS316 and pSS317 plasmids were constructed as follows: a 2.7-kb fragment containing *HOP1* ORF and the 5′ (648 bp) and 3′ (241 bp) UTR regions was first amplified by PCR from genomic DNA of a BR1919 strain using oligos HOP1-EcoRI(Fw) and HOP1-SalI(Rv) and blunt-cloned into the pJET1.2 vector (ThermoFisher Scientific) to originate pSS314. This *Eco*RI-*Sal*I fragment was then subcloned into pRS426 to generate the pSS316 plasmid. A 1.6-kb fragment spanning the *hop1-T318A* mutation was amplified from the JCY565 strain (6) (a gift from J. Carballo; CIB-CSIC), digested with BamHI-SacI and used to replace the same 1.0-kb fragment in pSS314 to generate pSS315. The 2.7-kb EcoRI-SalI fragment of pSS315 was then transferred to pRS426 to originate the pSS317 plasmid overexpressing *hop1-T318A*.

Genetic screen for high-copy suppressors of *zip1 pch2*

The *zip1 pch2-lacZ* mutant (DP221) was transformed with a yeast genomic library constructed in the multicopy vector YEp24 (46). Transformants were selected on SC-Ura and replica-plated to SPO plates containing a sterile Whatman 3MM filter paper on top. As positive controls, two colonies of DP221 transformed with pSS54 were placed at known positions on every plate. After incubation at 30°C for 3 days, the filters were removed, exposed to chloroform fumes for 10 min and assayed for β-galactosidase activity by incubating them at 30°C, colony side up, in empty dishes with a solution of 500 μl of Z-buffer (60 mM Na_2HPO_4, 40 mM NaH_2PO_4, 10 mM KCl, 1 mM $MgSO_4$, 40 mM β-mercatoethanol, pH 7.0) containing 100 μl of 20 mg/ml X-Gal. About 23 000 transformants were scored and 21 displayed blue color; plasmids were recovered for further analysis. The presence of *PCH2* in the plasmids was discarded by PCR using internal *PCH2* primers. Fifteen of the plasmids recovered fail to reproduce the phenotype when reintroduced into DP221, indicating that the suppression phenotype was not linked to the plasmids. The remaining six plasmids were analyzed by restriction mapping and sequencing of the insert ends and were grouped into two Pch-Two-Suppressors: *PTS10* containing *RPS9A* and a truncated form of *MOT1*, and *PTS11* containing *HOP1*, *PCI8*, *MAM33*, *RPS24B* and *SEC6*.

Western blotting and immunoprecipitation

Total cell extracts were prepared by trichloroacetic acid (TCA) precipitation from 5-ml aliquots of sporulation cultures as previously described (13). Analysis of Mek1 phosphorylation using Phos-tag gels was performed as reported (8). The antibodies used are listed in Supplementary Table S3. The ECL or ECL2 reagents (ThermoFisher Scientific) were used for detection. The signal was captured on films and/or with a ChemiDoc XRS system (Bio-Rad) and quantified with the Quantity One software (Bio-Rad).

For immunoprecipitation of Pch2, 5-ml aliquots from 16 h meiotic cultures were crosslinked with 1% formaldehyde for 10 min at 30°C. The reaction was quenched by adding glycine to 250 mM and incubating for 5 min on ice. Cells were collected, washed and broken with glass beads in lysis buffer (150 mM NaCl, 1% Triton X-100, 50 mM Tris HCl pH 8.0) containing protease inhibitors (Complete Ultra Tablets, Roche). Clarified extracts were immunoprecipitated with anti-HA antibodies conjugated with magnetic MicroBeads using the μMACS Epitope Tag Protein Isolation Kit (Miltenyi Biotec) following the manufacturer's protocol.

Cytology

Immunofluorescence of chromosome spreads and whole cells was performed essentially as described in (47) and (48), respectively. The antibodies used are listed in Supplementary Table S3. Images of spreads were captured with a Nikon Eclipse 90i fluorescence microscope controlled with MetaMorph software and equipped with a Hammamatsu Orca-AG CCD camera and a PlanApo VC 100 × 1.4 NA objective. Ddc2-GFP foci images were captured with an Olympus IX71 fluorescence microscope equipped with a personal DeltaVision system, a CoolSnap HQ2 (Photometrics) camera and 100x UPLSAPO 1.4 NA objective. Stacks of 10 planes at 0.4 μm intervals with 500 ms exposure time were captured. Maximum intensity projections of deconvolved images were generated using the SoftWorRx 5.0 software (Applied Precisions). Quantification of the fluorescence signal in individual spread nuclei or cells was performed with the Image J software. Background signal was subtracted using the Otsu's threshold method of Image J.

DAPI images were collected using a Leica DMRXA fluorescence microscope equipped with a Hammamatsu Orca-AG CCD camera and a 63 × 1.4 NA objective.

Dityrosine fluorescence assay, sporulation efficiency and spore viability

To examine dityrosine fluorescence as an indicator of the formation of mature asci, patches of cells grown on YPDA plates were replica-plated to sporulation plates overlaid with a nitrocellulose filter (Protran BA85, Whatman). After 3-days incubation at 30°C, fluorescence was visualized by illuminating the open plates from the top with a hand-held 302 nm UV lamp. Images were taken using a Gel Doc XR system (Bio-Rad). Sporulation efficiency was quantitated by microscopic examination of asci formation after 3 days on sporulation plates. Both mature and immature asci were scored. At least 300 cells were counted for every strain. Spore viability was assessed by tetrad dissection. At least 144 spores were scored for every strain.

Statistics

To determine the statistical significance of differences a two-tailed Student *t*-test was used. *P*-Values were calculated with the GraphPad Prism 5.0 software.

RESULTS

A genetic screen for high-copy suppressors of *zip1 pch2* identifies *HOP1*

The absence of Pch2 alleviates the checkpoint-induced meiotic arrest of the *zip1* mutant. To gain insight into the function of Pch2 in this checkpoint we devised a genetic screen to identify genes that, when overexpressed, restored the meiotic block in a *zip1 pch2* double mutant. This screen could potentially identify novel components of the checkpoint pathway and/or reveal additional functional interactions of Pch2 with previously known checkpoint factors. We took advantage of the fact that Pch2 is transiently produced during meiotic prophase in the wild type, but it accumulates in the prophase-arrested *zip1* mutant (18). To follow *PCH2* expression, we generated a construct containing the *PCH2* coding sequence corresponding to the first 90 amino acids (*pch2Δ$^{90\text{-}564}$*) fused the *E. coli lacZ* gene and expressed from the *PCH2* promoter in a centromeric plasmid (Figure 1A). β-galactosidase activity was used as a readout for *PCH2* expression and dityrosine fluorescence as an indicator of sporulation on plates. Consistent with the previously described *PCH2* expression pattern, meiotic-proficient wild-type cells containing this plasmid exhibited no or low levels of β-galactosidase activity, but the prophase-arrested *zip1* mutant accumulated high levels of β-galactosidase activity, manifested as blue color on sporulation plate assays (Figure 1B and C). Alleviation of the prophase arrest in a *zip1 dot1* mutant (8,19) eliminated β-galactosidase production (Figure 1B), whereas the checkpoint-independent meiotic block imposed by deletion of *NDT80* (49) resulted in β-galactosidase accumulation (Figure 1B). Thus, the *pch2Δ$^{90\text{-}564}$-lacZ* fusion gene (hereafter, *pch2Δ-lacZ*) serves as a useful reporter for meiotic prophase arrest.

We next generated diploid strains in which both copies of the *PCH2* gene were replaced by the *pch2Δ-lacZ* construct at the genomic locus (Figure 1D). As expected, *pch2Δ-lacZ* behaved like a null mutant; it bypassed checkpoint arrest as manifested by the presence of dityrosine fluorescence in *zip1 pch2Δ-lacZ*, but no β-galactosidase was detected (Figure 1E). Notably, introduction of a single-copy or a high-copy *PCH2* restored the meiotic block in *zip1 pch2Δ-lacZ* and resulted in conspicuous β-galactosidase accumulation (Figure 1E). Thus, we reasoned that we could use this assay to screen for high-copy suppressors of the unscheduled sporulation resulting from the defective checkpoint in *zip1 pch2Δ-lacZ*. After transformation with a 2μ-based high-copy genomic library and replica-plate to sporulation medium, we scored for the appearance of blue color as an indicator of restored meiotic prophase arrest (Figure 1F and G). The plasmids contained in the colonies displaying β-galactosidase activity were recovered, analyzed by restriction digestion and DNA sequencing, and re-transformed into the original *zip1 pch2Δ-lacZ* strain to confirm that the suppression phenotype was linked to the plasmid. In addition to clones containing *PCH2*, we isolated two different high-copy suppressor genes (*PTS*, for Pch Two-Suppressors). *PTS10* encoded a C-terminal truncated version of the Mot1 transcriptional regulator (50). Since *2μPTS10* only conferred a transient and partial restoration of the meiotic arrest (Figure 1H) it was not further analyzed. In contrast, the effect of *2μPTS11* was comparable to that of the *2μPCH2* control (Figure 1H). Sequencing analysis revealed that the *HOP1* gene was present in the *2μPTS11* plasmids isolated from the library. To confirm that high levels of Hop1 were indeed responsible for the phenotype we analyzed a previously characterized *2μHOP1* plasmid (8,45) and found a similar effect on suppression of *zip1 pch2Δ-lacZ* sporulation (Figure 1H). Thus, *HOP1* overexpression restores meiotic arrest in the checkpoint-deficient *zip1 pch2Δ-lacZ* mutant.

Overexpression of *HOP1* suppresses the checkpoint defect of *pch2*, *sir2* and *dot1*, but not that of *rad17*, *ddc1* and *rad24* mutants

To determine whether the effect of Hop1 overproduction was exclusively exerted when the checkpoint was inactivated by the absence of Pch2, we analyzed mutants in other checkpoint genes also required for the *zip1* meiotic block. The Rad17, Ddc1 and Rad24 proteins are members of the 9-1-1 and RFC complexes acting upstream in the checkpoint pathway and contributing to the activation of the Mec1-Ddc2 sensor kinase (6,51,52). On the other hand, the H3K79 methyltransferase Dot1 is required for proper phosphorylation and localization of the Hop1 adaptor and the Mek1 checkpoint effector kinase (8). Dot1 regulates the chromosomal distribution of the nucleolar-associated Pch2 and Sir2 proteins (8,19). As shown in Figure 2, Hop1 overproduction significantly reduced sporulation efficiency in *zip1 pch2*, *zip1 sir2* and *zip1 dot1*, but had no effect on *zip1 rad17*, *zip1 ddc1* and *zip1 rad24* mutants. Thus, *HOP1* overexpression specifically supports meiotic checkpoint function when the Dot1-Pch2 module is not operative.

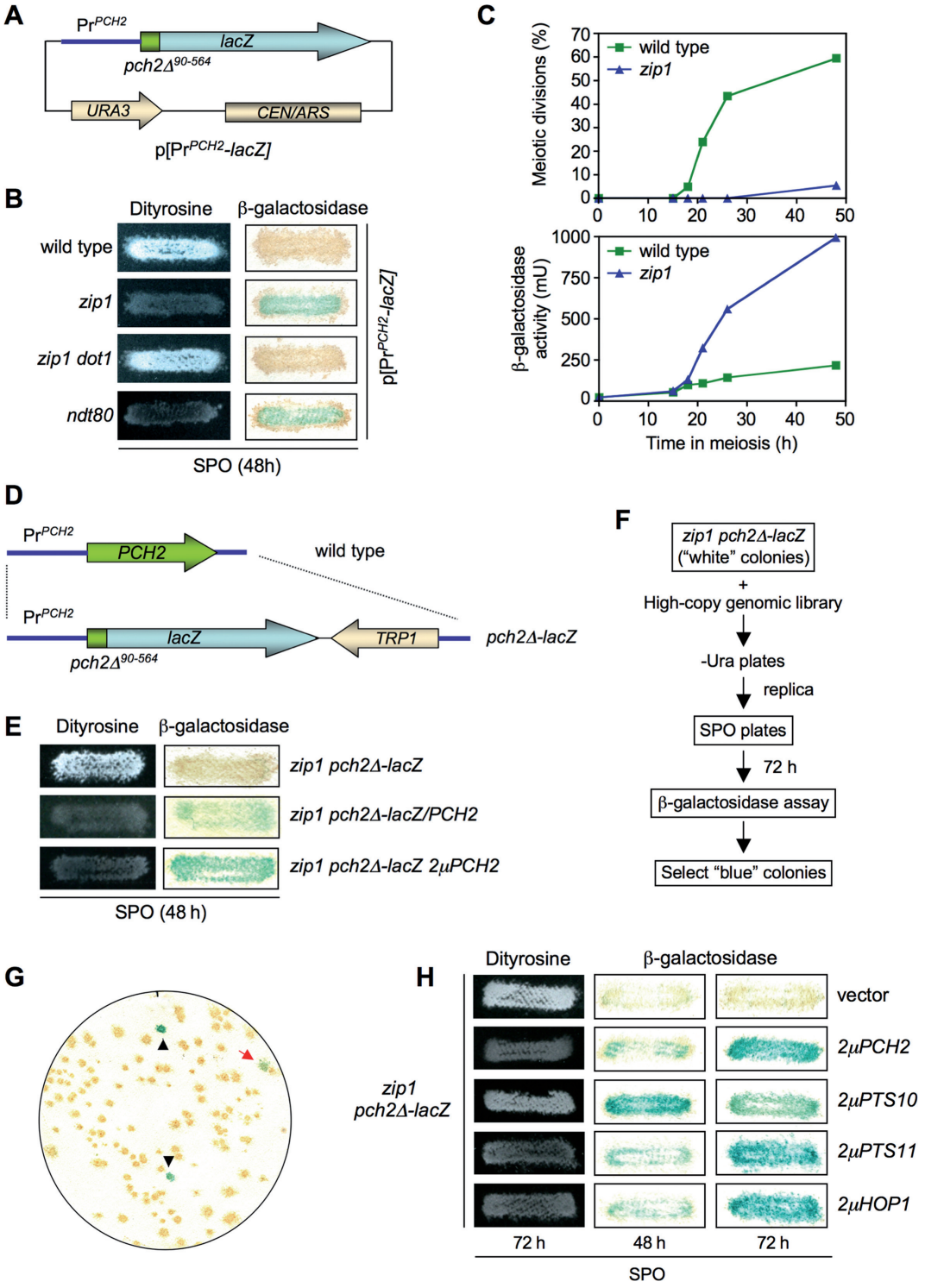

Figure 1. Identification of *HOP1* in a genetic screen for high-copy suppressors of the *zip1 pch2* checkpoint defect using a *pch2-lacZ* construct as a reporter for meiotic prophase arrest. (**A**) Schematic representation of a centromeric plasmid (pSS51) carrying the *PCH2* promoter and the coding sequence for the first N-terminal 90 amino acids fused in frame with the bacterial *lacZ* gene. (**B**) Dityrosine fluorescence and β-galactosidase assays of the indicated strains transformed with the pSS51 plasmid after 48 h on sporulation plates. (**C**) Kinetics of meiotic divisions and β-galactosidase activity in meiotic time courses of wild-type and *zip1* strains containing the pSS51 plasmid. (**D**) Schematic representation of the substitution of the *PCH2* gene for the *pch2-lacZ* construct at the genomic locus. (**E**) Dityrosine fluorescence and β-galactosidase assays of the indicated strains after 48 h on sporulation plates. (**F**) Scheme of the genetic screen. (**G**) Representative β-galactosidase assay of a plate from *zip1 pch2Δ-lacZ* transformed with the genomic high-copy library. Black triangles indicate positive controls deliberately placed at known positions on every plate of the screen. The red arrow points to a positive 'blue' candidate. (**H**) Dityrosine fluorescence and β-galactosidase assays of the *zip1 pch2Δ-lacZ* strain transformed with the indicated plasmids. Strains for (B) and (C) are: BR2495 (wild type), MY63 (*zip1*), DP174 (*zip1 dot1*) and S3483 (*ndt80*). Strains for (E), (F), (G) and (H) are: DP221 (*zip1 pch2Δ-lacZ*) and DP228 (*zip1 pch2Δ-lacZ/PCH2*). DP221 was transformed with empty vector or the indicated high-copy plasmids.

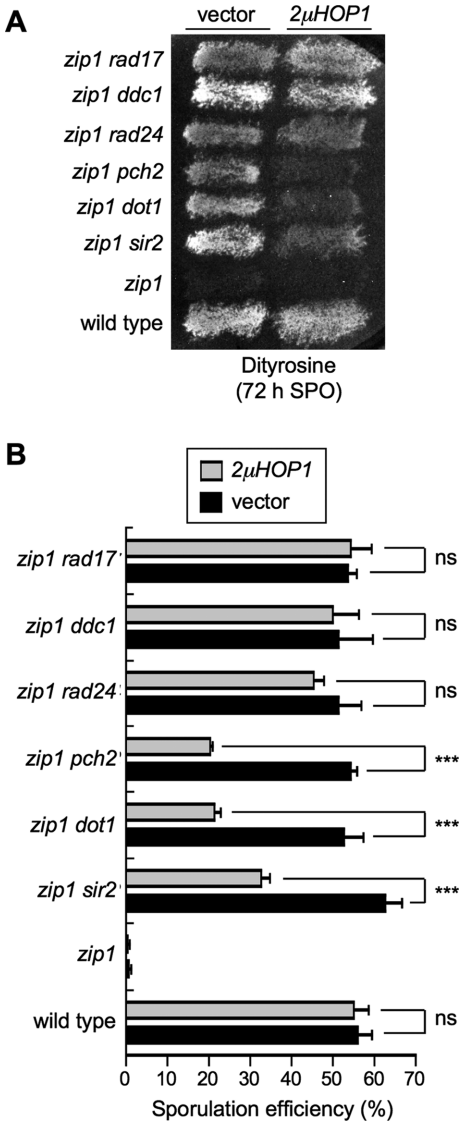

Figure 2. High-copy *HOP1* specifically suppresses the checkpoint defect of *zip1 pch2*, *zip1 sir2* and *zip1 dot1*. (**A**) Dityrosine fluorescence assay of the indicated strains transformed with empty vector (YEp352) of high-copy *HOP1* (R1692) after 3 days on sporulation plates. (**B**) Microscopic quantification of the sporulation efficiency of the strains analyzed in (A). Three independent counts were performed. Means and standard deviations are shown. (ns), no significant difference; (***), $P < 0.001$. Strains are: BR2495 (wild type), MY63 (*zip1*), DP174 (*zip1 dot1*), DP223 (*zip1 pch2*), DP267 (*zip1 sir2*), S4295 (*zip1 rad24*), S4278 (*zip1 ddc1*) and S4286 (*zip1 rad17*).

HOP1 overexpression restores meiotic checkpoint activity in *zip1 pch2*

To further explore the effect of *HOP1* overexpression, we next analyzed meiotic kinetics and molecular markers of checkpoint activation, such as Mek1 phosphorylation (in phostag gels) and Cdc5 inhibition, during meiotic time courses of wild-type, *zip1* and *zip1 pch2* strains with or without Hop1 overproduction (Figure 3). In the wild type, the Mek1 kinase was only weakly and transiently activated (Figure 3A) (8); *HOP1* overexpression slightly prolonged Mek1 activation resulting in a subtle meiotic delay (Figure 3A and B). As expected, the synapsis-deficient *zip1* mutant showed extensive Mek1 phosphorylation, delayed Cdc5 production and a significant meiotic delay; Hop1 overproduction slightly enhanced those effects (Figure 3C and D). Consistent with the defective checkpoint, Mek1 hyperactivation was not observed in the *zip1 pch2* mutant; moreover, Cdc5 production and meiotic divisions displayed roughly wild-type kinetics (Figure 3E and F). However, high doses of Hop1 markedly restored Mek1 phosphorylation, delayed Cdc5 production and provoked a significant meiotic delay in *zip1 pch2* (Figure 3E and F).

To elude the possible effect of the different kinetics of meiotic progression in the strains analyzed in these assays, we assessed Mek1 activation and localization in pachytene-arrested *ndt80* cells. To achieve full activation, Mek1 undergoes Mec1/Tel1-dependent phosphorylation followed by *in trans* autophosphorylation (6,9). The different forms resulting from these two phosphorylation events can be resolved in phostag gels (8) (Figure 3G, black and white arrows). We found that Mec1/Tel1-dependent phosphorylation occurred in the absence of Pch2 (Figure 3G, black arrow). However, the bands corresponding to Mek1 autophosphorylation were absent in *zip1 pch2* transformed with empty vector (Figure 3G, white arrows) indicating that, like Dot1, Pch2 is specifically required for Mek1 autophosphorylation. Strikingly, complete Mek1 activation was reestablished in *zip1 pch2* cells overproducing Hop1 (Figure 3G).

The *zip1*-induced meiotic checkpoint also promotes the formation of chromosome-associated Mek1 foci (8,53) (Figure 3H). Like Mek1 phosphorylation, formation of Mek1 foci was also impaired in *zip1 pch2*, which displayed fewer and dimmer foci. In contrast, numerous bright Mek1 foci were observed in the *zip1 pch2* mutant overexpressing *HOP1* (Figure 3H).

Taken together, these results indicate that Pch2 is required for Mek1 autophosphorylation and localization when the synapsis checkpoint is activated by the lack of Zip1. In the absence of Pch2, artificially-induced high levels of Hop1 can support checkpoint activity suggesting that Hop1 function is somehow compromised in the *zip1 pch2* mutant resulting in impaired Mek1 activation.

Pch2 is required for Hop1 phosphorylation induced by the synapsis checkpoint

Several lines of evidence indicate that, in unperturbed meiosis, Pch2 promotes the turnover of Hop1 from chromosomes; the *pch2* single mutant displays a more abundant and continuous localization of Hop1 along synapsed chromosomes (18,22). Thus, in principle, it was rather surprising that high doses of Hop1 could compensate for the absence of Pch2 supporting Mek1 activation and checkpoint function in the *zip1 pch2* mutant. To investigate this apparent contradiction, we examined Hop1 production, localization and phosphorylation in wild type, *pch2*, *zip1* and *zip1 pch2* prophase-arrested *ndt80* cells. Pachytene checkpoint activation leads to Mec1/Tel1-dependent phosphorylation of Hop1 at defined S/T-Q sites; in particular, phosphorylation of the T318 residue is critical for Hop1 checkpoint function promoting Mek1 activation (6,7). As expected, both on chromosome spreads and in whole-cell lysates, we found

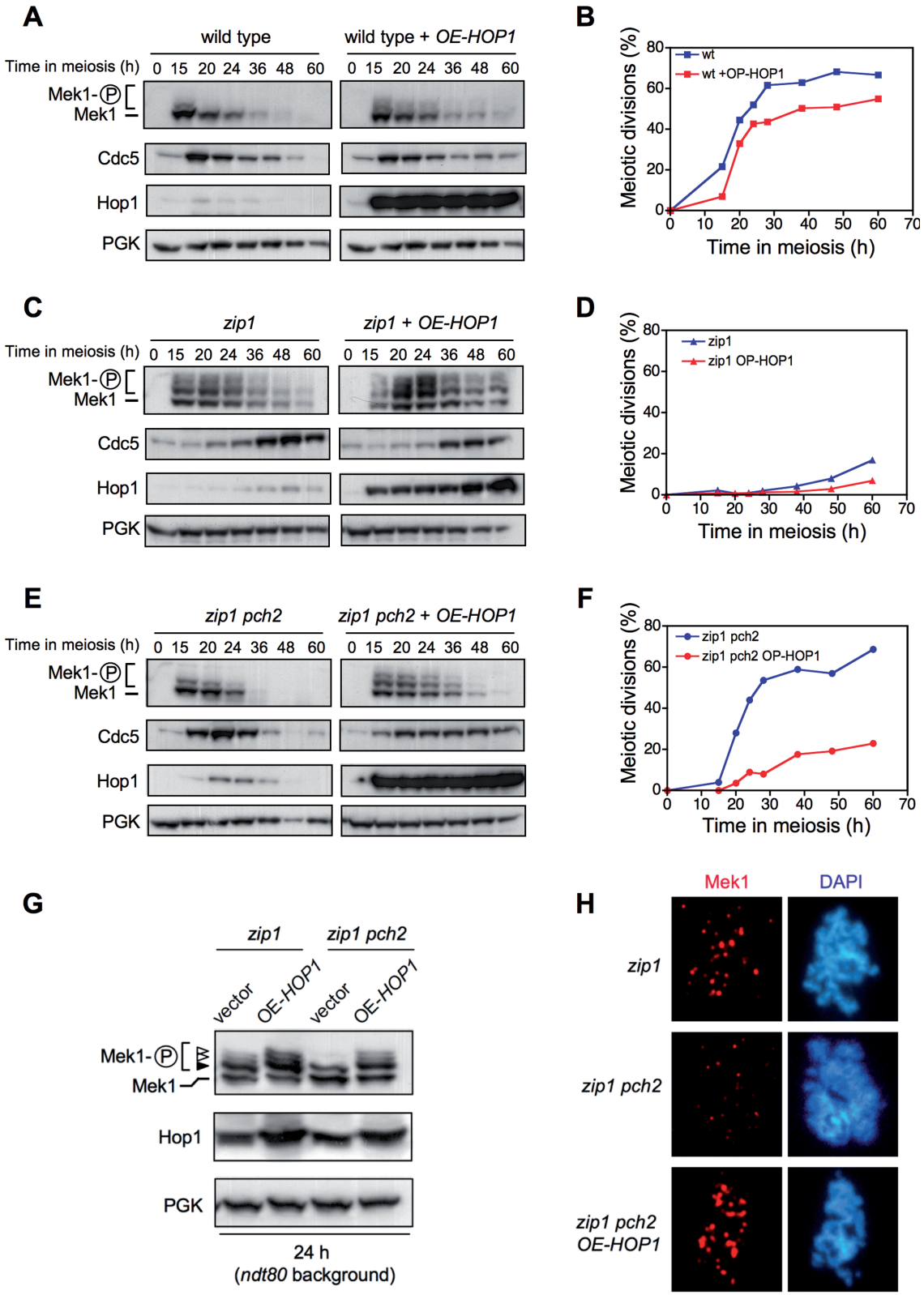

Figure 3. *HOP1* overexpression largely restores meiotic arrest, Mek1 activation, Mek1 localization and delayed Cdc5 production in *zip1 pch2*. Western blot analysis of the indicated proteins and meiotic kinetics of (**A** and **B**) wild type, (**C** and **D**) *zip1* and (**E** and **F**) *zip1 pch2* transformed with empty vector (pRS426) or high-copy *HOP1* (R1692). Strains are: DP421 (wild type), DP422 (*zip1*) and DP1029 (*zip1 pch2*). (**G**) Analysis of Mek1 phosphorylated forms in *ndt80*-arrested strains. The black arrowhead marks the Mec1/Tel1-dependent band and the white arrowheads point to the forms resulting from Mek1 autophosphorylation (8). Strains are: DP428 (*zip1*) and DP881 (*zip1 pch2*), transformed with pRS426 (empty vector) or R1692 (OE-*HOP1*). (**H**) Analysis of Mek1 localization by immunofluorescence of spread meiotic chromosomes using anti-GFP antibodies. Representative nuclei are shown. Strains are DP582 (*zip1*) and DP1111 (*zip1 pch2*).

higher levels of Hop1 in the *pch2* single mutant, compared with the wild type (Figure 4Aa,b; B and D). Paralleling the accumulation of total Hop1, an increased number of phospho-Hop1^{T318} foci (Figure 4Ae,f; C) and higher levels of the phosphorylated protein (Figure 4D) were also observed in *pch2*. Nevertheless, the ratio of phospho-Hop1^{T318} relative to total Hop1 was only moderately increased in *pch2* compared with the wild type (Figure 4E). In fact, the Mek1 kinase is minimally activated in *pch2* as manifested by the almost complete absence of autophosphorylation (Figure 4D, white arrow), the low level of histone H3T11 phosphorylation, which is a target of Mek1 (54) and, therefore, a useful reporter of its kinase activity (Figure 4D), and the rather normal kinetics of meiotic progression of *pch2*, which only shows a minor delay (20) (see also Figure 8D below).

On the other hand, the *zip1* mutant displayed continuous Hop1 signal along unsynapsed chromosome axes (55) (Figure 4Ac and B), numerous and strong phospho-Hop1^{T318} foci (Figure 4Ag and C), and high levels of phospho-Hop1^{T318} protein (Figure 4D). Importantly, the phospho-Hop1^{T318}/total Hop1 ratio was significantly raised in *zip1* (Figure 4E), leading to full activation of Mek1 and robust H3T11 phosphorylation (Figure 4D). Deletion of *PCH2* in *zip1* resulted in increased global levels of the Hop1 protein detected by Western blot, as compared with the *zip1* single mutant (Figure 4D); however, it was not massively incorporated on the axes; Hop1 chromosomal distribution in the *zip1 pch2* double mutant was less continuous than in *zip1* (Figure 4Ad and B). Importantly, *zip1*-induced Hop1^{T318} phosphorylation was dramatically reduced in the absence of Pch2 (Figure 4Ah, C, D and E), thus explaining the impaired Mek1 activation and defective checkpoint response in *zip1 pch2* (Figures 3 and 4D).

These observations reveal that the critical role of Pch2 in the *zip1*-induced checkpoint is to promote Hop1 phosphorylation at T318. Confirming this notion, overexpression of wild-type *HOP1*, but not that of a phosphorylation-deficient *hop1-T318A* mutant (6), restored Hop1^{T318} phosphorylation and checkpoint function (i.e. full Mek1 activation) in *zip1 pch2* (Figure 5).

The absence of PP4 restores checkpoint activity in *zip1 pch2* to a small extent

It has been reported that the protein phosphatase 4 (PP4) counteracts Mec1/Tel1-dependent Hop1^{T318} phosphorylation (7); therefore, to further explore the role of Pch2 in controlling Hop1^{T318} phosphorylation we examined the effect of deleting the *PPH3* gene, which encodes the catalytic subunit of PP4. We analyzed the kinetics of meiotic divisions (Figure 6A) and the activation of molecular markers of the checkpoint, including Hop1^{T318}, Mek1 and histone H3T11 phosphorylation (Figure 6B). Consistent with a role for PP4 in shutting off pachytene checkpoint signaling, the *pph3* mutant showed a transient Hop1-Mek1 activation (Figure 6B) manifested as a short meiotic delay (Figure 6A); moreover, the *zip1 pph3* double mutant displayed persistent checkpoint activity and strong meiotic arrest (Figure 6A and B). Although Hop1^{T318} phosphorylation is severely impaired in *zip1 pch2* (Figures 4D, E and 6B), the lack of PP4 resulted in higher levels of Hop1^{T318} phosphorylation and the ensuing Mek1 kinase activity (Figure 6B) leading to delayed meiotic divisions in *zip1 pch2 pph3* compared to *zip1 pch2* (Figure 6A). However, checkpoint function (i.e. Hop1^{T318} phosphorylation) was not completely restored in the *zip1 pch2 pph3* triple mutant, which showed faster meiotic progression than that of *zip1* and a weaker and shorter Mek1 activation (Figure 6A and B).

All together, these observations confirm that Pch2 specifically supports Hop1^{T318} phosphorylation when the synapsis checkpoint is triggered by the absence of Zip1 and reveal that the control of Hop1^{T318} phosphorylation by Pch2 is not, at least exclusively, exerted by modulating PP4 action.

To determine whether the defective Hop1^{T318} phosphorylation in *zip1 pch2* stems from an impaired general activation of the Mec1-Ddc2 complex, we performed immunofluorescence of spread meiotic chromosome using an antibody that recognizes the phosphorylated S/T-Q motifs. As shown in Supplementary Figure S1A, phospho-S/T-Q foci similarly decorated both *zip1* and *zip1 pch2* chromosomes. We also examined the localization of the Mec1-Ddc2 complex monitoring the induction of Ddc2-GFP foci when the meiotic checkpoint is triggered in *zip1* cells (43). We found that the formation of Ddc2 foci is not altered by the absence of Pch2 in *ndt80*-arrested cells (Supplementary Figure S1B). These observations suggest that Pch2 does not impact widespread Mec1 signaling.

Unsynapsed chromosomes and unrepaired DSBs remain in *zip1 pch2 ndt80*

Although the precise defect(s) triggering the checkpoint in *zip1* mutants (defective synapsis and/or unrepaired DSBs) remains unclear, since *pch2* affects meiotic DSB metabolism, it was formally possible that the reduced Hop1^{T318} phosphorylation observed in *zip1 pch2* resulted from the absence or the disappearance of the checkpoint-activating signal. However, the fact that Ddc2 foci formation and S/T-Q phosphorylation are conspicuous in *zip1 pch2* (Supplementary Figure S1) indicates that the *zip1* defects triggering the checkpoint are still present in the absence of Pch2. We also monitored the presence of Rad51 foci as a marker for unrepaired DSBs (56). To avoid again the effect of meiotic progression on DSB repair outcome we performed the analysis in *ndt80* cells. No or few Rad51 foci were observed in most wild-type (1.8 $\pm$ 0.3 SEM foci per nucleus; n = 40) and *pch2* (2.0 $\pm$ 0.5 SEM foci per nucleus; n = 35) nuclei, but the number was markedly increased in the *zip1* mutant (5.5 $\pm$ 0.5 SEM foci per nucleus; n = 35). Importantly, although the fraction of unrepaired DSBs was reduced in *zip1 pch2* (3.5 $\pm$ 0.5 SEM foci per nucleus; n = 45), likely due to intersister (IS) repair, the double mutant still showed prominent Rad51 foci (Figure 7A). In addition, chromosome axes are unsynapsed in *zip1 pch2*; i.e., the synapsis defect continues to exist (Figure 4Ac,d). Thus, these observations indicate that the inability of *zip1 pch2* to phosphorylate Hop1 at T318 does not stem from the absence of defects triggering the checkpoint and point to a more direct role for Pch2 in controlling Hop1-Mek1 activation.

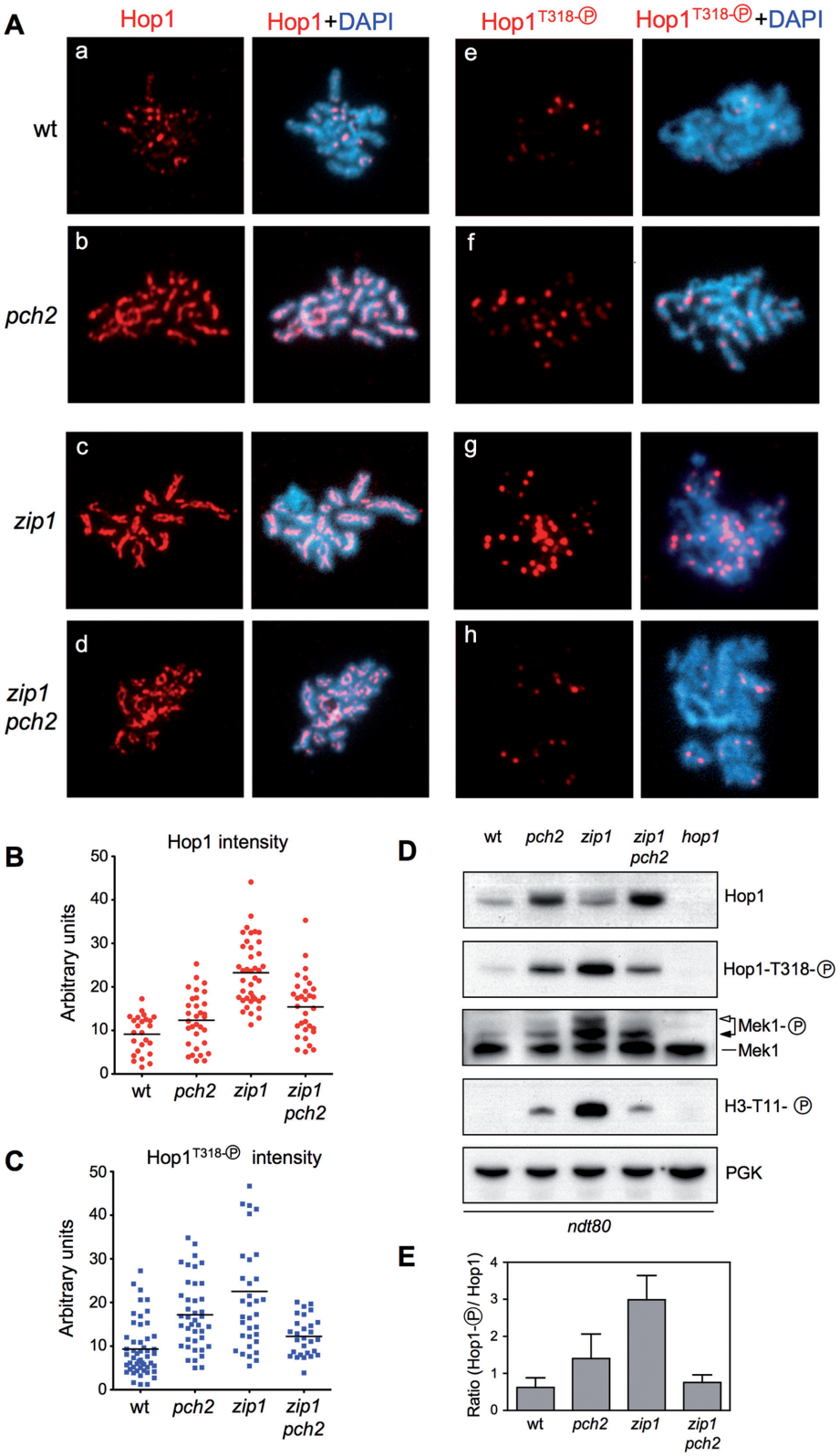

Figure 4. Pch2 promotes Hop1^{T318} phosphorylation in *zip1*. (**A**) Immunofluorescence of spread meiotic chromosomes stained with DAPI (blue) and anti-Hop1 (a-d panels) or anti-phospho-Hop1^{T318} (e–h panels) antibodies (red). Representative nuclei are shown. (**B** and **C**) Quantification of total Hop1 and phospho-Hop1^{T318} fluorescence signal, respectively, on the spreads analyzed in (A). Each spot in the plot represents the intensity of a nucleus scored. (**D**) Western blot analysis of the indicated proteins and phosphorylation events. (**E**) Quantification of relative Hop1^{T318} phosphorylation analyzed as in (D). The ratio of phospho-Hop1^{T318} versus total Hop1 chemiluminiscence signal is represented. Means and standard deviations from three independent experiments are shown. Strains are: DP424 (wild type), DP1058 (*pch2*), DP428 (*zip1*), DP881 (*zip1 pch2*) and DP700 (*hop1*). Spreads and lysates were prepared 24 h after meiotic induction of *ndt80* cells. For DP700 the sample was taken at 17 h.

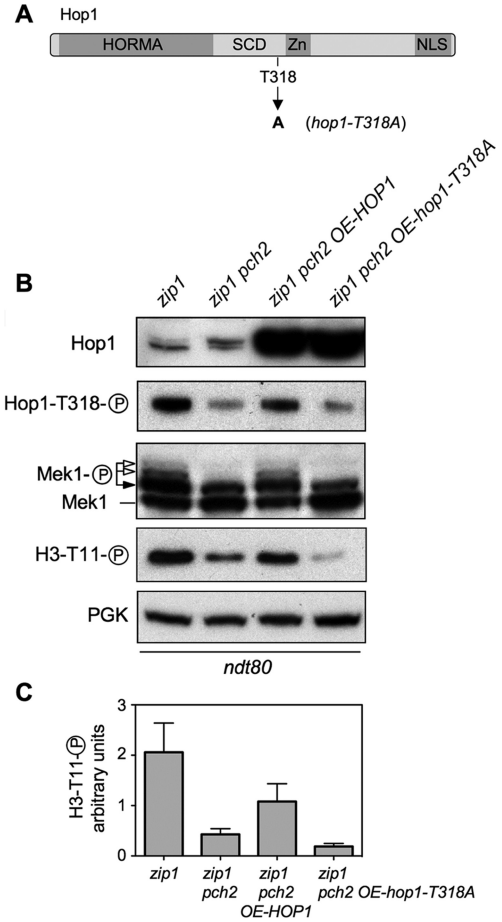

Figure 5. Hop1^{T318} phosphorylation is the critical checkpoint event impaired in *zip1 pch2*. (**A**) Schematic representation of the Hop1 protein domains and the position of the mutated T318 phosphosite (6) (**B**) Overexpression of wild-type *HOP1*, but not the *hop1-T318A* mutant, restores Mek1 activation in *zip1 pch2*. Western blot analysis of Hop1, phospho-Hop1^{T318}, Mek1 and phospho-H3^{T11} in *ndt80*-arrested cells. (**C**) Quantification of the phospho-H3^{T11} signal from three experiments. Note that Mek1 activity markedly increases, but is not fully restored in *zip1 pch2 OE-HOP1* cells due to plasmid-loss events in the meiotic cultures (43); those cells that lose the plasmid do not overproduce Hop1 and do not contribute to Mek1 phosphorylation. Strains are DP428 (*zip1*) and DP881 (*zip1 pch2*) transformed with pRS426 (empty vector), pSS316 (*OE-HOP1*) or pSS317 (*OE-hop1-T318A*).

The Pch2-Hop1-Mek1 signaling module impacts meiotic cell cycle progression

Since the analyses described above were performed in *ndt80*-arrested cells, we also explored the possibility that the mutation of *PCH2* suppresses *zip1* meiotic arrest exclusively by allowing the repair of DSBs by recombination between sister chromatids as a result of the impaired Mek1 function in *zip1 pch2* (28). If that were the case; that is, Mek1 only controls recombination partner choice and not cell cycle events, compromising repair by mutation of recombination factors would restore meiotic cell cycle arrest in *zip1 pch2* cells; therefore, we deleted *RAD51* to interfere with DNA repair. In parallel with monitoring meiotic divisions, we used the presence of multiple Ddc2-GFP foci as a reporter for unrepaired Spo11-dependent meiotic recombination intermedi-

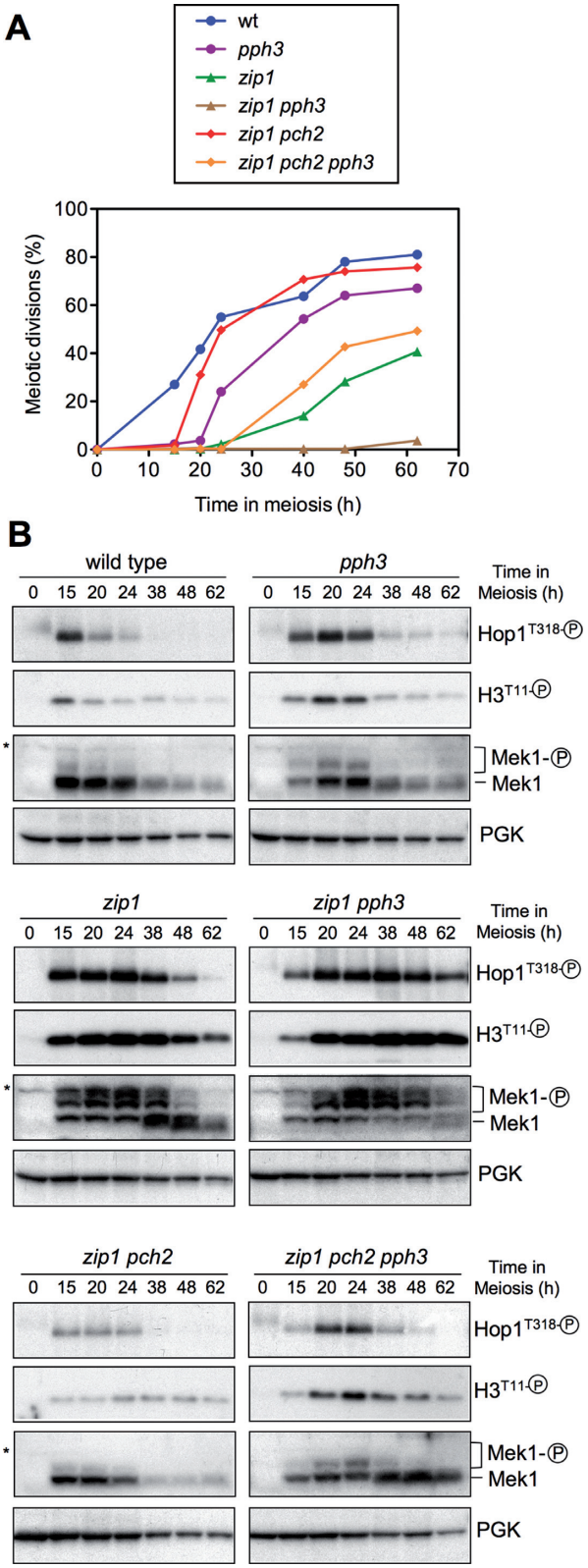

Figure 6. Impact of the PP4 phosphatase on Pch2-dependent meiotic checkpoint. (**A**) Time course of meiotic nuclear divisions; the percentage of cells containing two or more nuclei is represented. (**B**) Western blot analysis of Hop1^{T318} phosphorylation and Mek1 activity at the indicated time points in meiosis. PGK was used as a loading control. Strains are: DP421 (wild type), DP1247 (*pph3*), DP422 (*zip1*), DP1249 (*zip1 pph3*), DP1029 (*zip1 pch2*) and DP1245 (*zip1 pch2 pph3*).

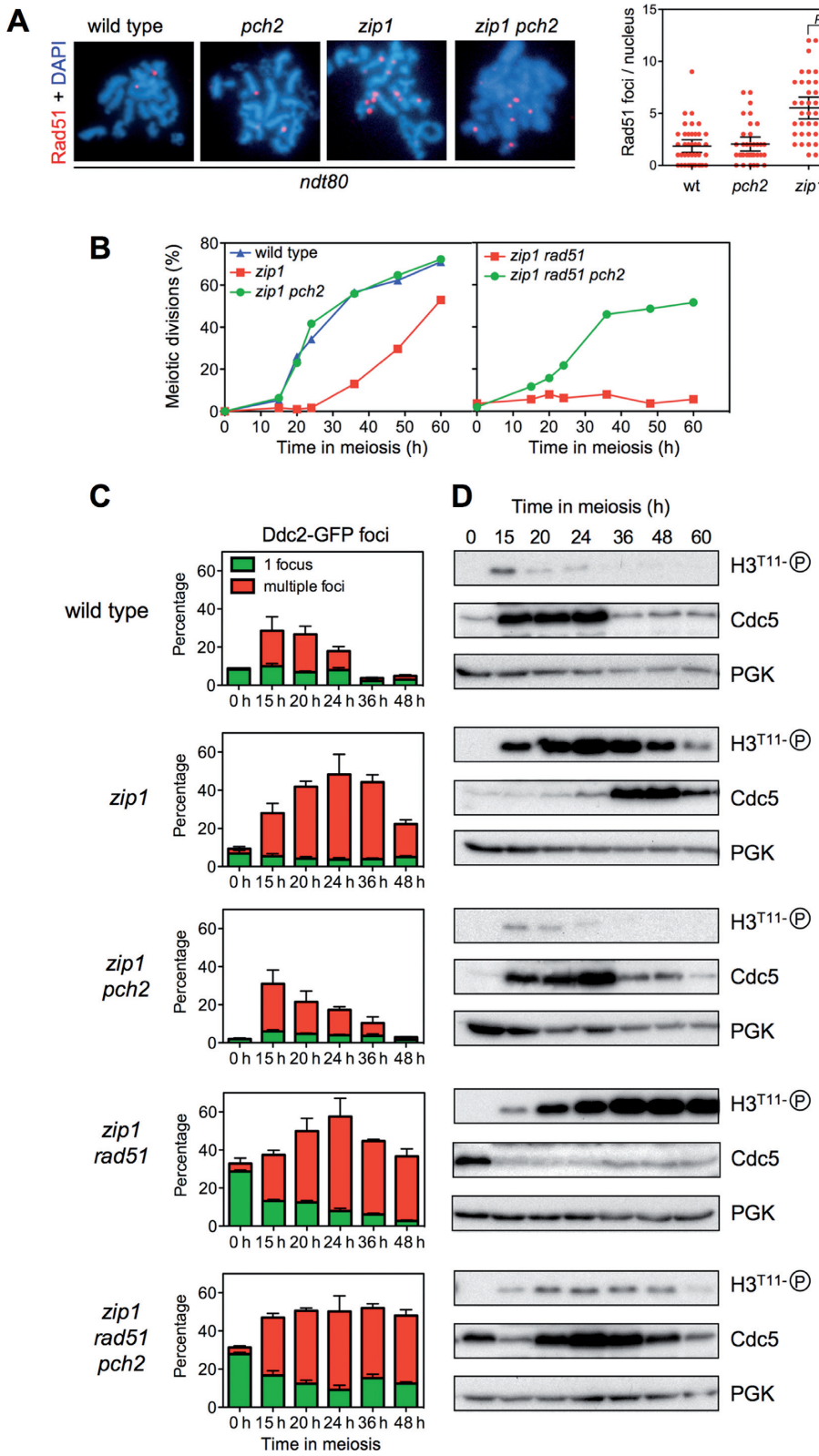

Figure 7. Effect of Pch2 on cell cycle progression and resolution of *zip1*-induced recombination intermediates. (**A**) Localization and quantification of Rad51 foci as markers for unrepaired DSBs on spread meiotic nuclei of *ndt80* cells after 24 h of meiotic induction. Strains are: DP424 (wild type), DP1058 (*pch2*), DP428 (*zip1*) and DP881 (*zip1 pch2*). (**B**) Time course of meiotic nuclear divisions. The percentage of cells with two or more nuclear masses is represented. (**C**) Quantification of Ddc2-GFP foci throughout meiosis. The percentage of cells containing a single non-meiotic Ddc2 focus (green bars) or multiple meiotic Ddc2 foci (red bars) from three different counts is represented. Note that *rad51* cells accumulate spontaneous non-meiotic Ddc2 foci at time zero. Between 150 and 800 cells were scored for each strain at every time point. (**D**) Western blot analysis of phospho-H3T11 (as a reporter for Mek1 activity), Cdc5 (as a marker for meiosis I entry) and PGK (as a loading control) from the same cultures analyzed in (B) and (C). Strains for (B), (C) and (D) are: DP448 (wild type), DP449 (*zip1*), DP1379 (*zip1 pch2*) DP1381 (*zip1 rad51*) and DP1382 (*zip1 pch2 rad51*).

ates (43), H3T11 phosphorylation as a reporter for Mek1 activity and Cdc5 production as a molecular indicator of prophase I exit and entry into meiotic divisions (Figure 7B, C and D). In the wild type, only a transient peak of Ddc2-containing cells was detected because recombination is normally completed. In the *zip1* mutant, cells containing multiple Ddc2 foci accumulate, leading to Mek1 activation and delayed Cdc5 production. As expected, the *zip1 pch2* double mutant showed impaired Mek1 activation allowing normal meiotic progression and the disappearance of recombination intermediates (Figure 7B, C and D). Notably, whereas at late time points a fraction of *zip1* cells underwent meiotic divisions after a delay, the *zip1 rad51* double mutant displayed a much tighter arrest (Figure 7B) and markedly reduced and delayed Cdc5 production (Figure 7D). Likewise, Ddc2 multiple foci and Mek1 activation persisted for longer in *zip1 rad51* (Figure 7C and D; Supplementary Figure S2). These observations indicate that compromising recombination by the *rad51* mutation prevents the resolution of recombination intermediates in *zip1* leading to a stronger meiotic block. Importantly, deletion of *PCH2* reduced Mek1 activation and restored meiotic progression and earlier Cdc5 production in *zip1 rad51* despite the persistence of multiple Ddc2 foci; that is, unrepaired recombination intermediates (Figure 7B,C,D; Supplementary Figure S2).

We also analyzed the effect of Rad54, which is a Rad51 accessory factor, and a direct Mek1 target (12). In addition to the action of Hed1, phosphorylation of Rad54 by Mek1 reduces its affinity for Rad51 binding; therefore, mutation of *RAD54* can be used also as a tool to interfere with meiotic recombinational repair (57–59). We observed that, like in *zip1 pch2*, the sporulation block of *zip1* was still relieved in the *zip1 pch2 rad54* triple mutant (Supplementary Figure S3A). Consistent with impaired repair in the absence of Rad54, spore viability was further reduced in *zip1 pch2 rad54* (29.1%, n = 144) compared with *zip1 pch2* (47.2%; n = 144). Moreover, we used chromosome spreads to monitor the presence of Ddc2 foci in combination with spindle staining as a sensitive cytological assay for checkpoint function (19,43,51). Whereas *zip1 rad54* cells arrested in prophase with unseparated SPBs and numerous Ddc2 foci (35.4 ± 2.5 SEM foci per nucleus; n = 13), *zip1 rad54 pch2* nuclei displaying elongated meiosis I spindle coexisting with persistent recombination intermediates (14.0 ± 3.0 SEM Ddc2 foci per nucleus; n = 10) could be detected (Supplementary Figure S3B). In wild-type nuclei, recombination intermediates never coexist with metaphase spindles (19,43,51). These findings indicate that, in the absence of Pch2, a late cell cycle event has been initiated before an earlier one has been completed; that is, checkpoint function is impaired.

In summary, these observations argue that Pch2 controls a general checkpoint response via Hop1-Mek1 regulation that includes the cell-cycle arrest outcome and not only the regulation of recombination.

To determine whether the effect of Pch2 was exerted exclusively in response to the meiotic defects resulting from the lack of Zip1, we examined other mutants affecting SC dynamics, such as *zip3* and *ecm11*. Zip3 is a SUMO ligase constituting the so-called synapsis initiating complex (60,61) and Ecm11 is a component of the central element of the SC (39,62). Similar to *zip1*, although to different extents, both *ecm11* and *zip3* single mutants displayed delayed meiotic progression (Supplementary Figure S4A), increased Hop1-T318 phosphorylation and induced Mek1 activity (Supplementary Figure S4B). Deletion of *PCH2* resulted in faster meiotic progression and impaired Hop1 and Mek1 activation (Supplementary Figure S4). Therefore, Pch2 impact on Hop1-Mek1 signaling is also required to restrain meiotic divisions in other mutants altering SC proper development.

The ATPase activity of Pch2 is required for its checkpoint function

Pch2 is a hexameric ring AAA+ ATPase (63). In order to investigate whether Pch2 ATPase activity is required for its meiotic checkpoint function, conserved critical residues in the AAA+ domain of Pch2 were mutated to abolish its catalytic activity (64). In particular, the lysine 320 in the Walker A motif required for ATP binding was changed to alanine, and the glutamic acid at position 399 in the Walker B motif, required for ATP hydrolysis, was substituted for glutamine to generate the *pch2-K320A* and *pch2-E399Q* mutants, respectively (Figure 8A). We used the *delitto perfetto* technique, which leaves no additional modifications, to introduce these mutations in the genomic loci of strains carrying functional N-terminal HA- or MYC-tagged versions of *PCH2* (18). Both Pch2-K320A and Pch2-E399Q mutant proteins were produced at normal levels and with normal kinetics (Figure 8B). Like *pch2Δ*, the *pch2-K320A* and *pch2-E399Q* single mutants showed no prominent phenotype in unperturbed meiosis; they were able to complete meiosis and sporulation with kinetics and efficiency similar to the wild type, producing high levels of viable spores (Figure 8C and D; Table 1). Interestingly, when the meiotic checkpoint was triggered by the lack of Zip1, we found that, like *pch2Δ*, the *pch2-K320A* and *pch2-E399Q* mutations completely suppressed the sporulation defect of *zip1* (Figure 8C); the *zip1 pch2-K320A* and *zip1 pch2-E399Q* double mutants displayed fairly normal kinetics of meiotic divisions (Figure 8D), but generate largely inviable meiotic products (Table 1). These observations imply that the ATPase activity of Pch2 is absolutely required to restrain meiotic progression when the checkpoint is induced by the absence of Zip1. To further confirm this interpretation we assessed the effect of the *pch2-K320A* and *pch2-E399Q* mutations on checkpoint function by monitoring molecular markers of checkpoint activation impacted by Pch2 (see above), such as Hop1^{T318} phosphorylation, Mek1 hyperphosphorylation and histone H3T11 phosphorylation (Figure 8E). Consistent with the alleviation of meiotic arrest (Figure 8C and D), the high levels of phospho-Hop1^{T318} and Mek1 hyperactivation observed in *zip1* were drastically reduced in both *zip1 pch2-K320A* and *zip1 pch2-E399Q* double mutants (Figure 8E). Like in *zip1 pch2Δ*, *HOP1* overexpression restored Hop1^{T318} phosphorylation and Mek1 activation in both ATPase mutants (Supplementary Figure S5). Thus, both ATP binding to the Walker A motif and ATP hydrolysis by the Walker B module are critical for Pch2's meiotic checkpoint function.

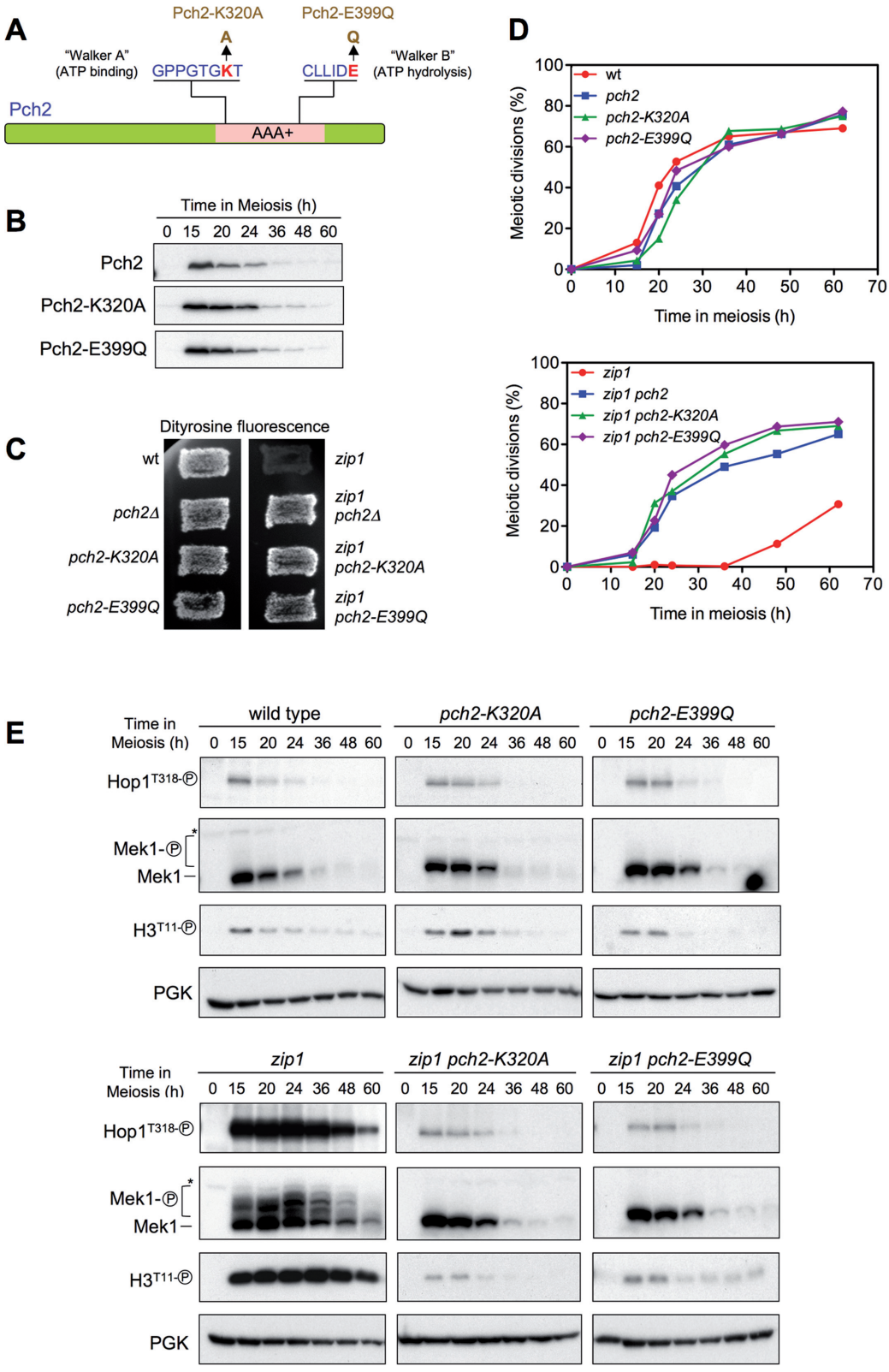

Figure 8. The ATPase activity of Pch2 is required for its checkpoint function. (**A**) Schematic representation of the Pch2 protein indicating the AAA+ domain, the conserved Walker A and Walker B motifs, and the mutations introduced at both sites. (**B**) Western blot analysis of Pch2, Pch2-K320A or Pch2-E399Q production (detected with anti-HA antibodies) during meiosis. (**C**) Dityrosine fluorescence assay. (**D**) Time course of meiotic nuclear divisions; the percentage of cells containing two or more nuclei is represented. (E) Western blot analysis of Hop1^{T318} phosphorylation and Mek1 activation. PGK was used as a loading control. Strains are: DP1151 (wild type), DP1164 (*pch2Δ*), DP1163 (*pch2-K320A*), DP1287 (*pch2-E399Q*), DP1152 (*zip1*), DP1161 (*zip1 pch2Δ*), DP1162 (*zip1 pch2-K320A*) and DP1288 (*zip1 pch2-E399Q*).

Table 1. Sporulation and spore viability

Genotype	Sporulation frequency (%)	Spore Viability (%)
Wild type	66.8	95.3
pch2Δ	73.9	90.7
pch2-K320A	64.6	96.5
pch2-E399Q	80.3	93.0
zip1	2.0	nd
zip1 pch2Δ	83.3	35.2
zip1 pch2-K320A	77.3	46.5
zip1 pch2-E399Q	80.3	31.2
Wild type + *OE-HOP1*	65.3	92.0
pch2Δ + *OE-HOP1*	20,3	94.4

Sporulation frequency and spore viability was determined as explained in Materials and Methods. nd, not determined.
OE-: overexpression.

ATP binding to Pch2 is required for its localization and complex stability

We also analyzed the localization of wild-type Pch2 and the ATPase-dead versions on pachytene chromosome spreads. As previously described, the wild-type Pch2 protein showed a conspicuous accumulation in a particular chromosomal region lacking Hop1 that corresponds to the rDNA array (18) (Figure 9Aa, Ad). In addition, faint foci outside the rDNA can be found on wild-type chromosomes displaying an exclusive localization with Hop1 (18,22) (Supplementary Figure S6, white arrows). Surprisingly, despite being present at normal levels in whole cell extracts (Figure 8B), the Walker A-deficient Pch2-K320A protein was not detectable at any location on meiotic chromosomes of either wild-type or *zip1* spread nuclei (Figure 9Ab and Ae). In contrast, the Pch2-E399Q protein showed normal rDNA localization (Figure 9Ac and Af) even though it is catalytically inactive (63) and lacks checkpoint function (Figure 8). Remarkably, like in *pch2Δ* (Figure 4Ab), the Hop1 protein was also more abundant on chromosomes and displayed a linear instead of a dotty pattern in both *pch2-K320A* and *pch2-E399Q* single mutants (Figure 9Ab and Ac). On the contrary, but also similar to *zip1 pch2Δ* (Figure 4Ad), Hop1 localization was disrupted and discontinuous in *zip1 pch2-K320A* and *zip1 pch2-E399Q* double mutants (Figure 9Ae and Af). In addition, the characteristic exclusion of Hop1 from the rDNA region (18,55) was lost in the ATPase-deficient mutants (Figure 9A; arrows); in fact, the Pch2-E399Q protein extensively colocalized with Hop1 at the rDNA (Figure 9Ac and Af). Moreover, in contrast to the wild type, chromosomal foci of Pch2-E399Q also colocalized with Hop1 (Supplementary Figure S6, yellow arrows).

Since the Pch2-K320A version was not associated to the meiotic chromatin, we next studied the subcellular localization of Pch2 and Pch2-K320A by immunofluorescence in whole meiotic *zip1* cells. The wild-type Pch2 was prominently detected in a discrete lateral nuclear region devoid of Hop1, presumably the nucleolus (Figure 9B, arrow). On the other hand, Pch2-K320A did not accumulate in the nucleus and was present rather evenly dispersed throughout the cell (Figure 9B). Interestingly, total cellular levels of Hop1 were higher in the *zip1 pch2-K320A* mutant (Figure 9B), although the protein was not massively incorporated onto the chromosome axes (Figure 9Ae).

Mutation of this conserved lysine in the Walker A motif of AAA+ family members commonly abolishes ATP binding and therefore ATPase activity *in vitro*, as has been demonstrated for Pch2 (63) but, in addition, it often leads to dissociation of the hexameric complex into monomers, as has been described for the HslU and SV40 LTag AAA+ ATPases (65). Therefore, we analyzed whether the *pch2-K320A* mutation compromises the formation of the Pch2 hexameric complex *in vivo*. We generated wild-type and *pch2-K320A* heterozygous diploid strains in which one copy of the *PCH2* (or *pch2-K320A*) gene was tagged with the HA epitope and the other copy with the Myc epitope (Figure 10). In the wild type (*PCH2-HA/PCH2-Myc*), the anti-HA antibody immunoprecipitated both Pch2-HA and Pch2-Myc, consistent with the formation of a stable complex. In contrast, the anti-HA antibody failed to immunoprecipitate the Myc-tagged subunits in the *pch2-K320A-HA/pch2-K320A-Myc* strain (Figure 10A), suggesting that ATP binding is required for the integrity or stability of the Pch2 hexameric ring *in vivo* (Figure 10B).

In summary, the ATPase activity of Pch2 is absolutely required for the checkpoint response to *zip1* meiotic defects and orchestrates proper Hop1 subcellular distribution, chromosomal localization and phosphorylation. ATP binding to the Walker A motif of Pch2, but not ATP hydrolysis, is essential for its nuclear accumulation and association to the meiotic chromosomes.

DISCUSSION

Suppression of *pch2* checkpoint defect by Hop1 overproduction

Previous studies have reported that the Pch2 protein is an important player in the meiotic checkpoint response triggered by the absence of Zip1, a major structural component of the central region of the synaptonemal complex. This work provides new insights into the role of Pch2 in this process; we show that the critical function of Pch2 in the *zip1*-induced checkpoint is to promote Mec1/Tel1-dependent Hop1 phosphorylation at T318 and, therefore, the ensuing Mek1 full activation leading to the meiotic cell cycle block. We also show here that the ATPase activity of Pch2 is essential for this checkpoint function.

We report the isolation of *HOP1* in a genetic screen for high-copy suppressors of the *pch2* checkpoint defect.

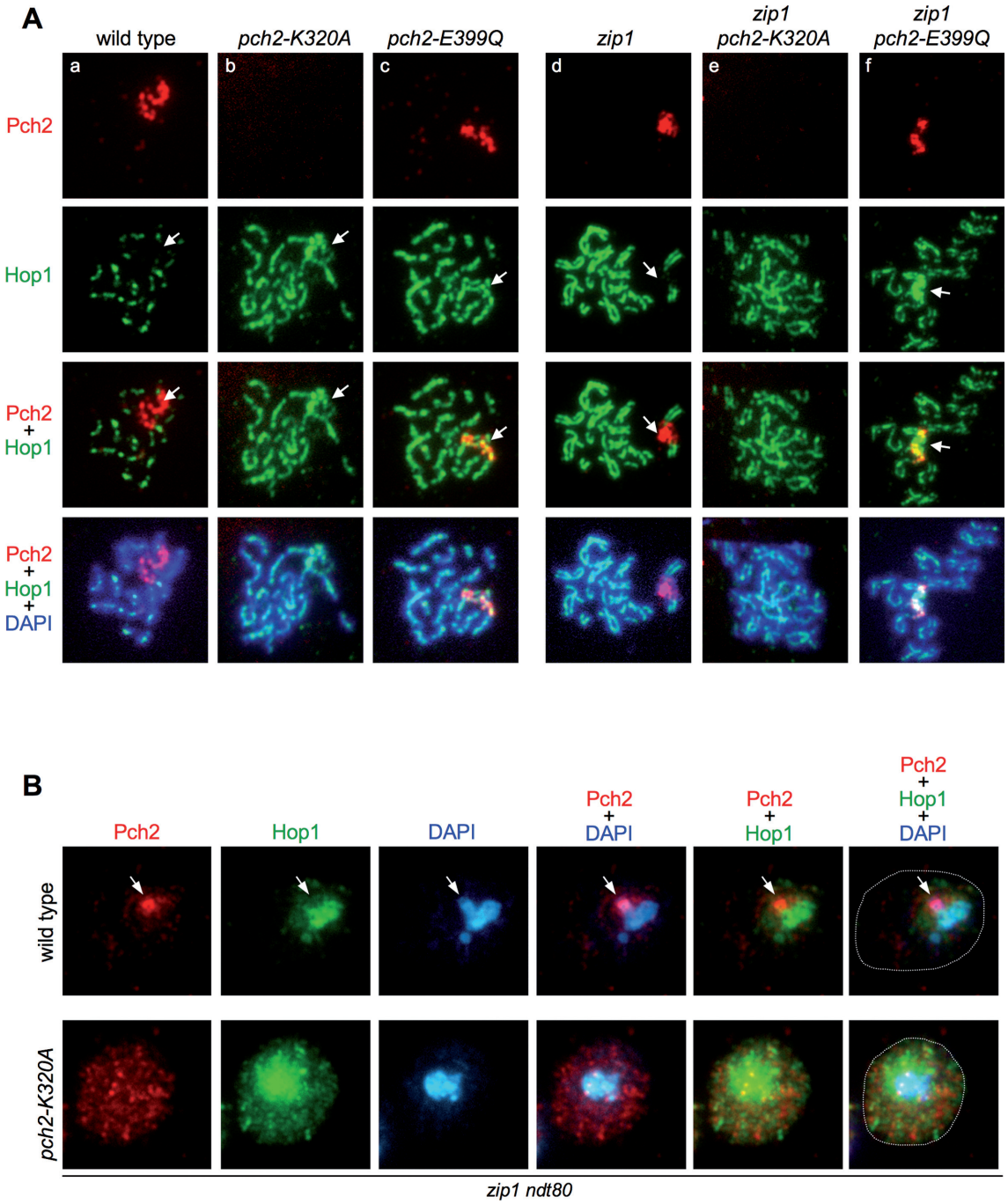

Figure 9. Localization of ATPase-deficient versions of Pch2. (**A**) Immunofluorescence of meiotic chromosomes stained with anti-HA or anti-MYC antibodies to detect Pch2, Pch2-K320A or Pch2-E399Q (red), anti-Hop1 antibodies (green) and DAPI (blue). Strains are: DP1243 (wild type), DP1193 (*pch2-K320A*), DP1262 (*pch2-E399Q*), DP1244 (*zip1*), DP1192 (*zip1 pch2-K320A*) and DP1263 (*zip1 pch2-E399Q*). (**B**) Immunofluorescence of whole meiotic cells stained with anti-HA antibodies (to detect Pch2 or Pch2-K320A; red), anti-Hop1 antibodies (green) and DAPI (blue). The contour of the cells is outlined in the rightmost panels. Representative cells 24 h after meiotic induction in *zip1 ndt80* background are shown. The arrows point to the rDNA region, which is distinguishable by the accumulation of Pch2 and the absence of Hop1. This region is not recognizable in the *pch2-K320A* mutant due to the mislocalization of Pch2-K320A and Hop1. Strains are: DP1190 (wild type) and DP1192 (*pch2-K320A*).

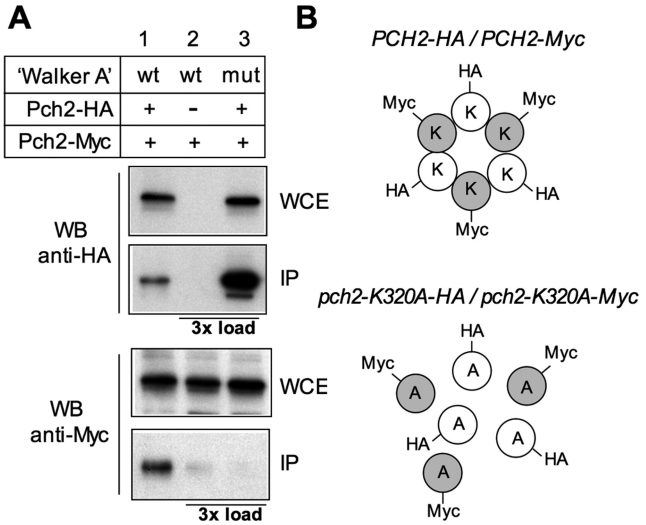

Figure 10. Mutation of the Pch2 ATP-binding site impairs the stability of the hexameric complex. (**A**) Whole cell extracts (WCE) prepared after 16 h in meiosis were immunoprecipitated with anti-HA antibodies. WCE and immunoprecipitates (IP) were analyzed by Western blot with both anti-HA and anti-Myc antibodies, as indicated. Strains are: DP1325 (*PCH2-HA/PCH2-Myc*; lane 1), DP1329 (*PCH2/PCH2-Myc*; lane 2) and DP1337 (*pch2-K320A-HA/pch2-K320A-Myc*; lane 3). To discard a problem with detection levels, in lane 2 (HA-untagged control) and lane 3, three more times of IP compared to lane 1 were loaded. (**B**) Schematic interpretation of the result described in (A). K and A represent a lysine and an alanine, respectively, at position 320 of Pch2.

Monitoring various cytological and molecular markers, we demonstrate that high levels of Hop1 restore checkpoint function in a *zip1 pch2* mutant restraining meiotic cell cycle progression. This finding was unanticipated, since it has been well established that Pch2 negatively regulates Hop1 abundance (at least on synapsed chromosomes) (18,21,22). Since Hop1 chromosomal levels are higher in the *pch2* mutant it was unexpected that additional amounts of Hop1 provided by an overexpression plasmid could suppress the phenotype resulting from the lack of Pch2. Nevertheless, the Hop1 remodeling function reported for Pch2 has been only analyzed in the context of synapsed chromosomes, where Pch2 determines an alternating pattern of Hop1 abundance (21) (Figure 11). We show here in the context of unsynapsed chromosomes that, although global cellular levels of Hop1 are higher in *zip1 pch2* compared with *zip1*, the extensive incorporation of Hop1 onto the lateral elements of *zip1* chromosomes is not further increased when *PCH2* is deleted. However, the rDNA region, normally devoid of Hop1, is decorated by the Hop1 protein in both *pch2* and *zip1 pch2* mutants, consistent with the nucleolar localization of Pch2 in both wild type and *zip1* nuclei. Notably, although Pch2 and Hop1 display largely exclusive localization patterns on wild-type chromosomes, we show that the catalytically-inactive Pch2-E399Q protein colocalizes with Hop1 both at chromosomal foci and the rDNA confirming that the ATPase activity of Pch2 is required for displacing Hop1 from the meiotic chromatin *in vivo* like it does *in vitro* (63).

Regulation of Hop1 phosphorylation

Phosphorylation of Hop1 at T318 by the Mec1/Tel1 checkpoint kinases is a requisite for Mek1 autophosphorylation and, therefore, for checkpoint activity. We show here that *zip1*-induced Hop1-T318 phosphorylation is drastically reduced in the absence of Pch2 or in ATPase-dead *pch2* mutants. This reduction is manifested both globally using western blot analysis of whole cell extracts and locally on chromosome spreads, indicating a general requirement for Pch2 to maintain high levels of Hop1-T318 phosphorylation when synapsis defects occur. The fact that overexpression of wild-type *HOP1*, but not that of a *hop1-T318A* mutant, restores the checkpoint in *zip1 pch2* reveals Hop1-T318 phosphorylation as the relevant target of Pch2's checkpoint function. Notably, although *HOP1* overexpression in the wild type has only minimal effects, it reduces sporulation efficiency in the *pch2* single mutant (Table 1), suggesting that Pch2 activity is required to maintain the proper balance of Hop1 abundance and phosphorylation also in the presence of synapsed chromosomes. We also note that Zip1 may contribute to the accumulation of phospho-Hop1^{T318} in *pch2* mutant chromosomes.

We show that meiotic defects persist in *zip1 pch2*; thus, in principle, two possibilities can be envisaged to explain the regulation of Hop1-T318 phosphorylation by the Pch2 ATPase: Pch2 might favor the action of the Mec1/Tel1 kinases on Hop1-T318 or, alternatively, may inhibit phospho-Hop1-T318 phosphatase(s). In line with the first option, Pch2 (together with Xrs2) promotes Tel1-dependent Hop1 phosphorylation in response to unresected DSBs in a *rad50S* mutant (29). However, Tel1 is not required for the *zip1*-induced synapsis checkpoint (29) pointing to a Tel1-independent function for Pch2 in this particular scenario. We also show here that the absence of Pch2 does not alter the localization of the Mec1-Ddc2 complex suggesting that Pch2 is not required for global Mec1 activity. Nevertheless, a local requirement for Pch2 in facilitating the access of Mec1 to the Hop1-T318 substrate on chromosome axes cannot be ruled out. In this scenario, Pch2's ATPase activity could be required to induce some conformational change in the vicinity of Hop1 enabling its phosphorylation at T318 by Mec1. The interaction of Red1 with SUMO chains promotes Hop1-T318 phosphorylation (66). It is possible that Pch2 differentially modulates this interaction in response to SC defects. In line with this possibility, a role for Pch2 in orchestrating the interdependence between Hop1 and Red1 for Hop1 phosphorylation has been proposed (67). Nevertheless, these studies have not been performed under checkpoint-inducing conditions (i.e. *zip1* mutant) where Pch2 may have different and/or additional functions (see below).

On the other hand, if Pch2 negatively regulates the phosphatase(s) involved in removing the phosphorylation of Hop1-T318, the lack of this phosphatase should reestablish the meiotic block in a *zip1 pch2* mutant. It has been proposed that PP4 is the main phosphatase reversing Hop1-T318 phosphorylation (7); therefore, we investigated the impact of PP4 in the response to *zip1* defects. In the BR1919 genetic background used in this study, the *zip1* mutant shows a checkpoint-induced meiotic block in prophase, but

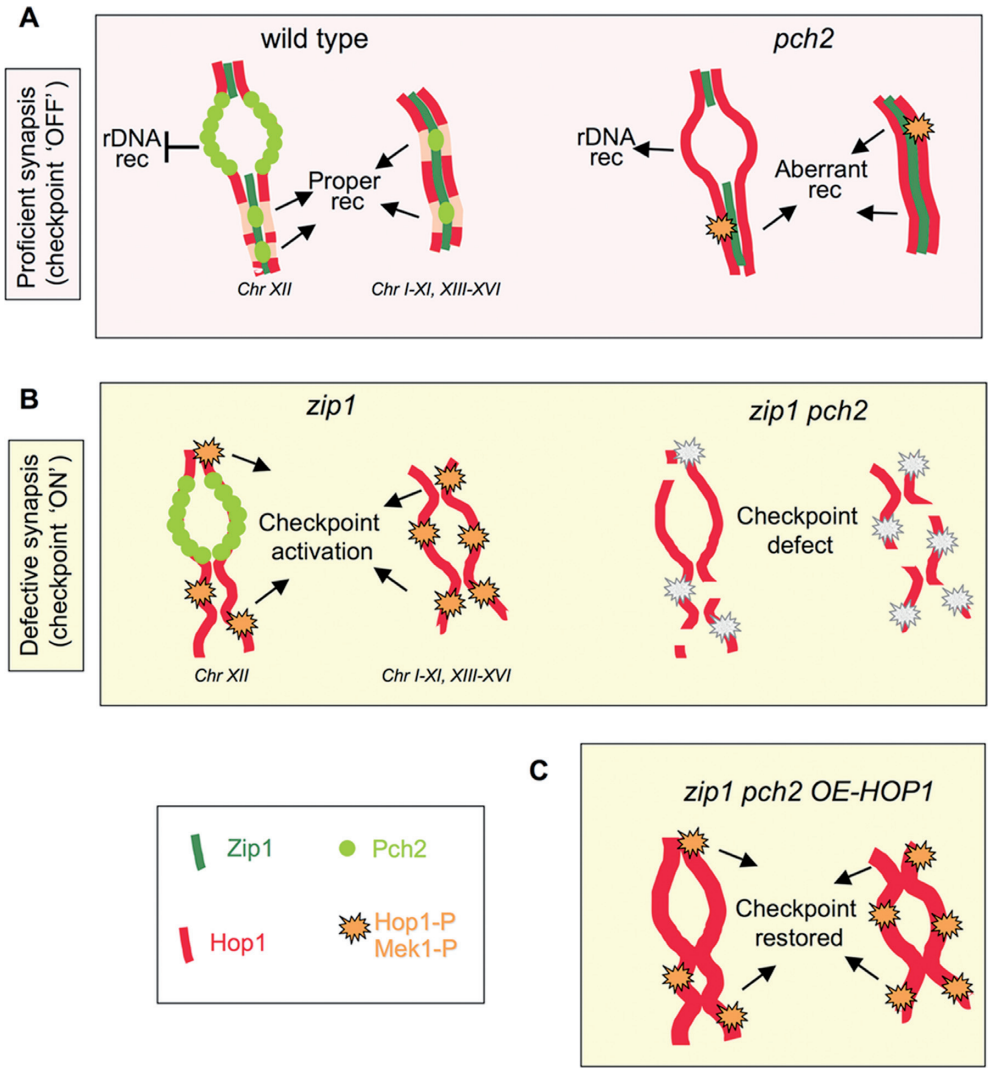

Figure 11. A model for Pch2 checkpoint function. (**A**) In unperturbed wild-type meiosis, nucleolar Pch2 excludes Hop1 from the rDNA preventing recombination at this chromosome XII array. In turn, chromosomal Pch2 dictates Hop1 discontinuous axis distribution sustaining proper synapsis and recombination. In the *pch2* single mutant, Hop1 localizes to the nucleolar region and unwanted rDNA recombination occurs. Hop1 is also more abundant on chromosome axes disturbing normal recombination events that slightly increase Hop1-T318 phosphorylation. Nevertheless, most recombination defects of the *pch2* mutant are only evident when DSBs are limiting (28,56). (**B**) In the synapsis-deficient *zip1* mutant, Pch2 is absent from the chromosomes and concentrated in the rDNA. This configuration supports continuous distribution of Hop1 along unsynapsed axes and high levels of Hop1-T318 phosphorylation relaying the checkpoint signal to Mek1 activation. When *PCH2* is deleted (or the ATPase inactivated), Hop1 loading and phosphorylation is impaired leading to inoperative checkpoint. (**C**) Despite the weakened Hop1/Mek1 activation, *HOP1* overexpression in *zip1 pch2* provides enough protein to restore high levels of global Hop1 phosphorylation and reinstate checkpoint function (see text for additional details).

at later time points at least a fraction of the cells resume cell cycle progression and complete the meiotic divisions. At the molecular level this meiotic resumption is manifested by an eventual decrease in Hop1-T318 phosphorylation and reduced Mek1 signaling (Figure 6). We found that the *zip1 pph3* double mutant displays more persistent Mek1 activation and a tighter meiotic block arguing that, indeed, PP4 is crucial for deactivation and/or adaptation of the *zip1*-induced checkpoint. However, we have observed that the absence of PP4 function only confers a partial restoration of Hop1-T318 phosphorylation in *zip1 pch2*, indicating that Pch2 does not primarily act on this phosphatase or that PP4 may not be the only phosphatase capable of dephosphorylating Hop1-T318. The simplest interpretation of this result is that the low levels of Hop1-T318 phosphorylation in *zip1 pch2*, perhaps resulting from crippled Mec1/Tel1 function, are increased to some extent when the inhibitory action of PP4 is removed. Regardless of the identity of the direct target of Pch2, these observations confirm that the crucial role of Pch2 in the *zip1* checkpoint is the fine regulation of Hop1-T318 phosphorylation status. In fact, these experiments reveal that manipulation of Hop1 phosphorylation in *zip1 pch2* by other means, such as deleting *PPH3*, but without altering *HOP1* expression levels also has an impact on the checkpoint.

Relevance of the ATPase activity for Pch2 checkpoint function

Recent *in vitro* analyses of the *S. cerevisiae* Pch2 protein have elegantly demonstrated that Pch2 is indeed an AAA+ ATPase that assembles into hexameric rings in the presence of nucleotides (63). That study also assessed the *in vivo* meiotic impact of mutations in the ATPase domain of Pch2 by determining the decrease in spore viability resulting from combining a *csm4* mutant with the loss of Pch2 function. However, since Csm4 is involved in chromosome movement during prophase driven by telomere attachment to the nuclear envelope (68–70) and there are multiple meiotic processes influenced by Pch2, the physiological basis of this synthetic spore viability defect with *csm4* is not obvious. Therefore, we analyzed the contribution of the ATPase activity to the well-established Pch2 role in the *zip1*-induced checkpoint. In contrast to the intermediate phenotype reported for the *pch2-K320A* mutant based on its combination with *csm4* (63), we show here that mutants defective in either ATP binding site (*pch2-K320A*) or ATP hydrolysis (*pch2-E399Q*) phenocopy the *pch2* deletion mutant for the checkpoint defect indicating that both activities are absolutely required for Pch2 checkpoint function. However, we observe a striking difference between both catalytically-inactive proteins in terms of localization on meiotic chromosome spreads. Whereas Pch2-E399Q displays the normal accumulation at the rDNA region on chromosome XII and some fainter interstitial chromosomal foci, the Pch2-K320A version completely fails to bind to the chromosomes. We found that the Pch2-K320A mutation preventing ATP binding compromises the integrity of the hexameric ring; this observation could explain the defect in localization, which may require an intact complex for its correct targeting. On the other hand, Pch2-E399Q does localize like the wild-type Pch2 protein; however, in contrast to Pch2, which does not overlap with Hop1 staining, the Pch2-E399Q version displays extensive colocalization with Hop1 both at chromosomal foci (in otherwise wild-type strains) and the rDNA, where Hop1 fails to be excluded in this mutant. These observations are consistent with the notion that Pch2/Trip13 utilizes the forces generated from ATP hydrolysis to displace or reorganize HORMA domain proteins, such as Hop1/HORMAD1 in meiosis or MAD2 in the SAC response (71). The effect of mammalian Trip13 on the conformational change of MAD2 is exerted with the help of the p31 adaptor (35). To determine whether yeast Pch2 requires additional cofactors or adaptors to disassemble Hop1 from meiotic chromosomes awaits further investigation. Nevertheless, *in vitro* assays show that purified Pch2 can directly alter Hop1 DNA binding properties (63).

A dual role for Pch2 on Hop1 regulation?

The Pch2 protein is predominantly found in the unsynapsed region of chromosome XII, which lacks Zip1 and Hop1, preventing recombination within the rDNA array (18,26). In addition, Pch2 is also present in SC-associated chromosomal foci promoting an alternating pattern of Zip1 and Hop1 during SC development (21). Curiously, whereas in yeast SK1 strains Pch2 chromosomal foci are conspicuous (22), in the BR strains used in this work, most Pch2 is detected in the nucleolar area with SC-associated foci showing a much weaker staining ((18); Figure 9 and Supplementary Figure S6). Importantly, in the synapsis-deficient *zip1* mutant, the chromosomal Pch2 protein is no longer detectable and it is exclusively observed in the rDNA ((18); Figure 9). These observations suggest that two populations of Pch2 with different requirements for chromosome binding may exist: the nucleolar Pch2 pool, which does not require Zip1 for being targeted to the unsynapsed rDNA array and the interstitial chromosomal Pch2 protein, which is likely dependent on Zip1 assembly for its localization. Both pools of Pch2 possess the ability to displace Hop1 from the chromosome axes because Hop1 is more abundant along the SC and accumulates in the rDNA region in *pch2* mutants lacking ATPase activity. However, since Pch2 function is critically required for the *zip1*-induced meiotic arrest, the fact that in the *zip1* mutant Pch2 is only present at the rDNA location implies that the nucleolar Pch2 protein is responsible for the checkpoint function by sustaining high levels of Hop1-T318 phosphorylation in response to synapsis defects (Figure 11).

How can Pch2 control Hop1 phosphorylation from the nucleolus where, precisely, Hop1 is excluded? A role for nucleolar proteins in the control of cell cycle events is a well-documented phenomenon (72). Perhaps, the most paradigmatic example is the regulation of mitotic exit in budding yeast by the FEAR/MEN pathways orchestrating the release of the Cdc14 phosphatase from the nucleolus during anaphase (73–75). In a similar scenario it is possible that, when synapsis is defective, Pch2 traps in the nucleolus a crucial regulator required for exit from pachytene. Upon synapsis completion this factor would be released promoting entry into meiosis I. The PP4 phosphatase was a good candidate to meet these requirements because it promotes Hop1-T318 dephosphorylation and, hence, checkpoint inactivation, but our results indicate that Pch2 does not primarily acts via PP4 regulation (see above). In addition, during meiotic prophase PP4 appears to be localized at centromeres, not the nucleolus (76). We have also tested another phosphatase, PP1, which displays nucleolar localization at least during some stages of the cell cycle (77). In contrast to a previous study reporting a role for Glc7 -the catalytic subunit of PP1- in reversing Mek1 activation (38), we have found a minimal, if any, effect of either a *glc7-T152K* allele or a meiotic-depletion *glc7-md* mutant in Hop1 or Mek1 phosphorylation, and no evidence of functional relationship between Glc7 and Pch2 (AL and PSS, unpublished results). Alternatively, nucleolar Pch2 could control the localization of a Mec1 activator in response to synapsis defects. Since the N-terminal domain of Xrs2 physically interacts with Pch2 (29), it will be interesting to further investigate how this interaction impinges on Hop1 regulation in response to SC defects.

In sum, our results are consistent with a differential regulation of Hop1 by chromosomal and nucleolar Pch2 in a wild-type (checkpoint OFF) versus a *zip1* (checkpoint ON) situation (Figure 11). The identification of Pch2 co-factors that may modulate its action on Hop1 depending on the specific chromosomal context or synapsis status will help to elucidate the basis of this differential effect.

SUPPLEMENTARY DATA

Supplementary Data are available at NAR Online.

ACKNOWLEDGEMENTS

The authors are grateful to Rodrigo Bermejo for a *pph3Δ* strain, Félix Prado for *delitto perfetto* reagents, Jesús Carballo for the phospho-Hop1-T318 antibody, Olga Calvo for the anti-GFP antibody, and Amy MacQueen and Shirleen Roeder for plasmids and strains. We also thank Vanessa Silva Dutra de Carvalho for help with some experiments, Isabel Acosta for technical assistance and Jesús Carballo and Andrés Clemente for helpful discussions and ideas.

FUNDING

Ministry of Economy and Competitiveness (MINECO) of Spain [BFU2012-35748 and BFU2015-65417-R]; Predoctoral contract from the University of Salamanca (Spain) (to E.H.); Predoctoral fellowship (JAE-predoc) (to D.O.) and a postdoctoral fellowship (JAE-doc) (to S.C.) from the CSIC (Spain). Funding for open access charge: Ministry of Economy and Competitiveness (MINECO) of Spain [BFU2012-35748 and BFU2015-65417-R].
Conflict of interest statement. None declared.

REFERENCES

1. MacQueen,A.J. and Hochwagen,A. (2011) Checkpoint mechanisms: the puppet masters of meiotic prophase. *Trends Cell. Biol.*, **21**, 393–400.
2. Roeder,G.S. and Bailis,J.M. (2000) The pachytene checkpoint. *Trends Genet.*, **16**, 395–403.
3. Subramanian,V.V. and Hochwagen,A. (2014) The meiotic checkpoint network: step-by-step through Meiotic Prophase. *Cold Spring Harb. Perspect. Biol.*, **6**, e1002369.
4. Schwacha,A. and Kleckner,N. (1997) Interhomolog bias during meiotic recombination: meiotic functions promote a highly differentiated interhomolog-only pathway. *Cell*, **90**, 1123–1135.
5. Sym,M., Engebrecht,J.A. and Roeder,G.S. (1993) ZIP1 is a synaptonemal complex protein required for meiotic chromosome synapsis. *Cell*, **72**, 365–378.
6. Carballo,J.A., Johnson,A.L., Sedgwick,S.G. and Cha,R.S. (2008) Phosphorylation of the axial element protein Hop1 by Mec1/Tel1 ensures meiotic interhomolog recombination. *Cell*, **132**, 758–770.
7. Chuang,C.N., Cheng,Y.H. and Wang,T.F. (2012) Mek1 stabilizes Hop1-Thr318 phosphorylation to promote interhomolog recombination and checkpoint responses during yeast meiosis. *Nucleic Acids Res.*, **40**, 11416–11427.
8. Ontoso,D., Acosta,I., van Leeuwen,F., Freire,R. and San-Segundo,P.A. (2013) Dot1-dependent histone H3K79 methylation promotes activation of the Mek1 meiotic checkpoint effector kinase by regulating the Hop1 adaptor. *PLoS Genet.*, **9**, e1003262.
9. Niu,H., Li,X., Job,E., Park,C., Moazed,D., Gygi,S.P. and Hollingsworth,N.M. (2007) Mek1 kinase is regulated to suppress double-strand break repair between sister chromatids during budding yeast meiosis. *Mol. Cell. Biol.*, **27**, 5456–5467.
10. Niu,H., Wan,L., Baumgartner,B., Schaefer,D., Loidl,J. and Hollingsworth,N.M. (2005) Partner choice during meiosis is regulated by Hop1-promoted dimerization of Mek1. *Mol. Biol. Cell*, **16**, 5804–5818.
11. Terentyev,Y., Johnson,R., Neale,M.J., Khisroon,M., Bishop-Bailey,A. and Goldman,A.S. (2010) Evidence that MEK1 positively promotes interhomologue double-strand break repair. *Nucleic Acids Res.*, **38**, 4349–4360.
12. Niu,H., Wan,L., Busygina,V., Kwon,Y., Allen,J.A., Li,X., Kunz,R.C., Kubota,K., Wang,B., Sung,P. *et al.* (2009) Regulation of meiotic recombination via Mek1-mediated Rad54 phosphorylation. *Mol. Cell*, **36**, 393–404.
13. Acosta,I., Ontoso,D. and San-Segundo,P.A. (2011) The budding yeast polo-like kinase Cdc5 regulates the Ndt80 branch of the meiotic recombination checkpoint pathway. *Mol. Biol. Cell*, **22**, 3478–3490.
14. Leu,J.Y. and Roeder,G.S. (1999) The pachytene checkpoint in *S. cerevisiae* depends on Swe1-mediated phosphorylation of the cyclin-dependent kinase Cdc28. *Mol. Cell*, **4**, 805–814.
15. Tung,K.S., Hong,E.J. and Roeder,G.S. (2000) The pachytene checkpoint prevents accumulation and phosphorylation of the meiosis-specific transcription factor Ndt80. *Proc. Natl. Acad. Sci. U.S.A.*, **97**, 12187–12192.
16. Wang,Y., Chang,C.Y., Wu,J.F. and Tung,K.S. (2011) Nuclear localization of the meiosis-specific transcription factor Ndt80 is regulated by the pachytene checkpoint. *Mol. Biol. Cell*, **22**, 1878–1886.
17. Eichinger,C.S. and Jentsch,S. (2010) Synaptonemal complex formation and meiotic checkpoint signaling are linked to the lateral element protein Red1. *Proc. Natl. Acad. Sci. U.S.A.*, **107**, 11370–11375.
18. San-Segundo,P.A. and Roeder,G.S. (1999) Pch2 links chromatin silencing to meiotic checkpoint control. *Cell*, **97**, 313–324.
19. San-Segundo,P.A. and Roeder,G.S. (2000) Role for the silencing protein Dot1 in meiotic checkpoint control. *Mol. Biol. Cell*, **11**, 3601–3615.
20. Wu,H.Y. and Burgess,S.M. (2006) Two distinct surveillance mechanisms monitor meiotic chromosome metabolism in budding yeast. *Curr. Biol.*, **16**, 2473–2479.
21. Borner,G.V., Barot,A. and Kleckner,N. (2008) Yeast Pch2 promotes domainal axis organization, timely recombination progression, and arrest of defective recombinosomes during meiosis. *Proc. Natl. Acad. Sci. U.S.A.*, **105**, 3327–3332.
22. Joshi,N., Barot,A., Jamison,C. and Borner,G.V. (2009) Pch2 links chromosome axis remodeling at future crossover sites and crossover distribution during yeast meiosis. *PLoS Genet.*, **5**, e1000557.
23. Wojtasz,L., Daniel,K., Roig,I., Bolcun-Filas,E., Xu,H., Boonsanay,V., Eckmann,C.R., Cooke,H.J., Jasin,M., Keeney,S. *et al.* (2009) Mouse HORMAD1 and HORMAD2, two conserved meiotic chromosomal proteins, are depleted from synapsed chromosome axes with the help of TRIP13 AAA-ATPase. *PLoS Genet.*, **5**, e1000702.
24. Farmer,S., Hong,E.J., Leung,W.K., Argunhan,B., Terentyev,Y., Humphryes,N., Toyoizumi,H. and Tsubouchi,H. (2012) Budding yeast Pch2, a widely conserved meiotic protein, is involved in the initiation of meiotic recombination. *PLoS One*, **7**, e39724.
25. Roig,I., Dowdle,J.A., Toth,A., de Rooij,D.G., Jasin,M. and Keeney,S. (2010) Mouse TRIP13/PCH2 is required for recombination and normal higher-order chromosome structure during meiosis. *PLoS Genet.*, **6**, e1001062.
26. Vader,G., Blitzblau,H.G., Tame,M.A., Falk,J.E., Curtin,L. and Hochwagen,A. (2011) Protection of repetitive DNA borders from self-induced meiotic instability. *Nature*, **477**, 115–119.
27. Zanders,S. and Alani,E. (2009) The *pch2Δ*; mutation in baker's yeast alters meiotic crossover levels and confers a defect in crossover interference. *PLoS Genet.*, **5**, e1000571.
28. Zanders,S., Sonntag Brown,M., Chen,C. and Alani,E. (2011) Pch2 modulates chromatid partner choice during meiotic double-strand break repair in *Saccharomyces cerevisiae*. *Genetics*, **188**, 511–521.
29. Ho,H.C. and Burgess,S.M. (2011) Pch2 acts through Xrs2 and Tel1/ATM to modulate interhomolog bias and checkpoint function during meiosis. *PLoS Genet.*, **7**, e1002351.
30. Eytan,E., Wang,K., Miniowitz-Shemtov,S., Sitry-Shevah,D., Kaisari,S., Yen,T.J., Liu,S.T. and Hershko,A. (2014) Disassembly of mitotic checkpoint complexes by the joint action of the AAA-ATPase TRIP13 and p31(comet). *Proc. Natl. Acad. Sci. U.S.A.*, **111**, 12019–12024.
31. Nelson,C.R., Hwang,T., Chen,P.H. and Bhalla,N. (2015) TRIP13^{PCH-2} promotes Mad2 localization to unattached kinetochores in the spindle checkpoint response. *J. Cell Biol.*, **211**, 503–516.
32. Wang,K., Sturt-Gillespie,B., Hittle,J.C., Macdonald,D., Chan,G.K., Yen,T.J. and Liu,S.T. (2014) Thyroid hormone receptor interacting protein 13 (TRIP13) AAA-ATPase is a novel mitotic checkpoint-silencing protein. *J. Biol. Chem.*, **289**, 23928–23937.

33. Banerjee,R., Russo,N., Liu,M., Basrur,V., Bellile,E., Palanisamy,N., Scanlon,C.S., van Tubergen,E., Inglehart,R.C., Metwally,T. *et al.* (2014) TRIP13 promotes error-prone nonhomologous end joining and induces chemoresistance in head and neck cancer. *Nat. Commun.*, **5**, 4527.
34. Martin,K.J., Patrick,D.R., Bissell,M.J. and Fournier,M.V. (2008) Prognostic breast cancer signature identified from 3D culture model accurately predicts clinical outcome across independent datasets. *PLoS One*, **3**, e2994.
35. Ye,Q., Rosenberg,S.C., Moeller,A., Speir,J.A., Su,T.Y. and Corbett,K.D. (2015) TRIP13 is a protein-remodeling AAA+ ATPase that catalyzes MAD2 conformation switching. *Elife*, **4**, e07367.
36. Rockmill,B. and Roeder,G.S. (1990) Meiosis in asynaptic yeast. *Genetics*, **126**, 563–574.
37. Agarwal,S. and Roeder,G.S. (2000) Zip3 provides a link between recombination enzymes and synaptonemal complex proteins. *Cell*, **102**, 245–255.
38. Bailis,J.M. and Roeder,G.S. (2000) Pachytene exit controlled by reversal of Mek1-dependent phosphorylation. *Cell*, **101**, 211–221.
39. Humphryes,N., Leung,W.K., Argunhan,B., Terentyev,Y., Dvorackova,M. and Tsubouchi,H. (2013) The Ecm11-Gmc2 complex promotes synaptonemal complex formation through assembly of transverse filaments in budding yeast. *PLoS Genet.*, **9**, e1003194.
40. Goldstein,A.L. and McCusker,J.H. (1999) Three new dominant drug resistance cassettes for gene disruption in *Saccharomyces cerevisiae*. *Yeast*, **15**, 1541–1553.
41. Voth,W.P., Jiang,Y.W. and Stillman,D.J. (2003) New 'marker swap' plasmids for converting selectable markers on budding yeast gene disruptions and plasmids. *Yeast*, **20**, 985–993.
42. Schneider,B.L., Seufert,W., Steiner,B., Yang,Q.H. and Futcher,A.B. (1995) Use of polymerase chain reaction epitope tagging for protein tagging in *Saccharomyces cerevisiae*. *Yeast*, **11**, 1265–1274.
43. Refolio,E., Cavero,S., Marcon,E., Freire,R. and San-Segundo,P.A. (2011) The Ddc2/ATRIP checkpoint protein monitors meiotic recombination intermediates. *J. Cell Sci.*, **124**, 2488–2500.
44. Stuckey,S., Mukherjee,K. and Storici,F. (2011) In vivo site-specific mutagenesis and gene collage using the delitto perfetto system in yeast *Saccharomyces cerevisiae*. *Methods Mol. Biol.*, **745**, 173–191.
45. Hollingsworth,N.M. and Ponte,L. (1997) Genetic interactions between *HOP1*, *RED1* and *MEK1* suggest that *MEK1* regulates assembly of axial element components during meiosis in the yeast *Saccharomyces cerevisiae*. *Genetics*, **147**, 33–42.
46. Carlson,M. and Botstein,D. (1982) Two differentially regulated mRNAs with different 5′ ends encode secreted with intracellular forms of yeast invertase. *Cell*, **28**, 145–154.
47. Rockmill,B. (2009) Chromosome spreading and immunofluorescence methods in *Saccharomyes cerevisiae*. *Methods Mol. Biol.*, **558**, 3–13.
48. Santos,B., Duran,A. and Valdivieso,M.H. (1997) *CHS5*, a gene involved in chitin synthesis and mating in *Saccharomyces cerevisiae*. *Mol. Cell. Biol.*, **17**, 2485–2496.
49. Xu,L., Ajimura,M., Padmore,R., Klein,C. and Kleckner,N. (1995) NDT80, a meiosis-specific gene required for exit from pachytene in *Saccharomyces cerevisiae*. *Mol. Cell. Biol.*, **15**, 6572–6581.
50. Collart,M.A. (1996) The *NOT*, *SPT3*, and *MOT1* genes functionally interact to regulate transcription at core promoters. *Mol. Cell. Biol.*, **16**, 6668–6676.
51. Lydall,D., Nikolsky,Y., Bishop,D.K. and Weinert,T. (1996) A meiotic recombination checkpoint controlled by mitotic checkpoint genes. *Nature*, **383**, 840–843.
52. Majka,J. and Burgers,P.M. (2007) Clamping the Mec1/ATR checkpoint kinase into action. *Cell Cycle*, **6**, 1157–1160.
53. Hong,E.J. and Roeder,G.S. (2002) A role for Ddc1 in signaling meiotic double-strand breaks at the pachytene checkpoint. *Genes Dev.*, **16**, 363–376.
54. Govin,J., Dorsey,J., Gaucher,J., Rousseaux,S., Khochbin,S. and Berger,S.L. (2010) Systematic screen reveals new functional dynamics of histones H3 and H4 during gametogenesis. *Genes Dev.*, **24**, 1772–1786.
55. Smith,A.V. and Roeder,G.S. (1997) The yeast Red1 protein localizes to the cores of meiotic chromosomes. *J. Cell Biol.*, **136**, 957–967.
56. Joshi,N., Brown,M.S., Bishop,D.K. and Borner,G.V. (2015) Gradual implementation of the meiotic recombination program via checkpoint pathways controlled by global DSB levels. *Mol. Cell*, **57**, 797–811.
57. Arbel,A., Zenvirth,D. and Simchen,G. (1999) Sister chromatid-based DNA repair is mediated by RAD54, not by DMC1 or TID1. *EMBO J.*, **18**, 2648–2658.
58. Liu,Y., Gaines,W.A., Callender,T., Busygina,V., Oke,A., Sung,P., Fung,J.C. and Hollingsworth,N.M. (2014) Down-regulation of Rad51 activity during meiosis in yeast prevents competition with Dmc1 for repair of double-strand breaks. *PLoS Genet.*, **10**, e1004005.
59. Raschle,M., Van Komen,S., Chi,P., Ellenberger,T. and Sung,P. (2004) Multiple interactions with the Rad51 recombinase govern the homologous recombination function of Rad54. *J. Biol. Chem.*, **279**, 51973–51980.
60. Cheng,C.H., Lo,Y.H., Liang,S.S., Ti,S.C., Lin,F.M., Yeh,C.H., Huang,H.Y. and Wang,T.F. (2006) SUMO modifications control assembly of synaptonemal complex and polycomplex in meiosis of *Saccharomyces cerevisiae*. *Genes Dev.*, **20**, 2067–2081.
61. Lynn,A., Soucek,R. and Borner,G.V. (2007) ZMM proteins during meiosis: crossover artists at work. *Chromosome Res.*, **15**, 591–605.
62. Voelkel-Meiman,K., Taylor,L.F., Mukherjee,P., Humphryes,N., Tsubouchi,H. and Macqueen,A.J. (2013) SUMO localizes to the central element of synaptonemal complex and is required for the full synapsis of meiotic chromosomes in budding yeast. *PLoS Genet.*, **9**, e1003837.
63. Chen,C., Jomaa,A., Ortega,J. and Alani,E.E. (2014) Pch2 is a hexameric ring ATPase that remodels the chromosome axis protein Hop1. *Proc. Natl. Acad. Sci. U.S.A.*, **111**, E44–E53.
64. Hanson,P.I. and Whiteheart,S.W. (2005) AAA+ proteins: have engine, will work. *Nat. Rev. Mol. Cell. Biol.*, **6**, 519–529.
65. Wendler,P., Ciniawsky,S., Kock,M. and Kube,S. (2012) Structure and function of the AAA+ nucleotide binding pocket. *Biochim. Biophys. Acta*, **1823**, 2–14.
66. Lin,F.M., Lai,Y.J., Shen,H.J., Cheng,Y.H. and Wang,T.F. (2010) Yeast axial-element protein, Red1, binds SUMO chains to promote meiotic interhomologue recombination and chromosome synapsis. *EMBO J.*, **29**, 586–596.
67. Lo,Y.H., Chuang,C.N. and Wang,T.F. (2014) Pch2 prevents Mec1/Tel1-mediated Hop1 phosphorylation occurring independently of Red1 in budding yeast meiosis. *PLoS One*, **9**, e85687.
68. Conrad,M.N., Lee,C.Y., Chao,G., Shinohara,M., Kosaka,H., Shinohara,A., Conchello,J.A. and Dresser,M.E. (2008) Rapid telomere movement in meiotic prophase is promoted by NDJ1, MPS3, and CSM4 and is modulated by recombination. *Cell*, **133**, 1175–1187.
69. Kosaka,H., Shinohara,M. and Shinohara,A. (2008) Csm4-dependent telomere movement on nuclear envelope promotes meiotic recombination. *PLoS Genet.*, **4**, e1000196.
70. Wanat,J.J., Kim,K.P., Koszul,R., Zanders,S., Weiner,B., Kleckner,N. and Alani,E. (2008) Csm4, in collaboration with Ndj1, mediates telomere-led chromosome dynamics and recombination during yeast meiosis. *PLoS Genet.*, **4**, e1000188.
71. Vader,G. (2015) Pch2(TRIP13): controlling cell division through regulation of HORMA domains. *Chromosoma*, **124**, 333–339.
72. Pederson,T. (2011) The nucleolus. *Cold Spring Harb. Perspect. Biol.*, **3**, a000638.
73. Shou,W., Seol,J.H., Shevchenko,A., Baskerville,C., Moazed,D., Chen,Z.W., Jang,J., Charbonneau,H. and Deshaies,R.J. (1999) Exit from mitosis is triggered by Tem1-dependent release of the protein phosphatase Cdc14 from nucleolar RENT complex. *Cell*, **97**, 233–244.
74. Stegmeier,F., Visintin,R. and Amon,A. (2002) Separase, polo kinase, the kinetochore protein Slk19, and Spo12 function in a network that controls Cdc14 localization during early anaphase. *Cell*, **108**, 207–220.
75. Visintin,R., Hwang,E.S. and Amon,A. (1999) Cfi1 prevents premature exit from mitosis by anchoring Cdc14 phosphatase in the nucleolus. *Nature*, **398**, 818–823.
76. Falk,J.E., Chan,A.C., Hoffmann,E. and Hochwagen,A. (2010) A Mec1- and PP4-dependent checkpoint couples centromere pairing to meiotic recombination. *Dev. Cell*, **19**, 599–611.
77. Bloecher,A. and Tatchell,K. (2000) Dynamic localization of protein phosphatase type 1 in the mitotic cell cycle of *Saccharomyces cerevisiae*. *J. Cell Biol.*, **149**, 125–140.

SUPPLEMENTARY DATA

The Pch2 AAA+ ATPase promotes phosphorylation of the Hop1 meiotic checkpoint adaptor in response to synaptonemal complex defects

Esther Herruzo[1], David Ontoso[1], Sara González-Arranz[1], Santiago Cavero[1], Ana Lechuga[1] and Pedro A. San-Segundo[1,*]

[1] Instituto de Biología Funcional y Genómica. Consejo Superior de Investigaciones Científicas and University of Salamanca, 37007 Salamanca, Spain

[*] To whom correspondence should be addressed. Tel: +34 923294902; Fax: +34 923224876; Email: pedross@usal.es

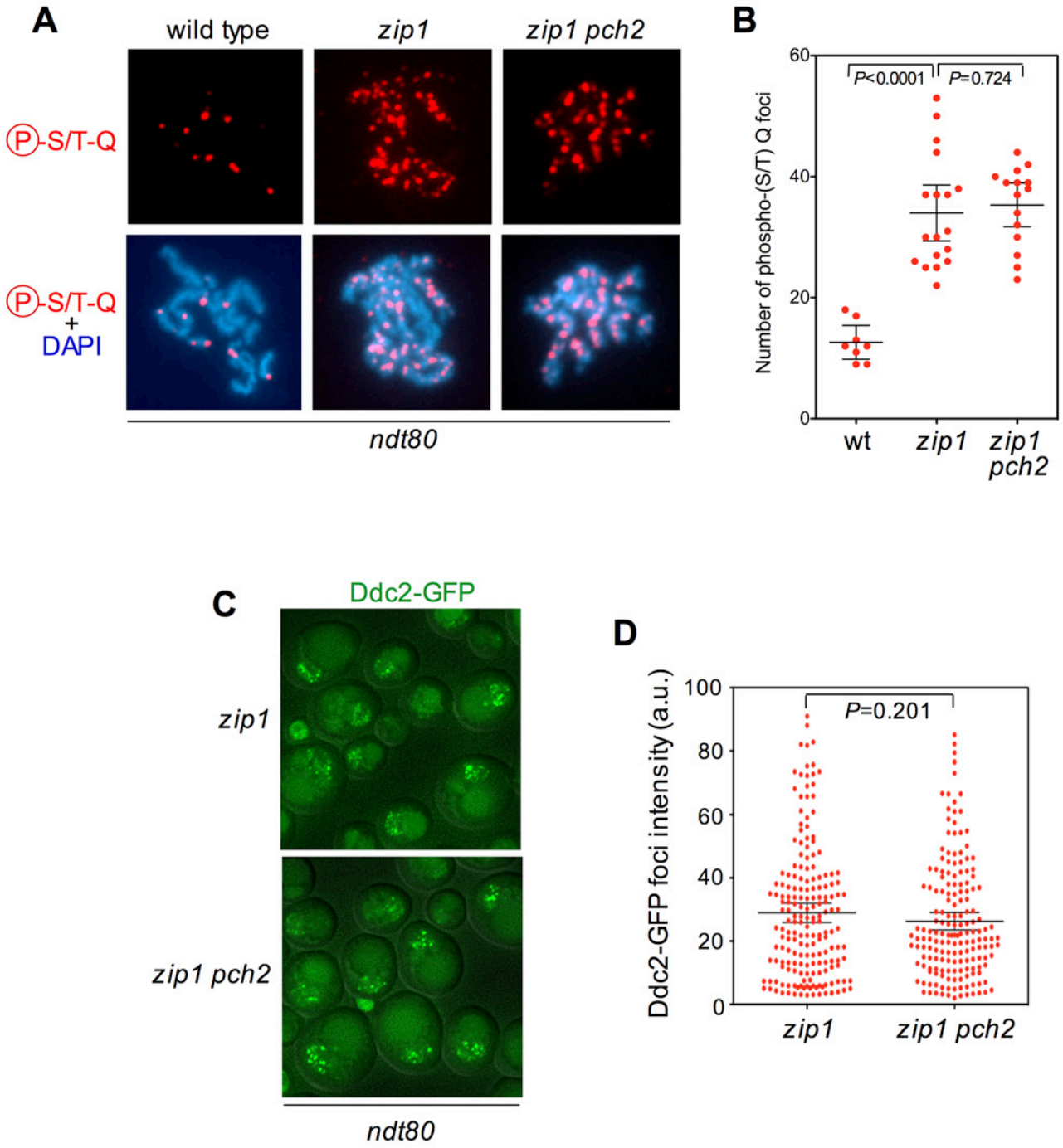

Figure S1. Pch2 does not affect widespread Mec1 signaling. (A) Immunofluorescence of meiotic chromosomes stained with anti-phospho-S/T-Q antibodies (red) and DAPI (blue). Representative nuclei are shown. (B) Quantification on the number of phospho-S/T-Q foci per nucleus. (C) Representative images of Ddc2-GFP foci formation in live cells. Maximum projection images of 10-plane stacks are shown. (D) Quantification of the Ddc2-GFP signal. Strains are: DP424 (wild type), DP460 (*zip1*) and DP1251 (*zip1 pch2*). Prophase-arrested *ndt80* cells were analyzed 24 h after meiotic induction.

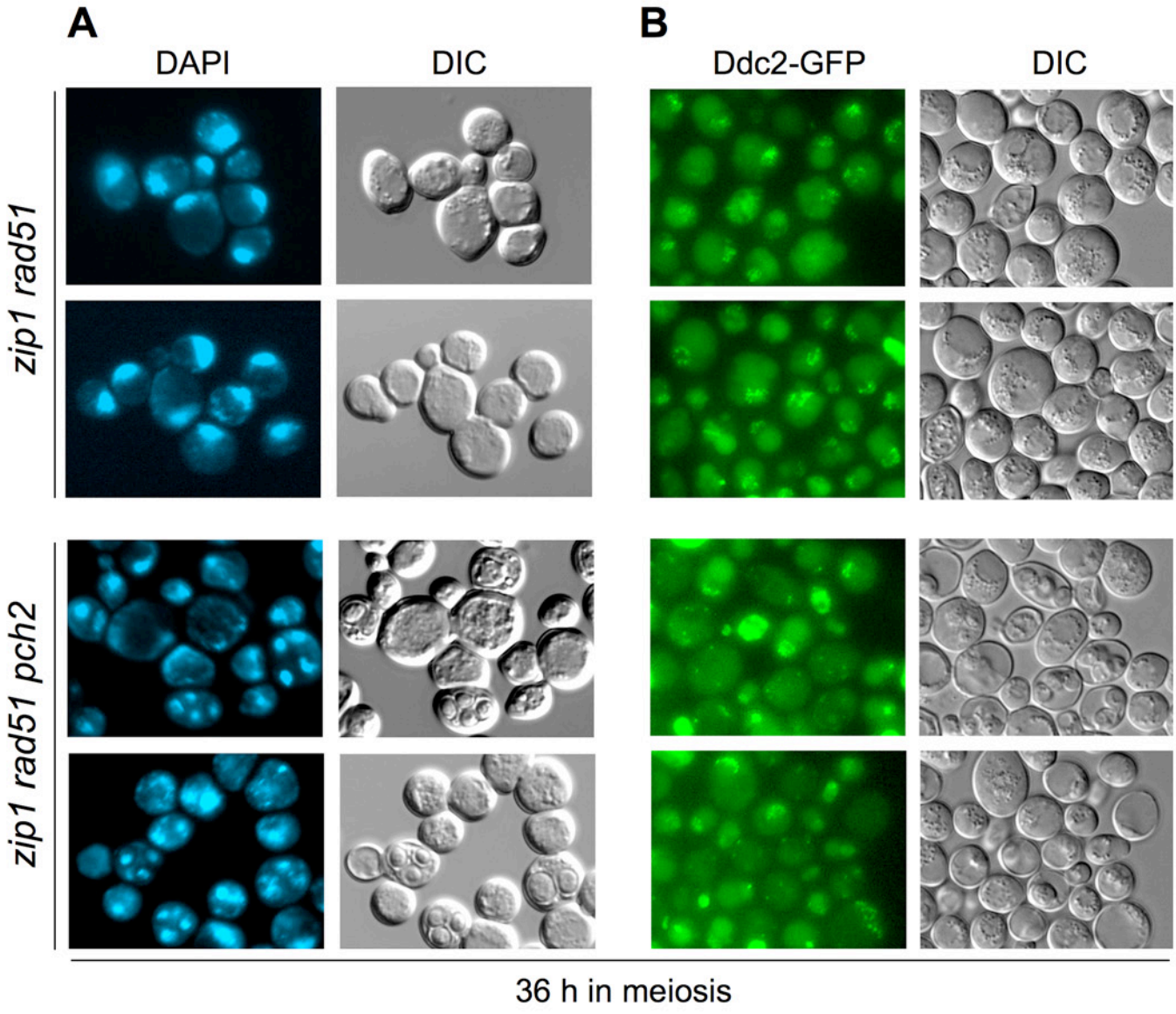

Figure S2. Representative images of meiotic nuclear divisions and Ddc2 foci detection for the analyses presented in Figure 7B and 7C.

(A) Aliquots from meiotic cultures were taken a different time points, fixed with ethanol and stained with DAPI to monitor meiotic nuclear divisions. (B) Independent aliquots from the same cultures were directly analyzed by live-cell fluorescence microscopy to detect Ddc2-GFP. Two different representative fields from the 36 h time point of the *zip1 rad51* (DP1381) and *zip1 rad51 pch2* (DP1382) strains are shown for DAPI and other two representative fields for Ddc2-GFP. The corresponding differential interference contrast (DIC) images are also presented.

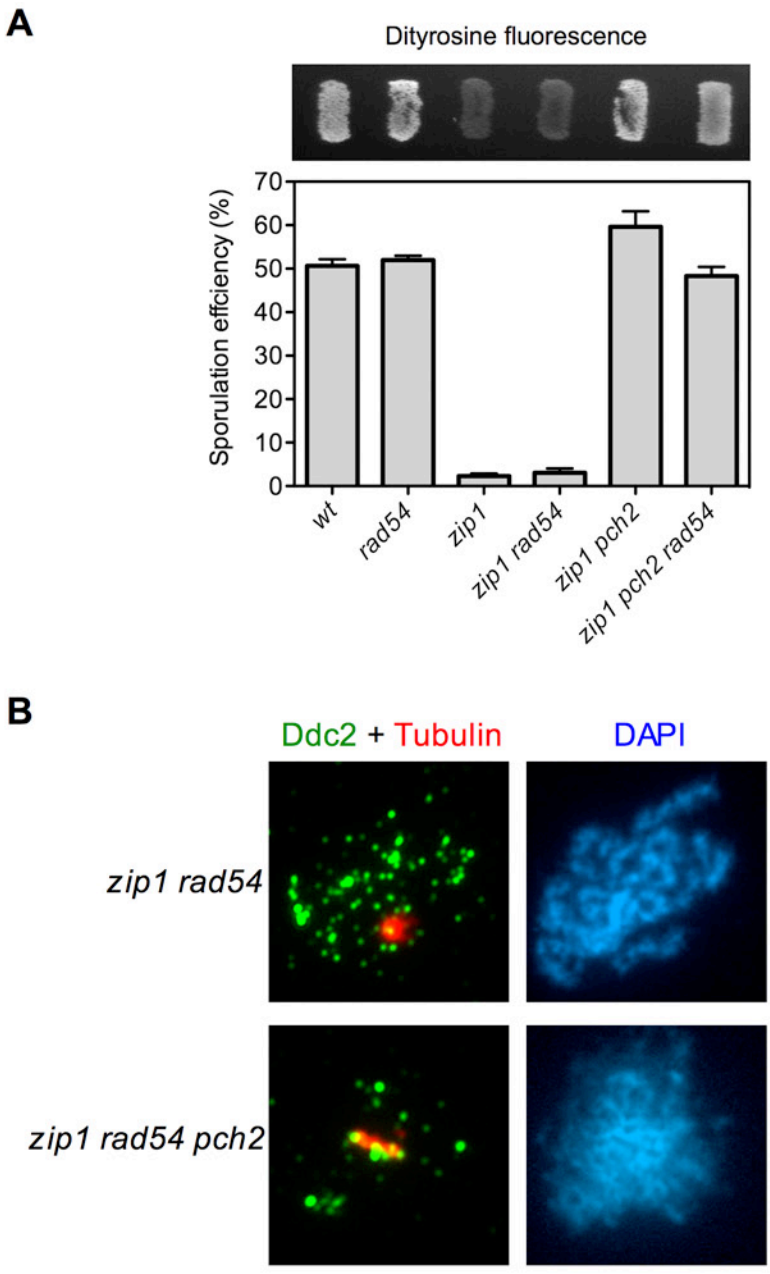

Figure S3. Deletion of *RAD54* does not prevent meiotic progression in *zip1 pch2*. (A) Dityrosine fluorescence and sporulation efficiency after three days on sporulation plates. Strains are: DP421 (wild type), DP1168 (*rad54*), DP422 (*zip1*), DP1169 (*zip1 rad54*), DP1161 (*zip1 pch2*) and DP1171 (*zip1 pch2 rad54*). (B) Immunofluorescence of spread meiotic chromosomes stained with anti-tubulin (red), anti-GFP antibodies to detect Ddc2 (green) and DAPI (blue). A representative prophase nucleus from *zip1 rad54* (DP1378) and a representative meiosis I nucleus from *zip1 rad54 pch2* (DP1387) are shown. Spreads were prepared 24 h after meiosis induction.

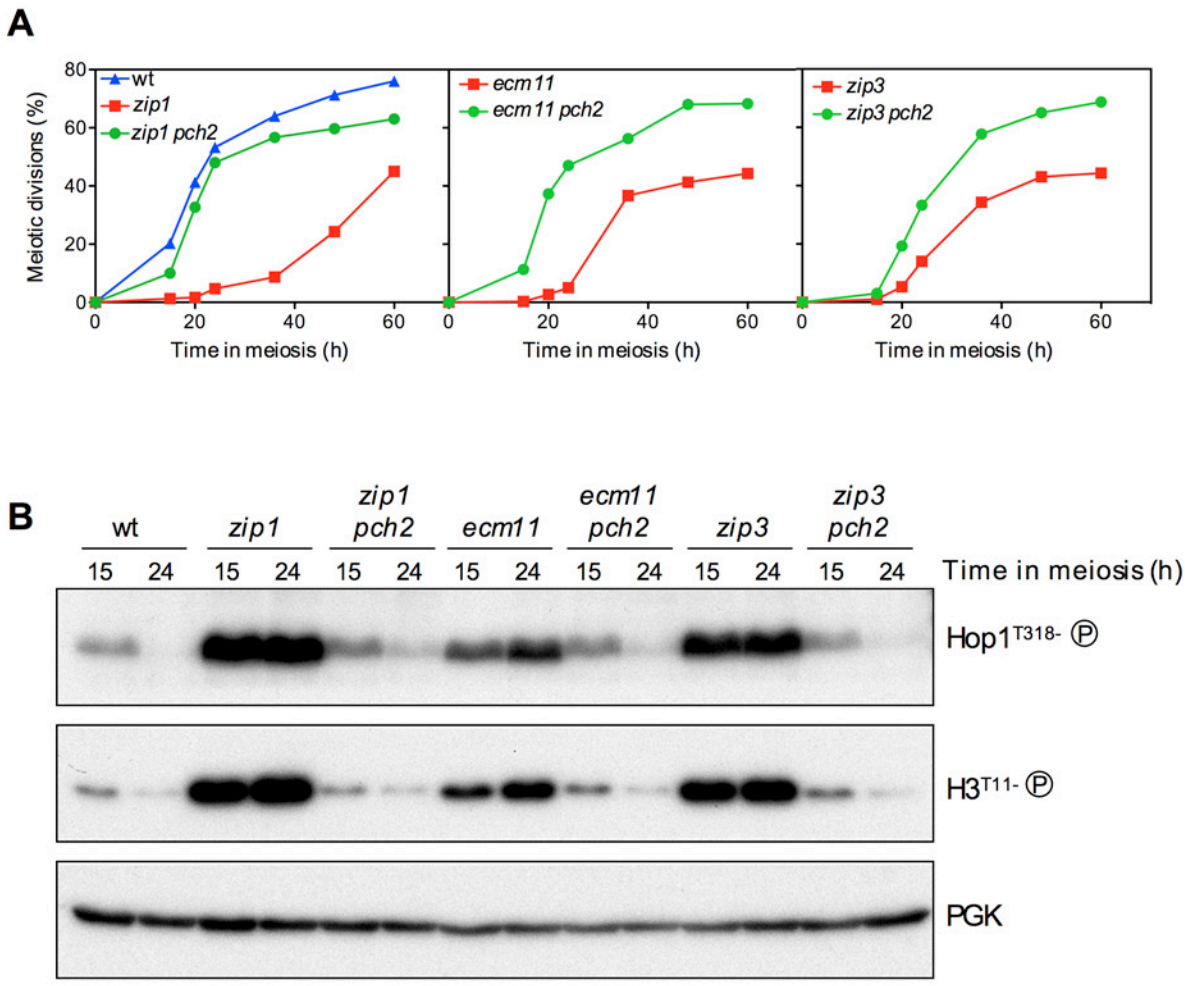

Figure S4. Pch2 is required for checkpoint activation in the SC-deficient *ecm11* and *zip3* mutants. (A) Time course of meiotic nuclear divisions; the percentage of cells containing more than two nuclei is represented. (B) Western blot analysis of phospho-Hop1^{T318}, phospho-H3^{T11} (as indicator of Mek1 activity) and PGK (as loading control). Extracts were prepared at 15 h and 24 h after meiotic induction. Strains are: DP421 (wild type), DP422 (*zip1*), DP1029 (*zip1 pch2*), DP1388 (*ecm11*), DP1390 (*ecm11 pch2*), DP1384 (*zip3*) and DP1386 *(zip3 pch2*).

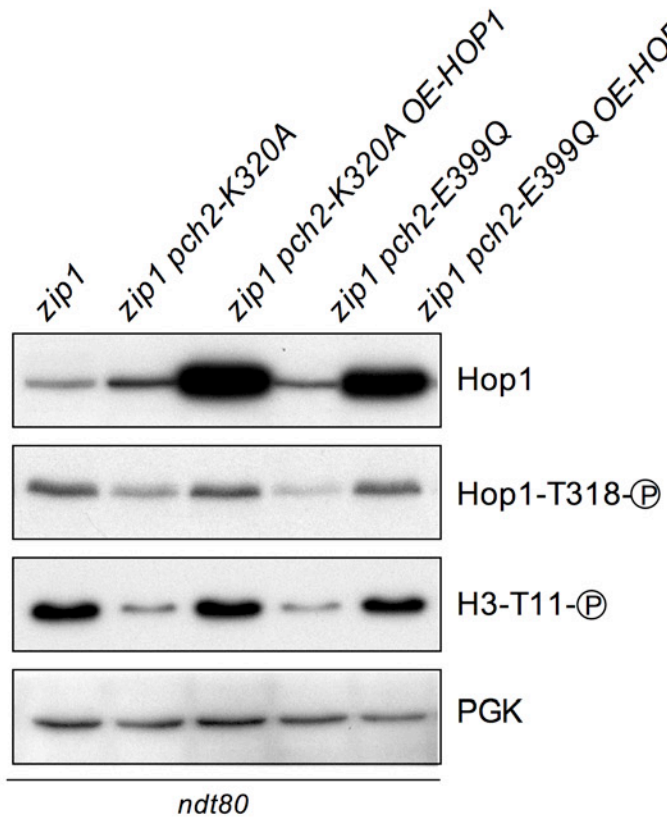

Figure S5. Hop1 overproduction restores *zip1*-induced checkpoint function in *pch2* ATPase mutants. Western blot analysis of total Hop1, phospho-Hop1^{T318}, phospho-H3^{T11} (as indicator of Mek1 activity) and PGK (as loading control). Extracts were prepared after 24 h of meiotic induction in *ndt80* strains. Strains are: DP1190 (*zip1*), DP1192 *(zip1 pch2-K320A*) and DP1302 (*zip1 pch2-E399Q*), transformed with empty vector or with R1692 (*OE-HOP1*).

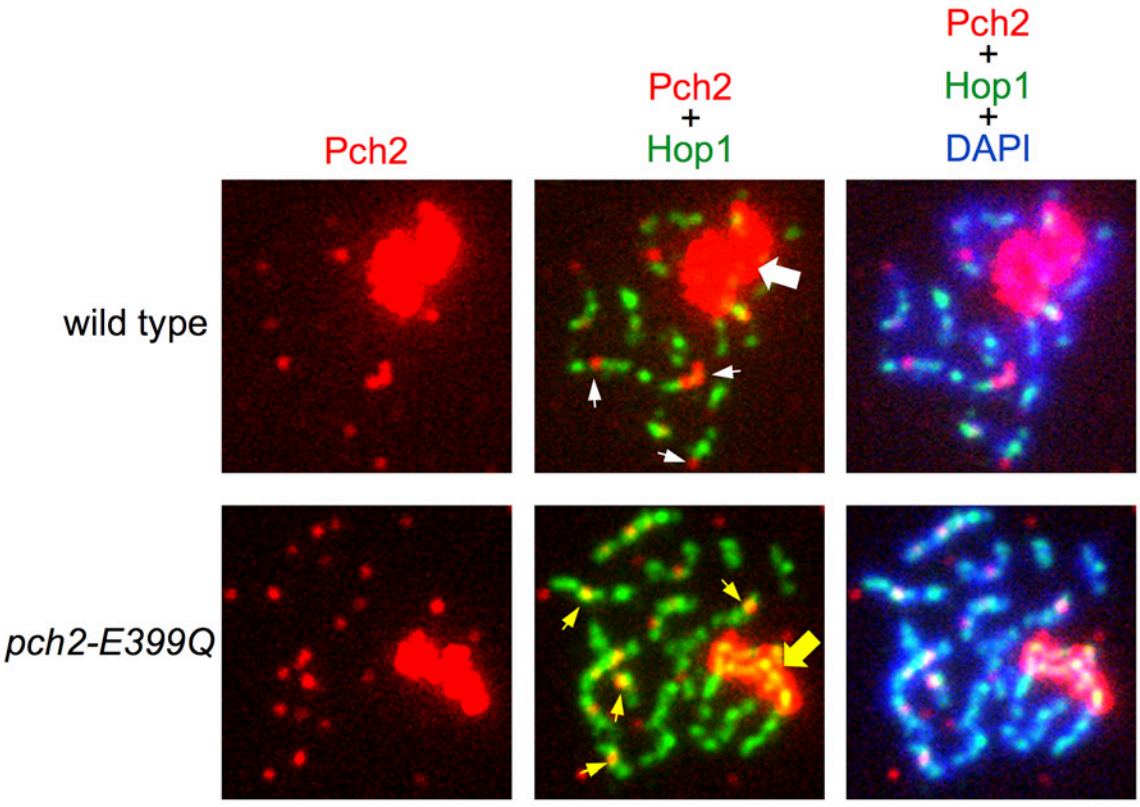

Figure S6. In contrast with wild-type Pch2, the ATPase-deficient Pch2-E399Q version colocalizes with Hop1 at the rDNA and chromosome axes.
Overexposed images of the corresponding panels shown in Figure 9A to reveal Pch2 chromosomal localization. Thick arrows point to the rDNA. Thin arrows point to interstitial Pch2 chromosomal foci. Strains are: DP1243 (wild type) and DP1262 (*pch2-E399Q*).

Table S1. *Saccharomyces cerevisiae* strains

Strain	Genotype*	Source
BR2495	*MAT***a**/*MATα leu2-27/leu2-3,112 his4-280/his4-260 arg4-8/ARG4 thr1-1/thr1-4 trp1-1/trp1-289 cyh10/CYH10 ura3-1 ade2-1*	Roeder Lab
MY63	BR2495 *zip1::LEU2*	Roeder Lab
S3483	BR2495 *ndt80::LEU2*	Roeder Lab
S4278	BR2495 *zip1::LEU2 ddc1::ADE2*	Roeder Lab
S4286	BR2495 *zip1::LYS2 rad17::LEU2 lys2*	Roeder Lab
S4295	BR2495 *zip1::LEU2 rad24::TRP1*	Roeder Lab
DP174	BR2495 *zip1::LEU2 dot1::TRP1*	PSS Lab
DP221	BR2495 *zip1::LEU2 pch2Δ$^{90-564}$-lacZ::TRP1*	This work
DP223	BR2495 *zip1::LEU2 pch2::TRP1*	PSS Lab
DP228	BR2495 *zip1::LEU2 pch2Δ$^{90-564}$-lacZ::TRP1/PCH2*	This work
DP267	BR2495 *zip1::LYS2 sir2::LEU2 lys2*	PSS Lab
BR1919-2N	*MAT***a**/*MATα leu2-3,112 his4-260 thr1-4 trp1-289 ura3-1 ade2-1*	Roeder Lab
DP421	BR1919-2N *lys2ΔNheI*	PSS Lab
DP422	DP421 *zip1::LYS2*	PSS Lab
DP424	DP421 *ndt80::LEU2*	PSS Lab
DP428	DP421 *zip1::LYS2 ndt80::LEU2*	PSS Lab
DP448	DP421 *DDC2-GFP::TRP1*	PSS Lab
DP449	DP421 *zip1::LYS2 DDC2-GFP::TRP1*	PSS Lab
DP460	DP421 *zip1::LYS2 ndt80::LEU2 DDC2-GFP::TRP1*	PSS Lab
DP582	DP421 *zip1::LYS2 ndt80::LEU2 MEK1-GFP::kanMX6*	PSS Lab
DP700	DP421 *hop1::hphMX4*	This work
DP881	DP421 *zip1::LYS2 pch2::TRP1 ndt80::LEU2*	This work
DP1029	DP421 *zip1::LYS2 pch2::TRP1*	This work
DP1058	DP421 *pch2::TRP1 ndt80::LEU2*	This work
DP1111	DP421 *zip1::LYS2 pch2::TRP1 ndt80::LEU2 MEK1-GFP::kanMX6*	This work
DP1151	BR1919-2N *PCH2-3HA*	This work
DP1152	BR1919-2N *zip1::LEU2 PCH2-3HA*	This work
DP1161	BR1919-2N *zip1::LEU2 pch2::TRP1*	This work

DP1162	BR1919-2N *zip1::LEU2 pch2-3HA-K320A*	This work
DP1163	BR1919-2N *pch2-3HA-K320A*	This work
DP1164	BR1919-2N *pch2::TRP1*	This work
DP1168	BR1919-2N *rad54::LEU2*	This work
DP1169	BR1919-2N *zip1::URA3 rad54::LEU2*	This work
DP1171	BR1919-2N *zip1::URA3 pch2::TRP1 rad54::LEU2*	This work
DP1190	BR1919-2N *zip1::LEU2 ndt80::kanMX3 PCH2-3HA*	This work
DP1192	BR1919-2N *zip1::LEU2 ndt80::kanMX3 pch2-3HA-K320A lys2/LYS2*	This work
DP1193	BR1919-2N *ndt80::kanMX3 pch2-3HA-K320A lys2/LYS2*	This work
DP1243	BR1919-2N *PCH2-3MYC*	This work
DP1244	BR1919-2N *zip1::LEU2 PCH2-3MYC*	This work
DP1245	DP421 *zip1::LYS2 pch2::TRP1 pph3::kanMX6*	This work
DP1247	DP421 *pph3::kanMX6*	This work
DP1249	DP421 *zip1::LYS2 pph3::kanMX6*	This work
DP1251	DP421 *zip1::LYS2 pch2::URA3 ndt80::LEU2 DDC2-GFP::TRP1*	This work
DP1262	BR1919-2N *pch2-3MYC-E399Q*	This work
DP1263	BR1919-2N *zip1::LEU2 pch2-3MYC-E399Q*	This work
DP1287	BR1919-2N *pch2-3HA-E399Q*	This work
DP1288	BR1919-2N *zip1::LEU2 pch2-3HA-E399Q*	This work
DP1302	BR1919-2N *zip1::LEU2 pch2-3HA-E399Q ndt80::kanMX3*	This work
DP1325	BR1919-2N *PCH2-3HA / PCH2-3MYC*	This work
DP1329	BR1919-2N *PCH2 / PCH2-3MYC*	This work
DP1337	BR1919-2N *pch2-3HA-K320A / pch2-3MYC-K320A*	This work
DP1378	DP421 *zip1::LYS2 rad54::LEU2 DDC2-GFP::TRP1*	This work
DP1379	DP421 *zip1::LYS2 pch2::URA3 DDC2-GFP::TRP1*	This work
DP1381	DP421 *zip1::LYS2 rad51::natMX4 DDC2-GFP::TRP1*	This work
DP1382	DP421 *zip1::LYS2 rad51::natMX4 pch2::URA3 DDC2-GFP::TRP1*	This work
DP1384	BR1919-2N *zip3::URA3*	This work
DP1386	BR1919-2N *zip3::URA3 pch2::TRP1*	This work
DP1387	DP421 *zip1::LYS2 rad54::LEU2 pch2::URA3 DDC2-GFP::TRP1*	This work

DP1388	BR1919-2N *ecm11::kanMX6*	This work
DP1390	BR1919-2N *ecm11::kanMX6 pch2::TRP1*	This work

* All strains are diploids isogenic to BR2495 or BR1919 and, unless specified, homozygous for the indicated markers. DP421 is a *lys2* version of the original BR1919-2N.

Table S2. Plasmids

Plasmid name	Vector	Relevant parts	Source
R1566	YCp50	*URA3 CEN4 lacZ*	Roeder Lab
pSS51	YCp50	*URA3 CEN4 pch2-lacZ*	This work
pSS67	pUC18	*pch2-lacZ::TRP1*	This work
pSS54	YEp352	*URA3 2μ PCH2*	This work
R1692	YEp24	*URA3 2μ HOP1*	Hollingsworth Lab
pSS314	pJET1.2	*HOP1*	This work
pSS315	pJET1.2	*hop1-T318A*	This work
pSS316	pRS426	*URA3 2μ HOP1*	This work
pSS317	pRS426	*URA3 2μ hop1-T318A*	This work

Table S3. Primary antibodies

Antibody	Host and type	Application* (Dilution)	Source / Reference
Mek1	Rabbit polyclonal	WB (1:2000)	(1)
Cdc5	Goat polyclonal	WB (1:1000)	Santa Cruz Biotechnology sc-6733
Hop1	Rabbit polyclonal	WB (1:2000) IF (1:400)	(2)
Hop1-T318-P	Rabbit polyclonal	WB (1:1000) IF (1:150)	Jesús Carballo (3)
H3-T11-P	Rabbit polyclonal	WB (1:2000)	Abcam ab5168
Rad51	Rabbit polyclonal	IF (1:300)	Santa Cruz Biotechnology sc-33626
GFP	Rabbit polyclonal	IF (1:400)	Molecular Probes A-6455
Phospho-(S/T)Q	Rabbit polyclonal	IF (1:400)	Cell Signaling Technology #2851
HA (12CA5)	Mouse monoclonal	WB (1:2000) IF (1:200)	Roche 11 666 606 001
Myc (4A6)	Mouse monoclonal	IF (1:200) WB (1:1000)	Millipore 05-724
GFP (JL-8)	Mouse monoclonal	IF (1:200)	Clontech 632381
PGK (22C5)	Mouse monoclonal	WB (1:10000)	Molecular Probes A-6457
Tubulin (TAT1)	Mouse monoclonal	IF (1:400)	(4)

*WB, western blot; IF, immunofluorescence

1. Ontoso, D., Acosta, I., van Leeuwen, F., Freire, R. and San-Segundo, P.A. (2013) Dot1-dependent histone H3K79 methylation promotes activation of the Mek1 meiotic checkpoint effector kinase by regulating the Hop1 adaptor. *PLoS genetics*, **9**, e1003262.

2. Smith, A.V. and Roeder, G.S. (1997) The yeast Red1 protein localizes to the cores of meiotic chromosomes. *J Cell Biol*, **136**, 957-967.

3. Carballo, J.A., Johnson, A.L., Sedgwick, S.G. and Cha, R.S. (2008) Phosphorylation of the axial element protein Hop1 by Mec1/Tel1 ensures meiotic interhomolog recombination. *Cell*, **132**, 758-770.

4. Refolio, E., Cavero, S., Marcon, E., Freire, R. and San-Segundo, P.A. (2011) The Ddc2/ATRIP checkpoint protein monitors meiotic recombination intermediates *J. Cell Sci.*, **124**, 2488-2500.

CONCLUSIONES

1. La sobre-producción de la proteína adaptadora del checkpoint Hop1 suprime el *checkpoint* defectivo del mutante *zip1Δ pch2Δ*, restaurando la fosforilación de Mek1, su localización en los cromosomas y el bloqueo de la progresión meiótica.

2. El papel principal de Pch2 en el *checkpoint* meiótico inducido por fallos en sinapsis es promover la fosforilación de Hop1 en la T318, ya que los niveles de fosforilación de Hop1 así como su acumulación en los ejes de los cromosomas se ve reducida al delecionar *PCH2*. La sobre-expresión ectópica de *HOP1*, pero no del fosfomutante *hop1-T318A*, restablece la actividad del *checkpoint* en *zip1Δ pch2Δ*.

3. Pch2 promueve la fosforilación de Hop1 en la T318, al menos en parte, modulando la acción de la fosfatasa PP4, puesto que el triple mutante *zip1Δ pch2Δ pph3Δ* restaura parcialmente la funcionalidad del *checkpoint*.

4. La regulación de la actividad del módulo Hop1-Mek1 por Pch2 durante la respuesta del *checkpoint* impacta directamente en el bloqueo del ciclo celular meiótico y no sólo en las rutas de recombinación.

5. La actividad ATPasa de Pch2 es necesaria para su función en el *checkpoint*. Además, el motivo de unión del ATP de Pch2 es esencial para el ensamblaje estable del complejo hexamérico y la correcta localización de la proteína.

CONCLUSIONS

1. Overproduction of the Hop1 checkpoint adaptor suppresses the checkpoint defect of the *zip1Δ pch2Δ* mutant, restoring Mek1 phosphorylation, its association to meiotic chromosomes and meiotic arrest.

2. The critical role of Pch2 in the synapsis checkpoint is to promote phosphorylation of the meiotic checkpoint adaptor Hop1 at T318; Hop1 phosphorylation and accumulation on chromosomes axes is reduced when *PCH2* is deleted. *HOP1* overexpression, but not that of the *hop1-T318A* phosphomutant, reinstates checkpoint function in *zip1Δ pch2Δ*.

3. Pch2 sustains Hop1 phosphorylation at T318, at least in part, by modulating PP4 phosphatase action, given that checkpoint function is partially restored in the *zip1Δ pch2Δ pph3Δ* triple mutant.

4. Pch2 regulation of the Hop1-Mek1 checkpoint signaling module directly impacts on meiotic cell cycle control and not only on recombination pathway choice.

5. The ATPase activity of Pch2 is required for its checkpoint function. Moreover, the ATP binding motif is necessary for stable assembly of the hexameric complex and proper Pch2 localization.

Artículo 2

ARTÍCULO 2: "*Impact of histone H4K16 acetylation on the meiotic recombination checkpoint in Saccharomyces cerevisiae*"

RESUMEN

En las células meióticas, el *checkpoint* de recombinación meiótica o de paquitene es un mecanismo de vigilancia que monitoriza procesos cruciales, como la sinapsis y la recombinación de los cromosomas, que son esenciales para la distribución correcta de los cromosomas entre los productos meióticos. Fallos en estos procesos dan lugar a la formación de gametos aneuploides. La recombinación meiótica ocurre en el contexto de la cromatina, de hecho, la histona metiltransferasa Dot1 y la histona deacetilasa Sir2 son reguladores bien conocidos del *checkpoint* de paquitene de *Saccharomyces cerevisiae*. Aquí describimos que la acetilación de la histona H4 en la lisina 16 mediada por Sas2 (H4K16ac), una de las dianas de Sir2, modula la actividad del *checkpoint* meiótico en respuesta a defectos en el complejo sinaptonémico. En este artículo mostramos que, al igual que el mutante *sir2Δ*, la mutación *H4-K16Q* que mimetiza la acetilación constitutiva de la H4K16, elimina el retraso de la progresión del ciclo celular meiótico impuesto por el *checkpoint* inducido por fallos en sinapsis en el mutante *zip1Δ*. También demostramos que, como en el mutante *dot1Δ*, la fosforilación del adaptador del *checkpoint* Hop1 en la treonina 318 y la consiguiente activación de Mek1 están afectadas en los mutantes de *H4-K16*. Sin embargo, al contrario que los mutantes *sir2Δ* y *dot1Δ*, las mutaciones *H4-K16R* y *H4-K16Q* solo tienen un pequeño efecto en la activación del *checkpoint* y en la localización nucleolar de Pch2 en células bloqueadas en profase (*ndt80Δ*). También aportamos evidencias de una interacción entre la H3K79me3 dependiente de Dot1 y la H4K16ac, y mostramos que Sir2 excluye la H4K16ac de la región del rDNA en cromosomas meióticos. Nuestros resultados desvelan que niveles adecuados de H4K16ac regulan este mecanismo de control de calidad meiótico y que Sir2 actúa sobre otras dianas adicionales para activar el *checkpoint* por completo.

GRAPHICAL ABSTRACT

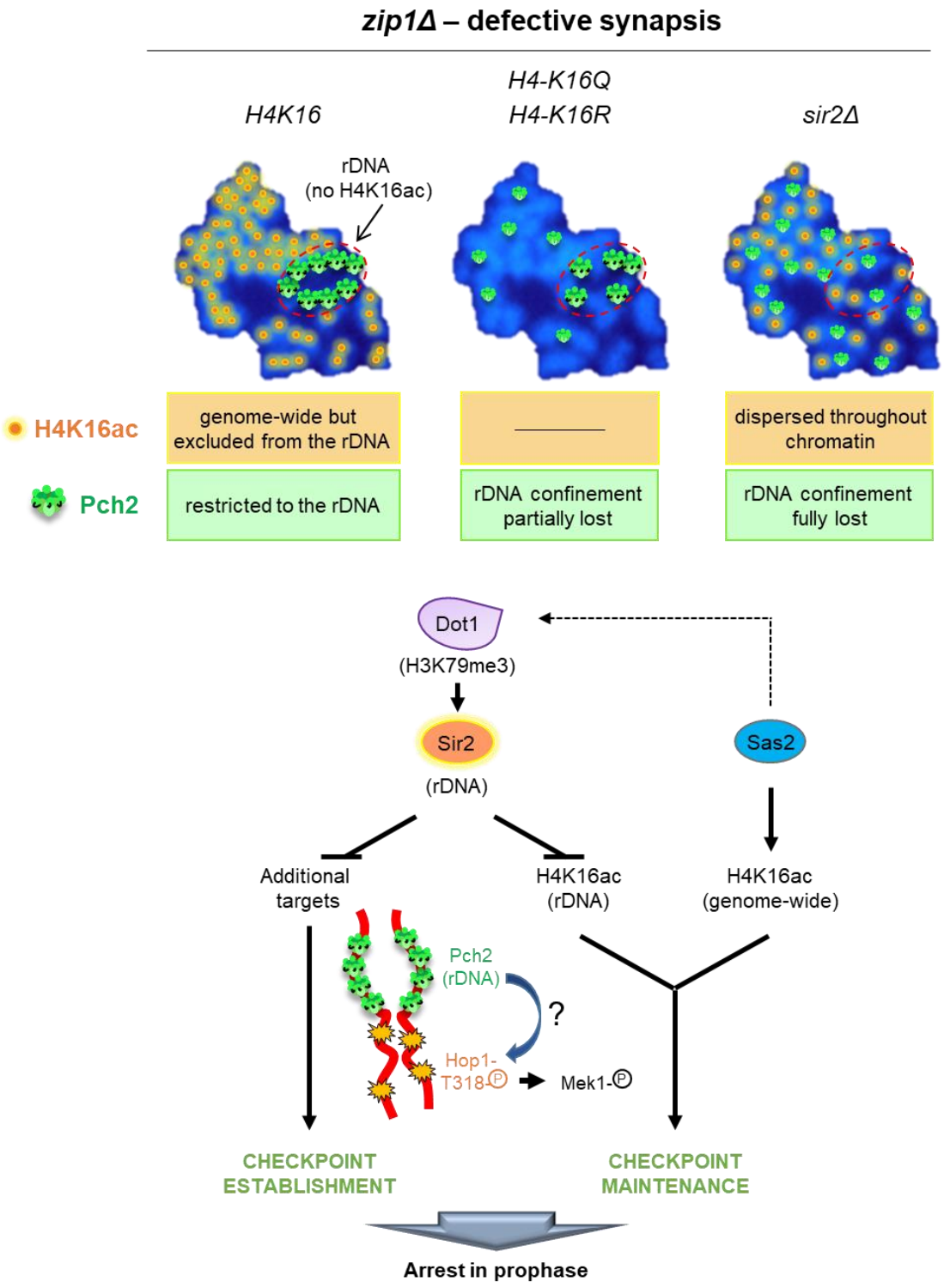

microbial cell

Research Article

www.microbialcell.com

Impact of histone H4K16 acetylation on the meiotic recombination checkpoint in *Saccharomyces cerevisiae*

Santiago Cavero[1,2], Esther Herruzo[1], David Ontoso[1,3] and Pedro A. San-Segundo[1,*]

[1] Instituto de Biología Funcional y Genómica. Consejo Superior de Investigaciones Científicas and University of Salamanca, 37007 Salamanca, Spain.

[2] Present address: Department of Experimental and Health Sciences, Pompeu Fabra University, 08003-Barcelona, Spain.

[3] Present address: Molecular Biology Program, Memorial Sloan Kettering Cancer Center, New York, New York 10065, USA.

* Corresponding Author:

Pedro San-Segundo. IBFG (CSIC-USAL), C/ Zacarías González, 2; 37007-Salamanca, Spain; Tel: +34 923294902; Fax: +34 923224876; E-mail: pedross@usal.es

ABSTRACT **In meiotic cells, the pachytene checkpoint or meiotic recombination checkpoint is a surveillance mechanism that monitors critical processes, such as recombination and chromosome synapsis, which are essential for proper distribution of chromosomes to the meiotic progeny. Failures in these processes lead to the formation of aneuploid gametes. Meiotic recombination occurs in the context of chromatin; in fact, the histone methyltransferase Dot1 and the histone deacetylase Sir2 are known regulators of the pachytene checkpoint in *Saccharomyces cerevisiae*. We report here that Sas2-mediated acetylation of histone H4 at lysine 16 (H4K16ac), one of the Sir2 targets, modulates meiotic checkpoint activity in response to synaptonemal complex defects. We show that, like *sir2*, the *H4-K16Q* mutation, mimicking constitutive acetylation of H4K16, eliminates the delay in meiotic cell cycle progression imposed by the checkpoint in the synapsis-defective *zip1* mutant. We also demonstrate that, like in *dot1*, *zip1*-induced phosphorylation of the Hop1 checkpoint adaptor at threonine 318 and the ensuing Mek1 activation are impaired in *H4-K16* mutants. However, in contrast to *sir2* and *dot1*, the *H4-K16R* and *H4-K16Q* mutations have only a minor effect in checkpoint activation and localization of the nucleolar Pch2 checkpoint factor in *ndt80*-prophase-arrested cells. We also provide evidence for a cross-talk between Dot1-dependent H3K79 methylation and H4K16ac and show that Sir2 excludes H4K16ac from the rDNA region on meiotic chromosomes. Our results reveal that proper levels of H4K16ac orchestrate this meiotic quality control mechanism and that Sir2 impinges on additional targets to fully activate the checkpoint.**

doi: *10.15698/mic2016.12.548*
Received *originally: 29.06.2016;*
in revised form: 30.09.2016,
Accepted *24.10.2016,*
Published *04.12.2016.*

Keywords*: meiosis, checkpoint, histone H4K16, chromatin modifications, Sir2, Pch2, Sas2.*

Abbreviations:
DSBs - double-strand breaks,
H4K16ac - acetylation of histone H4 at lysine 16,
PTMs - post-translational modifications,
SC - synaptonemal complex.

INTRODUCTION

Meiosis is a specialized type of cell division in which a single round of DNA replication is followed by two consecutive rounds of nuclear division (meiosis I and II), allowing the generation of haploid gametes from diploid progenitor cells [1, 2]. In the first meiotic division the segregation of homologous chromosomes (homologs) takes place, whereas during meiosis II sister chromatids separate one from each other.

Between DNA duplication and the first meiotic division, a complex series of events involving homologous chromosomes occur during the so-called meiotic prophase; namely, genetic recombination initiated by Spo11-induced DNA double-strand breaks (DSBs) [3], alignment of parental chromosomes (pairing) and tight association of homologs (synapsis) in the context of the synaptonemal complex (SC) [1, 4]. The SC is a highly conserved meiosis-specific tripartite structure that assembles along the lengths of paired homologous chromosomes. It consists of a central region, in which the *S. cerevisiae* Zip1 protein is the major component [5, 6], and two lateral elements composed of the Hop1 and Red1 proteins. Problems in the recombinational repair of meiotic DSBs as well as defects in pairing and synapsis of homologs are situations that trigger the activation of a meiosis-specific surveillance mechanism, the so-called pachytene checkpoint or meiotic recombination check-

point, that prevents meiotic nuclear division until those crucial processes have been completed [7-9]. In the yeast *Saccharomyces cerevisiae*, the activation of this evolutionarily-conserved pathway by unrepaired meiotic DSBs relies on the same sensor proteins that the canonical DNA damage checkpoint operating in vegetative growing cells, specifically the Mec1 and Tel1 kinases (the yeast homologs of mammalian DNA damage sensor kinases ATR and ATM), Rad24 and the 9-1-1 complex [10-14]. In addition, meiosis-specific proteins, present in the chromosomal axis, such as Red1 and Hop1 [15-17], act as adaptors sustaining the activation and hyperphosphorylation of the meiosis-specific downstream effector kinase Mek1 [18-23]. The delay in the exit from meiotic prophase in *S. cerevisiae* is imposed predominantly by controlling the expression and localization of the meiosis-specific transcription factor Ndt80, which in turn promotes the activation of the majority of genes required for late meiotic development, including B-type cyclins and the polo-like kinase Cdc5 [18, 24-27], as well as by inhibiting the major cyclin-dependent kinase (CDK) Cdc28 through its Swe1-dependent phosphorylation [28, 29]. Budding yeast meiotic mutants such as *zip1*, defective in SC and crossover formation that leads to the accumulation of recombination intermediates [5, 30, 31], are invaluable genetic tools to activate and study the pachytene checkpoint.

Meiotic recombination and the checkpoint response occur in the context of chromatin, which is subject to a wide variety of histone post-translational modifications (PTMs). These histone PTMs include acetylation, methylation, phosphorylation or ubiquitylation and exert their functions either influencing the overall structure of chromatin or regulating the binding of effector molecules. Histone PTMs have important roles in transcription, replication, repair, establishment of euchromatin/heterochromatin and other aspects of eukaryotic chromosome dynamics. Various histone PTMs have been described to be involved in crucial meiotic processes, such as recombination and the pachytene checkpoint [8, 9, 32]. In particular, it has been proposed that H3K4 trimethylation promotes the formation of Spo11-dependent meiotic DSBs in *S. cerevisiae* mediated by the tethering of the Ssp1 subunit of the Set1 complex to chromosome axes [33-35]. Nevertheless, further mechanistic studies are required to confirm this model. In addition, previous reports have also revealed the requirement of Dot1 and Sir2 for the meiotic block triggered by the pachytene checkpoint in *zip1* mutants lacking a component of the SC [21, 36, 37]. Dot1 is the methyltransferase required for H3K79 methylation (H3K79me), whereas Sir2 is a histone deacetylase that establishes and maintains silencing within yeast heterochromatic-like regions at telomeres, ribosomal DNA (rDNA) and silenced mating-type loci, and whose preferred histone substrates are H3K56ac and H4K16ac [38-42]. However, in some cases, the precise meiotic role of those epigenetic modifications is not well known yet.

In this work we have investigated the role of the acetylation of lysine 16 in histone H4 (H4K16ac) during meiosis and its regulation by Sas2 and Sir2. We demonstrate that global acetylation of H4K16 does not change in either unperturbed or challenged meiosis and found that proper H4K16ac is dispensable during normal meiotic divisions. However, it is required for meiotic checkpoint activity, as manifested by the effect of *H4-K16R* and *H4-K16Q* mutants on suppression of the checkpoint-induced meiotic delay of *zip1*. These mutants show a reduction in the activity of the Mek1 meiotic effector kinase, which is most probably due to impaired Hop1 phosphorylation at threonine 318. Our results also indicate that the effect of *H4-K16R* and *H4-K16Q* mutations on the meiotic checkpoint is exerted, at least in part, through a cross-talk between H4K16ac and H3K79me. We provide cytological evidence showing that Pch2 localization is slightly altered in the H4K16ac mutants and, finally, we unveil the meiotic chromosomal distribution of H4K16ac, which is excluded from the rDNA region in a Sir2-dependent manner.

RESULTS AND DISCUSSION

Global levels of H4K16ac do not change in either normal or challenged meiosis

In budding yeast, the lysine 16 of histone H4 (hereafter H4K16) is primarily acetylated by Sas2, a member of the MYST-type family of histone acetyltransferases (HATs) [43-47] and secondarily by the essential HAT Esa1 [48, 49]. In turn, at least *in vitro*, H4K16ac is the preferred substrate, but not the only one, of the NAD^+-dependent Sir2 deacetylase [40, 44, 50-52]. Importantly, disruption of *SIR2* leads to H4K16 hyperacetylation exclusively in heterochromatic-like regions, such as subtelomeric sequences, the rDNA locus and the silenced mating-type loci, but does not affect genome-wide H4K16ac [53]. In fact, Sir2-dependent deacetylation of H4K16ac is a characteristic feature of silenced chromatin at those particular genomic domains [54]. Since Sir2 has been shown to play a crucial role in the meiotic recombination checkpoint [36], we sought to explore the possible role of H4K16ac in this process.

To study the kinetics of H4K16ac accumulation during meiosis, we performed meiotic time courses as described in Materials and Methods and followed this histone mark by immunoblotting with an anti-H4K16ac antibody. A non-acetylatable *H4-K16R* mutant was used as a control for antibody specificity (Figure 1). In this preliminary approach to determine variations of this histone modification, we found that global levels of H4K16ac do not significantly change upon meiosis induction (compare time 0 with the remaining times) or during the whole length of the meiotic program (Figure 1, upper panels). Next, we wanted to determine if H4K16ac was affected by the activation of the meiotic recombination checkpoint; thus, we analyzed a *zip1* mutant, which triggers the checkpoint. We found that H4K16ac levels were also unaltered during the meiotic time courses in the *zip1* mutant (Fig. 1, lower panels), indicating that despite the role of Sir2 in the checkpoint, global levels of H4K16ac remain fairly constant when synapsis defects exist.

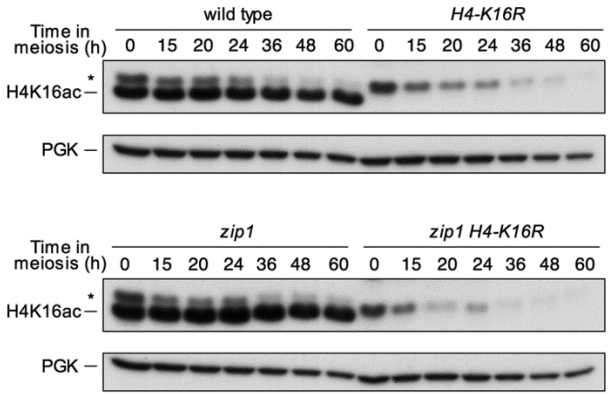

FIGURE 1: H4K16 acetylation remains unaltered during both normal and perturbed meiosis. Western blot analysis of H4K16 acetylation throughout meiosis in wild-type (DP421) and *zip1* (DP422) cells. The *H4-K16R* (DP994) and *zip1 H4-K16R* (DP995) mutant strains were used as controls for antibody specificity. PGK was used as a loading control. Asterisks mark a non-specific band.

Previous studies have shown that histone acetylation levels, including those of H4K16, dramatically increase during the induction of an HO-induced DSB lesion and decrease during the subsequent homologous recombinational repair, presumably due to the coordinated action of histone modifying enzymes, such as Esa1 and Sir2, that are recruited to the lesion [55]. This ability to modify the levels of histone acetylation is essential to maintain cell viability after exposure to DNA damaging agents or during DNA repair by homologous recombination, either because changes in histone acetylation are necessary for the recruitment of DNA repair enzymes and/or chromatin remodelers, or because they are important in downstream signaling. In fact, different H3 and H4 lysines are found acetylated upon DNA damage in yeast [56, 57]. Meiosis involves the generation and subsequent repair of multiple DSBs across the genome and signal transduction in the meiotic checkpoint pathway shares many components with the mitotic DNA damage checkpoint [8]. However, in this study, we show that global levels of H4K16ac do not change either with the induction of the meiotic program or when meiotic chromosome synapsis defects exist (Figure 1). Nevertheless, the precise meiotic errors (incomplete recombination, chromosome structural defects or both) triggering the checkpoint in the *zip1* mutant remain to be established. In addition, in contrast to the situation in mitotic cells, meiotic DSB repair occurs in the special context of the SC with probably different chromatin modifications requirements. Moreover, in our study we have measured global levels of H4K16 acetylation and we cannot rule out the possibility that local modifications of H4K16 acetylation may occur at particular genomic regions.

H4K16 normal acetylation is required for efficient meiotic checkpoint regulation

To further investigate the role of H4K16ac in meiosis, several meiotic events were analyzed in *H4-K16R* (non-acetylatable) and *H4-K16Q* (mimicking constitutive acetylation) mutants, both in a wild-type (unperturbed meiosis) and a *zip1* background (triggering meiotic checkpoint activation). The kinetics of meiotic nuclear divisions was monitored by DAPI staining of nuclei. Dityrosine fluorescence, a specific component of mature spores, was used as a semi-quantitative indicator for sporulation efficiency. Finally, spore viability that reflects the fidelity of meiotic chromosome segregation and the integrity of the spore genome

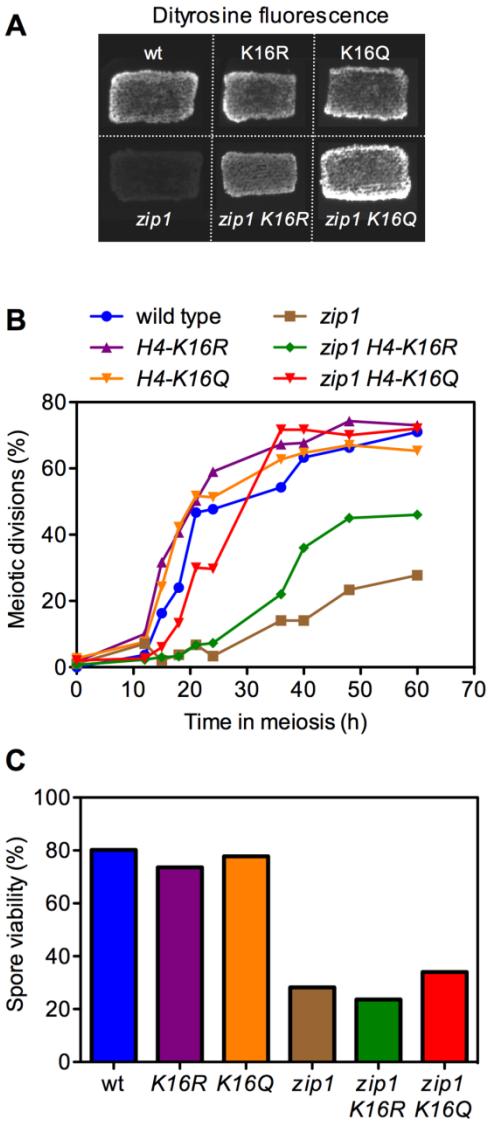

FIGURE 2: The meiotic recombination checkpoint is impaired in *H4-K16R* and *H4-K16Q* mutants. (A) Dityrosine fluorescence, as an indicator of sporulation, was examined after 3 days of sporulation on plates. **(B)** Time course of meiotic nuclear divisions; the percentage of cells containing two or more nuclei is represented. **(C)** Spore viability, as assessed by asci dissection, is presented. At least 144 spores were scored for each strain. Strains used in (A) are DP421 (wild type), DP994 (*H4-K16R*), DP1000 (*H4-K16Q*), DP422 (*zip1*), DP995 (*zip1 H4-K16R*) and DP1001 (*zip1 H4-K16Q*). Strains used in (B) and (C) are DP634 (wild type), DP635 (*H4-K16R)*, DP636 (*H4-K16Q)*, DP639 (*zip1)*, DP640 (*zip1 H4-K16R)* and DP641 (*zip1 H4-K16Q).*

was determined by tetrad dissection. In an otherwise wild-type background, the *H4-K16R* and *H4-K16Q* single mutants showed no or little meiotic defects (Figure 2). The progression through meiosis was normal (Figure 2B, S1A) and resulted in the formation of mature dityrosine-containing spores (Figure 2A) with a high viability similar to that of the wild type (Figure 2C). These observations suggest that normal regulation of H4K16ac is dispensable in unperturbed meiosis.

As previously described, the *zip1* mutant, where the pachytene checkpoint is triggered, showed a strong delay in meiotic progression and the formation of mature spores was dramatically reduced (Figure 2A, 2B, S1A). Notably, the *H4-K16R* and *H4-K16Q* mutations were able to partially (*K16R*) or completely (*K16Q*) alleviate the checkpoint-dependent meiotic block: the *zip1 H4-K16Q* and *zip1 H4-K16R* double mutants progressed faster into meiosis (Figure 2B, S1A) and formed dityrosine-containing spores in a higher proportion than *zip1* cells (Figure 2A); however, spore viability remained low (Figure 2C) indicating that although *zip1 H4-K16Q* and *zip1 H4-K16R* cells were able to progress into meiosis and to form mature spores, the problems caused by the lack of Zip1 persist. Thus, the status of H4K16ac modulates meiotic progression in the *zip1* mutant. Interestingly, the *H4-K16Q* mutant mimicking constitutive acetylation shows a stronger checkpoint defect, similar to the lack of the Sir2 deacetylase [36] (see below).

H4-K16R and *H4-K16Q* mutants are defective in the maintenance, but not the establishment, of checkpoint-induced Mek1 activation

To investigate the meiotic checkpoint role of H4K16ac more directly at a molecular level, we followed the status of Mek1 activation throughout meiotic time courses in the *zip1 H4-K16R* and *zip1 H4-K16Q* mutants using high-resolution Phos-tag gels. The appearance of hyper-phosphorylated Mek1 isoforms is indicative of meiotic checkpoint activation [21]. The threonine 11 of histone 3 has been identified as one of Mek1 downstream targets [58]. Although the role of H3T11ph in meiosis, if any, is still unclear, it is a useful additional reporter for Mek1 kinase activity (Figure 3) [59]. In wild-type cells, Mek1 levels rose transiently during meiotic prophase (peak at 20 hours) and then progressively declined as meiosis I and II and sporulation took place. Phosphorylated forms of Mek1 and H3T11ph remained at very low levels during the whole meiotic time course (Figure 3, upper panel). In contrast, robust Mek1 activation, as shown by the appearance of additional slow migrating and stronger phosphorylated Mek1 forms, and marked H3T11ph could be detected in the *zip1* mutant (Figure 3, second panel), consistent with its pronounced meiotic delay triggered by the checkpoint (Figure 2B). We next examined the *zip1 H4-K16R* and *zip1 H4-K16Q* double mutants. Remarkably, according with the complete suppression of the meiotic delay (Figure 2B), Mek1 activation was severely impaired in the *zip1 H4-K16Q* double mutant, as manifested by the absence of the upper Mek1 phosphorylated forms and low levels of H3T11ph (Figure 3, third panel). The *zip1 H4-K16R*, which shows only

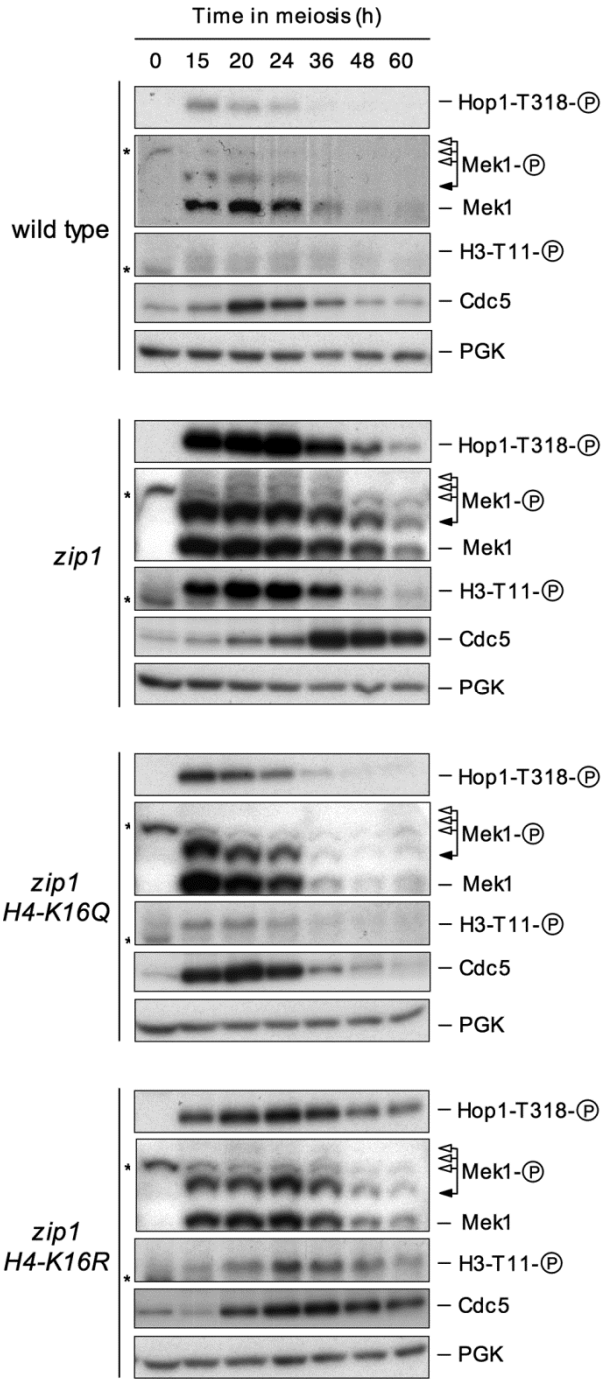

FIGURE 3: H4K16 acetylation is necessary for normal Mek1 and Hop1 phosphorylation. Western blot analysis of Mek1 and Hop1 activation in wild type (DP421), *zip1* (DP422), *zip1 H4-K16Q* (DP1001) and *zip1 H4-K16R* (DP995) strains throughout meiosis. Black arrows point the Mec1/Tel1-dependent phosphorylated form of Mek1, whereas white arrows mark the bands resulting from Mek1 autophosphorylation [21]. Asterisks mark non-specific bands. H3T11 phosphorylation and Cdc5 inhibition were used as additional molecular markers for checkpoint activation. PGK was used as a loading control.

a partial checkpoint defect (Figure 2B), showed a milder reduction in both the levels and the duration of Mek1 activation and H3T11ph (Figure 3, bottom panels).

Mec1/Tel1-dependent phosphorylation of Hop1 at defined S/T-Q sites is required for Mek1 hyperphosphorylation and activation, as well as for meiotic checkpoint activity [15]. Among the several S/T-Q sites targeted by Mec1/Tel1 in Hop1, phosphorylation of threonine 318 together with phosphorylation of serine 298 are crucial events in the meiotic checkpoint network to coordinate recombination and meiotic progression [60]. We examined the levels of Hop1-T318 phosphorylation throughout the meiotic time courses using a phospho-specific antibody as an upstream marker for *zip1*-induced checkpoint activation [59]. During normal meiosis, only a very weak and transient Hop1-T318ph signal could be detected during the meiotic prophase, coinciding with the weak activation observed in Mek1 (Figure 3, upper panel). However, in *zip1* mutant cells triggering the activation of the pachytene checkpoint, Hop1-T318ph dramatically increased (Figure 3, second panel). We next analyzed the *zip1 H4-K16R* and *zip1 H4-K16Q* double mutants and we found a reduction in Hop1-T318 phosphorylation, very similar to that observed in Mek1 activity (Figure 3, third and bottom panels). Again, the effect of *H4-K16Q* was much stronger.

To further support the results shown above, we also analyzed a downstream target of the meiotic recombination checkpoint, the Cdc5 polo-like kinase. Cdc5 is one of the most prominent members of a large set of genes under the control of the meiosis-specific Ndt80 transcription factor, with a number of functions in meiosis including the exit from pachytene and entry into the first meiotic division [18, 24, 61-64]. In wild-type cells, low levels of Cdc5 were detected in vegetative cell cycle, prior to entering meiosis; those levels peaked during mid-meiosis and then declined. Meanwhile, in a *zip1* mutant the production of Cdc5 was clearly delayed (Figure 3, top and second panels), according with the slower meiotic progression (Figure 2B). In contrast, earlier induction of Cdc5 production was completely or partially restored in the *zip1 H4-K16Q* and *zip1 H4-K16R* double mutants, respectively (Figure 3, third and bottom panels), which is again consistent with the meiotic progression of these mutants.

All together, these results confirm the effect of *H4-K16Q* and *H4-K16R* mutations in meiotic progression and indicate that the checkpoint defects observed most probably arise from the failure to efficiently phosphorylate Hop1 and Mek1. Thus, H4K16ac is required for both Hop1 phosphorylation and the ensuing Mek1 activation in the meiotic recombination checkpoint pathway.

Interestingly, the substitution of the lysine 16 of histone 4 with differently charged residues resulted in slightly different outcomes. Similar to the lack of the Sir2 deacetylase [36] the *H4-K16Q* substitution, mimicking the constitutively acetylated state of lysine, completely abolished the meiotic block imposed by *ZIP1* disruption, as well as the phosphorylation of Mek1 and Hop1. Conversely, substitution of the lysine by arginine, a residue that cannot be acetylated, *H4-K16R*, only showed a partial effect on the meiotic progression as well as in the Hop1 and Mek1 phosphorylation (Figures 2 and 3). Curiously, similar consequences have been observed regarding the impact of H4K16ac mutants on other biological processes. For example, the *H4-K16Q* substitution significantly reduces lifespan whereas *H4-K16R* shows only a marginal effect [65]. Likewise, the frequency of chromosome loss and the levels of rDNA recombination are also higher in *H4-K16Q* strains than in *H4-K16R* mutants [66, 67]. In line with these observations, our results raise the possibility that the dynamics of H4K16ac, more than only the exact state of such acetylation, is required to regulate the meiotic checkpoint, although the precise mechanism underlying such effect re-

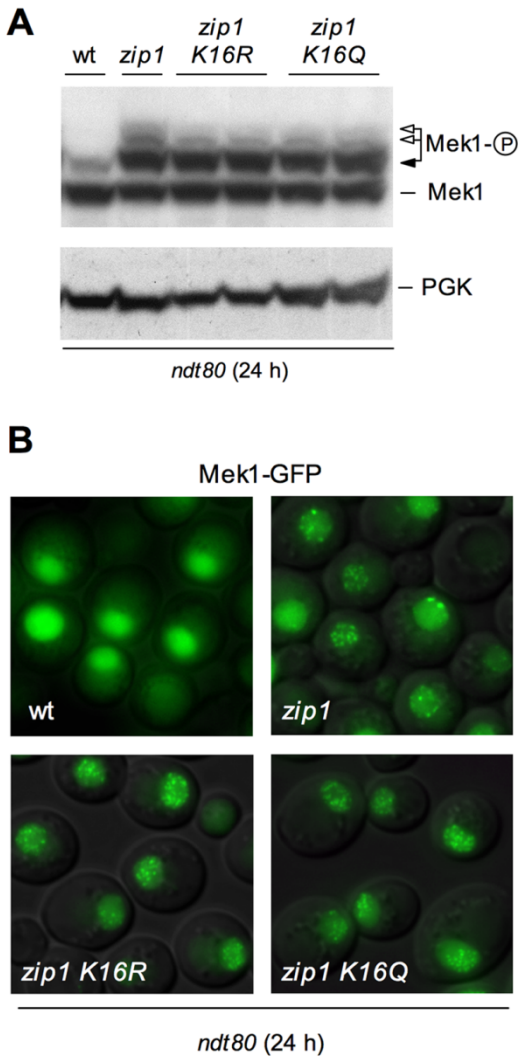

FIGURE 4: Analysis of Mek1 activation and localization in *ndt80*-arrested cells. (A) Western blot analysis of different Mek1 phosphorylation forms in *ndt80*-arrested cells after 24 h in meiosis. PGK is shown as a loading control. Strains are DP424 (wild type), DP428 (*zip1*), DP996 (*zip1 H4-K16R*) and DP1002 (*zip1 H4-K16Q*). Two independent clones of DP966 and DP1002 were analyzed. **(B)** Representative images of checkpoint-induced Mek1-GFP foci in wild type (DP584), *zip1* (DP582), *zip1 H4-K16R* (DP1089) and *zip1 H4-K16Q* (DP1090) *ndt80*-arrested cells after 24 h in meiosis.

mains to be elucidated.

In principle, the differences observed in Mek1 phosphorylation between *zip1 H4-K16R* and *zip1 H4-K16Q* double mutants and the *zip1* single mutant could be a consequence of their different kinetics in meiotic progression (*zip1* exhibits a profound delay that is bypassed in *zip1 H4-K16R* and *zip1 H4-K16Q*; Figure 2B) or could arise from a direct effect of H4K16 acetylation on Mek1 activation. To distinguish between these two possibilities, we monitored Mek1 phosphorylation in pachytene-arrested *ndt80* cells. Ndt80 is a meiosis-specific transcription factor required for induction of meiotic middle genes [25, 68, 69] promoting exit from prophase [70]; thus, *ndt80* cells arrest in pachytene independently of the meiotic checkpoint allowing us to analyze the status of checkpoint activation independent of meiotic progression. If H4K16 acetylation were not involved in the establishment of checkpoint-induced Mek1 activation but only in its maintenance, we will expect Mek1 phosphorylation to be similar in *zip1* and in *zip1 H4K16* acetylation mutants, in a *ndt80* background. As shown in Figure 4A, in an *ndt80* background, *zip1 H4-K16R* and *zip1 H4-K16Q* double mutants are only slightly impaired in Mek1 activation. Previous studies have shown that *zip1*-induced checkpoint activation results in different Mek1 phosphorylated forms [21]. In Figure 4A we can observe that *H4-K16R* and *H4-K16Q* mutants slightly affected only the upper phosphorylated bands, corresponding to Mek1 autophosphorylation (Figure 4A; white arrows), while the band immediately above the basal form, which depends on Mec1/Tel1 [21], remained intact (Figure 4A; black arrow). Moreover, when we analyzed the phosphorylation of H3T11 and Hop1-T318 as additional markers of checkpoint activation in *ndt80* cells, we observed little if any reduction in their phosphorylation levels in the *zip1 H4-K16R* and *zip1 H4-K16Q* mutants when compared to *zip1* (Figure 5). This is in clear contrast with the results of a *zip1 dot1* double mutant in which H3T11ph and Hop1-T318ph were practically abolished (Figure 5), consistent with Dot1 being absolutely required both for checkpoint activation and maintenance [21]. These results suggest that the correct acetylation of H4K16 is not required for the establishment of checkpoint-induced Mek1 and Hop1 phosphorylation, but more probably only for its maintenance. If the meiotic prophase block is artificially imposed by means of the *ndt80* mutation, then H4K16ac becomes dispensable to sustain Hop1 and Mek1 activation.

It has been previously demonstrated that, upon meiotic checkpoint activation, the Mek1 effector kinase localizes to discrete nuclear foci that can be detected both on chromosome spreads and in live meiotic cells [12, 21]. To investigate in more detail the role of H4K16ac in the meiotic checkpoint, we assessed the localization of Mek1-GFP in wild-type, *zip1*, *zip1 H4-K16R* and *zip1 H4-K16Q* cells, always in an *ndt80* background. As expected, *zip1* mutant cells accumulated multiple discrete Mek1-GFP foci during meiotic prophase (Figure 4B) and most *zip1 H4-K16R* and *zip1 H4-K16Q* cells displayed a similar pattern of Mek1 localization (Figure 4B), indicating that formation of *zip1*-induced Mek1 foci is not defective in the absence of normal H4K16ac. This observation suggests that, although H4K16ac is required for sustained meiotic checkpoint activity, it is not necessary for the checkpoint-induced association of Mek1 to meiotic chromosomes.

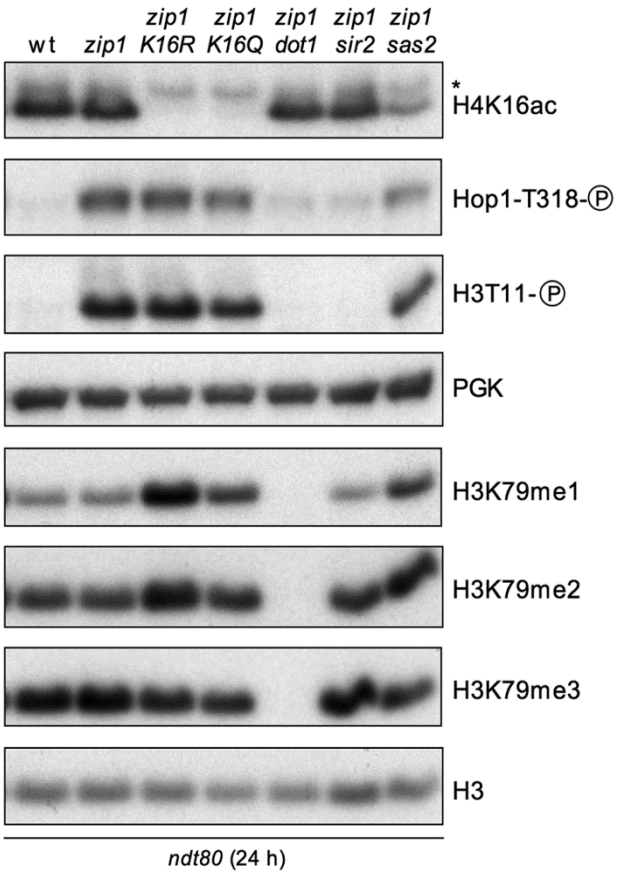

FIGURE 5: The *sir2* mutant, but not *H4-K16Q*, *H4-K16R* or *sas2*, is defective in establishing early markers of checkpoint activation. Western blot analysis of *zip1*-induced Hop1-T318 and H3-T11 phosphorylation, as well as H3K79 methylation, 24 h after meiosis induction in *ndt80*-arrested cells. PGK and total H3 were used as loading controls. Strains are: DP424 (wild type), DP428 (*zip1)*, DP996 (*zip1 H4-K16R*), DP1002 (*zip1 H4-K16Q*), DP655 (*zip1 dot1*), DP1086 (*zip1 sir2*) and DP1073 (*zip1 sas2*).

The Sir2 and Sas2 proteins are required for proper meiotic checkpoint response

To further investigate the role of H4K16ac in the meiotic recombination checkpoint we studied mutants affecting the metabolism of this residue, such as *sir2* (deficient in a H4K16ac deacetylase), and *sas2* (lacking the main H4K16 acetyltransferase). The relationship of Sir2 with the meiotic checkpoint has been previously reported [36], but a detailed analysis of meiotic progression and checkpoint activity was not described.

We found that deletion of *SIR2* completely suppressed the meiotic delay imposed by the checkpoint in the *zip1* mutant; that is, the *zip1 sir2* double mutant showed similar kinetics of meiotic progression than the wild type (Figure 6A, S1B) and displayed high levels of sporulation (Figure

6B). Hop1T318 phosphorylation and H3T11 phosphorylation (as a marker of Mek1 activity) were drastically reduced in *zip1 sir2* compared to *zip1* and, according with the meiotic progression, Cdc5 production was restored to wild-type kinetics in *zip1 sir2* (Figure 6C). Disruption of *SAS2* also alleviated the *zip1* meiotic block, but to a lesser extent than *zip1 sir2* did (Figure 6A, 6B, S1B). Consistent with this intermediate effect, Hop1T318 and H3T11 phosphorylation showed a moderate reduction, and Cdc5 dynamics was only partially restored in *zip1 sas2* (Figure 6C). Thus, in

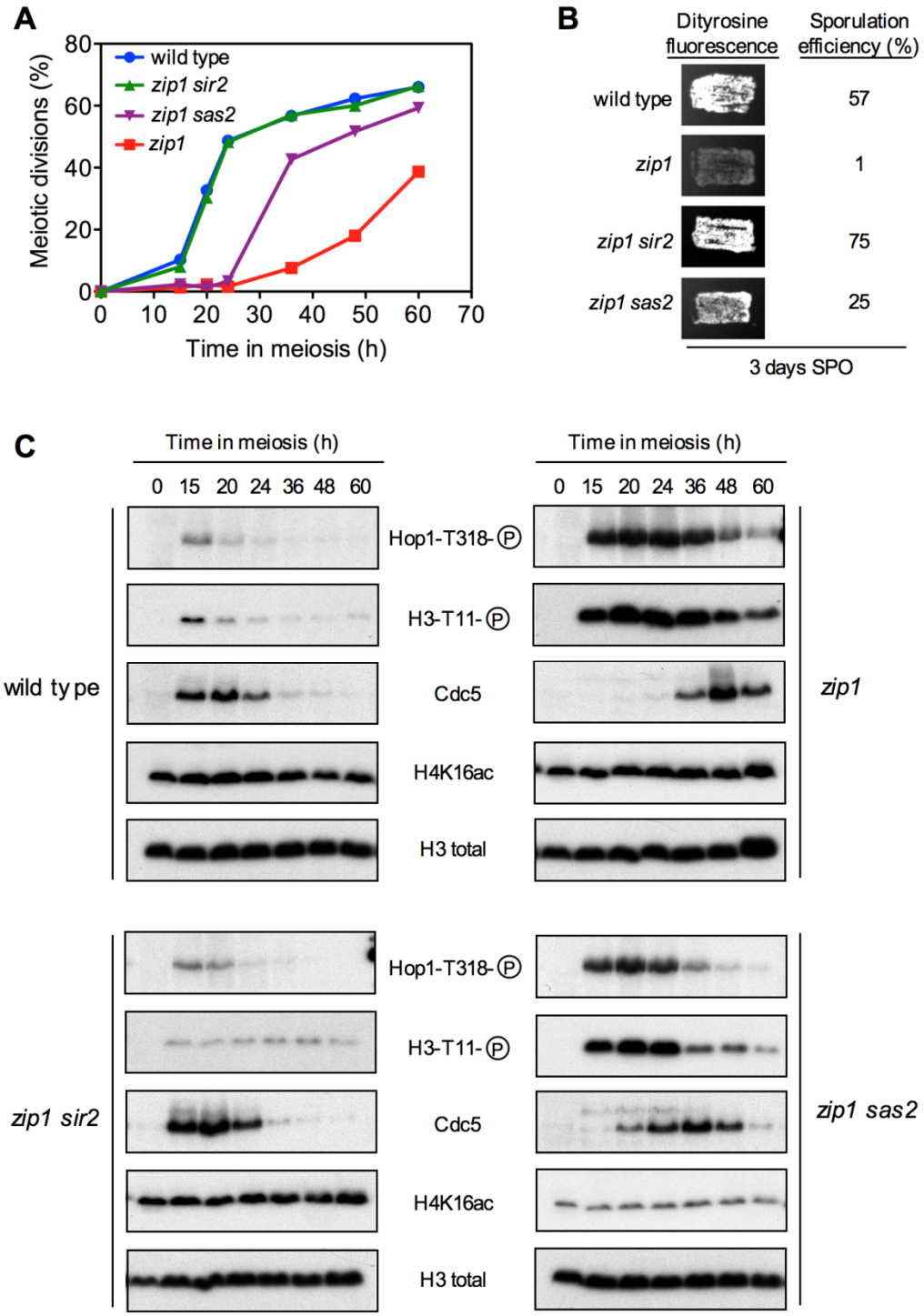

FIGURE 6: The meiotic recombination checkpoint response is impaired in the absence of Sir2 or Sas2. (A) Time course of meiotic nuclear divisions; the percentage of cells containing two or more nuclei is represented. **(B)** Dityrosine fluorescence, as a visual indicator of sporulation, and sporulation efficiency, quantified by microscopic examination of at least 300 cells, were examined after 3 days of sporulation on plates. **(C)** Western blot analysis of the indicated proteins during meiosis. Strains are DP421 (wild type), DP422 (*zip1*), DP1401 (*zip1 sir2*) and DP1410 (*zip1 sas2*).

NDT80+ cells competent for meiotic progression, the checkpoint phenotype resulting from the lack of the Sir2 deacetylase is similar to that produced by the *H4-K16Q* mutation mimicking constitutive acetylation, and the effect produced by the absence of the Sas2 acetyltransferase parallels that of the *H4-K16R* mutation preventing acetylation of this residue (Figures 2 and 3).

The checkpoint impact of *SIR2* and *SAS2* deletions was also analyzed in *ndt80* mutant cells by monitoring the levels of *zip1*-induced Hop1T318 and H3T11 phosphorylation. In the case of *sir2*, we found a complete abrogation of both phosphorylation events (Figure 5), indicating that, in contrast to *H4-K16Q*, the *sir2* mutant is defective both in the establishment and maintenance of the meiotic checkpoint, in a similar way to *dot1*. The fact that the lack of the H4K16ac Sir2 deacetylase does not cause exactly the same effect as the mimicked constitutive acetylation of the *H4-K16Q* mutant in *ndt80* strains suggests that Sir2 has additional checkpoint functions. On the other hand, in *ndt80* cells, *SAS2* disruption only showed a marginal effect on both H3T11 and Hop1 phosphorylation, similar to what we observed with the acetylation-defective *H4-K16R* mutant (Figure 5), indicating that Sas2 is primarily involved in checkpoint maintenance.

We also monitored the state of H4K16ac and, as we showed above (Figure 1), it was also unaffected when the checkpoint was triggered by *zip1* in *ndt80*-arrested cells (Figure 5). Strikingly, we found that the disruption of *SIR2* did not significantly increase global levels of H4K16ac in either *NDT80* or *ndt80* cells (Figures 5 and 6C), consistent with the notion that Sir2 is not the main genome-wide H4K16ac deacetylase and its action may be specifically restricted to precise heterochromatic domains [53, 54]. On the other hand, *SAS2* deletion clearly, but not completely, reduced H4K16ac (Figures 5 and 6C), suggesting that Sas2 is the main, but not the only, H4K16 acetyltransferase acting in the meiotic cell cycle.

Cross-talk between H4K16 acetylation and H3K79 methylation

Previous studies have shown that some histone PTMs positively or negatively affect other histone marks in what has been described as histone cross-talk, adding an extra layer of complexity to the control of different chromatin processes [71-73]. One example is the tri-methylation of H3K79 by Dot1, which is completely dependent upon the prior ubiquitylation of H2BK123 by Rad6/Bre1 [74]. It has also been described that H4K16ac modulates Dot1-dependent H3K79 methylation by promoting Dot1 binding to a short basic patch in the histone H4 tail in competition with Sir3 [75]. Since Dot1-dependent H3K79 methylation is required for the meiotic recombination checkpoint [21, 37] it was possible that the impact of H4K16ac on the checkpoint (Figures 2 and 3) was exerted via regulation of H3K79me. To explore this possibility, we first analyzed the effect of *H4-K16R* and *H4-K16Q* mutations on H3K79 mono-, di- and tri-methylation in *zip1 ndt80* checkpoint-activated and pachytene-arrested cells (Figures 5 and 7A, 7B). Given the distributive mode of action of the Dot1 methyltransferase [76], an impaired Dot1 catalytic activity is manifested as a reduction in H3K79me3 concomitant with an increase in H3K79me1 and H3K79me2 [21, 76]. Indeed, we observed higher levels of H3K79me1 and H3K79me2 in both H4K16ac-defective mutants, as well as a reduction in those of H3K79me3 (Figures 5 and 7A, 7B), which is the most relevant form to sustain the meiotic checkpoint response [21]. Thus, these findings suggest that H4K16ac mutants affect the activity of Dot1. We also observed that, like *H4-K16R*, the absence of the H4K16 acetyltransferase Sas2 also increased H3K79me1 and H3K79me2 and reduced H3K79me3 (Figure 5). Curiously, disruption of *SIR2*, did not have any effect on global H3K79me levels (Figure 5), again consistent with the notion that Sir2 meiotic checkpoint function can be exerted, at least in part, in a way that is independent from a global activity on H4K16ac.

Since Dot1 catalytic activity appears to be compromised in H4K16ac mutants, we explored whether *DOT1* overexpression would restore normal H3K79me3 levels and meiotic checkpoint function in *zip1 H4-K16R* or *zip1 H4-K16Q* double mutants. *DOT1* was overexpressed from a high-copy plasmid (Figure S2) and the pattern of H3K79me was analyzed at 0 h and 20 h after meiotic induction (Figure 7A, 7B). We found that the increased H3K79me1 and H3K79me2 levels observed in the *zip1 H4-K16R* and *zip1 H4-K16Q* mutants were reduced upon *DOT1* overexpression (Figure 7A, 7B). On the contrary, high doses of Dot1 increased the amount of H3K79me3 in *zip1 H4-K16R* and *zip1 H4-K16Q*, although it did not reach normal wild-type levels (Figure 7A, 7B). These observations confirm that overexpression of *DOT1* can partially compensate for the crippled Dot1 methyltransferase activity when H4K16ac metabolism is altered; therefore, we analyzed the effect on the meiotic checkpoint by monitoring the kinetics of meiotic divisions.

We have shown before that *H4-K16R* releases the checkpoint-dependent *zip1* meiotic delay to some extent and *H4-K16Q* completely alleviates the *zip1* block (Figure 2B). Interestingly, *DOT1* overexpression resulted in less efficient meiotic progression in *zip1 H4-K16R* and *zip1 H4-K16Q* cells compared to the controls transformed with empty vector (Figure 7C, S1C), consistent with a partial restoration of the checkpoint. Altogether, these results suggest that the effect of *H4-K16R* and *H4-K16Q* mutations on the meiotic checkpoint triggered by a *zip1* mutant is exerted, at least in part, through their effect on modulating proper H3K79 methylation pattern.

Relationship between Sir2, H4K16ac and Pch2 nucleolar localization

In *Saccharomyces cerevisiae*, the Pch2 protein is a negative regulator of Hop1 chromosomal abundance in synapsed chromosomes [77, 78], but it is required for the *zip1*-induced meiotic checkpoint promoting Hop1 phosphorylation at T318 [36, 59]. The majority of Pch2 localizes to the unsynapsed nucleolar region of chromosome XII that contains the ribosomal RNA genes (rDNA), where it is required to exclude the meiosis-specific Hop1 protein from the nucleolus. This nucleolar localization of Pch2 is completely

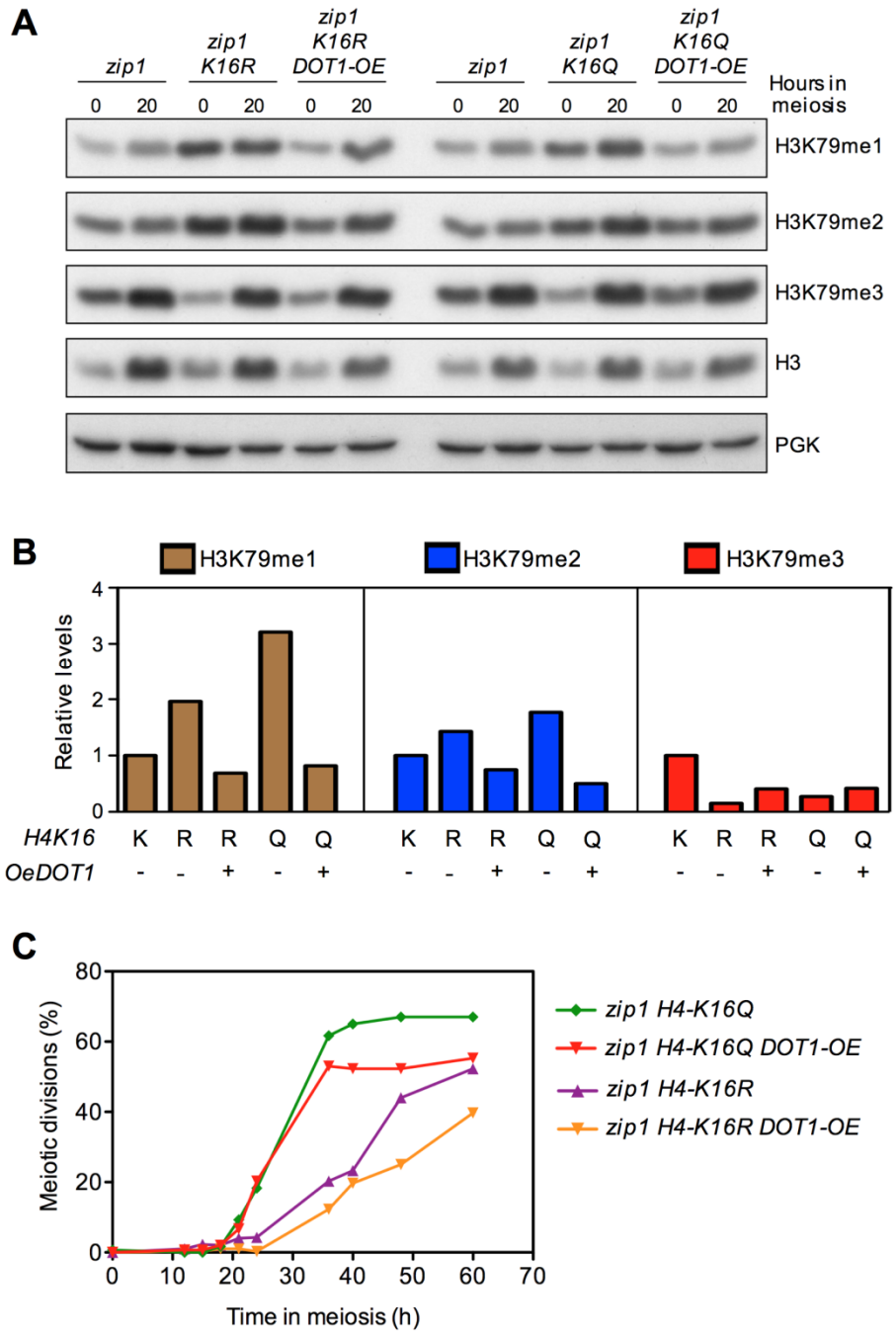

FIGURE 7: *DOT1* overexpression partially restores the meiotic checkpoint in H4K16ac-deficient mutants. **(A)** Western blot analysis of H3K79 methylation species in vegetative (T=0h) and meiotic cells (T=20h). Total H3 and PGK were used as loading controls. **(B)** Quantification of relative levels of the H3K79 methylation forms at T=0 from the blots shown in (A). Total H3 signal was used for normalization. **(C)** Time course of meiotic nuclear divisions; the percentage of cells with two or more nuclei is presented. Strains are DP422 (*zip1*), DP995 (*zip1 H4-K16R*) and DP1001 (*zip1 H4-K16Q*), transformed either with an empty vector or with the high-copy pSS63 *DOT1* overexpression plasmid (*DOT1-OE*).

dependent on the Sir2 deacetylase, which is also located in the rDNA [36], and deletion of *SIR2* impairs the meiotic checkpoint (Figures 5 and 6). Moreover, the Dot1 meiotic checkpoint factor regulates both Sir2 and Pch2 nucleolar localization [21, 37]. This scenario points to a pivotal role for the nucleolar Pch2 in the pachytene checkpoint [59] and prompted us to investigate if *H4-K16R* and/or *H4-K16Q* mutations affected the nucleolar localization of Pch2 on meiotic chromosome spreads.

In *zip1* cells, when the meiotic checkpoint is activated, Pch2 localization is limited to the nucleolar (rDNA) region (Figure 8). As it has been previously shown [36], in *zip1 sir2* cells the nucleolar concentration of Pch2 was lost and the protein appeared in form of foci dispersed throughout the meiotic chromosomes (Figure 8). Then, we analyzed Pch2 distribution in the *zip1 H4-K16Q* and *zip1 H4-K16R* mutants. We found that the Pch2 signal was still located in a restricted chromosomal area, presumably the rDNA region, but it was somehow more diffused although to a lesser extent than in *zip1 sir2* (Figure 8). Thus, like Dot1 and Sir2, these findings point to a role for H4K16ac in delimiting the nucleolar confinement of Pch2 and its exclusion from the rest of the chromatin, although the action of Sir2 must not be exerted only on H4K16ac because the effect of *SIR2* deletion on Pch2 localization is stronger than that of H4K16 mutations.

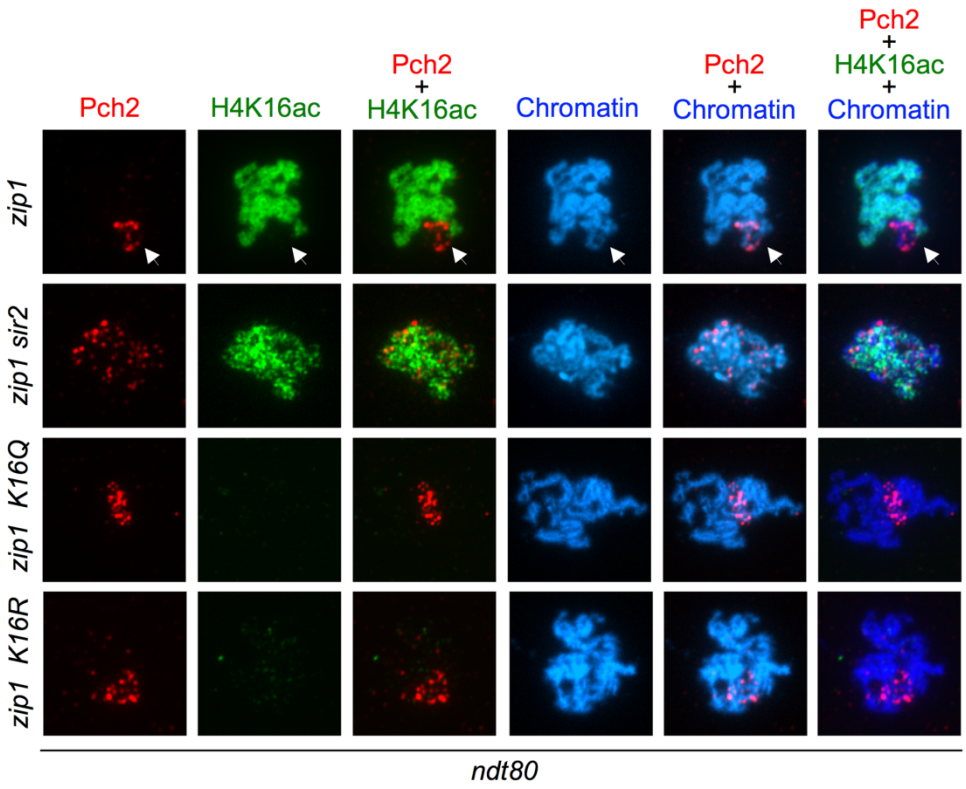

FIGURE 8: Analysis of Pch2 localization in H4K16ac-deficient mutants. Immunofluorescence of meiotic chromosome spreads from *zip1* (DP1123), *zip1 sir2* (DP1124), *zip1 H4-K16R* (DP1121) and *zip1 H4-K16Q* (DP1139) stained with DAPI (blue) as well as with anti-HA to detect Pch2-HA (red) and anti-H4K16ac (green) antibodies. The arrows point to the rDNA region where Pch2 accumulates and is devoid of H4K16ac. Representative nuclei are shown. Spreads were prepared after 24 h of meiotic induction in *ndt80* strains.

In addition, we also examined the distribution of H4K16ac on meiotic chromosomes. We used an antibody that recognizes the nucleolar Nsr1 protein involved in ribosome biogenesis [79] to unambiguously identify the rDNA region, which often appears as a chromatin loop on preparations of spread meiotic chromosomes. Strikingly, the H4K16ac histone mark was completely excluded from the rDNA in both wild-type and *zip1* nuclei (Figure 9), also displaying an exclusive localization pattern with that of nucleolar Pch2 (Figure 8, arrow). However, in the absence of Sir2, H4K16ac was distributed all along the chromatin, showing a complete co-localization with the DAPI staining, including the rDNA region marked by the nucleolar Nsr1 protein (Figure 9). Consistent with microarray studies in vegetative cells [53] and with our western blot analysis of global meiotic levels of H4K16ac (Figures 5 and 6), the H4K16ac signal on the bulk of the genome was not significantly altered in *sir2* mutants (Figure 9). These results indicate that Sir2 is the major deacetylase specifically responsible for preventing H4K16 acetylation in the rDNA during meiosis.

Besides the impact on the meiotic recombination checkpoint, it has been shown that *SIR2* disruption significantly alters the genomic distribution of Spo11-induced DSBs; with some genes displaying increased levels of DSBs whereas others experience reduced levels of DSBs in the absence of Sir2 [80]. Two defined genomic domains, such as subtelomeric regions and the rDNA array, show elevated recombination in the *sir2* mutant [80]. Pch2 also prevents recombination at the rDNA by excluding Hop1 from the nucleolar region [36, 59]. Moreover, Sir2 and Pch2 modulate the protection of DSB-induced meiotic instability at the rDNA borders [81]. It has been proposed that the effect of Sir2 on recombination at subtelomeric regions is exerted through the regulation of H4K16ac; however, the heterogeneous effect of Sir2 on the global meiotic DSB landscape implies that multiple factors and targets must be involved in addition to H4K16ac [80].

Concluding remarks

In this work we have explored the functional contribution of H4K16ac, the Sir2 deacetylase and the Sas2 acetyltransferase in the meiotic recombination checkpoint triggered by synaptonemal complex defects. In line with previous observations, our results indicate that an intricate network of histone PTMs fine-tune this meiotic quality control mechanism (Figure 10). We propose that reduced levels of Dot1-mediated H3K79me3 at the rDNA enable the enrichment of Sir2 in the nucleolus. The presence of Sir2 at the rDNA region is responsible for the low level of H4K16ac in this area and, together with an additional unknown Sir2 target, confines Pch2 in the nucleolus. The Pch2 ATPase is critical to orchestrate the proper balance between the amount of Hop1 bound to chromosome axes and phosphorylated Hop1, which in turn sustains Mek1 activation [21, 59]. Nevertheless, the precise mechanism by which nucleolar Pch2 regulates the phosphorylation status of the Hop1 checkpoint adaptor located at the axes and excluded from the rDNA remains to be determined.

Curiously, when meiotic progression is prevented by the *ndt80* mutation, we have observed different checkpoint activity phenotypes resulting from deletion of *SIR2* compared with *H4-K16* or *sas2* mutants. Whereas Sir2 is required for Mek1 activation in any condition, Sas2/H4K16ac only affect the maintenance of Mek1 activa-

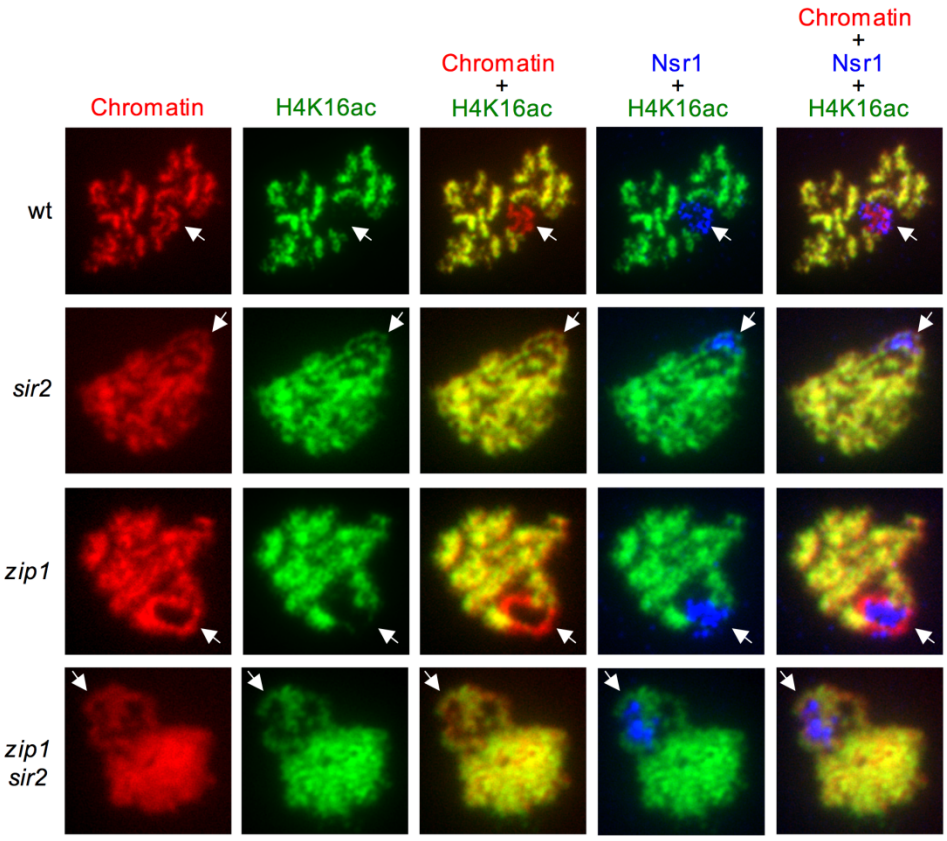

FIGURE 9: Sir2 excludes H4K16ac from the rDNA region. Immunofluorescence of meiotic chromosome spreads from wild type (BR2495), *sir2* (DP262), *zip1* (DP1123) and *zip1 sir2* (DP1124), stained with DAPI (red) as well as with anti-H4K16ac (green) and anti-Nsr1 (blue) antibodies. The arrows point to the rDNA region identified by Nsr1 staining. Representative nuclei are shown. Spreads were prepared after 16 h of meiotic induction for BR2495 and DP262 and 24 h for DP1123 and DP1124.

tion in *NDT80*-proficient cells, thus supporting the notion that Sir2 acts on additional targets.

We hypothesize that the general status of H4K16ac modulates DNA repair pathways involved in the resolution of recombination intermediates accumulated in *zip1* triggering the checkpoint arrest. Alteration of H4K16ac dynamics by *SAS2* deletion or *H4-K16* mutations, would allow the Ndt80-dependent repair of those intermediates thus allowing meiotic progression in *zip1.* Further experimental work will be required to explore this possibility.

MATERIALS AND METHODS

Yeast strains

Yeast strains genotypes are listed in Table S1. All the strains are in the BR1919 or BR2495 genetic background [82]. Gene deletion and tagging were performed using a PCR-based approach or by genetic crosses always in an isogenic background. The *dot1::URA3*, *zip1::LYS2, zip1::LEU2, sir2::URA3* and *ndt80::LEU2* deletions were previously described [5, 26, 31, 37, 83]. In the plasmid-borne *H4-K16R and H4-K16Q* mutants, both genomic copies of the histone H3-H4 encoding genes (*HHT1-HHF1* and *HHT2-HHF2*) were deleted and the wild-type *HHT2-HHF2* genes or the modified *HHT2-hhf2(K16R)* or *HHT2-hhf2(K16Q)* versions were expressed from the centromeric plasmids pRM204, pWD23 and pWD25, respectively, as the only source of H3-H4 histones [65]. Alternatively, both copies of the histone H4-encoding genes *HHF1* and *HHF2* were mutated in their genomic loci to *K16R* and *K16Q* following the *delitto perfetto* approach [84]. N-terminal tagging of Pch2 with three copies of the HA epitope and the *MEK1-GFP* construct were previously described [21, 36]. *DOT1-HA* was overexpressed from the pSS63 plasmid [37].

Meiotic time courses

Strains were grown on 2xSC (3,5 ml) for 20-24 h and then transferred to 2,5 ml of YPDA where they were incubated to saturation for an additional 8 h. Cells were then harvested, washed with 2% potassium acetate (KAc), resuspended into 10 ml of KAc and incubated at 30°C with vigorous shaking (235 rpm) to induce meiosis and sporulation. 20 mM adenine and 10 mM uracil was added to both YPDA and KAc media. Culture volumes were scaled up when needed. Aliquots of cells were removed at different time points for analysis. To analyze meiotic divisions, cells were fixed in 70% ethanol, washed in phosphate-buffered saline (PBS) and stained with 1 mg/ml DAPI for 15 min at room temperature. Nuclei were observed by fluorescence microscopy and at least 300 cells were scored for each strain at each time point in every experiment. Meiotic kinetics experiments were repeated several times and representative experiments are shown. Dityrosine fluorescence was analyzed as previously described [37] and spore viability was determined by tetrad dissection.

Western blotting

TCA yeast whole cell extracts from 5-10 ml aliquots of meiotic cultures were prepared as described previously [18] and proteins were resolved by SDS-PAGE and then transferred to PVDF membranes. To resolve the phosphorylated forms of Mek1, 10% SDS-PAGE gels with a 29:1 ratio of acrylamide:bisacrylamide containing 37,5 µM Phos-tag reagent (Wako) and 75 µM $MnCl_2$ were prepared as described [18, 21],

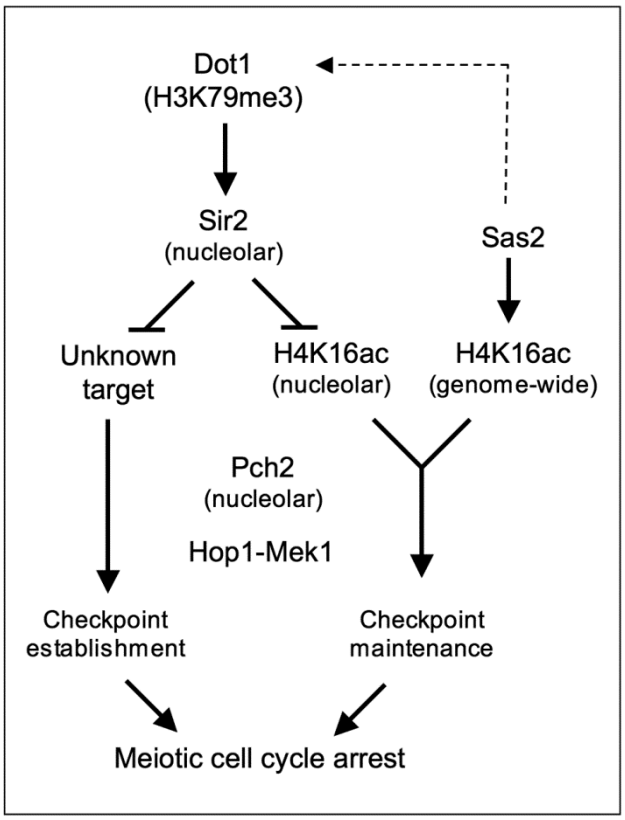

FIGURE 10: A model for the regulation of the meiotic checkpoint by histone post-translational modifications. See text for details.

whereas normal 15% or 10% gels (acrylamide:bisacrylamide 37,5:1) were used for detection of H4K16ac, H3T11ph and H3K79me or Mek1, Hop1-T318ph, Cdc5 and Dot1-HA, respectively. Blots were probed with the following primary antibodies: rabbit polyclonal antibodies raised against Mek1 (1:1000) [13], Hop1-T318 (1:1000; kindly provided by J. Carballo), H3T11ph (1:2000; Abcam 5168), H4K16ac (1:2000; Millipore 07-329), H3K79-me1 (1:1000; Abcam ab2886), H3K79-me2 (1:2000; Abcam ab3594) and H3K79-me3 (1:2000; Abcam ab2621); goat polyclonal antibody against Cdc5 (1:1000; Santa Cruz Biotechnology sc-6733); mouse monoclonal antibody against the HA epitope (1:2000; Roche 12CA5). A mouse monoclonal antibody directed against 3-phosphoglycerate kinase (PGK) (1:10000; Molecular Probes A-6457) or a rabbit polyclonal antibody against histone H3 (1:5000; Abcam ab1791) were used as loading controls. HRP-conjugated secondary antibodies were from GE Healthcare (NA934 and NA931) or Santa Cruz Biotechnology (sc-2033). The Pierce ECL or ECL-2 reagents (Thermo Scientific) were used for detection and the signal was captured on film (Amersham Hyperfilm ECL; GE Healthcare) and/or with a ChemiDoc XRS (BioRad) system, using the Quantity One software (Bio-Rad). The same software was used to quantify protein levels.

Cytology

Whole cell images were captured with a Nikon Eclipse 90i fluorescence microscope controlled with the MetaMorph software (Molecular Devices) and equipped with an Orca-AG (Hamamatsu) CCD camera and a PlanApo VC 100X 1.4 NA objective. To analyze Mek1-GFP foci in live meiotic cells, exposure time was 1 second and stacks of 11 planes at 0,4 µm were captured. Maximum intensity projections were generated with the NIH ImageJ software (http://rsb.info.nih.gov/ij/). To outline the contour of the cells in the representative whole-cell images presented, an overlay of the DIC image with 15-20% transparency over the GFP signal is shown. Immunofluorescence of meiotic chromosome spreads was performed as previously described [36]. To detect the HA-tagged Pch2 and H4K16ac, a mouse monoclonal anti-HA antibody (12CA5, Roche) or a rabbit polyclonal anti H4K16ac (Millipore 07-329) were used at 1:200 dilution. Nsr1 was detected with a mouse monoclonal antibody (clone 31C4, ThermoFisher MA1-10030) used at 1:200 dilution. Alexa-Fluor-488 and Alexa-Fluor-594-conjugated secondary antibodies from Molecular Probes were used at 1:200 dilution. Images were captured with the same equipment as indicated above.

ACKNOWLEDGEMENTS

We are grateful to Shelly Berger, Félix Prado and Jesús Carballo for plasmids and antibodies and to Natalia Calixto for help with strain construction. SC was partially supported by a postdoctoral JAE-Doc contract and DO by a predoctoral JAE-Predoc contract from the Consejo Superior de Investigaciones Científicas (CSIC) of Spain. This work was funded by grants BFU2012-35748 and BFU2015-65417-R, from the Ministry of Economy and Competitiveness of Spain (MINECO), and grant CSI084U16 from Junta de Castilla y León (Spain), to PSS.

SUPPLEMENTAL MATERIAL

All supplemental data for this article are available online at www.microbialcell.com.

CONFLICT OF INTEREST

The authors declare there is no conflict of interest.

Please cite this article as: Santiago Cavero, Esther Herruzo, David Ontoso and Pedro A. San-Segundo (2016). Impact of histone H4K16 acetylation on the meiotic recombination checkpoint in *Saccharomyces cerevisiae*. **Microbial Cell** 3(12): 606-620. doi: 10.15698/mic2016.12.548

REFERENCES

1. Petronczki M, Siomos MF, Nasmyth K (**2003**). Un menage a quatre: the molecular biology of chromosome segregation in meiosis. **Cell** 112(4): 423-440.

2. Kleckner N (**1996**). Meiosis: how could it work? **Proc Natl Acad Sci USA** 93(16): 8167-8174.

3. Keeney S (**2001**). Mechanism and control of meiotic recombination initiation. **Curr Top Dev Biol** 52(1-53).

4. Roeder GS (**1997**). Meiotic chromosomes: it takes two to tango. **Genes Dev** 11(20): 2600-2621.

5. Sym M, Engebrecht JA, Roeder GS (**1993**). ZIP1 is a synaptonemal complex protein required for meiotic chromosome synapsis. **Cell** 72(3): 365-378.

6. Dong H, Roeder GS (**2000**). Organization of the yeast Zip1 protein within the central region of the synaptonemal complex. **J Cell Biol** 148(3): 417-426.

7. Roeder GS, Bailis JM (**2000**). The pachytene checkpoint. **Trends Genet** 16(9): 395-403.

8. Subramanian VV, Hochwagen A (**2014**). The meiotic checkpoint network: step-by-step through meiotic prophase. **Cold Spring Harb Perspect Biol** 6(10): a016675.

9. MacQueen AJ, Hochwagen A (**2011**). Checkpoint mechanisms: the puppet masters of meiotic prophase. **Trends Cell Biol** 21(7): 393-400.

10. Harrison JC, Haber JE (**2006**). Surviving the breakup: the DNA damage checkpoint. **Annu Rev Genet** 40(209-235).

11. Lovejoy CA, Cortez D (**2009**). Common mechanisms of PIKK regulation. **DNA Repair (Amst)** 8(9): 1004-1008.

12. Hong EJ, Roeder GS (**2002**). A role for Ddc1 in signaling meiotic double-strand breaks at the pachytene checkpoint. **Genes Dev** 16(3): 363-376.

13. Refolio E, Cavero S, Marcon E, Freire R, San-Segundo PA (**2011**). The Ddc2/ATRIP checkpoint protein monitors meiotic recombination intermediates. **J Cell Sci** 124(Pt 14): 2488-2500.

14. Lydall D, Nikolsky Y, Bishop DK, Weinert T (**1996**). A meiotic recombination checkpoint controlled by mitotic checkpoint genes. **Nature** 383(6603): 840-843.

15. Carballo JA, Johnson AL, Sedgwick SG, Cha RS (**2008**). Phosphorylation of the axial element protein Hop1 by Mec1/Tel1 ensures meiotic interhomolog recombination. **Cell** 132(5): 758-770.

16. Woltering D, Baumgartner B, Bagchi S, Larkin B, Loidl J, de los Santos T, Hollingsworth NM (**2000**). Meiotic segregation, synapsis, and recombination checkpoint functions require physical interaction between the chromosomal proteins Red1p and Hop1p. **Mol Cell Biol** 20(18): 6646-6658.

17. Eichinger CS, Jentsch S (**2010**). Synaptonemal complex formation and meiotic checkpoint signaling are linked to the lateral element protein Red1. **Proc Natl Acad Sci USA** 107(25): 11370-11375.

18. Acosta I, Ontoso D, San-Segundo PA (**2011**). The budding yeast polo-like kinase Cdc5 regulates the Ndt80 branch of the meiotic recombination checkpoint pathway. **Mol Biol Cell** 22(18): 3478-3490.

19. Bailis JM, Roeder GS (**2000**). Pachytene exit controlled by reversal of Mek1-dependent phosphorylation. **Cell** 101(2): 211-221.

20. Niu H, Li X, Job E, Park C, Moazed D, Gygi SP, Hollingsworth NM (**2007**). Mek1 kinase is regulated to suppress double-strand break repair between sister chromatids during budding yeast meiosis. **Mol Cell Biol** 27(15): 5456-5467.

21. Ontoso D, Acosta I, van Leeuwen F, Freire R, San-Segundo PA (**2013**). Dot1-dependent histone H3K79 methylation promotes activation of the Mek1 meiotic checkpoint effector kinase by regulating the Hop1 adaptor. **PLoS Genet** 9(1): e1003262.

22. Rockmill B, Roeder GS (**1991**). A meiosis-specific protein kinase homolog required for chromosome synapsis and recombination. **Genes Dev** 5(12B): 2392-2404.

23. Wan L, de los Santos T, Zhang C, Shokat K, Hollingsworth NM (**2004**). Mek1 kinase activity functions downstream of *RED1* in the regulation of meiotic double strand break repair in budding yeast. **Mol Biol Cell** 15(1): 11-23.

24. Sourirajan A, Lichten M (**2008**). Polo-like kinase Cdc5 drives exit from pachytene during budding yeast meiosis. **Genes Dev** 22(19): 2627-2632.

25. Chu S, Herskowitz I (**1998**). Gametogenesis in yeast is regulated by a transcriptional cascade dependent on Ndt80. **Mol Cell** 1(5): 685-696.

26. Tung KS, Hong EJ, Roeder GS (**2000**). The pachytene checkpoint prevents accumulation and phosphorylation of the meiosis-specific transcription factor Ndt80. **Proc Natl Acad Sci USA** 97(22): 12187-12192.

27. Wang Y, Chang CY, Wu JF, Tung KS (**2011**). Nuclear localization of the meiosis-specific transcription factor Ndt80 is regulated by the pachytene checkpoint. **Mol Biol Cell** 22(11): 1878-1886.

28. Leu JY, Roeder GS (**1999**). The pachytene checkpoint in *S. cerevisiae* depends on Swe1-mediated phosphorylation of the cyclin-dependent kinase Cdc28. **Mol Cell** 4(5): 805-814.

29. Pak J, Segall J (**2002**). Role of Ndt80, Sum1, and Swe1 as targets of the meiotic recombination checkpoint that control exit from pachytene and spore formation in *Saccharomyces cerevisiae*. **Mol Cell Biol** 22(18): 6430-6440.

30. Storlazzi A, Xu L, Schwacha A, Kleckner N (**1996**). Synaptonemal complex (SC) component Zip1 plays a role in meiotic recombination independent of SC polymerization along the chromosomes. **Proc Natl Acad Sci USA** 93(17): 9043-9048.

31. Sym M, Roeder GS (**1994**). Crossover interference is abolished in the absence of a synaptonemal complex protein. **Cell** 79(2): 283-292.

32. Brachet E, Sommermeyer V, Borde V (**2012**). Interplay between modifications of chromatin and meiotic recombination hotspots. **Biol Cell** 104(2): 51-69.

33. Borde V, Robine N, Lin W, Bonfils S, Geli V, Nicolas A (**2009**). Histone H3 lysine 4 trimethylation marks meiotic recombination initiation sites. **EMBO J** 28(2): 99-111.

34. Acquaviva L, Drogat J, Dehe PM, de La Roche Saint-Andre C, Geli V (**2013**). Spp1 at the crossroads of H3K4me3 regulation and meiotic recombination. **Epigenetics** 8(4): 355-360.

35. Sommermeyer V, Beneut C, Chaplais E, Serrentino ME, Borde V (**2013**). Spp1, a member of the Set1 Complex, promotes meiotic DSB formation in promoters by tethering histone H3K4 methylation sites to chromosome axes. **Mol Cell** 49(1): 43-54.

36. San-Segundo PA, Roeder GS (**1999**). Pch2 links chromatin silencing to meiotic checkpoint control. **Cell** 97(3): 313-324.

37. San-Segundo PA, Roeder GS (**2000**). Role for the silencing protein Dot1 in meiotic checkpoint control. **Mol Biol Cell** 11(10): 3601-3615.

38. Feng Q, Wang H, Ng HH, Erdjument-Bromage H, Tempst P, Struhl K, Zhang Y (**2002**). Methylation of H3-lysine 79 is mediated by a new family of HMTases without a SET domain. **Curr Biol** 12(12): 1052-1058.

39. Ng HH, Feng Q, Wang H, Erdjument-Bromage H, Tempst P, Zhang Y, Struhl K (**2002**). Lysine methylation within the globular domain of histone H3 by Dot1 is important for telomeric silencing and Sir protein association. **Genes Dev** 16(12): 1518-1527.

40. Imai S, Armstrong CM, Kaeberlein M, Guarente L (**2000**). Transcriptional silencing and longevity protein Sir2 is an NAD-dependent histone deacetylase. **Nature** 403(6771): 795-800.

41. Rusche LN, Kirchmaier AL, Rine J (**2003**). The establishment, inheritance, and function of silenced chromatin in *Saccharomyces cerevisiae*. **Annu Rev Biochem** 72(481-516).

42. Xu F, Zhang Q, Zhang K, Xie W, Grunstein M (**2007**). Sir2 deacetylates histone H3 lysine 56 to regulate telomeric heterochromatin structure in yeast. **Mol Cell** 27(6): 890-900.

43. Meijsing SH, Ehrenhofer-Murray AE (**2001**). The silencing complex SAS-I links histone acetylation to the assembly of repressed chromatin by CAF-I and Asf1 in *Saccharomyces cerevisiae*. **Genes Dev** 15(23): 3169-3182.

44. Suka N, Luo K, Grunstein M (**2002**). Sir2p and Sas2p opposingly regulate acetylation of yeast histone H4 lysine16 and spreading of heterochromatin. **Nat Genet** 32(3): 378-383.

45. Kimura A, Umehara T, Horikoshi M (**2002**). Chromosomal gradient of histone acetylation established by Sas2p and Sir2p functions as a shield against gene silencing. **Nat Genet** 32(3): 370-377.

46. Sutton A, Shia WJ, Band D, Kaufman PD, Osada S, Workman JL, Sternglanz R (**2003**). Sas4 and Sas5 are required for the histone acetyltransferase activity of Sas2 in the SAS complex. **J Biol Chem** 278(19): 16887-16892.

47. Shia WJ, Osada S, Florens L, Swanson SK, Washburn MP, Workman JL (**2005**). Characterization of the yeast trimeric-SAS acetyltransferase complex. **J Biol Chem** 280(12): 11987-11994.

48. Chang CS, Pillus L (**2009**). Collaboration between the essential Esa1 acetyltransferase and the Rpd3 deacetylase is mediated by H4K12 histone acetylation in *Saccharomyces cerevisiae*. **Genetics** 183(1): 149-160.

49. Suka N, Suka Y, Carmen AA, Wu J, Grunstein M (**2001**). Highly specific antibodies determine histone acetylation site usage in yeast heterochromatin and euchromatin. **Mol Cell** 8(2): 473-479.

50. Borra MT, Langer MR, Slama JT, Denu JM (**2004**). Substrate specificity and kinetic mechanism of the Sir2 family of NAD+-dependent histone/protein deacetylases. **Biochemistry** 43(30): 9877-9887.

51. Smith JS, Brachmann CB, Celic I, Kenna MA, Muhammad S, Starai VJ, Avalos JL, Escalante-Semerena JC, Grubmeyer C, Wolberger C, Boeke JD (**2000**). A phylogenetically conserved NAD+-dependent protein deacetylase activity in the Sir2 protein family. **Proc Natl Acad Sci USA** 97(12): 6658-6663.

52. Braunstein M, Sobel RE, Allis CD, Turner BM, Broach JR (**1996**). Efficient transcriptional silencing in *Saccharomyces cerevisiae* requires a heterochromatin histone acetylation pattern. **Mol Cell Biol** 16(8): 4349-4356.

53. Robyr D, Suka Y, Xenarios I, Kurdistani SK, Wang A, Suka N, Grunstein M (**2002**). Microarray deacetylation maps determine genome-wide functions for yeast histone deacetylases. **Cell** 109(4): 437-446.

54. Gartenberg MR, Smith JS (**2016**). The Nuts and Bolts of Transcriptionally Silent Chromatin in *Saccharomyces cerevisiae*. **Genetics** 203(4): 1563-1599.

55. Tamburini BA, Tyler JK (**2005**). Localized histone acetylation and deacetylation triggered by the homologous recombination pathway of double-strand DNA repair. **Mol Cell Biol** 25(12): 4903-4913.

56. Masumoto H, Hawke D, Kobayashi R, Verreault A (**2005**). A role for cell-cycle-regulated histone H3 lysine 56 acetylation in the DNA damage response. **Nature** 436(7048): 294-298.

57. Yu Y, Teng Y, Liu H, Reed SH, Waters R (**2005**). UV irradiation stimulates histone acetylation and chromatin remodeling at a repressed yeast locus. **Proc Natl Acad Sci USA** 102(24): 8650-8655.

58. Govin J, Dorsey J, Gaucher J, Rousseaux S, Khochbin S, Berger SL (**2010**). Systematic screen reveals new functional dynamics of histones H3 and H4 during gametogenesis. **Genes Dev** 24(16): 1772-1786.

59. Herruzo E, Ontoso D, Gonzalez-Arranz S, Cavero S, Lechuga A, San-Segundo PA (**2016**). The Pch2 AAA+ ATPase promotes phosphorylation of the Hop1 meiotic checkpoint adaptor in response to synaptonemal complex defects. **Nucleic Acids Res** 44(16): 7722-7741.

60. Penedos A, Johnson AL, Strong E, Goldman AS, Carballo JA, Cha RS (**2015**). Essential and Checkpoint Functions of Budding Yeast ATM and ATR during Meiotic Prophase Are Facilitated by Differential Phosphorylation of a Meiotic Adaptor Protein, Hop1. **PLoS One** 10(7): e0134297.

61. Hollingsworth NM (**2008**). Deconstructing meiosis one kinase at a time: polo pushes past pachytene. **Genes Dev** 22(19): 2596-2600.

62. Lee BH, Amon A (**2003**). Polo kinase--meiotic cell cycle coordinator. **Cell Cycle** 2(5): 400-402.

63. Lee BH, Amon A (**2003**). Role of Polo-like kinase *CDC5* in programming meiosis I chromosome segregation. **Science** 300(5618): 482-486.

64. Clyne RK, Katis VL, Jessop L, Benjamin KR, Herskowitz I, Lichten M, Nasmyth K (**2003**). Polo-like kinase Cdc5 promotes chiasmata formation and cosegregation of sister centromeres at meiosis I. **Nat Cell Biol** 5(5): 480-485.

65. Dang W, Steffen KK, Perry R, Dorsey JA, Johnson FB, Shilatifard A, Kaeberlein M, Kennedy BK, Berger SL (**2009**). Histone H4 lysine 16 acetylation regulates cellular lifespan. **Nature** 459(7248): 802-807.

66. Choy JS, Acuna R, Au WC, Basrai MA (**2011**). A role for histone H4K16 hypoacetylation in *Saccharomyces cerevisiae* kinetochore function. **Genetics** 189(1): 11-21.

67. Cesarini E, D'Alfonso A, Camilloni G (**2012**). H4K16 acetylation affects recombination and ncRNA transcription at rDNA in *Saccharomyces cerevisiae*. **Mol Biol Cell** 23(14): 2770-2781.

68. Hepworth SR, Friesen H, Segall J (**1998**). *NDT80* and the meiotic recombination checkpoint regulate expression of middle sporulation-specific genes in *Saccharomyces cerevisiae*. **Mol Cell Biol** 18(10): 5750-5761.

69. Chu S, DeRisi J, Eisen M, Mulholland J, Botstein D, Brown PO, Herskowitz I (**1998**). The transcriptional program of sporulation in budding yeast. **Science** 282(5389): 699-705.

70. Xu L, Ajimura M, Padmore R, Klein C, Kleckner N (**1995**). *NDT80*, a meiosis-specific gene required for exit from pachytene in *Saccharomyces cerevisiae*. **Mol Cell Biol** 15(12): 6572-6581.

71. Bannister AJ, Kouzarides T (**2011**). Regulation of chromatin by histone modifications. **Cell Res** 21(3): 381-395.

72. Kouzarides T (**2007**). Chromatin modifications and their function. **Cell** 128(4): 693-705.

73. Millar CB, Grunstein M (**2006**). Genome-wide patterns of histone modifications in yeast. **Nat Rev Mol Cell Biol** 7(9): 657-666.

74. Lee JS, Shukla A, Schneider J, Swanson SK, Washburn MP, Florens L, Bhaumik SR, Shilatifard A (**2007**). Histone crosstalk between H2B monoubiquitination and H3 methylation mediated by COMPASS. **Cell** 131(6): 1084-1096.

75. Altaf M, Utley RT, Lacoste N, Tan S, Briggs SD, Cote J (**2007**). Interplay of chromatin modifiers on a short basic patch of histone H4 tail defines the boundary of telomeric heterochromatin. **Mol Cell** 28(6): 1002-1014.

76. Frederiks F, Tzouros M, Oudgenoeg G, van Welsem T, Fornerod M, Krijgsveld J, van Leeuwen F (**2008**). Nonprocessive methylation by Dot1 leads to functional redundancy of histone H3K79 methylation states. **Nat Struct Mol Biol** 15(6): 550-557.

77. Borner GV, Barot A, Kleckner N (**2008**). Yeast Pch2 promotes domainal axis organization, timely recombination progression, and arrest of defective recombinosomes during meiosis. **Proc Natl Acad Sci USA** 105(9): 3327-3332.

78. Joshi N, Barot A, Jamison C, Borner GV (**2009**). Pch2 links chromosome axis remodeling at future crossover sites and crossover distribution during yeast meiosis. **PLoS Genet** 5(7): e1000557.

79. Yan C, Melese T (**1993**). Multiple regions of NSR1 are sufficient for accumulation of a fusion protein within the nucleolus. **J Cell Biol** 123(5): 1081-1091.

80. Mieczkowski PA, Dominska M, Buck MJ, Lieb JD, Petes TD (**2007**). Loss of a histone deacetylase dramatically alters the genomic distribution of Spo11p-catalyzed DNA breaks in *Saccharomyces cerevisiae*. **Proc Natl Acad Sci USA** 104(10): 3955-3960.

81. Vader G, Blitzblau HG, Tame MA, Falk JE, Curtin L, Hochwagen A (**2011**). Protection of repetitive DNA borders from self-induced meiotic instability. **Nature** 477(7362): 115-119.

82. Rockmill B, Roeder GS (**1990**). Meiosis in asynaptic yeast. **Genetics** 126(3): 563-574. PMID: 2249756.

83. Chien CT, Buck S, Sternglanz R, Shore D (**1993**). Targeting of SIR1 protein establishes transcriptional silencing at *HM* loci and telomeres in yeast. **Cell** 75(3): 531-541.

84. Storici F, Resnick MA (**2006**). The *Delitto Perfetto* approach to *in vivo* site-directed mutagenesis and chromosome rearrangements with synthetic oligonucleotides in yeast. **Methods Enzymol** 409(329-345).

SUPPLEMENTAL INFORMATION

Impact of histone H4K16 acetylation on the meiotic recombination checkpoint in *Saccharomyces cerevisiae*

Santiago Cavero[1, 2], Esther Herruzo[1], David Ontoso[1, 3] and Pedro A. San-Segundo[1, *]

[1] Instituto de Biología Funcional y Genómica. Consejo Superior de Investigaciones Científicas and University of Salamanca, 37007 Salamanca, Spain

[*] To whom correspondence should be addressed: Email: pedross@usal.es

Table S1. *Saccharomyces cerevisiae* strains

Strain	Genotype *
BR1919-2N	*MAT***a**/*MATα leu2-3,112 his4-260 ura3-1 ade2-1 thr1-4 trp1-289*
BR2495	*MAT***a**/*MATα leu2-27/leu2-3,112 his4-280/his4-260 trp1-1/trp1-289 arg4-8/ARG4 thr1-1/thr1-4 cyh10/CYH10 ura3-1 ade2-1*
DP262	BR2495 *sir2::URA3 PCH2-3HA*
DP421	BR1919-2N *lys2ΔNheI*
DP422	DP421 *zip1::LYS2*
DP424	DP421 *ndt80::LEU2*
DP428	DP421 *zip1::LYS2 ndt80::LEU2*
DP582	DP421 *zip1::LYS2 ndt80::LEU2 MEK1-GFP::kanMX6*
DP584	DP421 *ndt80::LEU2 MEK1-GFP::kanMX6*
DP634	DP421 *(hht1-hhf1)::kanMX6 (hht2-hhf2)::natMX4 p(HHT2-HHF2)::TRP1*
DP635	DP421 *(hht1-hhf1)::kanMX6 (hht2-hhf2)::natMX4 p(HHT2-hhf2-K16R)::TRP1*
DP636	DP421 *(hht1-hhf1)::kanMX6 (hht2-hhf2)::natMX4 p(HHT2-hhf2-K16Q)::TRP1*
DP639	DP421 *(hht1-hhf1)::kanMX6 (hht2-hhf2)::natMX4 p(HHT2-HHF2)::TRP1 zip1::LYS2*
DP640	DP421 *(hht1-hhf1)::kanMX6 (hht2-hhf2)::natMX4 p(HHT2-hhf2-K16R)::TRP1 zip1::LYS2*
DP641	DP421 *(hht1-hhf1)::kanMX6 (hht2-hhf2)::natMX4 p(HHT2-hhf2-K16Q)::TRP1 zip1::LYS2*
DP655	DP421 *zip1::LYS2 ndt80::LEU2 dot1::kanMX6*
DP994	DP421 *hhf1-K16R hhf2-K16R*
DP995	DP421 *hhf1-K16R hhf2-K16R zip1::LYS2*
DP996	DP421 *hhf1-K16R hhf2-K16R zip1::LYS2 ndt80::LEU2*
DP1000	DP421 *hhf1-K16Q hhf2-K16Q*
DP1001	DP421 *hhf1-K16Q hhf2-K16Q zip1::LYS2*
DP1002	DP421 *hhf1-K16Q hhf2-K16Q zip1::LYS2 ndt80::LEU2*
DP1073	DP421 *zip1::LYS2 ndt80::LEU2 sas2::natMX4*
DP1086	DP421 *zip1::LYS2 ndt80::LEU2 sir2::URA3*
DP1089	DP421 *zip1::LYS2 ndt80::LEU2 hhf1-K16R hhf2-K16R MEK1-GFP::kanMX6*
DP1090	DP421 *zip1::LYS2 ndt80::LEU2 hhf1-K16Q hhf2-K16Q MEK1-GFP::kanMX6*
DP1121	DP421 *zip1::LEU2 ndt80::kanMX6 hhf1-K16R hhf2-K16R PCH2-3HA*
DP1123	DP421 *zip1::LEU2 ndt80::kanMX6 PCH2-3HA*
DP1124	DP421 *zip1::LEU2 ndt80::kanMX6 sir2::URA3 PCH2-3HA*
DP1139	DP421 *zip1::LEU2 ndt80::kanMX6 hhf1-K16Q hhf2-K16Q PCH2-3HA*
DP1401	DP421 *zip1::LYS2 sir2::URA3*
DP1410	DP421 *zip1::LYS2 sas2::natMX4*

* Unless indicated, all diploid strains are homozygous for the markers.

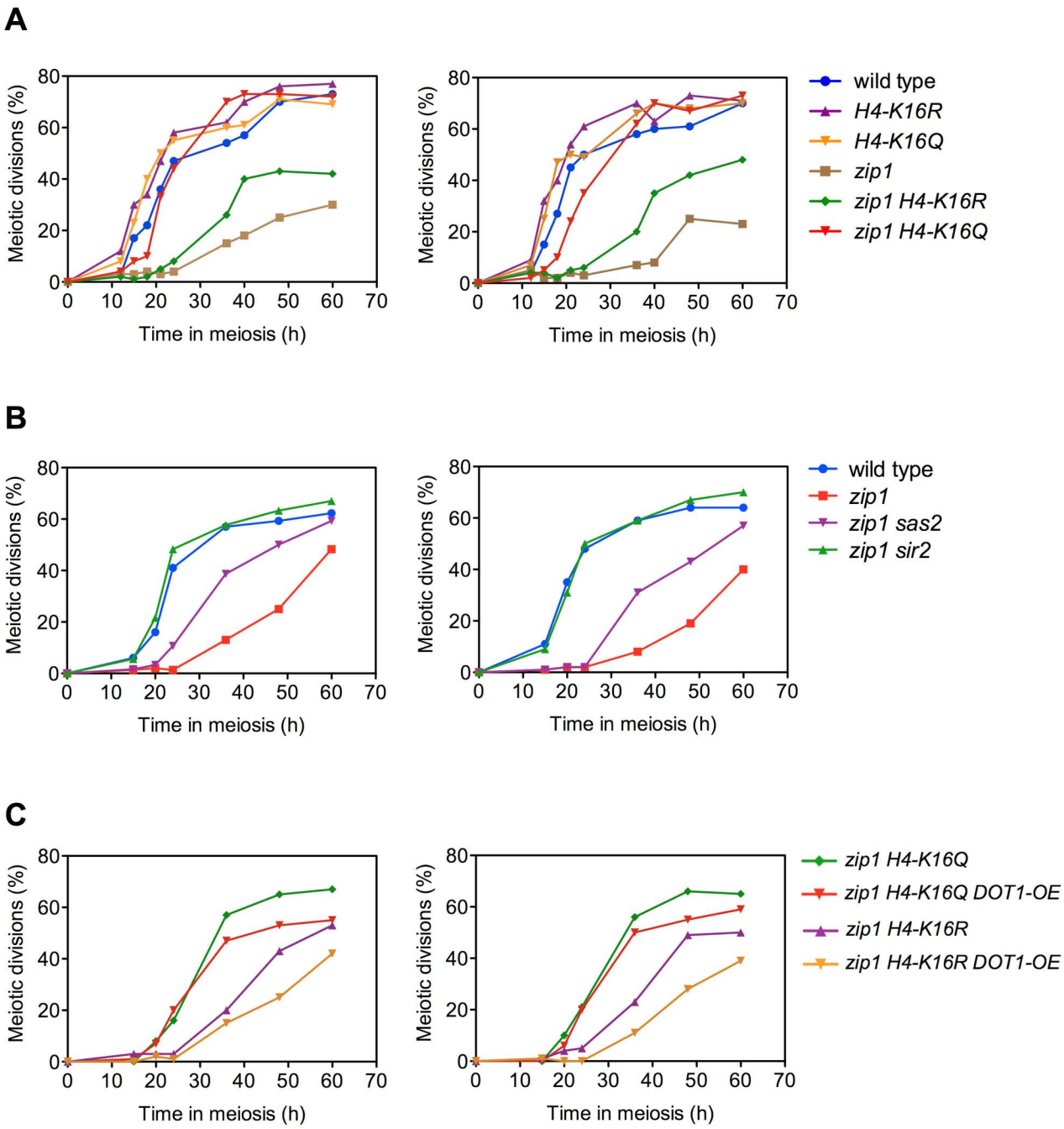

Figure S1. Additional replicates of the representative meiotic time courses shown in main figures

(A) Two replicates of the time course shown in Figure 2B

(B) Two replicates of the time course shown in Figure 6A

(C) Two replicates of the time course shown in Figure 7C

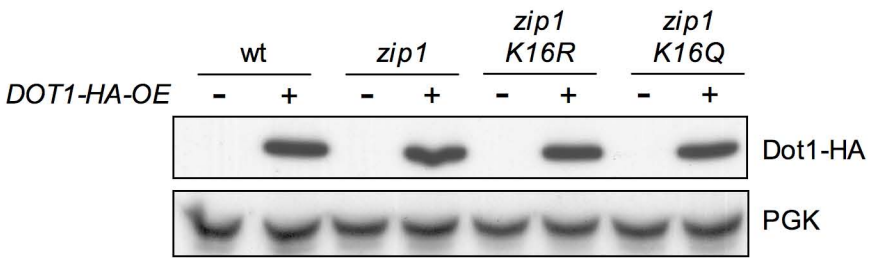

Figure S2. *DOT1* overexpression in H4K16ac mutants
Western blot analysis of *DOT1* overexpression in wild-type (DP421), *zip1* (DP422), *zip1 H4-K16R* (DP995) and *zip1 H4-K16Q* (DP1001) strains transformed either with an empty vector or with a high-copy plasmid expressing *DOT1-HA* (pSS63). PGK was used as a loading control.

CONCLUSIONES

1. Los niveles globales de H4K16ac no varían a lo largo de la meiosis en el mutante *zip1Δ*, a pesar del importante papel que desempeña Sir2 en el *checkpoint* meiótico.

2. El control de los niveles adecuados de H4K16ac es necesario para mantener el *checkpoint*, pero no para su activación.

3. Las mutaciones *sir2Δ* y *sas2Δ* suprimen, completa y parcialmente, el bloqueo meiótico del mutante *zip1Δ*, respectivamente.

4. Además de regular los niveles de H4K16ac, Sir2 tiene funciones adicionales en el *checkpoint*, puesto que el efecto de la ausencia de Sir2 es mayor que el provocado por una acetilación constitutiva de H4K16.

5. La función de H4K16ac en el *checkpoint* meiótico viene dada, al menos en parte, por el efecto en la metilación de H3K79.

6. Sir2 previene la acetilación de H4K16 en el rDNA y actúa sobre alguna diana adicional para mantener la reclusión de Pch2 en el nucleolo.

CONCLUSIONS

1. Global levels of H4K16ac do not change in the *zip1* mutant, despite the important role of Sir2 in the meiotic checkpoint.

2. Proper levels of H4K16ac are required for checkpoint maintenance, but not for checkpoint activation.

3. Mutation of *SIR2* and *SAS2* partially and completely suppress the *zip1*-induced checkpoint, respectively.

4. The checkpoint defect caused by the lack of Sir2 is stronger than the one resulting from mimicking constitutive acetylation of H4K16, implying that Sir2 possesses additional checkpoint functions besides H4K16ac regulation.

5. The effect of H4K16ac in the meiotic checkpoint is exerted, at least in part, through the modulation of proper H3K79 methylation pattern.

6. Sir2 prevents H4K16 acetylation in the rDNA and impinges into additional target(s) to sustain Pch2 nucleolar confinement.

Artículo

3

ARTÍCULO 3: "*Characterization of Pch2 localization determinants reveals a nucleolar-independent role in the meiotic recombination checkpoint*"

RESUMEN

El *checkpoint* de recombinación meiótica bloquea la progresión del ciclo celular meiótico en respuesta a fallos en sinapsis o recombinación para impedir la segregación aberrante de cromosomas. La ATPasa AAA+ Pch2^{TRIP13} de levadura, conservada en la evolución, participa en esta ruta promoviendo la fosforilación del adaptador Hop1^{HORMAD} en T318. En una cepa silvestre, Pch2 se localiza en los cromosomas que han completado la sinapsis así como en la región sin sinapsis del DNA ribosómico (nucleolo), excluyendo a Hop1. Por el contrario, en el mutante *zip1Δ* defectivo en el complejo sinaptonémico (SC), que induce la activación del *checkpoint*, Pch2 sólo se detecta en el nucleolo. Alteraciones en algunas marcas epigenéticas que dan lugar a la dispersión de Pch2 del nucleolo suprimen el bloqueo del mutante *zip1Δ*. Estas observaciones han dado origen a la idea de que la localización nucleolar de Pch2 podría ser importante para el *checkpoint* de recombinación meiótica. En este trabajo investigamos cómo afecta la distribución de Pch2 en los cromosomas a la función del *checkpoint*. Hemos generado y caracterizado varias mutaciones que alteran la localización de Pch2 provocando una distribución aberrante de Hop1 y una respuesta del *checkpoint* comprometida. Además del motivo AAA+, hemos identificado un motivo básico dentro del extremo N-terminal crítico para la función de Pch2 en el *checkpoint* y para su localización. También hemos examinado la relevancia funcional de la interacción Orc1-Pch2 ya descrita. Ambas proteínas colocalizan en el rDNA, y la degradación inducida de Orc1 durante la profase meiótica impide la localización de Pch2 en el rDNA permitiendo la acumulación no deseada de Hop1 en dicha región. Sin embargo, la asociación de Pch2 con los componentes del SC permanece intacta en ausencia de Orc1. Finalmente, mostramos que la activación del *checkpoint* no se ve afectada por la falta de Orc1 lo que demuestra que, contrariamente a hipótesis previas, realmente la localización nucleolar de Pch2 es prescindible para el *checkpoint* meiótico.

GRAPHICAL ABSTRACT

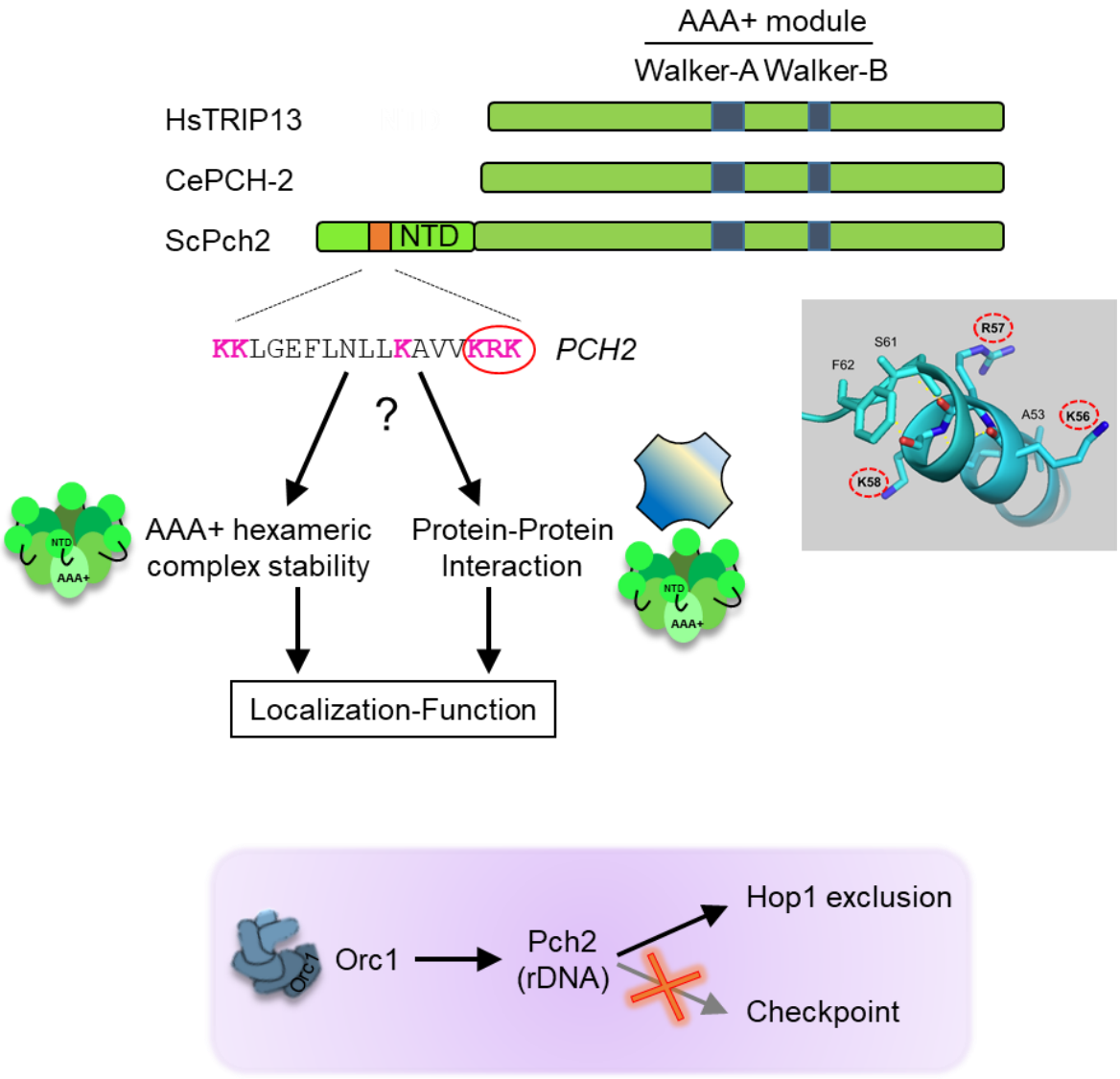

Chromosoma (2019) 128:297–316
https://doi.org/10.1007/s00412-019-00696-7

ORIGINAL ARTICLE

Characterization of Pch2 localization determinants reveals a nucleolar-independent role in the meiotic recombination checkpoint

Esther Herruzo[1] · Beatriz Santos[1,2] · Raimundo Freire[3] · Jesús A. Carballo[4] · Pedro A. San-Segundo[1]

Received: 2 November 2018 / Revised: 5 February 2019 / Accepted: 20 February 2019 / Published online: 12 March 2019

Abstract

The meiotic recombination checkpoint blocks meiotic cell cycle progression in response to synapsis and/or recombination defects to prevent aberrant chromosome segregation. The evolutionarily conserved budding yeast Pch2^{TRIP13} AAA+ ATPase participates in this pathway by supporting phosphorylation of the Hop1^{HORMAD} adaptor at T318. In the wild type, Pch2 localizes to synapsed chromosomes and to the unsynapsed rDNA region (nucleolus), excluding Hop1. In contrast, in synaptonemal complex (SC)–defective *zip1Δ* mutants, which undergo checkpoint activation, Pch2 is detected only on the nucleolus. Alterations in some epigenetic marks that lead to Pch2 dispersion from the nucleolus suppress *zip1Δ*-induced checkpoint arrest. These observations have led to the notion that Pch2 nucleolar localization could be important for the meiotic recombination checkpoint. Here we investigate how Pch2 chromosomal distribution impacts checkpoint function. We have generated and characterized several mutations that alter Pch2 localization pattern resulting in aberrant Hop1 distribution and compromised meiotic checkpoint response. Besides the AAA+ signature, we have identified a basic motif in the extended N-terminal domain critical for Pch2's checkpoint function and localization. We have also examined the functional relevance of the described Orc1-Pch2 interaction. Both proteins colocalize in the rDNA, and Orc1 depletion during meiotic prophase prevents Pch2 targeting to the rDNA allowing unwanted Hop1 accumulation on this region. However, Pch2 association with SC components remains intact in the absence of Orc1. We finally show that checkpoint activation is not affected by the lack of Orc1 demonstrating that, in contrast to previous hypotheses, nucleolar localization of Pch2 is actually dispensable for the meiotic checkpoint.

Keywords Meiosis · Checkpoint · Synapsis · Recombination · Pch2 · Orc1

This article is part of a Special Issue on Recent advances in meiosis from DNA replication to chromosome segregation "edited by Valérie Borde and Francesca Cole, co-edited by Paula Cohen and Scott Keeney."

Electronic supplementary material The online version of this article (https://doi.org/10.1007/s00412-019-00696-7) contains supplementary material, which is available to authorized users.

✉ Pedro A. San-Segundo
pedross@usal.es

[1] Instituto de Biología Funcional y Genómica (IBFG), Consejo Superior de Investigaciones Científicas (CSIC) and University of Salamanca, 37007 Salamanca, Spain

[2] Departamento de Microbiología y Genética, University of Salamanca, 37007 Salamanca, Spain

[3] Instituto de Tecnologías Biomédicas, Hospital Universitario de Canarias, 38320 La Laguna, Tenerife, Spain

[4] Department of Cellular and Molecular Biology, Centro de Investigaciones Biológicas, Consejo Superior de Investigaciones Científicas (CSIC), 28040 Madrid, Spain

Introduction

During gametogenesis, a tight spatiotemporal control of a myriad of interrelated events that integrate the meiotic program must occur in order to achieve the successful generation of gametes with the adequate chromosome complement. This control is reinforced by the action of surveillance mechanisms, or checkpoints, that block meiotic progression in response to defects in critical meiotic processes thus preventing errors in the distribution of chromosomes to the meiotic progeny (Subramanian and Hochwagen 2014). Checkpoint pathways involve a series of molecular events frequently relying on protein phosphorylation, to eventually give rise to the adequate cellular responses including cell cycle arrest among others. The so-called pachytene checkpoint or meiotic recombination checkpoint operates during meiosis to face failures in the synapsis and/or recombination processes. Depending on the nature

of the triggering signal, different sensing mechanisms are involved. For example, while RPA-coated processed meiotic DNA double-strand breaks (DSBs) activate the Mec1^{ATR} sensor kinase via 9-1-1 complex and Ddc2^{ATRIP}-mediated recruitment (Lydall et al. 1996; Hong and Roeder 2002; Eichinger and Jentsch 2010; Refolio et al. 2011), unresected DSBs activate Tel1^{ATM} via the Mre11-Rad50-Xrs2^{NBS1} (MRX) complex (Usui et al. 2001). In any case, irrespective of the checkpoint-inducing event, the final outcome involves a block in meiotic progression by downregulation of the cell cycle machinery (Acosta et al. 2011; Prugar et al. 2017).

The evolutionarily conserved Pch2^{TRIP13} protein was initially discovered in *Saccharomyces cerevisiae* in a genetic screen for mutations that alleviate the checkpoint-induced meiotic arrest of the *zip1Δ* mutant lacking a main component of the central region of the synaptonemal complex (SC) (Sym et al. 1993; San-Segundo and Roeder 1999; Wu and Burgess 2006; Herruzo et al. 2016). Pch2 is also required for the checkpoint response elicited by unresected DSBs involving the interaction with Xrs2 (Ho and Burgess 2011). The participation of Pch2 orthologs in the checkpoint response to various meiotic stimuli has been also reported in other organisms, such as worms (Bhalla and Dernburg 2005) and flies (Joyce and McKim 2009). Besides the checkpoint role, Pch2 additionally impinges on multiple interrelated meiotic recombination events, including DSB formation (Farmer et al. 2012; Joshi et al. 2015), chromosome axis morphogenesis (Börner et al. 2008; Joshi et al. 2009), crossover control (Medhi et al. 2016; Chakraborty et al. 2017), interhomolog bias (Zanders et al. 2011; Subramanian et al. 2016), crossover interference (Zanders and Alani 2009), and ribosomal DNA (rDNA) array stability (San-Segundo and Roeder 1999; Vader et al. 2011). Pch2^{TRIP13} belongs to the AAA+ family of ATPases (Chen et al. 2014; Vader 2015) that utilize the energy generated from ATP hydrolysis to produce conformational changes on the substrates (Hanson and Whiteheart 2005). In the case of Pch2^{TRIP13}, many of its meiotic functions involve the action on the Hop1^{HORMAD1,2} SC component; in particular, Pch2 promotes Hop1 disengagement from chromosome axes as synapsis progresses (San-Segundo and Roeder 1999; Li and Schimenti 2007; Börner et al. 2008; Wojtasz et al. 2009; Roig et al. 2010; Herruzo et al. 2016; Subramanian et al. 2016). Although budding yeast *PCH2* is only expressed in meiotic cells, recent studies have revealed a crucial role for Pch2 orthologs in the mitotic spindle assembly checkpoint in worms and mammals, also acting on a HORMA domain–containing protein, namely MAD2 (Nelson et al. 2015; Ye et al. 2015; Ma and Poon 2018; West et al. 2018).

Since Pch2 removes Hop1 from meiotic chromosomes, the *pch2Δ* single mutant displays more abundant and continuous Hop1 distribution on synapsed chromosomes (San-Segundo and Roeder 1999; Börner et al. 2008). In contrast, unexpectedly, our previous work has demonstrated that under checkpoint-inducing conditions (*zip1Δ*), the Pch2 protein is critically required for maintaining linear Hop1 localization along chromosome axes and, more important, for sustaining high levels of Hop1 phosphorylation at Thr318. In other words, chromosomal Hop1 is less abundant and Hop1-T318 phosphorylation is drastically reduced in *zip1Δ pch2Δ* compared to *zip1Δ* (Herruzo et al. 2016). Deficient Mec1-dependent Hop1-T318 phosphorylation leads to impaired Mek1 activation (Carballo et al. 2008), thus explaining the defective checkpoint response in *zip1Δ pch2Δ* cells. Importantly, *HOP1* overexpression restores checkpoint function in *zip1Δ pch2Δ* (Herruzo et al. 2016). Cytological studies have uncovered a peculiar localization pattern for the Pch2 protein on meiotic chromosomes. Pch2 displays a prominent localization in the unsynapsed rDNA region of chromosome XII and a weaker distribution on interstitial synapsed chromosomal sites (San-Segundo and Roeder 1999; Börner et al. 2008; Herruzo et al. 2016). The association of Pch2 with the SC is clearly evidenced by the presence of Pch2 on Zip1-containing polycomplexes (San-Segundo and Roeder 1999; Dong and Roeder 2000). Remarkably, in a checkpoint-activated scenario like the SC-deficient *zip1Δ* mutant, Pch2 has been only detected in the nucleolar region. Nucleolar accumulation of Pch2 requires histone H3K79 methylation by Dot1 and proper levels of H4K16 acetylation controlled by Sir2 (Ontoso et al. 2013; Cavero et al. 2016). The fact that both *dot1* and *sir2* mutations impair the meiotic recombination checkpoint is consistent with the notion that nucleolar Pch2 is important for checkpoint activity. However, this hypothesis has not yet been tested directly.

In this work, we have identified a basic motif in the non-conserved N-terminal domain (NTD) of Pch2 that is necessary for its localization to both SC and rDNA. Mutation of this motif results in impaired checkpoint response suggesting that it may be required for proper Pch2 chromatin association and/or interaction with additional critical factors. The Orc1 protein targets Pch2 to the rDNA to repress meiotic DSB formation (Vader et al. 2011); thus, in order to definitely assess the functional relevance of Pch2 nucleolar localization for the *zip1Δ*-induced checkpoint, we have engineered a conditional *orc1-3mAID* degron allele. We found that induced Orc1 degradation during meiotic prophase precludes Pch2 localization to the rDNA, but association with SC components is unaltered. Using various cytological and molecular assays, we show that checkpoint activation remains intact in the absence of Orc1. Thus, we conclude that Pch2 nucleolar localization is dispensable for the checkpoint response to SC defects.

Results

An NLS-like element in the Pch2 N-terminal domain is required for checkpoint function and localization

Alignment of the protein sequences of Pch2/TRIP13 orthologs of different species revealed the presence of a non-

conserved extended N-terminal domain (NTD) in the Pch2 protein of *S. cerevisiae* (Fig. 1a and Fig. S1). In wild-type yeast meiotic chromosomes, Pch2 accumulates at the SC-devoid nucleolar rDNA region of chromosome XII and a minor fraction also associates to the SC along synapsed chromosomes (San-Segundo and Roeder 1999; Börner et al. 2008; Herruzo et al. 2016; Subramanian et al. 2016). In other organisms such as plants and worms, Pch2 orthologs have been localized only to the SC (Miao et al. 2013; Deshong et al. 2014; Lambing et al. 2015). The fact that nucleolar accumulation of Pch2 appears to be restricted to budding yeast suggests that the NTD of Pch2 may be involved in this characteristic distribution pattern. Several observations point to a critical role for the nucleolar Pch2 in meiotic recombination checkpoint function (see "Introduction"); therefore, we searched the NTD sequence for motifs possibly involved in nucleolar targeting. We found a 17-amino-acid stretch at positions 42 to 58 containing several basic residues that could resemble a nuclear or nucleolar localization signal (NLS/NoLS) (Fig. 1a and Fig. S1). To explore the meiotic relevance of this NLS-like sequence, we used the *delitto perfetto* approach to generate *PCH2* mutants carrying a precise deletion of this motif in the genomic loci (*pch2-nlsΔ*) (Fig. 1a). Like the *pch2Δ* null mutant, the *pch2-nlsΔ* single mutant completed meiosis and sporulation with similar kinetics and efficiency than the wild type generating high levels of viable spores (Fig. 1b, c; Table 1). Notably, when the checkpoint was triggered by the absence of Zip1, the *pch2-nlsΔ* mutation suppressed the sporulation defect of *zip1Δ* (Fig. 1b) to produce largely inviable spores (Table 1). Likewise, the substantial delay in the kinetics of meiotic divisions of *zip1Δ* was drastically suppressed in *zip1Δ pch2-nlsΔ* to reach near wild-type kinetics (Fig. 1d). Western blot analysis revealed that, in both the wild-type strain and the *pch2-nlsΔ* single mutant, the Pch2 and Pch2-nlsΔ proteins were induced during meiotic prophase (15 h) and then disappeared with similar kinetics as meiosis and sporulation progresses (Herruzo et al. 2016) (Fig. 1c, e). In the *zip1Δ* mutant, high levels of the wild-type Pch2 protein persisted until late time points (Fig. 1e) according to its strong meiotic prophase block (Fig. 1d). In contrast, in *zip1Δ pch2-nlsΔ*, the levels of Pch2-nlsΔ drastically diminished as meiotic divisions took place (Fig. 1d, e). To determine whether the reduced levels of Pch2-nlsΔ in *zip1Δ pch2-nlsΔ* cells were responsible for the bypass of *zip1Δ* arrest or simply reflected the consequences of meiotic progression beyond the point when the Pch2 protein is normally produced, we quantified Pch2 protein levels in the *ndt80Δ* mutant at the 24-h time point, when most cells in the BR strain background display a uniform prophase arrest (Voelkel-Meiman et al. 2012). We found that in *ndt80Δ*-arrested cells, Pch2-nlsΔ levels were not significantly reduced compared to those of the wild-type Pch2 (Fig. 1f, g), demonstrating that the disappearance of Pch2-nlsΔ at late time points in the *zip1Δ pch2-nlsΔ* double mutant (Fig. 1e) is the consequence, and not the cause, of meiotic cell cycle progression. We also analyzed molecular markers of checkpoint activation influenced by Pch2 function, such as Mec1-dependent Hop1-T318 phosphorylation and Mek1-dependent H3-T11 phosphorylation (Govin et al. 2010; Penedos et al. 2015; Herruzo et al. 2016; Kniewel et al. 2017). The *zip1Δ* mutant showed high levels of these phosphorylation events that were largely abolished in both *zip1Δ pch2Δ* and *zip1Δ pch2-nlsΔ* (Fig. 1e) consistent with suppression of the meiotic block. Thus, the *zip1Δ pch2-nlsΔ* mutant phenocopies the checkpoint defects of *zip1Δ pch2Δ*, indicating that the NLS-like sequence is absolutely required for meiotic checkpoint function.

We also examined the localization of the Pch2-nlsΔ protein by immunofluorescence of spread pachytene chromosomes at 24 h after meiotic induction in an *ndt80Δ* background. We used antibodies recognizing the Nsr1 protein as a nucleolar marker. Nuclei with a zygotene/pachytene chromosomal morphology based on DAPI staining of chromatin were scored in all localization analyses. As previously described, in both wild-type and *zip1Δ* nuclei, Pch2 displayed a conspicuous accumulation at the rDNA region marked by the presence of Nsr1 in the vicinity (Fig. 2b; Table S1). In contrast, the Pch2-nlsΔ protein was not detected associated to the meiotic rDNA chromatin (Fig. 2a; Table S1) despite the fairly normal levels observed in whole-cell extracts (Fig. 1f, g). Thus, the NLS-like stretch is required for Pch2 nucleolar localization.

The faint rDNA-independent SC-associated foci of Pch2 on wild-type prophase chromosomes are difficult to detect in most nuclear spread preparations (at least from BR strains) because their intensity is only slightly above the background level and they are often masked by the intense nucleolar signal (Herruzo et al. 2016). To circumvent this issue, we devised an alternative strategy to monitor the ability of Pch2 (or mutant derivatives) to bind SC components by inducing the formation of polycomplexes. The polycomplex is an extrachromosomal aggregate of SC proteins formed under certain circumstances (i.e., *ZIP1* overexpression or Spo11 deficiency) that mimics the same ultrastructure as the native SC (Dong and Roeder 2000). The formation of this structure provides an excellent and prominent readout for SC assembly allowing us to easily assess Pch2 interaction with SC components (Fig. 2b). Therefore, we examined the presence of different Pch2 versions in the polycomplexes of strains overexpressing *ZIP1*. As expected, the wild-type Pch2 protein extensively colocalized with Zip1 in the polycomplex (San-Segundo and Roeder 1999); in contrast, Pch2-nlsΔ failed to be detected in this structure (Fig. 2b; Table S1). We conclude that the NTD portion deleted in Pch2-nlsΔ is necessary not only for rDNA localization, but also for interaction with SC proteins.

We also analyzed the ability of the checkpoint-deficient ATPase-dead versions of Pch2 previously generated (Pch2-K320A and Pch2-E399Q) (Fig. 1a) to interact with Zip1 in

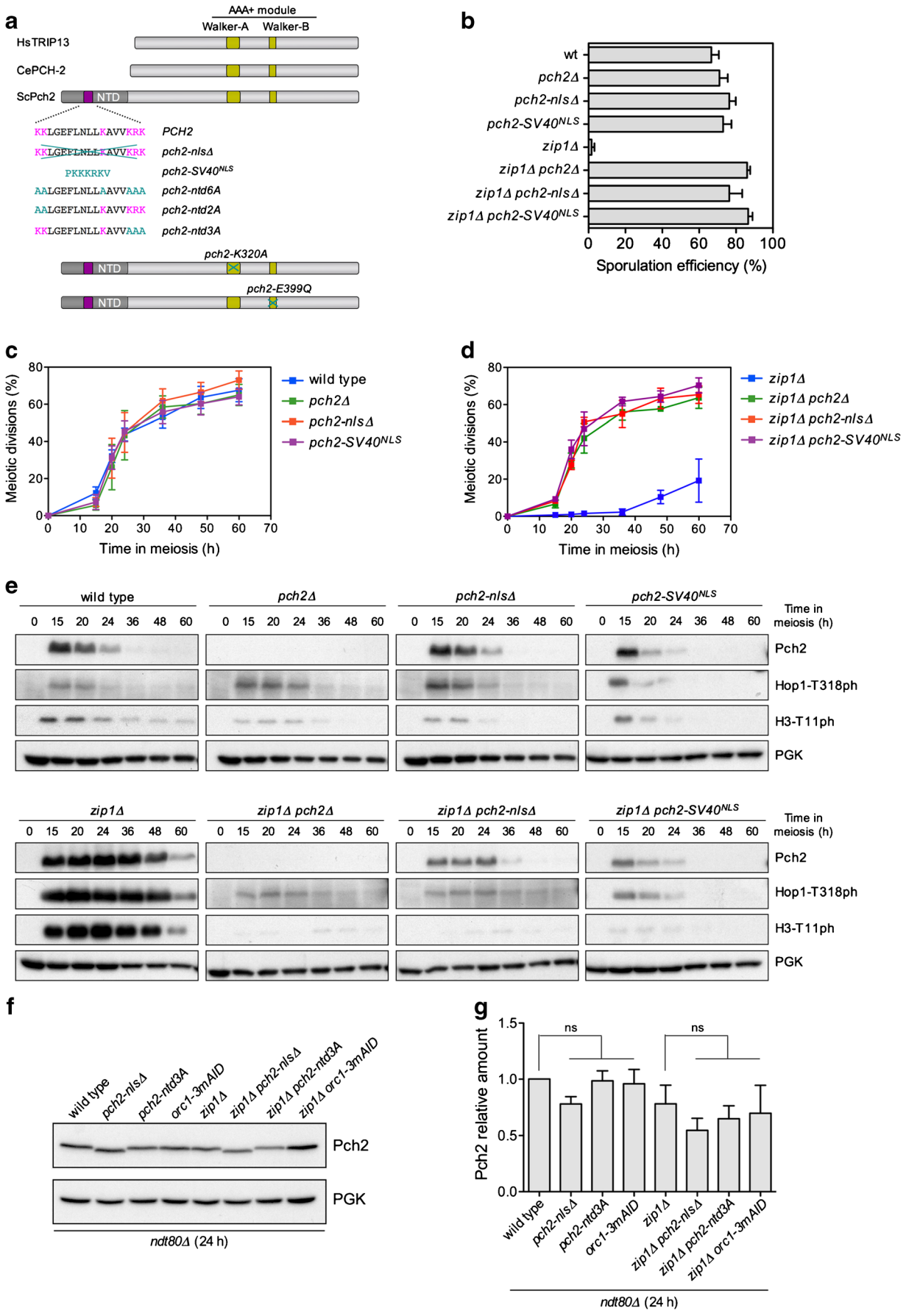
a
AAA+ module
Walker-A
Walker-B
HsTRIP13
CePCH-2
ScPch2
NTD
KKLGEFLNLLKAVVKRK PCH2
KKLGEFLNLLKAVVKRK pch2-nlsΔ
PKKKRKV pch2-SV40NLS
AALGEFLNLLAAVVAAA pch2-ntd6A
AALGEFLNLLKAVVKRK pch2-ntd2A
KKLGEFLNLLKAVVAAA pch2-ntd3A
pch2-K320A
pch2-E399Q
b
wt
pch2Δ
pch2-nlsΔ
pch2-SV40NLS
zip1Δ
zip1Δ pch2Δ
zip1Δ pch2-nlsΔ
zip1Δ pch2-SV40NLS
0 20 40 60 80 100
Sporulation efficiency (%)
c
Meiotic divisions (%)
Time in meiosis (h)
wild type
pch2Δ
pch2-nlsΔ
pch2-SV40NLS
d
Meiotic divisions (%)
Time in meiosis (h)
zip1Δ
zip1Δ pch2Δ
zip1Δ pch2-nlsΔ
zip1Δ pch2-SV40NLS
e
wild type
pch2Δ
pch2-nlsΔ
pch2-SV40NLS
0 15 20 24 36 48 60
Time in meiosis (h)
Pch2
Hop1-T318ph
H3-T11ph
PGK
zip1Δ
zip1Δ pch2Δ
zip1Δ pch2-nlsΔ
zip1Δ pch2-SV40NLS
f
wild type
pch2-nlsΔ
pch2-ntd3A
orc1-3mAID
zip1Δ
zip1Δ pch2-nlsΔ
zip1Δ pch2-ntd3A
zip1Δ orc1-3mAID
Pch2
PGK
ndt80Δ (24 h)
g
Pch2 relative amount
0.0
0.5
1.0
1.5
ns
ns
wild type
pch2-nlsΔ
pch2-ntd3A
orc1-3mAID
zip1Δ
zip1Δ pch2-nlsΔ
zip1Δ pch2-ntd3A
zip1Δ orc1-3mAID
ndt80Δ (24 h)

◀ **Fig. 1** A basic-rich motif in the Pch2 NTD is essential for its checkpoint function. **a** Pch2-relevant motifs and mutants generated. A schematic representation of the *S. cerevisiae* Pch2 protein (ScPch2) and the orthologs from *C. elegans* (CePCH-2) and human (HsTRIP13) is depicted indicating the characteristic AAA+ ATPase motifs. The sequence of the basic-rich motif (purple) in the extended N-terminal domain of Pch2 (NTD) is shown along with the modifications introduced (light blue) in the different mutants generated in this work (see text). Walker A and Walker B mutants previously constructed are also shown (Herruzo et al. 2016). **b** Sporulation efficiency, determined by microscopic counting, after 3 days on sporulation plates. Error bars: SD; $n = 3$. **c**, **d** Time course analysis of meiotic nuclear divisions; the percentage of cells containing two or more nuclei is represented. Error bars: SD; $n = 6$ in **c**; $n = 3$ in **d**. **e** Western blot analysis of Pch2 production during meiosis (detected with anti-HA antibodies), Hop1-T318 phosphorylation, and Mek1 activation (H3-T11 phosphorylation). PGK was used as a loading control. Strains in (**b**, **c**, **d**, **e**) are DP1151 (wild type), DP1164 (*pch2Δ*), DP1408 (*pch2-nlsΔ*), DP1455 (*pch2-SV40^{NLS}*), DP1152 (*zip1Δ*), DP1161 (*zip1Δ pch2Δ*), DP1409 (*zip1Δ pch2-nlsΔ*), and DP1456 (*zip1Δ pch2-SV40^{NLS}*). **f** Western blot analysis of Pch2 production in *ndt80Δ*-arrested strains of the indicated genotypes. Auxin (500 μM) was added to *orc1-m3AID* cultures 12 h after meiotic induction and all cell extracts were prepared at 24 h. **g** Quantification of Pch2 levels normalized with PGK and relativized to wild type. Errors bars: SD; $n = 3$; ns, not significant. The *ndt80Δ* strains in **f** and **g** are DP1191 (wild type), DP1411 (*pch2-nlsΔ*), DP1569 (*pch2-ntd3A*), DP1451 (*orc1-m3AID*), DP1190 (*zip1Δ*), DP1412 (*zip1Δ pch2-nlsΔ*), DP1570 (*zip1Δ pch2-ntd3A*), and DP1452 (*zip1Δ orc1-3mAID*)

the polycomplex. Pch2-K320A lacks the ATP-binding site in the Walker A motif; this protein fails to maintain a stable AAA+ hexameric complex and also fails to localize to meiotic chromatin. Pch2-E399Q lacks the ATP-hydrolysis site in the Walker B motif, but it does localize to the rDNA region despite being catalytically inactive (Chen et al. 2014; Herruzo et al. 2016). Consistent with those observations, we found that Pch2-K320A does not localize to polycomplexes, whereas the Pch2-E399Q version retains the capacity to associate with SC components (Fig. 2b; Table S1). Thus, the ATPase activity of Pch2 is not intrinsically a requisite for its proper localization.

Table 1 Sporulation and spore viability

Relevant genotype	Sporulation frequency (%)	Spore Viability (%)
Wild type	69.2	95.3[a]
pch2Δ	77.2	90.7[a]
pch2-nlsΔ	76.3	93.1
pch2-SV40^{NLS}	73.0	91.0
orc1-6HA	79.0	95.1
orc1-3mAID	67.6	91.7
zip1Δ	3.6	nd
zip1Δ pch2Δ	82.4	35.2[a]
zip1Δ pch2-nlsΔ	76.3	41.7
zip1Δ pch2-SV40^{NLS}	86.6	45.1
zip1Δ orc1-6HA	1.6	nd
zip1Δ orc1-3mAID	2.8	nd

[a] Data obtained from Herruzo et al., 2016

nd not determined

To assess whether the basic-rich 17-amino-acid NTD sequence is actually acting as a true NLS to sustain Pch2 function, we replaced it by a bona fide NLS from the SV40 virus generating the *pch2-SV40^{NLS}* version (Fig. 1a). Albeit with slightly reduced levels, the Pch2-SV40^{NLS} protein displayed the characteristic kinetics of prophase induction and eventual disappearance coincident with meiotic progression similar to Pch2 and Pch2-nlsΔ (Fig. 1e). Like *pch2Δ* and *pch2-nlsΔ*, the *pch2-SV40^{NLS}* single mutant sustained normal sporulation and high levels of spore viability (Fig. 1b, Table 1). In addition, similar to *zip1Δ pch2Δ* and *zip1Δ pch2-nlsΔ*, the *zip1Δ*-induced checkpoint-dependent meiotic block was alleviated in the *zip1Δ pch2-SV40^{NLS}* double mutant resulting in increased spore death (Fig. 1b, d; Table 1). Consistently, *zip1Δ pch2-SV40^{NLS}* displayed impaired Hop1-T318 and H3-T11 phosphorylation as compared to *zip1Δ* (Fig. 1e). Moreover, like Pch2-nlsΔ, the Pch2-SV40^{NLS} version also failed to localize to the rDNA region and to the polycomplex on meiotic chromosome spreads (Fig. 2a, b; Table S1). Thus, these findings are consistent with the possibility that the function of the Pch2 NTD motif is not, at least exclusively, driving Pch2 nuclear or nucleolar targeting/import by a canonical NLS-dependent mechanism.

The "KRK" basic motif in the Pch2 NTD is required for checkpoint function and localization

In order to pinpoint the residues within the 17-amino-acid stretch that are relevant for Pch2's checkpoint function, we constructed several mutants in which the basic residues were changed to alanine in different combinations (Fig. 1a): in *pch2-ntd6A*, all lysines (K) and the arginine (R) were mutated; in *pch2-ntd2A*, the KK at positions 42–43 were mutated; and in *pch2-ntd3A*, the KRK at positions 56–58 were mutated. We introduced these mutations into centromeric plasmids containing 3HA-tagged *PCH2* and transformed a checkpoint-deficient *zip1Δ pch2Δ* strain to assess their ability to restore checkpoint function by monitoring sporulation efficiency (Fig. 3a). As controls, the *zip1Δ pch2Δ* strain was also transformed with the empty vector (checkpoint fully inactive) or with the wild-type *PCH2* (checkpoint active). We found that *pch2-ntd6A* and *pch2-ntd3A* completely suppressed the *zip1Δ* sporulation defect, whereas *pch2-ntd2A* only conferred a partial decrease in sporulation efficiency. Note that the wild-type *PCH2* did not fully restore checkpoint arrest in this plasmid-based assay as a consequence of plasmid-loss events. Those *zip1Δ pch2Δ* cells that lose the plasmid (about 25%) become completely checkpoint defective and complete sporulation (Refolio et al. 2011). In any case, these observations suggest that the Pch2-ntd6A and Pch2-ntd3A proteins do not support checkpoint function, but the Pch2-ntd2A version retains

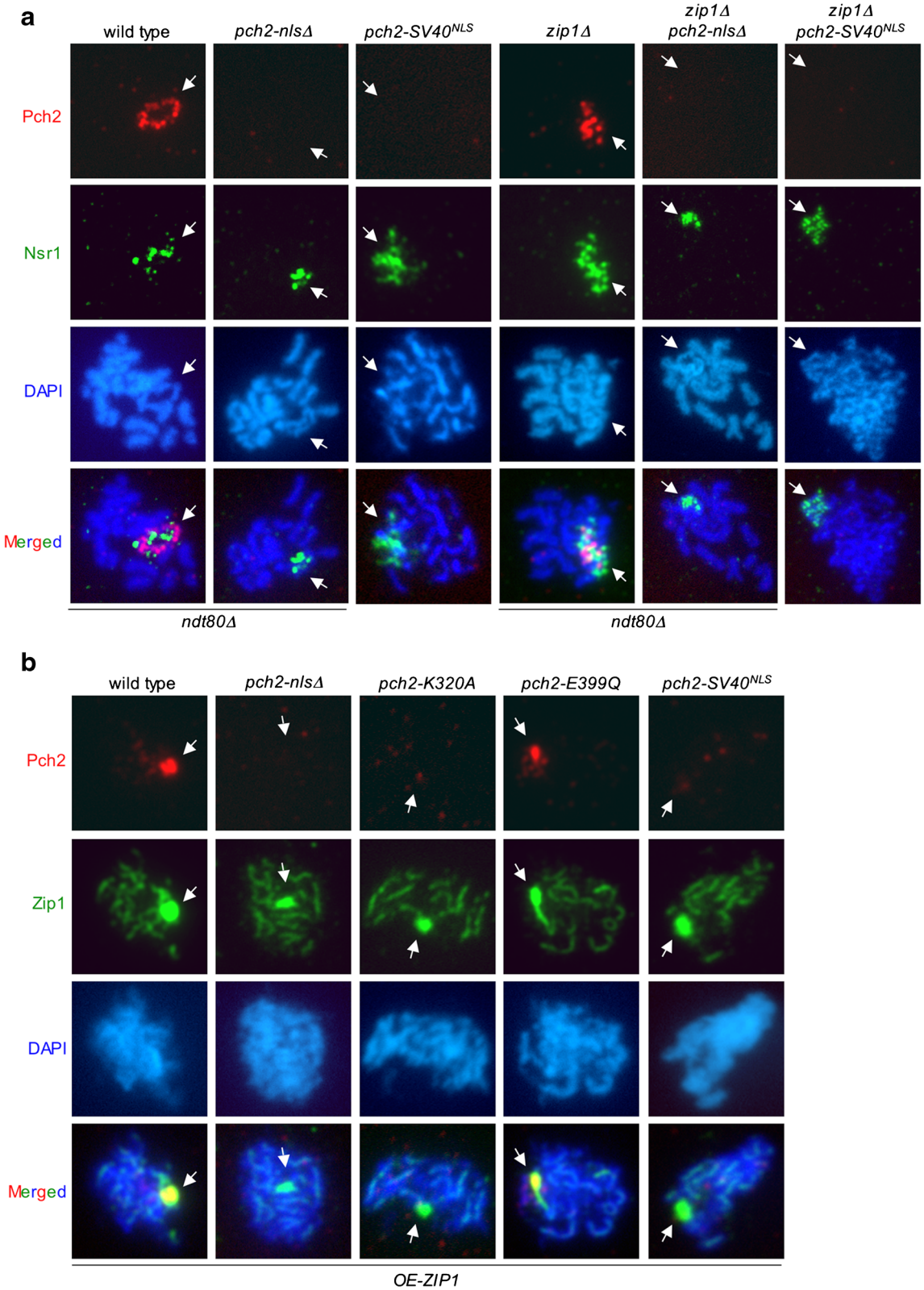

partial activity. To confirm this conclusion, we analyzed H3-T11 phosphorylation as a reporter for Mek1 activity. Consistent with the meiotic phenotype, H3-T11ph was severely impaired in the strains harboring *pch2-ntd6A* and *pch2-ntd3A* mutations and only partially reduced in *pch2-ntd2A* (Fig. 3b) indicating that the KRK motif at positions

◀ **Fig. 2** The basic-rich motif in the Pch2 NTD is essential for its nucleolar localization and for its association with SC components. **a** Immunofluorescence of meiotic chromosomes stained with anti-Pch2 antibodies to detect Pch2, Pch2-nlsΔ, or Pch2-SV40^{NLS} (red); anti-Nsr1 antibodies (green); and DAPI (blue). Representative nuclei are shown. Arrows point to the rDNA region. Samples were prepared 24 h after meiotic induction for the *ndt80Δ* strains DP1191 (wild type), DP1411 (*pch2-nlsΔ*), DP1190 (*zip1Δ*), and DP1412 (*zip1Δ pch2-nlsΔ*), or at 15 h for DP1455 (*pch2-SV40^{NLS}*) and DP1456 (*zip1Δ pch2-SV40^{NLS}*). **b** Immunofluorescence of meiotic chromosomes stained with anti-HA antibodies to detect Pch2, Pch2-nlsΔ, Pch2-K320A, Pch2-E399Q, or Pch2-SV40^{NLS} (red); anti-Zip1 antibodies (green); and DAPI (blue). Representative nuclei are shown. Samples were prepared 15 h after meiotic induction. Arrows point to the polycomplex. Strains in **b** are DP1151 (wild type), DP1408 (*pch2-nlsΔ*), DP1163 (*pch2-K320A*), DP1287 (*pch2-E399Q*), and DP1455 (*pch2-SV40^{NLS}*), all of them transformed with a high-copy plasmid overexpressing *ZIP1* (pSS343)

56–58 of the Pch2 NTD is critical for the meiotic recombination checkpoint. Note that the absence of the Pch2-nlsΔ, Pch2-ntd6A, and Pch2-ntd3A proteins at the 24-h time point (Fig. 3b) is the consequence of meiotic progression in these checkpoint-deficient mutants since both Pch2-nlsΔ and Pch2-ntd3A are produced at fairly normal levels in prophase-arrested *ndt80Δ* strains (Fig. 1f, g).

We next examined the localization of these Pch2-ntd mutant versions on spread *zip1Δ* meiotic nuclei in combination with Hop1 staining at the 15-h time point when all the proteins are present. Both Pch2-ntd6A and Pch2-ntd3A failed to decorate the rDNA meiotic chromatin. Moreover, like *zip1Δ pch2Δ* (Herruzo et al. 2016), the *zip1Δ pch2-ntd6A* and *zip1Δ pch2-ntd3A* mutants displayed fragmented and discontinuous Hop1 distribution, in contrast to the linear Hop1 axial configuration characteristic of the *zip1Δ* mutant (Fig. 3c; Table S1). On the other hand, the Pch2-ntd2A protein, which confers partial checkpoint activity, did localize to the rDNA retaining the capacity to exclude Hop1 from the nucleolar region (Fig. 3c; Table S1). We also determined the ability to interact with SC components by analyzing colocalization with Zip1 in polycomplexes. We overexpressed *ZIP1* from a high-copy vector in *pch2Δ* strains co-transformed with centromeric plasmids expressing either wild-type *PCH2* or the different *pch2-ntd* mutant versions. As expected, we observed extensive colocalization of wild-type Pch2 and Zip1 within the polycomplex (Fig. 3d; Table S1). In contrast, Pch2-ntd6A and Pch2-ntd3A did not associate with polycomplexes, whereas Pch2-ntd2A could be detected in this structure (Fig. 3d; Table S1). Thus, both *pch2-ntd6A* and *pch2-ntd3A* mutants, but not *pch2-ntd2A*, appear to be defective in Pch2 localization and meiotic recombination checkpoint function, suggesting that the KRK motif in the context of the Pch2 NTD is crucial for Pch2 action in the response to *zip1Δ*-induced meiotic defects.

The *PCH2* intron is not relevant for the meiotic checkpoint

The mRNA produced by the *PCH2* gene contains an intron close to the end that undergoes Tgs1-dependent and Mer1-independent splicing (Fig. S2) (Qiu et al. 2011). Although most budding yeast genes do not possess introns, their presence is relatively frequent among meiotic genes; indeed, controlled intron processing is crucial for certain meiotic events (Munding et al. 2010). In order to investigate if the regulated splicing of the *PCH2* mRNA is required for a proper meiotic checkpoint response, we constructed a centromeric plasmid carrying a *PCH2* allele lacking the intron sequence (*pch2-intΔ*) (Fig. S2) and assessed its ability to restore checkpoint function when transformed into a *zip1Δ pch2Δ* mutant. The Pch2 protein was produced from the *pch2-intΔ* allele with similar dynamics as the protein produced from the wild-type *PCH2* gene (Fig. 3b). Introduction of the *pch2-intΔ* allele decreased sporulation efficiency of *zip1Δ pch2Δ* to the same levels as the wild-type *PCH2* did (Fig. 3a), and it sustained high levels of H3-T11 phosphorylation (Fig. 3b). Moreover, like the protein produced from the wild-type *PCH2* gene, the Pch2 protein generated from the *pch2-intΔ* allele localized to the rDNA excluding Hop1 from this region (Fig. 3c; Table S1) and also was capable of interacting with Zip1 in the polycomplex (Fig. 3d; Table S1). Therefore, although we cannot rule out a subtle effect in other meiotic events controlled by Pch2, we conclude that the *PCH2* intron is dispensable for the *zip1Δ*-induced meiotic recombination checkpoint and for Pch2 chromosomal localization.

Analysis of Pch2 localization in whole meiotic cells

Using chromosome spreading, we have shown above that deletion or mutation of the NLS-like motif in the Pch2 NTD prevents its rDNA localization and association with SC proteins also leading to defective checkpoint function. Insertion of a bona-fide NLS from SV40 restores neither Pch2 chromosome binding nor function. Therefore, to further investigate the contribution of this basic NTD motif to govern Pch2 location, we explored Pch2 subcellular localization in whole meiotic cells. For this purpose, we initially generated diploid strains (*GFP-PCH2*) expressing a version of the *PCH2* gene containing the sequence of the green fluorescent protein (GFP) inserted at the second codon in its own genomic locus. A flexible linker encoding five Gly-Ala repeats was also introduced between the *GFP* and *PCH2* sequences (Fig. S3a). Several lines of evidence demonstrated that the GFP-Pch2 protein is functional. First, *zip1Δ GFP-PCH2* strains displayed a tight sporulation block similar to that of *zip1Δ* (Fig. S3b). Second, like the *zip1Δ* mutant, *zip1Δ GFP-PCH2* showed a marked meiotic delay in meiotic time courses (Fig. S3c), and sustained Hop1-T318 and H3-T11 phosphorylation (Fig. S3d). Third, Hop1 was excluded from the rDNA

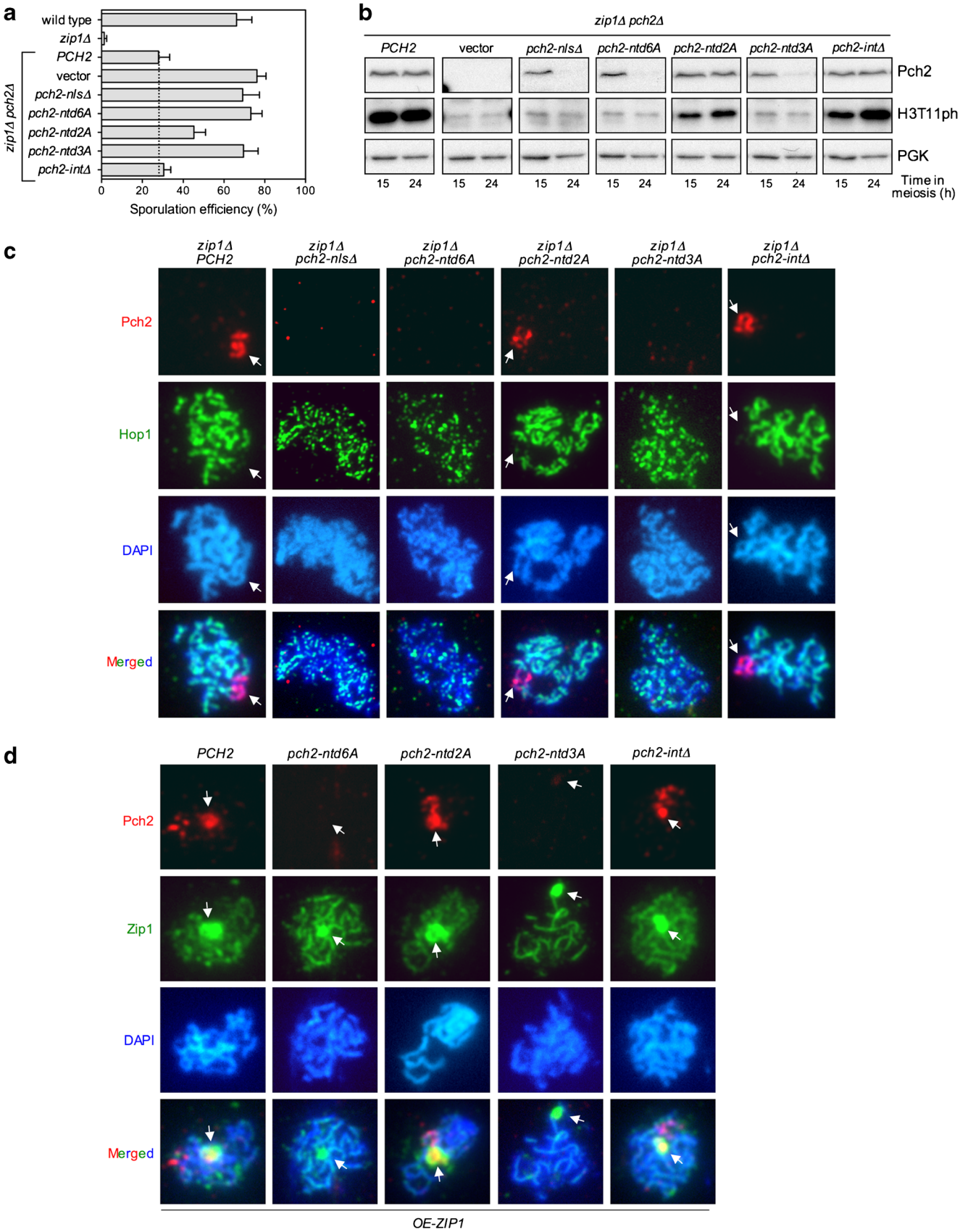
a
wild type
zip1Δ
PCH2
vector
pch2-nlsΔ
pch2-ntd6A
pch2-ntd2A
pch2-ntd3A
pch2-intΔ
zip1Δ pch2Δ
0 20 40 60 80 100
Sporulation efficiency (%)
b
zip1Δ pch2Δ
PCH2
vector
pch2-nlsΔ
pch2-ntd6A
pch2-ntd2A
pch2-ntd3A
pch2-intΔ
Pch2
H3T11ph
PGK
15 24
Time in meiosis (h)
c
zip1Δ PCH2
zip1Δ pch2-nlsΔ
zip1Δ pch2-ntd6A
zip1Δ pch2-ntd2A
zip1Δ pch2-ntd3A
zip1Δ pch2-intΔ
Pch2
Hop1
DAPI
Merged
d
PCH2
pch2-ntd6A
pch2-ntd2A
pch2-ntd3A
pch2-intΔ
Pch2
Zip1
DAPI
Merged
OE-ZIP1

◀ **Fig. 3** The KRK sequence within the basic motif in the Pch2 NTD is essential for its checkpoint function, nucleolar localization, and association with SC components. **a** Sporulation efficiency, determined by microscopic counting, after 3 days on sporulation plates. Error bars: SD; $n = 3$. The dotted line marks the basal level of complementation of *zip1Δ pch2Δ* checkpoint defect with the wild-type *PCH2* plasmid discarding the plasmid-loss effect. **b** Western blot analysis of Pch2 production and Mek1 activation (H3-T11 phosphorylation) at the indicated times after meiotic induction. PGK was used as a loading control. Strains in **a** and **b** are DP421 (wild type), DP422 (*zip1Δ*), and DP1405 (*zip1Δ pch2Δ*). The *zip1Δ pch2Δ* strain was transformed with pSS75 (*PCH2*), pRS314 (vector), pSS338 (*pch2-nlsΔ*), pSS358 (*pch2-ntd6A*), pSS363 (*pch2-ntd2A*), pSS364 (*pch2-ntd3A*), and pSS362 (*pch2-intΔ*). **c** Immunofluorescence of meiotic chromosomes stained with anti-HA antibodies to detect Pch2, Pch2-nlsΔ, Pch2-ntd6A, Pch2-ntd2A, Pch2-ntd3A, or Pch2-intΔ (red); anti-Hop1 antibodies (green); and DAPI (blue). Representative nuclei are shown. Samples were prepared 15 h after meiotic induction. Arrows point to the rDNA region. The DP1405 (*zip1Δ pch2Δ*) strain was transformed with pSS75 (*PCH2*), pSS338 (*pch2-nlsΔ*), pSS358 (*pch2-ntd6A*), pSS363 (*pch2-ntd2A*), pSS364 (*pch2-ntd3A*), and pSS362 (*pch2-intΔ*). **d** Immunofluorescence of meiotic chromosomes stained with anti-HA antibodies to detect Pch2, Pch2-ntd6A, Pch2-ntd2A, Pch2-ntd3A, or Pch2-intΔ (red); anti-Zip1 antibodies (green); and DAPI (blue). Representative nuclei are shown. Samples were prepared 15 h after meiotic induction. Arrows point to the polycomplex. The DP186 (*pch2Δ*) strain, transformed with pSS75 (*PCH2*), pSS358 (*pch2-ntd6A*), pSS363 (*pch2-ntd2A*), pSS364 (*pch2-ntd3A*), and pSS362 (*pch2-intΔ*), was also co-transformed with a high-copy plasmid overexpressing *ZIP1* (pSS343)

region in *zip1Δ GFP-PCH2* meiotic chromosomes (Fig. S3e). Nevertheless, despite being functional, western blot analysis revealed that GFP-Pch2 was produced in meiotic cells at about 10-fold reduced levels compared to the wild-type Pch2 protein and was barely detectable (Fig. 4a; second lane; Fig. S3d). These observations indicate that extremely low levels of Pch2 are sufficient to establish the meiotic checkpoint response, but prevent the use of the endogenous *GFP-PCH2* fusion for precise and sensitive localization studies. Thus, we placed the *GFP-PCH2* construct (as well as *GFP-pch2-nlsΔ* and *GFP-pch2-SV40^{NLS}*) under control of the meiosis-specific *HOP1* promoter in centromeric plasmids (Fig. 4b). In this situation, GFP-Pch2 and GFP-Pch2-nlsΔ were produced at roughly similar levels as the untagged Pch2 protein, and GFP-Pch2-SV40^{NLS} at only slightly reduced levels (Fig. 4a). Moreover, this plasmid-borne version of *GFP-PCH2* was capable of restoring sporulation arrest to large extent when transformed into *zip1Δ pch2Δ* (Fig. 4c) (sporulation was not completely blocked due to plasmid-loss events; see previous sections for explanation). In contrast, GFP-Pch2-nlsΔ and GFP-Pch2-SV40^{NLS} did not confer checkpoint functionality (Fig. 4c), consistent with the results shown above (Fig. 1b, d). Consequently, we used these constructs to examine Pch2 distribution in whole meiotic prophase cells. These plasmids were transformed into *zip1Δ* strains, also harboring *HOP1-mCherry* in heterozygosis as a marker for meiotic prophase chromosomes, and were analyzed by fluorescence microscopy.

We found that the wild-type GFP-Pch2 localized mainly to a discrete reduced area in one side of the nucleus (Fig. 4d; Fig. S4). According to the prominent localization pattern of Pch2 on chromosome spreads (Fig. 2a) (San-Segundo and Roeder 1999; Herruzo et al. 2016) and with the fact that this conspicuous GFP-Pch2 structure did not overlap with Hop1-mCherry (Fig. 4d; Fig. S4), we conclude that it likely corresponds to the nucleolus. In addition, GFP-Pch2 also displayed a diffuse homogenous cytoplasmic signal (Fig. 4d; Fig. S4). In contrast, GFP-Pch2-nlsΔ was largely excluded from the nucleus and found mostly in the cytoplasm (Fig. 4d; Fig. S4), as demonstrated by the reduced nuclear/cytoplasm fluorescence ratio of *GFP-pch2-nlsΔ* cells compared to that of wild-type *GFP-PCH2* (Fig. 4e). On the other hand, GFP-Pch2-SV40^{NLS} was more concentrated inside the nucleus (Fig. 4e) displaying a diffuse nucleoplasmic signal, but did not show nucleolar accumulation (Fig. 4d; Fig. S4). The use of the LineScan tool of MetaMorph software to trace fluorescent signals confirmed the differential distribution of GFP-Pch2, GFP-Pch2-nlsΔ, and GFP-Pch2-SV40^{NLS} across nucleolar, nuclear, and cytoplasmic compartments (Fig. 4d; Fig. S4).

These results indicate that the basic-rich motif in the NTD of Pch2 is required for its nuclear/nucleolar accumulation, but it is not simply acting as a canonical NLS sequence. The substitution of this motif for the SV40 NLS is capable of bringing Pch2 back to the nucleus, but it does not restore its normal distribution or its checkpoint function. We conclude that Pch2's NTD basic motif drives Pch2 subcellular localization and function by additional mechanisms besides the mere control of nuclear import.

Orc1 and Pch2 colocalize in the nucleolar region

The results presented above allowed us to identify a short motif in the Pch2 NTD important for its function and localization. We next sought for possible Pch2-interacting factors that could orchestrate Pch2 chromosomal distribution to support its checkpoint role. It has been described that Orc1 interacts with Pch2 promoting its nucleolar targeting to exert a repressive effect on meiotic DSB formation in the rDNA region (Vader et al. 2011). However, the possible implication of Orc1 in the meiotic recombination checkpoint remains to be tested. We first analyzed the localization of Pch2 and Orc1 on spread preparations of meiotic chromosomes. In order to detect Orc1, we constructed a C-terminal 6HA-tagged version of the protein. The *ORC1-6HA* strain (also carrying *3MYC-PCH2*) sporulated to normal levels and displayed high levels of spore viability (Fig. S5a; Table 1). Moreover, the *zip1Δ ORC1-6HA 3MYC-PCH2* diploid showed a strong sporulation block (Fig. S5a) indicating that Orc1 tagging does not disturb the meiotic checkpoint response. Immunofluorescence analysis of spread nuclei revealed that Pch2 and Orc1 at least partially colocalize in the rDNA region (Fig. 5a; arrows).

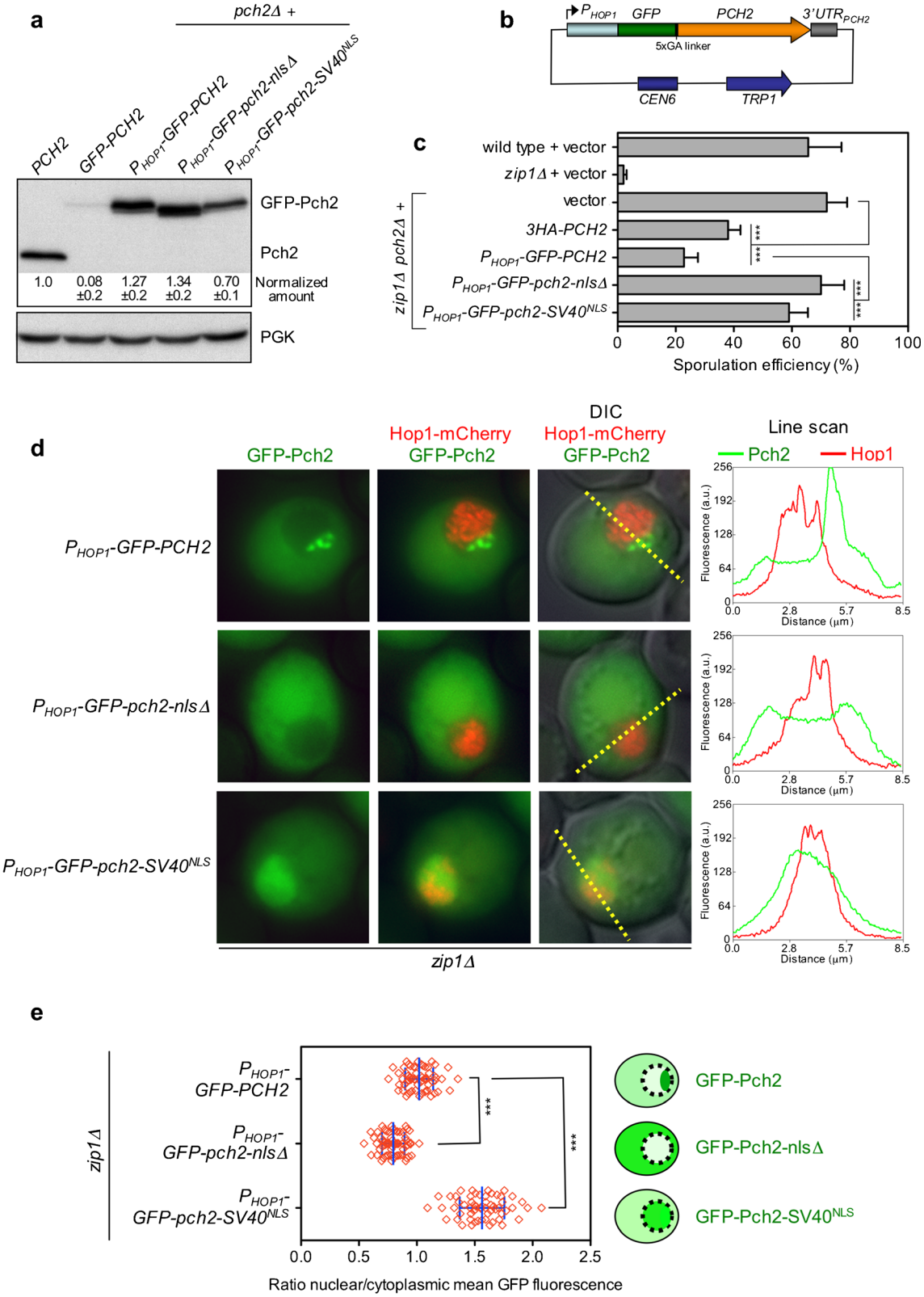

Nevertheless, we note that Pch2 was somewhat mislocalized from the nucleolar area in the strain harboring Orc1-6HA, displaying an additional chromosomal punctate pattern that was not observed in Orc1-untagged nuclei (Fig. 5a; arrowheads; Table S1). These and other observations with additional Orc1-tagging attempts (data not shown; see below)

◀ **Fig. 4** The basic NLS-like motif in Pch2 NTD orchestrates its proper subcellular distribution. **a** Production of untagged Pch2 and different versions of GFP-Pch2 were analyzed by western blot 15 h after meiotic induction. Protein levels were normalized with PGK and relativized to untagged wild-type Pch2; $n = 4$. Strains are BR2495 (*PCH2*), DP1508 (*GFP-PCH2*), and DP186 (*pch2Δ*). DP186 was transformed with pSS393 (P_{HOP1}-*GFP-PCH2*), pSS396 (P_{HOP1}-*GFP-pch2-nlsΔ*), and pSS397 (P_{HOP1}-*GFP-pch2-SV40*^{NLS}). **b** Schematic representation of the P_{HOP1}-*GFP-PCH2* construct in the pSS393 plasmid. The pSS396 and pSS397 plasmids (not depicted) are similar, but express *GFP-pch2-nlsΔ* and *GFP-pch2-SV40*^{NLS}, respectively. **c** Sporulation efficiency, determined by microscopic counting, after 3 days on sporulation plates. Error bars: SD; $n = 6$. Strains are DP421 (wild type), DP422 (*zip1Δ*), and DP1405 (*zip1Δ pch2Δ*), transformed with pRS314 (vector), pSS75 (*3HA-PCH2*), pSS393 (P_{HOP1}-*GFP-PCH2*), pSS396 (P_{HOP1}-*GFP-pch2-nlsΔ*), or pSS397 (P_{HOP1}-*GFP-pch2-SV40*^{NLS}), as indicated. **d** Fluorescence microscopy analysis of GFP-Pch2 (green) and Hop1-mCherry (red) distribution in whole meiotic cells 15 h after meiotic induction. The overlay with differential interference contrast (DIC) images is also displayed to show the cell morphology. The plots represent the GFP and mCherry fluorescent signals (green and red, respectively) along the depicted yellow lines from left to right. Representative cells are shown. Additional cells and line-scan plots are presented in Fig. S4. **e** Quantification of the ratio between the nuclear (including the nucleolar) and cytoplasmic GFP fluorescent signal. The cartoon illustrates the subcellular localization of the different Pch2 versions. The strains in **d** and **e** are DP1500 (*zip1Δ*) transformed with pSS393 (P_{HOP1}-*GFP-PCH2*), pSS396 (P_{HOP1}-*GFP-pch2-nlsΔ*), or pSS397 (P_{HOP1}-*GFP-pch2-SV40*^{NLS}); 62, 72, and 59 cells, respectively, were scored

indicate that this essential protein appears to be extremely sensitive to structural alterations produced by the fusion to ectopic epitopes. Although the essential replicative function of Orc1-6HA likely remains intact (growth and sporulation are normal in the tagged strains), other functions, such as Pch2 localization, appear to be slightly affected without compromising checkpoint functionality. To corroborate that the nuclear location where Orc1 colocalizes with Pch2 corresponds to the nucleolus, we took advantage of the fact that acetylation of histone H4 at lysine 16 (H4K16ac) is absent from the rDNA region (Cavero et al. 2016). As shown in Fig. 5b, Orc1 accumulation occurred in a region completely devoid of H4K16ac confirming that it coincides with the nucleolus.

Nucleolar localization of Pch2, but not polycomplex association, is impaired in Orc1-depleted cells

Since *ORC1* is an essential gene, in order to investigate in detail the requirement for Orc1 to target Pch2 to the rDNA and/or to the SC and the implication in the checkpoint, we aimed to generate conditional *orc1* alleles using the auxin-inducible degron (AID) system (Nishimura and Kanemaki 2014). We initially fused the C terminus of Orc1 to either the original full degron tag (AID), a shorter version (mAID), or three tandem copies of it (3mAID), in haploid strains expressing plant *TIR1* from the *ADH1* promoter and assessed the ability to grow on plates containing auxin (Fig. S5b, c). Only the *orc1-3mAID* mutant showed auxin-dependent growth inhibition (Fig. S5c); therefore, we selected this *orc1-3mAID* construct to generate diploid strains harboring the *TIR1* gene under control of the meiosis-specific *HOP1* promoter to use this system for depleting Orc1 in meiotic cultures. The *orc1-3mAID* mutant sustained normal levels of sporulation and spore viability and, like *zip1Δ*, the *zip1Δ orc1-3mAID* double mutant showed a tight sporulation block (Table 1; Fig. S5d). To explore the consequences of Orc1-3mAID depletion in meiotic time courses, we added auxin (or ethanol, as the solvent control) 12 h after meiotic induction, coinciding with prophase initiation in the BR strain background. We found that Orc1-3mAID was indeed efficiently degraded upon auxin treatment, but Pch2 global levels were not altered when Orc1 was depleted (Fig. 1f, g, 6a). Analysis of chromosome spreads revealed that, consistent with a previous report using an *orc1-161* thermosensitive allele (Vader et al. 2011), Pch2 was not detected in the nucleolar region of *orc1-3mAID* nuclei in either the presence or the absence of added auxin (Fig. 6b; Table S1). This result confirms that Orc1 is required for nucleolar targeting of Pch2 and reveals that C-terminal tagging of Orc1 with the 3mAID degron impairs this particular function without altering other essential roles of Orc1. Thus, Pch2 localization in the rDNA is exquisitely sensitive to Orc1 integrity. In any case, although *orc1-3mAID* per se prevents Pch2 normal distribution, we performed all the ensuing experiments involving this allele with auxin addition to promote Orc1-3mAID degradation (Fig. 6a) and using the untagged version as control thus avoiding uncertainties in the conclusions.

Since Pch2 prevents Hop1 binding to the rDNA, we examined the impact of Orc1 depletion on Hop1 localization in both wild-type and *zip1Δ* cells. Consistent with the absence of nucleolar Pch2 in the *orc1-3mAID* mutant (Fig. 6b), Hop1 decorated the rDNA region distinguished by the Nsr1 nucleolar marker (Fig. 6c; Table S1). These observations suggest that Pch2/Orc1-dependent exclusion of Hop1 from the rDNA likely underlies the meiotic DSB repressive effect in this region. We next determined the ability of Pch2 to bind to SC components in the absence of Orc1 by analyzing the colocalization with Zip1 in the polycomplex. In an initial attempt to induce the formation of polycomplexes by overexpressing *ZIP1* from a high-copy plasmid (see above), we found that the *orc1-3mAID* allele precludes *ZIP1* overexpression (Fig. S6), likely as a consequence of a fully functional Orc1 requirement for plasmid maintenance (Fox et al. 1995). Therefore, we took advantage of the recombination and synapsis-defective *spo11Δ* mutant as an alternative tool to promote polycomplex formation (Cheng et al. 2006). In contrast to the *pch2-ntd* mutants characterized above, we observed that Pch2 does colocalize with Zip1 in the polycomplexes formed in the *orc1-3mAID* mutant treated with

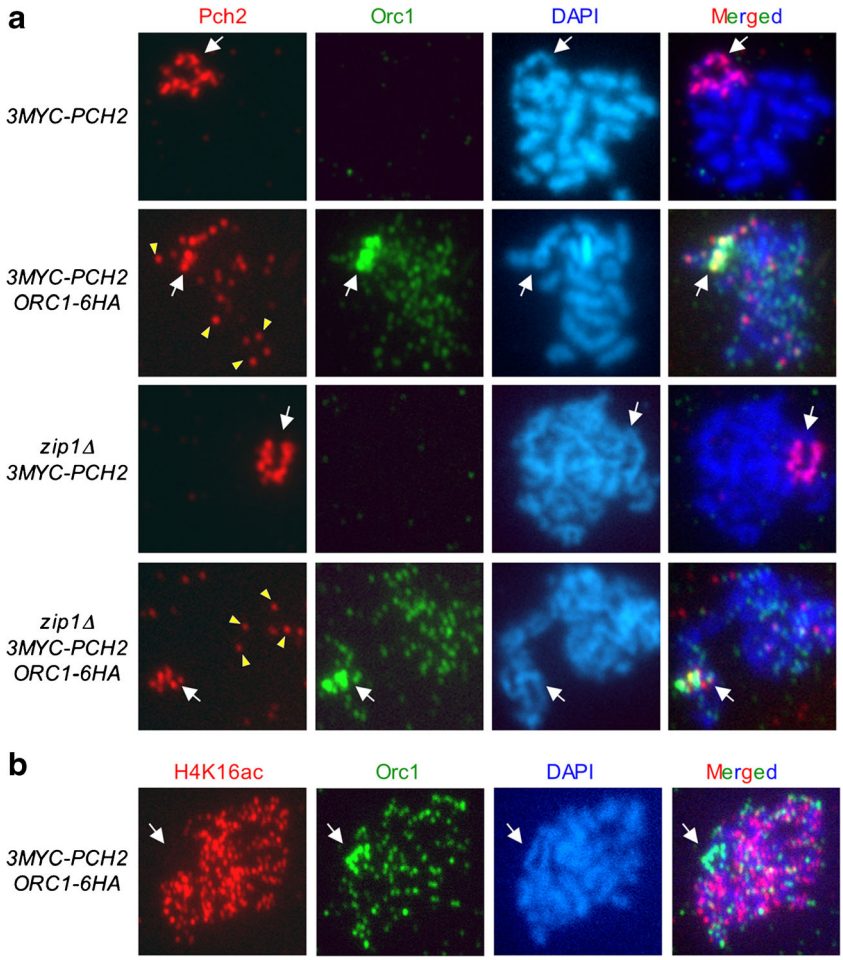

Fig. 5 Colocalization of Pch2 and Orc1 in the rDNA region. **a** Immunofluorescence of meiotic chromosomes stained with anti-Pch2 antibodies to detect Pch2 (red), anti-HA antibodies to detect Orc1 (green), and DAPI (blue). Representative nuclei are shown. Samples were prepared 15 h after meiotic induction. Arrows point to the rDNA region. Arrowheads point to some of the extranucleolar Pch2 dots observed in *ORC1-6HA* nuclei. Strains are DP1243 (*3MYC-PCH2*), DP1426 (*3MYC-PCH2 ORC1-6HA*), DP1244 (*zip1Δ 3MYC-PCH2*), and DP1427 (*zip1Δ 3MYC-PCH2 ORC1-6HA*). **b** Immunofluorescence of meiotic chromosomes stained with anti-H4K16ac (red), anti-HA antibodies to detect Orc1 (green), and DAPI (blue). A representative nucleus is shown. Samples were prepared 15 h after meiotic induction. Arrows point to the rDNA region. The strain is DP1426 (*3MYC-PCH2 ORC1-6HA*)

auxin (Fig. 6d; Table S1). The presence of Pch2 in the *spo11Δ*-induced polycomplexes tended to be even more frequent in *orc1-3mAID* compared to the wild type, although the statistical difference was not significant (Fig. 6e). In sum, these observations indicate that, unlike the rDNA, Pch2 interaction with SC components does not involve Orc1. Thus, the *orc1-3mAID* allele provides a unique scenario to determine whether Pch2 nucleolar localization is specifically required for the meiotic recombination checkpoint response.

The *zip1Δ*-triggered meiotic recombination checkpoint is active in the absence of Orc1

We analyzed the impact of auxin-induced Orc1-3mAID depletion on the meiotic recombination checkpoint during meiotic time courses (Fig. 7). The *orc1-3mAID* single mutant displayed normal kinetics of nuclear divisions and, more important, like *zip1Δ*, the *zip1Δ orc1-3mAID* double mutant showed a strong delay in meiotic progression (Fig. 7a) suggesting that the checkpoint remains functional in the absence of Orc1. Moreover, the meiotic block of *zip1Δ orc1-3mAID* was alleviated by deletion of *PCH2* (Fig. 7b) indicating that it stems from activation of the meiotic recombination

Fig. 6 Nucleolar localization of Pch2, but not interaction with SC components, depends on Orc1. **a** Western blot analysis of Pch2 production (detected with anti-HA antibodies) and Orc1-m3AID (detected with anti-mAID antibodies) at the indicated times in meiosis. Auxin (500 μM) or ethanol (as control) was added 12 h after meiotic induction. PGK was used as a loading control. **b** Immunofluorescence of meiotic chromosomes stained with anti-Pch2 antibodies to detect Pch2 (red), anti-Nsr1 antibodies (green), and DAPI (blue). Representative nuclei are shown. Auxin (500 μM) or ethanol (as control) was added 12 h after meiotic induction and samples were prepared at 17 h. Arrows point to the rDNA region. **c** Orc1 prevents Hop1 localization to the rDNA. Immunofluorescence of meiotic chromosomes stained with anti-Nsr1 antibodies (red), anti-Hop1 antibodies (green), and DAPI (blue). Representative nuclei are shown. Auxin (500 μM) was added 12 h after meiotic induction and samples were prepared at 17 h. Arrows point to the rDNA region. Strains in **a**, **b** and **c** are DP1151 (wild type), DP1437 (*orc1-3mAID*), DP1152 (*zip1Δ*), and DP1438 (*zip1Δ orc1-3mAID*). **d** Orc1 is dispensable for Pch2 association with the polycomplex. Immunofluorescence of meiotic chromosomes stained with anti-HA antibodies to detect Pch2 (red), anti-Zip1 antibodies (green), and DAPI (blue). Representative nuclei are shown. Auxin (500 μM) was added 12 h after meiotic induction and samples were prepared at 17 h. Arrows point to the polycomplex. **e** Quantification of the nuclei displaying Pch2 in the Zip1-containing polycomplex. Error bars, SD; $n = 3$; ns, not significant. Strains in **d** and **e** are DP1425 (*spo11Δ*) and DP1444 (*spo11Δ orc1-3mAID*)

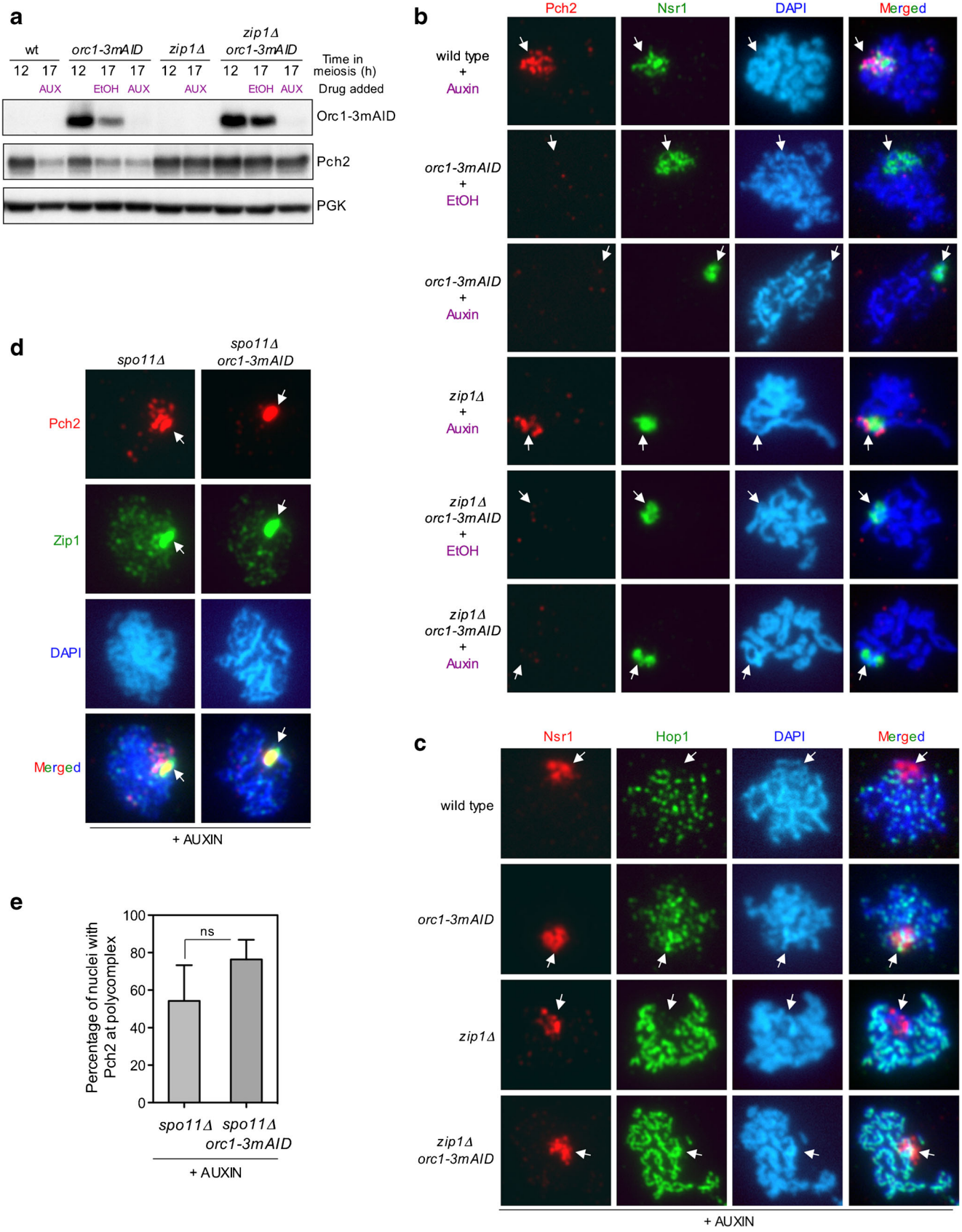
a
wt
orc1-3mAID
zip1Δ
zip1Δ orc1-3mAID
Time in meiosis (h)
12 17 12 17 17 12 17 12 17 17
AUX EtOH AUX AUX EtOH AUX
Drug added
Orc1-3mAID
Pch2
PGK
b
Pch2
Nsr1
DAPI
Merged
wild type + Auxin
orc1-3mAID + EtOH
orc1-3mAID + Auxin
zip1Δ + Auxin
zip1Δ orc1-3mAID + EtOH
zip1Δ orc1-3mAID + Auxin
c
Nsr1
Hop1
DAPI
Merged
wild type
orc1-3mAID
zip1Δ
zip1Δ orc1-3mAID
+ AUXIN
d
spo11Δ
spo11Δ orc1-3mAID
Pch2
Zip1
DAPI
Merged
+ AUXIN
e
Percentage of nuclei with Pch2 at polycomplex
100
80
60
40
20
0
ns
spo11Δ
spo11Δ orc1-3mAID
+ AUXIN

checkpoint. To validate this interpretation, we analyzed Hop1-T318 and H3-T11 phosphorylation as markers of checkpoint activation. In *zip1Δ orc1-3mAID* cells treated with auxin to induce Orc1-m3AID degradation (Fig. 7c), we found high levels of these checkpoint phospho-targets (Fig. 7d), confirming that Orc1 is dispensable for activation and maintenance of the meiotic checkpoint. In addition, to avoid the influence of the different kinetics of meiotic progression of the strains examined, we also quantified the ratio of phospho-Hop1-T318/total Hop1 as a selective indicator of Pch2 checkpoint function in *ndt80Δ*-arrested cells harboring various *pch2* and *orc1* mutations (Herruzo et al. 2016) (Fig. 7e, f).

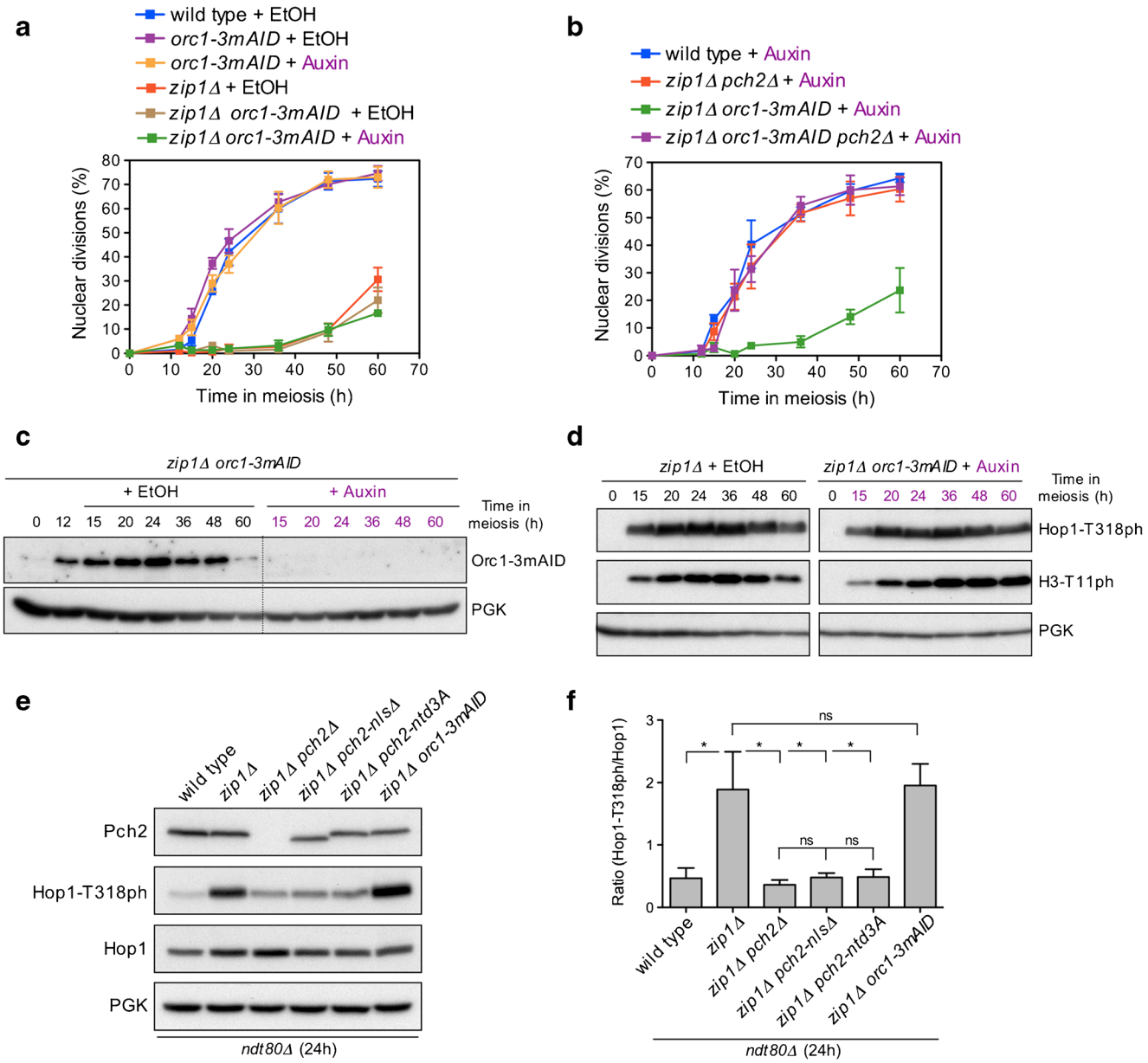

Fig. 7 Orc1 is not required for activation of the meiotic recombination checkpoint. **a**, **b** Time course analysis of meiotic nuclear divisions; the percentage of cells containing two or more nuclei is represented. Error bars: SD; $n = 3$. **c** Western blot analysis of Orc1-m3AID production detected with anti-mAID antibodies. **d** Western blot analysis of Hop1-T318 phosphorylation and Mek1 activation (H3-T11 phosphorylation). In **a**, **b**, **c**, and **d**, auxin (500 μM) or ethanol (as control) was added 12 h after meiotic induction. PGK was used as a loading control. Strains in **a**, **b**, **c**, and **d** are DP1151 (wild type), DP1152 (*zip1Δ*), DP1437 (*orc1-3mAID*), DP1438 (*zip1Δ orc1-3mAID*), DP1161 (*zip1Δ pch2Δ*), and DP1586 (*zip1Δ orc1-3mAID pch2Δ*). **e** Western blot analysis of Pch2 and Hop1 production, and Hop1-T318 phosphorylation in *ndt80Δ*-arrested strains of the indicated genotypes. Auxin (500 μM) was added to the *zip1Δ orc1-m3AID* culture 12 h after meiotic induction and all cell extracts were prepared at 24 h. **f** Quantification of relative Hop1-T318 phosphorylation analyzed as in **e**. The ratio of phospho-Hop1-T318 versus total Hop1 is represented. Errors bars: SD; $n = 3$. Asterisk: $p < 0.05$; ns, not significant. The *ndt80Δ* strains in **e** and **f** are DP1191 (wild type), DP1190 (*zip1Δ*), DP881 (*zip1Δ pch2Δ*), DP1412 (*zip1Δ pch2-nlsΔ*), DP1570 (*zip1Δ pch2-ntd3A*), and DP1452 (*zip1Δ orc1-3mAID*)

We found that, like in *zip1Δ pch2Δ*, the relative levels of Hop1-T318 phosphorylation were drastically reduced in *zip1Δ pch2-nlsΔ* and *zip1Δ pch2-ntd3A*, accounting for the defective Mek1 activation and according to the results presented above; in contrast, Hop1-T318 levels were not significantly altered in *zip1Δ orc1-3mAID*, confirming that the checkpoint was not abrogated. In sum, we can conclude that the Orc1-dependent conspicuous presence of Pch2 in the rDNA region is not required for its function in triggering the meiotic recombination checkpoint, namely sustaining Hop1-T318 phosphorylation.

Discussion

Previous work has spotted Pch2 as a crucial player in the meiotic recombination checkpoint triggered by the defects provoked by the absence of SC components, such as Zip1 and others (Sym et al. 1993; San-Segundo and Roeder 1999; Wu and Burgess 2006; Herruzo et al. 2016). Pch2 is critically required to sustain high levels of Mec1-dependent Hop1-T318 phosphorylation in order to relay the checkpoint signal to the downstream Mek1 effector kinase. Strikingly, cytological studies reveal that under checkpoint-inducing conditions, such as in the *zip1Δ* mutant lacking the central region of the SC, Pch2 is only detected in the rDNA region raising the possibility that Pch2 exerts its checkpoint function from this particular location. Consistent with this notion, mutations in certain chromatin modifiers that provoke Pch2 mislocalization from the rDNA impair the meiotic checkpoint (San-Segundo and Roeder 2000; Ontoso et al. 2013; Cavero et al. 2016) and also recombination control in perturbed meiosis (Börner et al. 2008). The rDNA array in chromosome XII of budding yeast possesses a unique heterochromatin-like structure that represses recombination (Gottlieb and Esposito 1989). In the case of meiosis, SC formation does not occur in the rDNA and Hop1 binding is prevented (Smith and Roeder 1997). Thus, previous to this study, a puzzling question in the field was how the nucleolar Pch2 could control the phosphorylation status of the axial component Hop1 that is particularly absent in the rDNA region. A paradigm of a crucial cell cycle regulator governed by the nucleolus is the Cdc14 phosphatase; controlled release of Cdc14 from the nucleolar RENT complex impinges on various processes such as mitotic exit (Stegmeier and Amon 2004), DNA repair (Villoria et al. 2017), and meiotic chromosome segregation (Fox et al. 2017). By analogy with this mechanism, it was possible to speculate that Pch2 may orchestrate the timely nucleolar sequestration and/or release of a critical factor involved in Hop1 phosphorylation.

In order to directly assess the requirement for the nucleolar Pch2 in the meiotic recombination checkpoint, we have identified and characterized *cis* and *trans* localization and functional determinants of Pch2. Table 2 summarizes our findings. The extended NTD of Pch2 was an opportune element to dissect, because it is not conserved in the Pch2 orthologs of other species where the nucleolar localization has not been reported. We have pinpointed a short stretch in Pch2's NTD containing a KRK basic motif that is essential for its checkpoint function. Nevertheless, this motif is not specific for Pch2 nucleolar targeting; it is also required for interaction with SC components raising the possibility that this basic amino acid stretch may direct global binding of Pch2 to meiotic chromosomes. Alternatively, it was also possible that the only function of this motif is to drive Pch2 nuclear import. The functional analysis of a Pch2-SV40^{NLS} version combined with cytological studies, both in spread chromosomes and whole meiotic cells, has allowed us to address this question. Consistent with the observation that the Pch2-nlsΔ protein does not associate with

Table 2 Summary of functional and localization analysis of Pch2

Relevant genotype	Pch2 rDNA localization	Pch2 SC association[a]	Checkpoint function[b]
PCH2	+	+	+
pch2Δ	NA	NA	–
pch2-K320A[c]	–	–	–
pch2-E399Q[c]	+	+	–
pch2-nlsΔ	–	–	–
pch2-SV40^{NLS}	–	–	–
pch2-ntd6A	–	–	–
pch2-ntd2A	+	+	±
pch2-ntd3A	–	–	–
pch2-intΔ	+	+	+
orc1-3mAID	–	+	+

[a] Inferred from Zip1-Pch2 colocalization in polycomplexes

[b] Checkpoint induced by *ZIP1* deletion

[c] ATPase-dead mutants described in Herruzo et al., 2016

NA not applicable

chromatin on nuclear spreads, it is largely excluded from the nucleus displaying a prominent cytoplasmic localization. Substitution of the NLS-like region by a well-defined NLS from the SV40 virus is capable of promoting the transport of Pch2 to the nucleus but, remarkably, it shows a diffuse nucleoplasmic distribution and, unlike the wild-type Pch2, does not accumulate in the nucleolus. Thus, the fact that Pch2-SV40^{NLS} restores neither Pch2 function nor chromosomal association, despite being present inside the nucleus, implies that the NLS-like region in Pch2's NTD is not solely acting in Pch2 nuclear transport. This basic patch, which is located in a predicted alpha-helical structure (Fig. S7), may be involved in the interaction of Pch2 with additional factors required for its proper localization and/or function. The N-terminal domain of the Xrs2 protein, a component of the MRX complex, interacts with Pch2 to modulate the Tel1-dependent checkpoint response to unresected meiotic DSBs (Ho and Burgess 2011). Since Tel1 is not required for the *zip1Δ*-induced meiotic block, it is possible to speculate that Xrs2 acts together with Pch2 in the checkpoint response induced by the absence of Zip1 without involving the MRX complex. In fact, MRX-independent functions of Xrs2 have been described in the vegetative DNA damage response (Oh et al. 2016). Perhaps, the NTD of Pch2 is required to form a complex with Xrs2 to sustain the *zip1Δ* checkpoint. Alternatively, mutation of the basic motif in Pch2's NTD may disrupt the AAA+ hexameric complex thus preventing its binding to normal Pch2 chromosomal target sites. Indeed, the ATPase-dead Pch2-K320A mutant version, defective in ATP binding, also fails to form a stable AAA+ complex (Wendler et al. 2012; Chen et al. 2014; Herruzo et al. 2016) and, like Pch2-ntd6A and Pch2-ntd3A, it is unable to localize to either the rDNA or the SC (Herruzo et al. 2016) (Fig. 3c, d). However, ATPase activity per se is not required for Pch2 localization because the ATP hydrolysis–deficient Pch2-E399Q version does localize normally to both rDNA and SC despite being inactive, as manifested by its inability to exclude Hop1 from the nucleolar area (Herruzo et al. 2016) (Fig. 2b). Future experiments will address these and other possibilities to delineate the precise role of the essential NTD motif identified in this work.

As an additional strategy to elucidate whether the nucleolar Pch2 population is involved in the meiotic recombination checkpoint response, in this work, we have also studied the participation of Orc1 in this surveillance mechanism and its requirement for targeting Pch2 to distinct chromosomal locations. Orc1 is an essential component of the Origin Recognition Complex (ORC), which is necessary for initiation of DNA replication during both the mitotic and meiotic cell cycles (Bell et al. 1993; Vader et al. 2011). Besides the replicative function, Orc1 collaborates with Pch2 in maintaining meiotic stability of the rDNA array by preventing DSB formation and the unwanted non-allelic homologous recombination that could potentially arise (Vader et al. 2011). Curiously, Orc1 protein levels are meticulously regulated during meiosis by intricate transcriptional and post-transcriptional mechanisms that ultimately rely on the Ndt80 transcription factor (Xie et al. 2016). Ndt80 is a key target of the meiotic recombination checkpoint raising the possibility of a functional coupling between Orc1 levels and the control of exit from prophase I by the status of checkpoint activation.

In our work, we describe the localization pattern of Orc1 on meiotic chromosomes. In accordance with the multiple replication origins in the rDNA repeats representing ORC binding sites, Orc1 often accumulates on this region partially colocalizing with Pch2. In addition, we also find a general distribution of Orc1 throughout meiotic chromatin likely reflecting Orc1 binding to genomic replication origins. Although we cannot discard a sensitivity issue, Pch2 appears to be absent from these sites suggesting that Orc1 and Pch2 interaction may occur exclusively in the nucleolus. Consistent with this notion, we show that Orc1 is specifically required for localization of Pch2 to the rDNA, but not for its association with SC proteins. Like Pch2, the Orc1 protein also belongs to the AAA+ family of ATPases (Duncker et al. 2009). While Pch2 forms homohexamers in vitro (Chen et al. 2014), the possibility of heteromeric complexes between Pch2 and Orc1 has been suggested (Vader 2015). Supporting this hypothesis, we note that Pch2 nucleolar localization, but not other Orc1 essential functions, is extremely sensitive to Orc1 fusion to small tags that could somehow disrupt proper complex structure. If this were the case, these Pch2-Orc1 heteromeric complexes would be involved exclusively in the rDNA-related functions, whereas Pch2 homohexamers would possess the capacity for removing Hop1 only from synapsed chromosomes. Alternatively, it is also possible that nucleolar Pch2 catalytic activity on the Hop1 substrate does not require Orc1, whose main function would be targeting Pch2 to the rDNA to exert the protective function on undesirable DSB formation.

The *orc1-3mAID* allele generated in this work solely compromises Pch2 nucleolar localization allowing us to unequivocally address the direct contribution of this particular genomic location to Pch2's role in the *zip1Δ*-induced meiotic checkpoint. We show multiple cytological and molecular pieces of evidence demonstrating that in the absence of Orc1 the checkpoint-launching response remains intact, thus indicating that Orc1 and, hence, nucleolar Pch2 are dispensable for the activation of this quality control mechanism. In the *zip1Δ* mutant lacking the central region of the SC, and thus triggering the checkpoint, Pch2 is only detectable in the rDNA by the chromosome spreading technique. In auxin-treated *zip1Δ orc1-3mAID* nuclei, Pch2 is no longer detected on chromosomes, but the checkpoint is still active. The DNA content profile of the *zip1Δ orc1-3mAID* double mutant is similar to that of *zip1Δ* (Fig. S5e) and, importantly, its strong delay in meiotic progression still relies on Pch2 (Fig. 7b), supporting the conclusion that the meiotic arrest of *zip1Δ orc1-3mAID* results from activation of the Pch2-dependent

meiotic recombination checkpoint and not from other unrelated defects. Our results, therefore, open the question of the precise localization and/or distribution of the Pch2 population relevant for the checkpoint response when Zip1 is absent. Although a technical sensitivity issue in Pch2 localization studies cannot be ruled out, it is also possible that a fraction of Pch2 loosely associated to chromatin is responsible for the checkpoint role. In line with this possibility, it has been suggested that the *Drosophila* PCH2 protein exerts its meiotic checkpoint function from a location associated to the nuclear envelope, but at a distance from the chromosomes (Joyce and McKim 2010). Previous studies have revealed a correlation between Pch2 nucleolar mislocalization and meiotic checkpoint deficiency in *sir2* and *dot1* mutants (San-Segundo and Roeder 1999, 2000; Ontoso et al. 2013; Cavero et al. 2016). However, we show here that the checkpoint remains intact when Pch2 is removed from the nucleolus upon Orc1 depletion. Therefore, Dot1 and Sir2 may also control the nucleolar-independent population of Pch2 important for checkpoint function. Consistent with the results presented here, the meiotic recombination checkpoint is functional in *zip1Δ rdnΔ* strains lacking the rDNA array on chromosome XII (San-Segundo and Roeder 1999). In this *rdnΔ* scenario, Pch2 shows a substantial redistribution to chromosome ends, and both Pch2 telomeric localization and checkpoint function become dependent on the Sir3 silencing factor, which is not normally required for *zip1Δ* arrest in RDN^{+} cells. Curiously, the budding yeast Sir3 protein is a paralog of Orc1 that arose by gene duplication and subsequent functional specialization during evolution (Hanner and Rusche 2017). Thus, multiple regulatory networks impact Pch2 function and localization in different circumstances. In sum, our results have contributed to narrow down the factors impinging on at least some of the paramount roles of Pch2, such as the *zip1Δ*-induced checkpoint response. Additional future studies will be aimed to discriminate the critical spatiotemporal regulatory mechanisms underlying the meiotic functions of this enigmatic conserved meiotic protein.

Materials and methods

Yeast strains and meiotic time courses

The genotypes of yeast strains are listed in Supplementary Table S2. All strains are in the BR1919 or BR2495 background (Rockmill and Roeder 1990). The *zip1Δ::LEU2*, *zip1Δ::LYS2*, *ndt80Δ::LEU2*, *ndt80Δ::kanMX3*, *pch2Δ::URA3*, and *pch2Δ::TRP1* gene deletions were previously described (Herruzo et al. 2016). The *spo11Δ::natMX4* deletion was generated using a polymerase chain reaction (PCR)–based approach (Goldstein and McCusker 1999). N-terminal tagging of Pch2 with three copies of the -HA or -MYC epitopes was previously described (San-Segundo and Roeder 1999; Herruzo et al. 2016). The *ORC1-6HA* and *orc1-3mAID* constructs were generated by a PCR-based method using the pYM16 (Janke et al. 2004) and pMK152 (Nishimura and Kanemaki 2014) plasmids, respectively. To direct expression of the *Oryza sativa TIR1* gene during meiosis in yeast for the auxin-induced degron technique, P_{HOP1}-*OsTIR1* was targeted to the genomic *ura3-1* locus by *Stu*I digestion of pSS346 (see below). The *pch2-nlsΔ*, *pch2-SV40*^{NLS}, and *pch2-ntd3A* mutations were introduced into the genomic *3HA-PCH2* locus using the *delitto perfetto* method that leaves no additional marker (Stuckey et al. 2011). Essentially, the CORE cassette (*URA3-kanMX4*) was first inserted into the *3HA-PCH2* gene in the vicinity of the location where the mutation was to be made. Then, the strains carrying *3HA-pch2-CORE* were transformed with DNA fragments containing the desired mutation and homologous flanking sequences to both sides of the CORE insertion point to evict the cassette. 5-Fluoroorotic acid (FOA)–resistant and G418-sensitive clones were selected and further checked for the presence of the desired mutation. Generation of *pch2-K320A* and *pch2-E399Q* was previously reported (Herruzo et al. 2016). Strains harboring N-terminal tagging of Pch2 with GFP (*GFP-PCH2*) were also constructed using the *delitto perfetto* approach. Basically, a PCR fragment containing the *PCH2* promoter followed by GFP inserted at the second codon of *PCH2* with a five Gly-Ala linker in between (Fig. S3A) was transformed into a strain carrying the CORE cassette close to the 5′ end of *PCH2* and correct FOA-resistant clones were selected. All constructions and mutations were verified by PCR analysis and/or sequencing. The sequences of all primers used in strain construction are available upon request. All strains were made by direct transformation of haploid parents or by genetic crosses always in an isogenic background. Sporulation conditions for meiotic time courses have been described (Ontoso et al. 2013). To score meiotic nuclear divisions, samples were taken at different time points, fixed in 70% ethanol, washed in phosphate-buffered saline (PBS) and stained with 1 μg/μl 4′,6-diamidino-2-phenylindole (DAPI) for 15 min. At least 300 cells were counted at each time point. Meiotic time courses were repeated several times; averages and error bars from at least three replicates are shown.

Plasmids

The plasmids used are listed in Supplementary Table S3. The pSS346 plasmid, in which *OsTIR1* is placed under control of the *HOP1* promoter, was constructed by cloning a PCR-amplified 660-bp fragment containing the *HOP1* promoter flanked by *Eco*RI-*Spe*I into the same sites of pMK200 to replace the *ADH1* promoter by the *HOP1* promoter. The different *pch2* mutations in pSS338, pSS358, pSS362, pSS363,

and pSS364 were generated following essentially the procedure described in the Q5 site-directed mutagenesis kit (New England Biolabs) using the pSS75 plasmid as template. To analyze the localization of functional GFP-Pch2 in live meiotic prophase cells, the pSS393 plasmid was constructed using several cloning steps. Essentially, pSS393 is a pRS314-derived centromeric plasmid harboring the *HOP1* promoter to drive the prophase-specific expression of the *GFP* coding sequence fused at the second codon of the *PCH2* ORF lacking the intron (Fig. 4b). A flexible linker of five Gly-Ala repeats was also placed between GFP and the Pch2 N-terminus. The pSS396 and pSS397 plasmids driving the production of GFP-Pch2-nlsΔ and GFP-Pch2-SV40^{NLS}, respectively, were derived from pSS393 by using the Q5 site-directed mutagenesis procedure (pSS396) or the NEBuilder assembly kit (New England Biolabs) (pSS397). Specific details on plasmid construction and the sequences of all primers used are available upon request.

Antibody generation

To raise rabbit polyclonal antibodies against Pch2, a DNA fragment encoding amino acids 91–300 was cloned into the pET30a vector (Novagen) for expression in *Escherichia coli*. The His-tagged protein was purified using Ni-NTA resin (Qiagen) following the manufacturer's instructions and was used for rabbit immunization. Serum was collected after five injections and was affinity purified against the recombinant antigen as described (Petkovic et al. 2005).

To obtain the mouse anti-Hop1 monoclonal antibody, the MonoExpress Gold Antibody service from Genescript was used. In brief, a recombinant fragment of *HOP1* encoding Hop1$^{20\text{-}250}$ was used to immunize mice. Hybridomas were generated and positive clones were selected for antibody production and affinity purification.

Western blotting

Total cell extracts were prepared by trichloroacetic acid (TCA) precipitation from 5-ml aliquots of sporulation cultures as previously described (Acosta et al. 2011). The antibodies used are listed in Supplementary Table S4. The ECL, ECL2, or SuperSignal West Femto reagents (ThermoFisher Scientific) were used for detection. The signal was captured on films and/or with a ChemiDoc XRS system (Bio-Rad) and quantified with the Quantity One software (Bio-Rad).

Cytology

Immunofluorescence of chromosome spreads was performed essentially as described (Rockmill 2009). The antibodies used are listed in Supplementary Table S4. Images of spreads were captured with a Nikon Eclipse 90i fluorescence microscope controlled with MetaMorph software (Molecular Devices) and equipped with a Hammamatsu Orca-AG charge-coupled device (CCD) camera and a PlanApo VC 100 × 1.4 NA objective. DAPI images were collected using a Leica DMRXA fluorescence microscope equipped with a Hammamatsu Orca-AG CCD camera and a 63 × 1.4 NA objective. Images of whole live cells expressing *GFP-PCH2* and *HOP1-mCherry* were captured with an Olympus IX71 fluorescence microscope equipped with a personal DeltaVision system, a CoolSnap HQ2 (Photometrics) camera, and × 100 UPLSAPO 1.4 NA objective. Stacks of 7 planes at 0.8-μm intervals were collected. Maximum intensity projections of planes containing Hop1-mCherry signal and single planes of GFP-Pch2 are shown in Fig. 4d and Fig. S4. The line-scan tool of the MetaMorph software was used to measure and plot the fluorescence intensity profile across the cytoplasm and nucleus/nucleolus. To determine the nuclear/cytoplasm GFP fluorescence ratio, the ROI manager tool of Fiji software (Schindelin et al. 2012) was used to define the cytoplasm and nuclear (including the nucleolus) areas and the mean intensity values were measured. Background values were subtracted prior to ratio calculation.

Dityrosine fluorescence assay, sporulation efficiency, and spore viability

To examine dityrosine fluorescence as an indicator of the formation of mature asci, patches of cells grown on YPDA plates were replica-plated to sporulation plates overlaid with a nitrocellulose filter (Protran BA85, Whatman). After 3-day incubation at 30 °C, fluorescence was visualized by illuminating the open plates from the top with a hand-held 302-nm ultraviolet (UV) lamp. Images were taken using a Gel Doc XR system (Bio-Rad). Sporulation efficiency was quantitated by microscopic examination of asci formation after 3 days on sporulation plates. Both mature and immature asci were scored. At least 300 cells were counted for every strain. Spore viability was assessed by tetrad dissection. At least 144 spores were scored for every strain.

Statistics

To determine the statistical significance of differences, a two-tailed Student *t* test was used. *P* values were calculated with the GraphPad Prism 5.0 software.

Acknowledgements We are grateful to David Ontoso, Andrés Clemente, and Shirleen Roeder for reagents. We also thank Isabel Acosta and Sara González-Arranz for the technical assistance, Carlos Vázquez for the advice on microscopy analysis, and José Pérez-Martín and Andrés Clemente for the helpful discussions and ideas.

Funding This work was supported by grants from the Ministry of Economy and Competitiveness (MINECO) of Spain to JAC and PSS

(grants BFU2015-64361-P and BFU2015-65417-R, respectively). EH was supported by a predoctoral contract (FPU1502035) from the Ministry of Education of Spain. JAC is supported by a Ramón y Cajal contract (RYC2013-13950). The IBFG is funded in part by an institutional grant from Junta de Castilla y León (CLU-2017-03).

Compliance with ethical standards

Conflict of interest The authors declare that they have no conflict of interest.

References

Acosta I, Ontoso D, San-Segundo PA (2011) The budding yeast polo-like kinase Cdc5 regulates the Ndt80 branch of the meiotic recombination checkpoint pathway. Mol Biol Cell 22:3478–3490

Bell SP, Kobayashi R, Stillman B (1993) Yeast origin recognition complex functions in transcription silencing and DNA replication. Science 262:1844–1849

Bhalla N, Dernburg AF (2005) A conserved checkpoint monitors meiotic chromosome synapsis in *Caenorhabditis elegans*. Science 310: 1683–1686

Börner GV, Barot A, Kleckner N (2008) Yeast Pch2 promotes domainal axis organization, timely recombination progression, and arrest of defective recombinosomes during meiosis. Proc Natl Acad Sci U S A 105:3327–3332

Carballo JA, Johnson AL, Sedgwick SG, Cha RS (2008) Phosphorylation of the axial element protein Hop1 by Mec1/Tel1 ensures meiotic interhomolog recombination. Cell 132:758–770

Cavero S, Herruzo E, Ontoso D, San-Segundo PA (2016) Impact of histone H4K16 acetylation on the meiotic recombination checkpoint in *Saccharomyces cerevisiae*. Microb Cell 3:606–620

Chakraborty P, Pankajam AV, Lin G, Dutta A, Krishnaprasad GN, Tekkedil MM, Shinohara A, Steinmetz LM, Nishant KT (2017) Modulating crossover frequency and interference for obligate crossovers in *Saccharomyces cerevisiae* meiosis. G3 7:1511–1524

Chen C, Jomaa A, Ortega J, Alani EE (2014) Pch2 is a hexameric ring ATPase that remodels the chromosome axis protein Hop1. Proc Natl Acad Sci U S A 111:E44–E53

Cheng CH, Lo YH, Liang SS, Ti SC, Lin FM, Yeh CH, Huang HY, Wang TF (2006) SUMO modifications control assembly of synaptonemal complex and polycomplex in meiosis of *Saccharomyces cerevisiae*. Genes Dev 20:2067–2081

Deshong AJ, Ye AL, Lamelza P, Bhalla N (2014) A quality control mechanism coordinates meiotic prophase events to promote crossover assurance. PLoS Genet 10:e1004291

Dong H, Roeder GS (2000) Organization of the yeast Zip1 protein within the central region of the synaptonemal complex. J Cell Biol 148: 417–426

Duncker BP, Chesnokov IN, McConkey BJ (2009) The origin recognition complex protein family. Genome Biol 10:214

Eichinger CS, Jentsch S (2010) Synaptonemal complex formation and meiotic checkpoint signaling are linked to the lateral element protein Red1. Proc Natl Acad Sci U S A 107:11370–11375

Farmer S, Hong EJ, Leung WK, Argunhan B, Terentyev Y, Humphryes N, Toyoizumi H, Tsubouchi H (2012) Budding yeast Pch2, a widely conserved meiotic protein, is involved in the initiation of meiotic recombination. PLoS One 7:e39724

Fox CA, Loo S, Dillin A, Rine J (1995) The origin recognition complex has essential functions in transcriptional silencing and chromosomal replication. Genes Dev 9:911–924

Fox C, Zou J, Rappsilber J, Marston AL (2017) Cdc14 phosphatase directs centrosome re-duplication at the meiosis I to meiosis II transition in budding yeast. Wellcome Open Res 2:2

Goldstein AL, McCusker JH (1999) Three new dominant drug resistance cassettes for gene disruption in *Saccharomyces cerevisiae*. Yeast 15: 1541–1553

Gottlieb S, Esposito RE (1989) A new role for a yeast transcriptional silencer gene, SIR2, in regulation of recombination in ribosomal DNA. Cell 56:771–776

Govin J, Dorsey J, Gaucher J, Rousseaux S, Khochbin S, Berger SL (2010) Systematic screen reveals new functional dynamics of histones H3 and H4 during gametogenesis. Genes Dev 24:1772–1786

Hanner AS, Rusche LN (2017) The yeast heterochromatin protein Sir3 experienced functional changes in the AAA+ domain after gene duplication and subfunctionalization. Genetics 207:517–528

Hanson PI, Whiteheart SW (2005) AAA+ proteins: have engine, will work. Nat Rev Mol Cell Biol 6:519–529

Herruzo E, Ontoso D, Gonzalez-Arranz S, Cavero S, Lechuga A, San-Segundo PA (2016) The Pch2 AAA+ ATPase promotes phosphorylation of the Hop1 meiotic checkpoint adaptor in response to synaptonemal complex defects. Nucleic Acids Res 44:7722–7741

Ho HC, Burgess SM (2011) Pch2 acts through Xrs2 and Tel1/ATM to modulate interhomolog bias and checkpoint function during meiosis. PLoS Genet 7:e1002351

Hong EJ, Roeder GS (2002) A role for Ddc1 in signaling meiotic double-strand breaks at the pachytene checkpoint. Genes Dev 16:363–376

Janke C, Magiera MM, Rathfelder N, Taxis C, Reber S, Maekawa H, Moreno-Borchart A, Doenges G, Schwob E, Schiebel E, Knop M (2004) A versatile toolbox for PCR-based tagging of yeast genes: new fluorescent proteins, more markers and promoter substitution cassettes. Yeast 21:947–962

Joshi N, Barot A, Jamison C, Börner GV (2009) Pch2 links chromosome axis remodeling at future crossover sites and crossover distribution during yeast meiosis. PLoS Genet 5:e1000557

Joshi N, Brown MS, Bishop DK, Börner GV (2015) Gradual implementation of the meiotic recombination program via checkpoint pathways controlled by global DSB levels. Mol Cell 57:797–811

Joyce EF, McKim KS (2009) Drosophila PCH2 is required for a pachytene checkpoint that monitors double-strand-break-independent events leading to meiotic crossover formation. Genetics 181:39–51

Joyce EF, McKim KS (2010) Chromosome axis defects induce a checkpoint-mediated delay and interchromosomal effect on crossing over during *Drosophila* meiosis. PLoS Genet 6:e1001059

Kniewel R, Murakami H, Liu Y, Ito M, Ohta K, Hollingsworth NM, Keeney S (2017) Histone H3 threonine 11 phosphorylation is catalyzed directly by the meiosis-specific kinase Mek1 and provides a molecular readout of Mek1 activity in vivo. Genetics 207:1313–1333

Lambing C, Osman K, Nuntasoontorn K, West A, Higgins JD, Copenhaver GP, Yang J, Armstrong SJ, Mechtler K, Roitinger E, Franklin FC (2015) Arabidopsis PCH2 mediates meiotic chromosome remodeling and maturation of crossovers. PLoS Genet 11: e1005372

Li XC, Schimenti JC (2007) Mouse pachytene checkpoint 2 (trip13) is required for completing meiotic recombination but not synapsis. PLoS Genet 3:e130

Lydall D, Nikolsky Y, Bishop DK, Weinert T (1996) A meiotic recombination checkpoint controlled by mitotic checkpoint genes. Nature 383:840–843

Ma HT, Poon RYC (2018) TRIP13 functions in the establishment of the spindle assembly checkpoint by replenishing O-MAD2. Cell Rep 22:1439–1450

Medhi D, Goldman AS, Lichten M (2016) Local chromosome context is a major determinant of crossover pathway biochemistry during budding yeast meiosis. Elife 5:e19699

Miao C, Tang D, Zhang H, Wang M, Li Y, Tang S, Yu H, Gu M, Cheng Z (2013) Central region component1, a novel synaptonemal complex component, is essential for meiotic recombination initiation in rice. Plant Cell 25:2998–3009

Munding EM, Igel AH, Shiue L, Dorighi KM, Trevino LR, Ares M Jr (2010) Integration of a splicing regulatory network within the meiotic gene expression program of *Saccharomyces cerevisiae*. Genes Dev 24:2693–2704

Nelson CR, Hwang T, Chen PH, Bhalla N (2015) TRIP13^{PCH-2} promotes Mad2 localization to unattached kinetochores in the spindle checkpoint response. J Cell Biol 211:503–516

Nishimura K, Kanemaki MT (2014) Rapid depletion of budding yeast proteins via the fusion of an auxin-inducible degron (AID). Curr Protoc Cell Biol 64:20.9.1–20.916

Oh J, Al-Zain A, Cannavo E, Cejka P, Symington LS (2016) Xrs2 dependent and independent functions of the Mre11-Rad50 complex. Mol Cell 64:405–415

Ontoso D, Acosta I, van Leeuwen F, Freire R, San-Segundo PA (2013) Dot1-dependent histone H3K79 methylation promotes activation of the Mek1 meiotic checkpoint effector kinase by regulating the Hop1 adaptor. PLoS Genet 9:e1003262

Penedos A, Johnson AL, Strong E, Goldman AS, Carballo JA, Cha RS (2015) Essential and checkpoint functions of budding yeast ATM and ATR during meiotic prophase are facilitated by differential phosphorylation of a meiotic adaptor protein, Hop1. PLoS One 10: e0134297

Petkovic M, Dietschy T, Freire R, Jiao R, Stagljar I (2005) The human Rothmund-Thomson syndrome gene product, RECQL4, localizes to distinct nuclear foci that coincide with proteins involved in the maintenance of genome stability. J Cell Sci 118:4261–4269

Prugar E, Burnett C, Chen X, Hollingsworth NM (2017) Coordination of double strand break repair and meiotic progression in yeast by a Mek1-Ndt80 negative feedback loop. Genetics 206:497–512

Qiu ZR, Shuman S, Schwer B (2011) An essential role for trimethylguanosine RNA caps in *Saccharomyces cerevisiae* meiosis and their requirement for splicing of *SAE3* and *PCH2* meiotic pre-mRNAs. Nucleic Acids Res 39:5633–5646

Refolio E, Cavero S, Marcon E, Freire R, San-Segundo PA (2011) The Ddc2/ATRIP checkpoint protein monitors meiotic recombination intermediates. J Cell Sci 124:2488–2500

Rockmill B (2009) Chromosome spreading and immunofluorescence methods in *Saccharomyces cerevisiae*. Methods Mol Biol 558:3–13

Rockmill B, Roeder GS (1990) Meiosis in asynaptic yeast. Genetics 126: 563–574

Roig I, Dowdle JA, Toth A, de Rooij DG, Jasin M, Keeney S (2010) Mouse TRIP13/PCH2 is required for recombination and normal higher-order chromosome structure during meiosis. PLoS Genet 6: 1001062

San-Segundo PA, Roeder GS (1999) Pch2 links chromatin silencing to meiotic checkpoint control. Cell 97:313–324

San-Segundo PA, Roeder GS (2000) Role for the silencing protein Dot1 in meiotic checkpoint control. Mol Biol Cell 11:3601–3615

Schindelin J, Arganda-Carreras I, Frise E, Kaynig V, Longair M, Pietzsch T, Preibisch S, Rueden C, Saalfeld S, Schmid B, Tinevez JY, White DJ, Hartenstein V, Eliceiri K, Tomancak P, Cardona A (2012) Fiji: an open-source platform for biological-image analysis. Nat Methods 9:676–682

Smith AV, Roeder GS (1997) The yeast Red1 protein localizes to the cores of meiotic chromosomes. J Cell Biol 136:957–967

Stegmeier F, Amon A (2004) Closing mitosis: the functions of the Cdc14 phosphatase and its regulation. Annu Rev Genet 38:203–232

Stuckey S, Mukherjee K, Storici F (2011) In vivo site-specific mutagenesis and gene collage using the delitto perfetto system in yeast *Saccharomyces cerevisiae*. Methods Mol Biol 745:173–191

Subramanian VV, Hochwagen A (2014) The meiotic checkpoint network: step-by-step through meiotic prophase. Cold Spring Harb Perspect Biol 6:a016675

Subramanian VV, MacQueen AJ, Vader G, Shinohara M, Sanchez A, Borde V, Shinohara A, Hochwagen A (2016) Chromosome synapsis alleviates Mek1-dependent suppression of meiotic DNA repair. PLoS Biol 14:e1002369

Sym M, Engebrecht JA, Roeder GS (1993) ZIP1 is a synaptonemal complex protein required for meiotic chromosome synapsis. Cell 72: 365–378

Usui T, Ogawa H, Petrini JH (2001) A DNA damage response pathway controlled by Tel1 and the Mre11 complex. Mol Cell 7:1255–1266

Vader G (2015) Pch2(TRIP13): controlling cell division through regulation of HORMA domains. Chromosoma 124:333–339

Vader G, Blitzblau HG, Tame MA, Falk JE, Curtin L, Hochwagen A (2011) Protection of repetitive DNA borders from self-induced meiotic instability. Nature 477:115–119

Villoria MT, Ramos F, Duenas E, Faull P, Cutillas PR, Clemente-Blanco A (2017) Stabilization of the metaphase spindle by Cdc14 is required for recombinational DNA repair. EMBO J 36:79–101

Voelkel-Meiman K, Moustafa SS, Lefrancois P, Villeneuve AM, MacQueen AJ (2012) Full-length synaptonemal complex grows continuously during meiotic prophase in budding yeast. PLoS Genet 8:e1002993

Wendler P, Ciniawsky S, Kock M, Kube S (2012) Structure and function of the AAA+ nucleotide binding pocket. Biochim Biophys Acta 1823:2–14

West AMV, Komives EA, Corbett KD (2018) Conformational dynamics of the Hop1 HORMA domain reveal a common mechanism with the spindle checkpoint protein Mad2. Nucleic Acids Res 46:279–292

Wojtasz L, Daniel K, Roig I, Bolcun-Filas E, Xu H, Boonsanay V, Eckmann CR, Cooke HJ, Jasin M, Keeney S, McKay MJ, Toth A (2009) Mouse HORMAD1 and HORMAD2, two conserved meiotic chromosomal proteins, are depleted from synapsed chromosome axes with the help of TRIP13 AAA-ATPase. PLoS Genet 5: e1000702

Wu HY, Burgess SM (2006) Two distinct surveillance mechanisms monitor meiotic chromosome metabolism in budding yeast. Curr Biol 16:2473–2479

Xie B, Horecka J, Chu A, Davis RW, Becker E, Primig M (2016) Ndt80 activates the meiotic *ORC1* transcript isoform and SMA2 via a bidirectional middle sporulation element in *Saccharomyces cerevisiae*. RNA Biol 13:772–782

Ye Q, Rosenberg SC, Moeller A, Speir JA, Su TY, Corbett KD (2015) TRIP13 is a protein-remodeling AAA+ ATPase that catalyzes MAD2 conformation switching. Elife 4:e07367

Zanders S, Alani E (2009) The pch2Delta mutation in baker's yeast alters meiotic crossover levels and confers a defect in crossover interference. PLoS Genet 5:e1000571

Zanders S, Sonntag Brown M, Chen C, Alani E (2011) Pch2 modulates chromatid partner choice during meiotic double-strand break repair in *Saccharomyces cerevisiae*. Genetics 188:511–521

SUPPLEMENTAL DATA

Characterization of Pch2 localization determinants reveals a nucleolar-independent role in the meiotic recombination checkpoint

Esther Herruzo[1], Beatriz Santos[1,2], Raimundo Freire[3], Jesús Carballo[4] and Pedro A. San-Segundo[1],*

[1]Instituto de Biología Funcional y Genómica (IBFG). Consejo Superior de Investigaciones Científicas (CSIC) and University of Salamanca. 37007-Salamanca, Spain. [2]Departamento de Microbiología y Genética. University of Salamanca. 37007-Salamanca, Spain. [3]Hospital Universitario de Canarias, Instituto de Tecnologías Biomédicas. 38320-La Laguna, Tenerife, Spain. [4]Centro de Investigaciones Biológicas. Consejo Superior de Investigaciones Científicas (CSIC). 28040-Madrid, Spain.

*Corresponding author: pedross@usal.es; +34 923294902

Supplemental Figures (Fig. S1-S7)
Table S1 (Quantitative data for spreads)
Table S2 (strains list)
Table S3 (plasmids list)
Table S4 (antibodies list)
Supplemental references

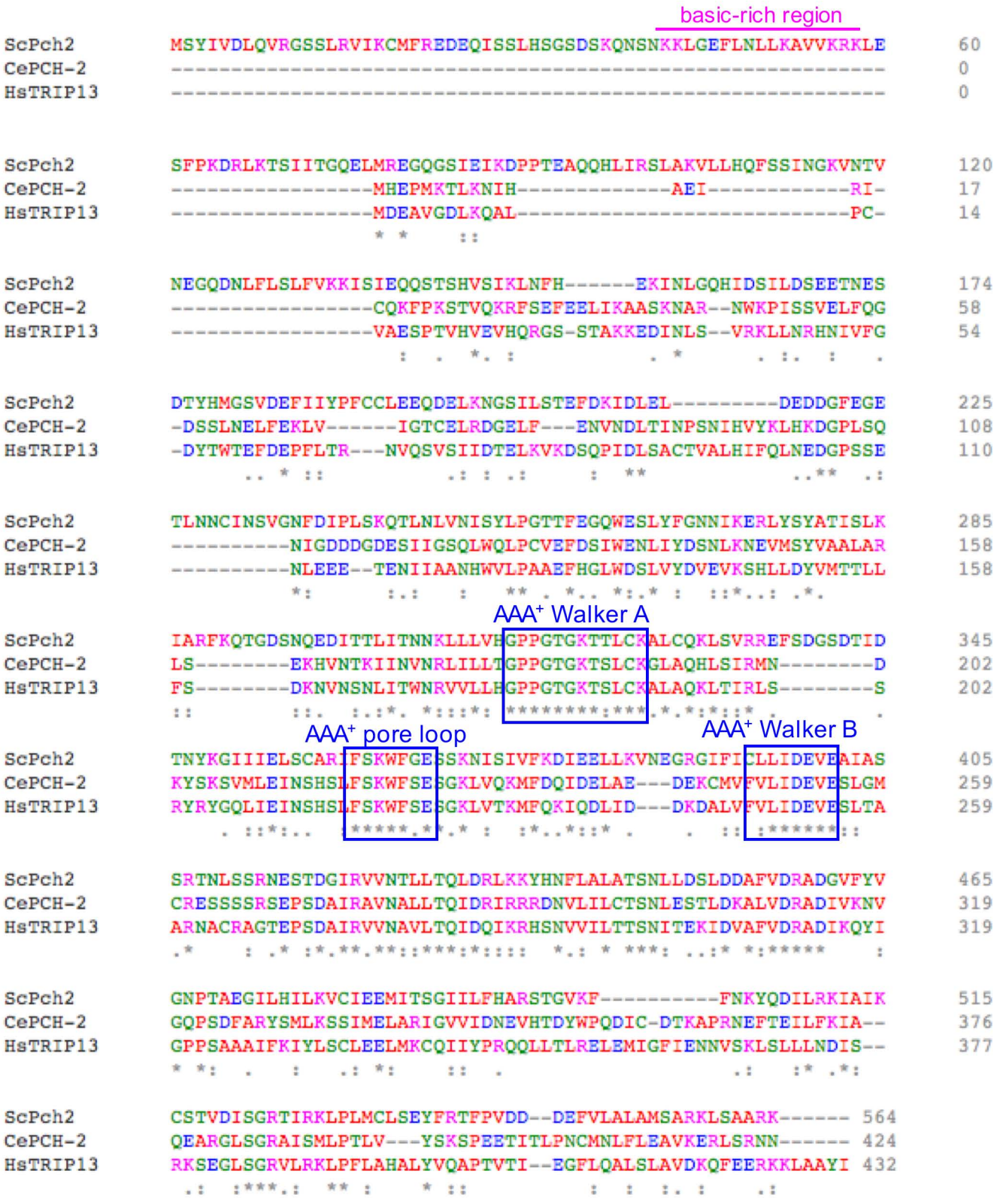

Fig. S1 ClustalW alignment of the protein sequences of Pch2 orthologs from *S. cerevisiae* (ScPch2), *C. elegans* (CePCH-2) and human (HsTRIP13). The characteristic AAA+ ATPase features are boxed (blue). The basic-rich motif in the ScPch2 NTD is underlined (magenta). The color code for amino acids is the following: AVFPMILW (small + hydrophobic -Y): red. DE (acidic): blue. RK (basic -H): magenta. STYHCNGQ (hydroxyl +sulfhydryl + amine + G): green. Alignment was performed at https://www.ebi.ac.uk/Tools/msa/clustalo/.

PCH2/YBR186w

Feature	Relative Coordinates	Coordinates
CDS	1..1551	chrII:600553..602103
intron	1552..1664	chrII:602104..602216
CDS	1665..1808	chrII:602217..602360

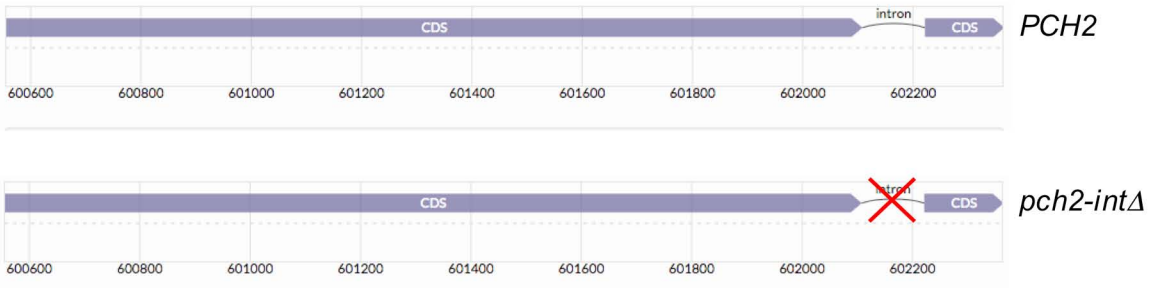

Fig. S2 The *S. cerevisiae PCH2* locus. Schematic representation of the intron-containing *PCH2* gene displaying the chromosome II coordinates. In the *pch2-intΔ* allele the intron was deleted, but the coding sequence is unchanged. Data obtained and representation modified from the Saccharomyces Genome Database (https://www.yeastgenome.org/).

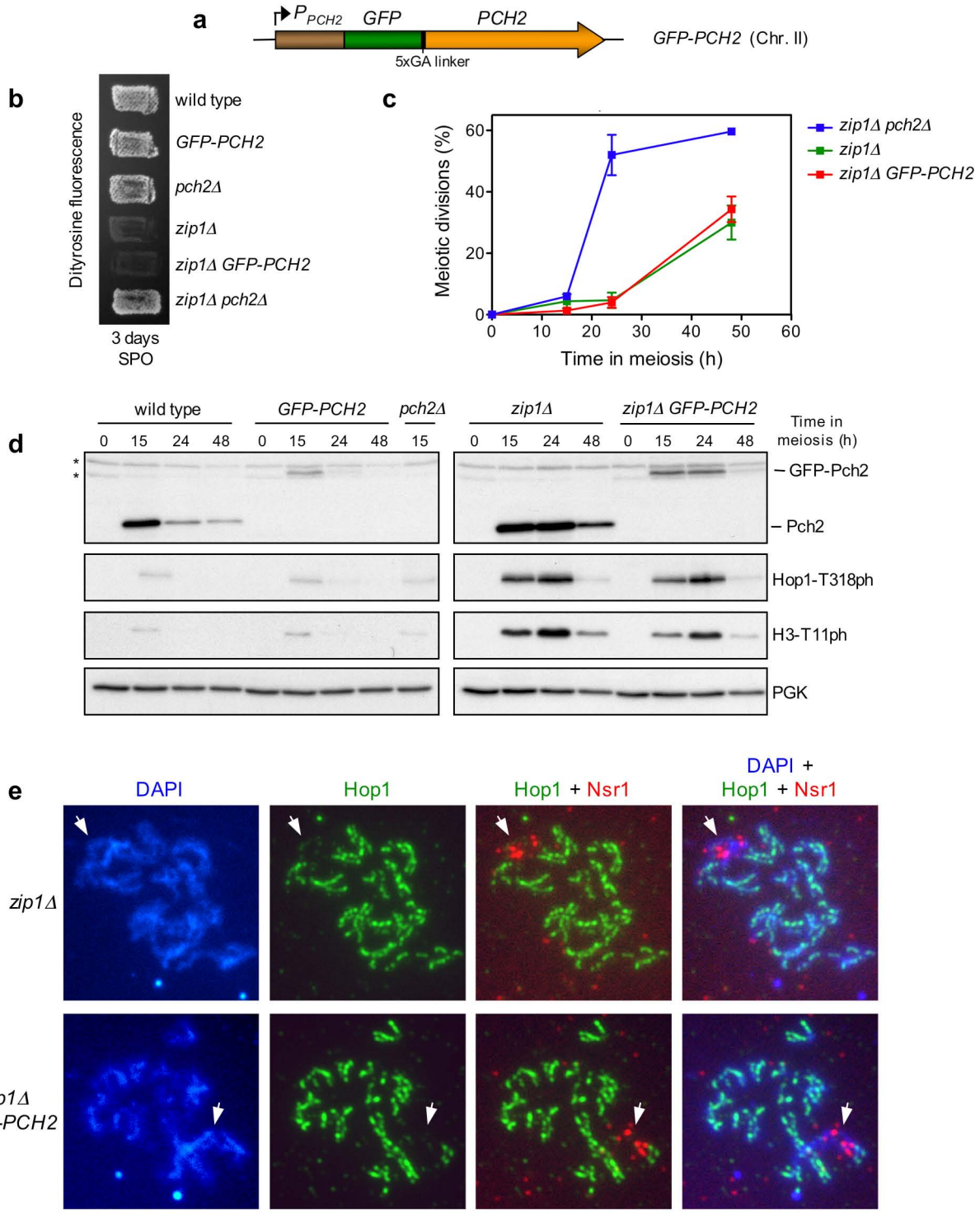

Fig. S3 The GFP-Pch2 protein fully supports meiotic checkpoint function. **a** Schematic representation of the *PCH2* gene tagged with *GFP* at its own genomic locus in chromosome II to generate *GFP-PCH2* strains. **b** Dityrosine fluorescence, as an indicator of sporulation, was examined after 3 days of sporulation on plates. **c** Time course analysis of meiotic nuclear divisions; the percentage of cells containing two or more nuclei is represented. Error bars: SD; n=3. **d** Western blot analysis of Pch2 and GFP-Pch2 production during meiosis (detected with anti-Pch2 antibodies), Hop1-T318 phosphorylation and Mek1 activation (H3-T11 phosphorylation). PGK was used as a loading control. **e** Immunofluorescence of meiotic chromosomes stained with anti-Nsr1 antibodies (red), anti-Hop1 antibodies (green) and DAPI (blue). Representative nuclei are shown Strains in (**b, c, d, e**) are: DP421 (wild type), DP1508 (*GFP-PCH2*), DP1023 (*pch2*Δ), DP422 (*zip1Δ*), DP1509 (*zip1Δ GFP-PCH2*) and DP1029 (*zip1Δ pch2Δ*).

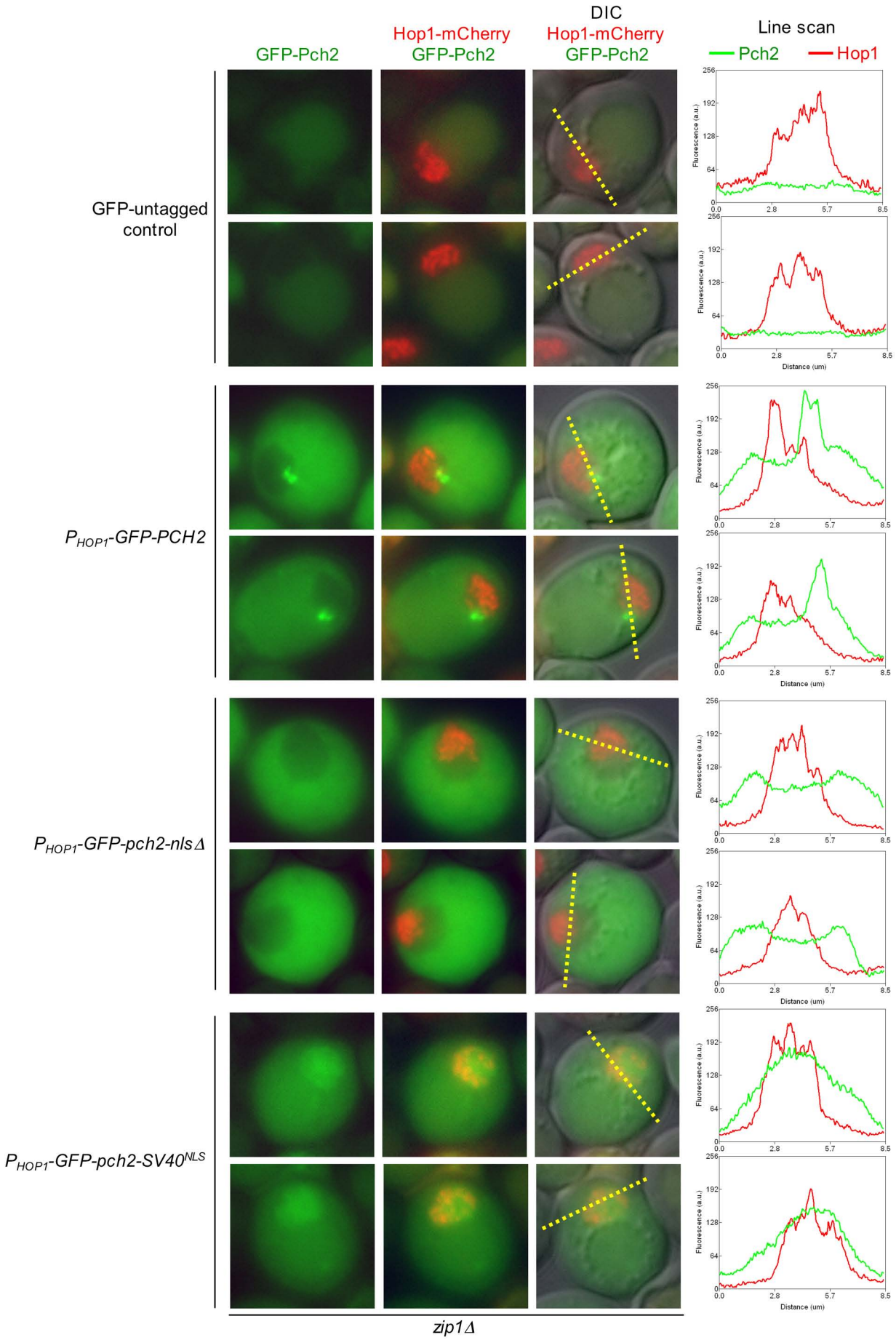

Fig. S4 Localization of GFP-Pch2, GFP-Pch2-nlsΔ and GFP-Pch2-SV40NLS in whole meiotic cells. Fluorescence microscopy images, and the corresponding line scan plots, of additional cells to those shown in Fig. 4d. The DP1500 (*zip1Δ*) strain was transformed with pSS393 (P_{HOP1}-*GFP-PCH2*), pSS396 (P_{HOP1}-*GFP-pch2-nlsΔ*) or pSS397 (P_{HOP1}-*GFP-pch2-SV40^{NLS}*).

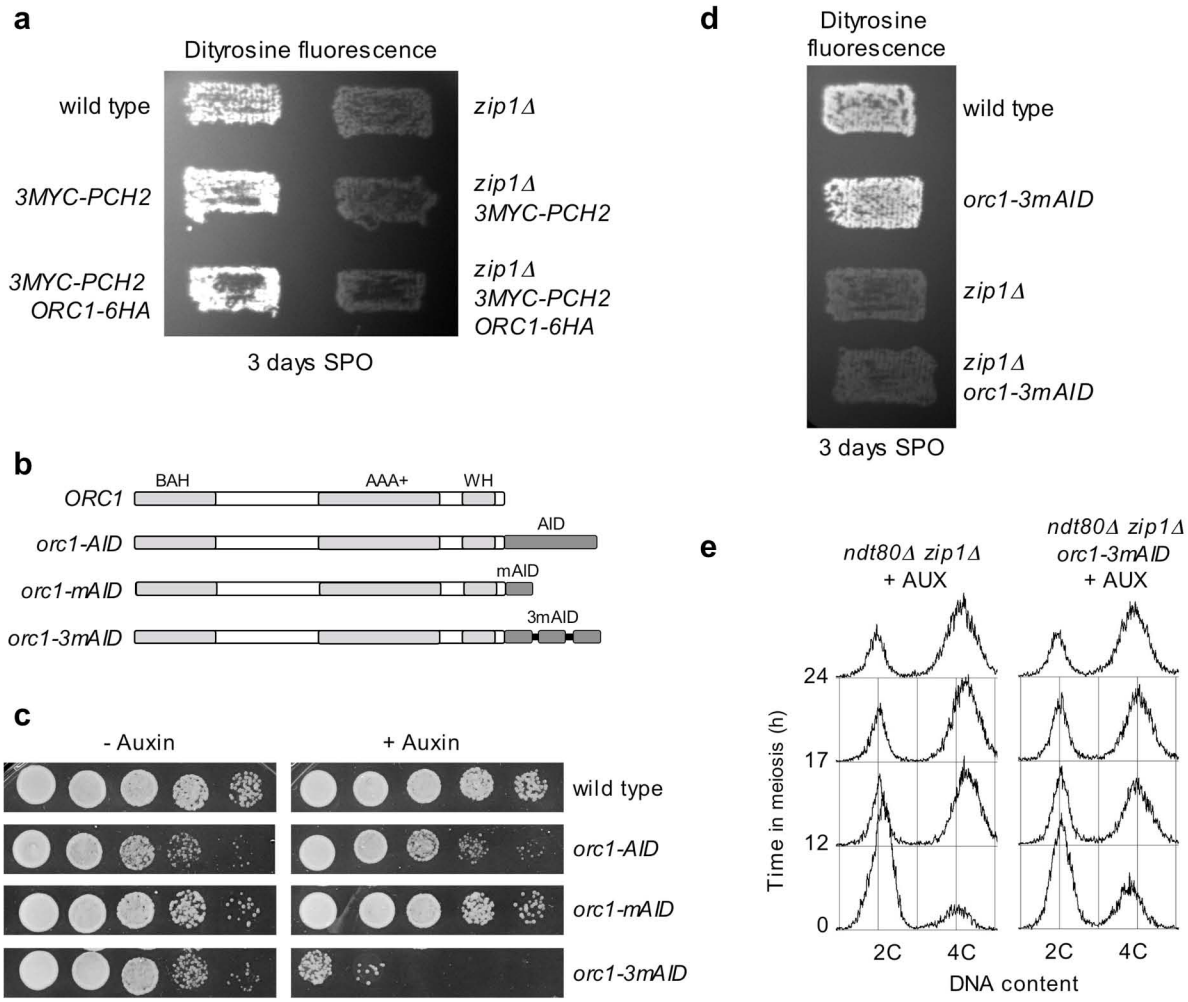

Fig. S5 Functional analysis of different tagged versions and degron alleles of *ORC1*. **a** Dityrosine fluorescence, as an indicator of sporulation, was examined after 3 days of sporulation on plates. Strains in (**a**) are: DP421 (wild type), DP1243 (*3MYC-PCH2*), DP1426 (*3MYC-PCH2 ORC1-6HA*), DP422 (*zip1Δ*), DP1244 (*zip1Δ 3MYC-PCH2*) and DP1427 (*zip1Δ 3MYC-PCH2ORC1-6HA*). **b, c** Construction and analysis of auxin-induced *orc1* degron alleles. **b** Schematic representation of the Orc1 protein indicating relevant functional domains (Kawakami et al. 2015). BAH: bromo-adjacent homology. WH: winged helix. The different versions of the auxin-induced degron used (AID, mAID and 3mAID) are also depicted. **c** Growth analysis of the different *orc1* alleles. Ten-fold serial dilutions of late log-phase cultures were spotted onto YPDA plates without auxin or containing 500 μM auxin. Representative clones of several transformants tested containing P_{ADH1}-*OsTIR1* (pMK200) are shown. **d** Dityrosine fluorescence, as an indicator of sporulation, was examined after 3 days of sporulation on plates. Strains in (**d**) are DP421 (wild type), DP1437 (*orc1-3mAID*), DP422 (*zip1Δ*) and DP1438 (*zip1Δ orc1-3mAID*). **e** FACS analysis of DNA content during meiosis. Auxin (500 μM) was added to cultures 12 h after meiotic induction. Strains in (**e**) are: DP1190 (*ndt80Δ zip1Δ*) and DP1452 (*ndt80Δ zip1Δ orc1-m3AID*).

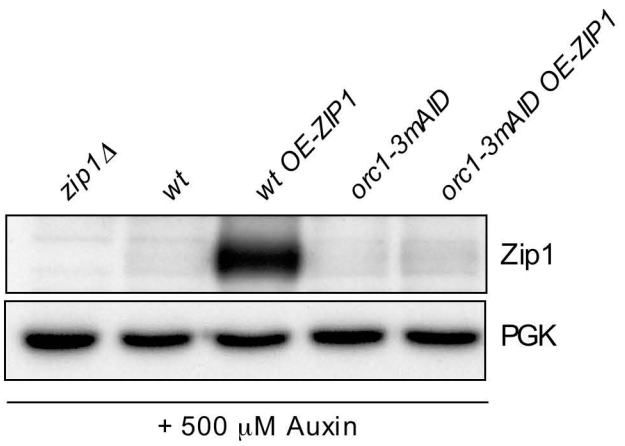

Fig. S6 Deficient *ZIP1* overexpression in the *orc1-3mAID* mutant. Western blot analysis of Zip1 overproduction. Auxin (500 μM) was added to cultures 12 h after meiotic induction and cell extracts were prepared at 18 hours. Strains are: DP1152 (*zip1Δ*), DP1151 (wt), DP1151 + pSS343 (wt *OE-ZIP1*), DP1437 (*orc1-3mAID*) and DP1437 + pSS343 *(orc1-3mAID OE-ZIP1*).

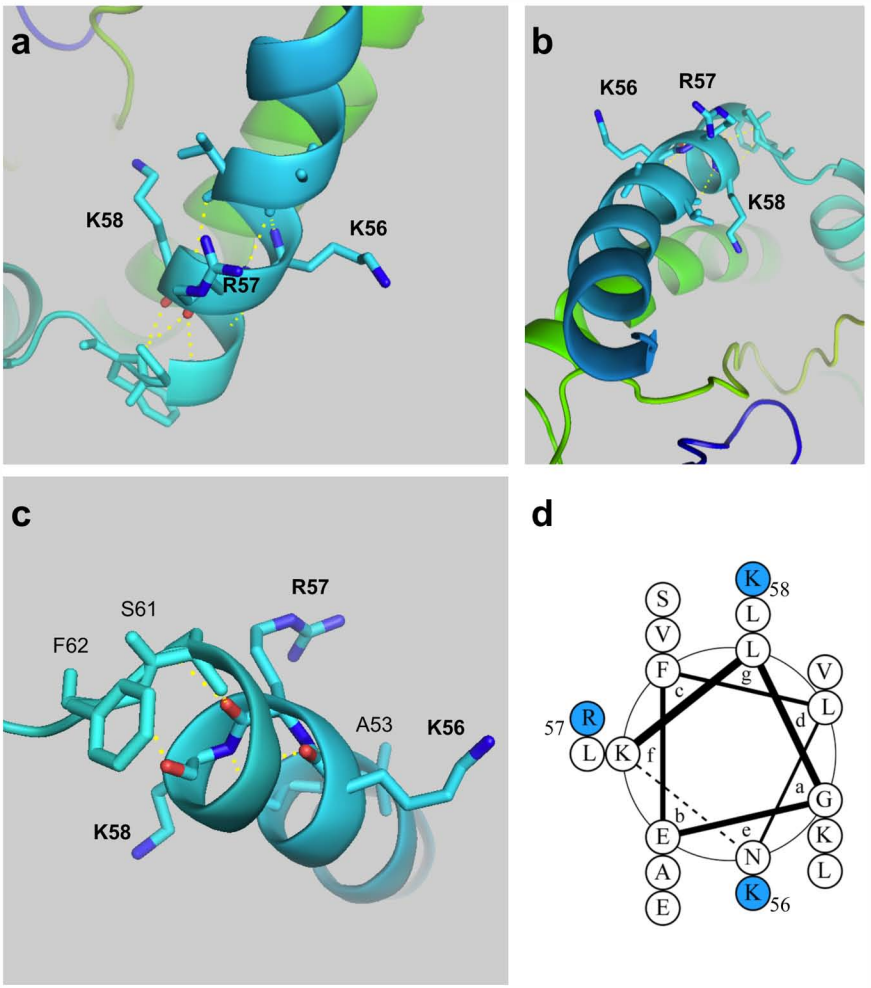

Fig. S7 Structural prediction of the basic motif in Pch2's NTD containing the $K_{56}R_{57}K_{58}$ residues. (**a-c**) Different views of the positions of the three amino acids K_{56}, R_{57}, and K_{58} within an α-helix. Relevant amino acids are depicted. Dark blue lines represent basic groups in lysines 56 and 58, and arginine 57. Red lines represent carbonyl groups. Yellow dotted lines represent polar contacts of these three residues with other nearby amino acids. Protein structure was modeled using the Phyre2 web portal (Kelley et al. 2015). Files were visualized, and images obtained, using the PyMOL Molecular Graphics System, Version 2.0 Schrödinger, LLC. (**d**) Two-dimensional distribution of residues $K_{56}R_{57}K_{58}$ (blue circles) within the predicted coiled-coil domain assembled from residues 43-KLGEFLNLLKAVVKRKLES-61. The diagram was generated using the DrawCoil 1.0 web tool available from https://grigoryanlab.org/drawcoil/.

Table S1. Quantitative data corresponding to spread immunolocalization figures

Figure 2a	**Pch2 rDNA localization**		
Relevant genotype (Strain)	**YES (%)**	**NO (%)**	**Nuclei scored**
wild type (DP1191)	100	0	58
pch2-nlsΔ (DP1411)	0	100	30
pch2-SV40^{NLS} (DP1455)	0	100	25
zip1Δ (DP1190)	100	0	20
zip1Δ pch2-nlsΔ (DP1412)	0	100	31
zip1Δ pch2-SV40^{NLS} (DP1456)	0	100	20

Figure 2b	**Pch2 localization at polycomplex**		
Relevant genotype (Strain)	**YES (%)**	**NO (%)**	**Nuclei scored**
wild type *OE-ZIP1* (DP1151/pSS343)	81.8	18.2	33
pch2-nlsΔ OE-ZIP1 (DP1408/pSS343)	0	100	22
pch2-K320A OE-ZIP1 (DP1163/pSS343)	0	100	20
pch2-E399Q OE-ZIP1 (DP1287/pSS343)	78.9	21.1	19
pch2-SV40^{NLS} OE-ZIP1 (DP1455/pSS343)	0	100	21

Figure 3c	**Pch2 rDNA localization**		
Relevant genotype (Strain)	**YES (%)**	**NO (%)**	**Nuclei scored**
zip1Δ PCH2 (DP1405/pSS75)	60	40	40
zip1Δ pch2-nlsΔ (DP1405/pSS338)	0	100	40
zip1Δ pch2-ntd6A (DP1405/pSS358)	2.5	97.5	40
zip1Δ pch2-ntd2A (DP1405/pSS363)	53.7	46.3	41
zip1Δ pch2-ntd3A (DP1405/pSS364)	0	100	40
zip1Δ pch2-intΔ (DP1405/pSS362)	62.2	37.8	37
	Hop1 localization pattern		
Relevant genotype (Strain)	**Linear (%)**	**Fragmented (%)**	**Nuclei scored**
zip1Δ PCH2 (DP1405/pSS75)	58	42	50
zip1Δ pch2-nlsΔ (DP1405/pSS338)	0	100	40
zip1Δ pch2-ntd6A (DP1405/pSS358)	2.1	97.9	47
zip1Δ pch2-ntd2A (DP1405/pSS363)	52.9	47.1	51
zip1Δ pch2-ntd3A (DP1405/pSS364)	2.3	97.7	43
zip1Δ pch2-intΔ (DP1405/pSS362)	52.5	47.5	40

Figure 3d	**Pch2 localization at polycomplex**		
Relevant genotype (Strain)	**YES (%)**	**NO (%)**	**Nuclei scored**
PCH2 (DP186/pSS75+pSS343)	68.4	31.6	19
pch2-ntd6A (DP186/pSS358+pSS343)	0	100	18
pch2-ntd2A (DP186/pSS363+pSS343)	30.8	69.2	26
pch2-ntd3A (DP186/pSS364+pSS343)	0	100	16
pch2-intΔ (DP186/pSS362+pSS343)	57.9	42.1	19

Figure 5a	Pch2 rDNA accumulation		
Relevant genotype (Strain)	**YES (%)**	**NO (%)**	**Nuclei scored**
3MYC-PCH2 ORC1-6HA (DP1426)	84.7	15.3	72
zip1Δ 3MYC-PCH2 ORC1-6HA (DP1427)	58.8	41.2	51
3MYC-PCH2 (DP1243)	100	0	12
zip1Δ 3MYC-PCH2 (DP1244)	100	0	13
	Pch2-Orc1 colocalization in the rDNA		
Relevant genotype (Strain)	**YES (%)**	**NO (%)**	**Nuclei scored**
3MYC-PCH2 ORC1-6HA (DP1426)	100	0	61
zip1Δ 3MYC-PCH2 ORC1-6HA (DP1427)	100	0	30

Figure 5b	Orc1 rDNA localization		
Relevant genotype (Strain)	**YES (%)**	**NO (%)**	**Nuclei scored**
3MYC-PCH2 ORC1-6HA (DP1426)	100	0	26
	Orc1 rDNA accumulation		
Relevant genotype (Strain)	**YES (%)**	**NO (%)**	**Nuclei scored**
3MYC-PCH2 ORC1-6HA (DP1426)	53.9	46.1	26

Figure 6b	Pch2 rDNA localization		
Relevant genotype (Strain)	**YES (%)**	**NO (%)**	**Nuclei scored**
wild type + Auxin (DP1151)	100	0	16
orc1-3mAID + EtOH (DP1437)	0	100	15
orc1-3mAID + Auxin (DP1437)	0	100	18
zip1Δ + Auxin (DP1152)	100	0	20
zip1Δ orc1-3mAID + EtOH (DP1438)	0	100	20
zip1Δ orc1-3mAID + Auxin (DP1438)	0	100	20

Figure 6c	Hop1 exclusion from the nucleolus		
Relevant genotype (Strain)	**YES (%)**	**NO (%)**	**Nuclei scored**
wild type + Auxin (DP1151)	100	0	29
orc1-3mAID + Auxin (DP1437)	0	100	20
zip1Δ + Auxin (DP1152)	100	0	23
zip1Δ orc1-3mAID + Auxin (DP1438)	0	100	21

Figure 6d	Pch2 localization at polycomplex		
Relevant genotype (Strain)	**YES (%)**	**NO (%)**	**Nuclei scored**
spo11Δ + Auxin (DP1425)	54.2	45.8	24
spo11Δ orc1-3mAID + Auxin (DP1444)	76.0	24.0	25

Table S2. *Saccharomyces cerevisiae* strains

Strain	Genotype*	Source
BR2495-2N	*MAT***a**/*MAT*α *leu2-27/leu2-3,112 his4-280/his4-260 arg4-8/ARG4 thr1-1/thr1-4 trp1-1/trp1-289 cyh10/CYH10 ura3-1 ade2-1*	Roeder Lab
DP186	BR2495-2N *pch2Δ::URA3*	PSS Lab
BR1919-2N	*MAT***a**/*MAT*α *leu2-3,112 his4-260 thr1-4 trp1-289 ura3-1 ade2-1*	Roeder Lab
DP421	BR1919-2N *lys2ΔNheI*	PSS Lab
DP422	DP421 *zip1Δ::LYS2*	PSS Lab
DP881	DP421 *zip1Δ::LYS2 pch2Δ::TRP1 ndt80Δ::LEU2*	PSS Lab
DP1023	DP421 *pch2Δ::TRP1*	PSS Lab
DP1029	DP421 *zip1Δ::LYS2 pch2Δ::TRP1*	PSS Lab
DP1151	BR1919-2N *3HA-PCH2*	PSS Lab
DP1152	BR1919-2N *zip1Δ::LEU2 3HA-PCH2*	PSS Lab
DP1161	BR1919-2N *zip1Δ::LEU2 pch2Δ::TRP1*	PSS Lab
DP1163	BR1919-2N *3HA-pch2-K320A*	PSS Lab
DP1164	BR1919-2N *pch2Δ::TRP1*	PSS Lab
DP1190	BR1919-2N *zip1Δ::LEU2 ndt80Δ::kanMX3 3HA-PCH2*	PSS Lab
DP1191	BR1919-2N *ndt80Δ::kanMX3 3HA-PCH2*	PSS Lab
DP1243	BR1919-2N *3MYC-PCH2*	PSS Lab
DP1244	BR1919-2N *zip1Δ::LEU2 3MYC-PCH2*	PSS Lab
DP1287	BR1919-2N *3HA-pch2-E399Q*	PSS Lab
DP1405	DP421 *zip1Δ::LEU2 pch2Δ::URA3*	This work
DP1408	BR1919-2N *3HA-pch2-nlsΔ*	This work
DP1409	BR1919-2N *zip1Δ::LEU2 3HA-pch2-nlsΔ*	This work
DP1411	BR1919-2N *ndt80::kanMX3 3HA-pch2-nlsΔ*	This work
DP1412	DP421 *zip1Δ::LEU2 ndt80Δ::kanMX3 3HA-pch2-nlsΔ*	This work
DP1425	BR1919-2N *spo11Δ::natMX4 3HA-PCH2*	This work
DP1426	BR1919-2N *3MYC-PCH2 ORC1-6HA::hphNT1*	This work
DP1427	BR1919-2N *zip1Δ::LEU2 3MYC-PCH2 ORC1-6HA::hphNT1*	This work
DP1437	BR1919-2N *orc1-3mAID::hphNT* P_{HOP1}*-OsTIR1::URA3 3HA-PCH2*	This work

DP1438	BR1919-2N *orc1-3mAID::hphNT* P_{HOP1}*-OsTIR1::URA3 zip1Δ::LEU2 3HA-PCH2*	This work
DP1444	BR1919-2N *orc1-3mAID::hphNT* P_{HOP1}*-OsTIR1::URA3 spo11Δ::natMX4 3HA-PCH2*	This work
DP1451	BR1919-2N *orc1-3mAID::hphNT* P_{HOP1}*-OsTIR1::URA3 ndt80Δ::kanMX3 3HA-PCH2*	This work
DP1452	BR1919-2N *orc1-3mAID::hphNT* P_{HOP1}*-OsTIR1::URA3 zip1Δ::LEU2 ndt80Δ::kanMX3 3HA-PCH2*	This work
DP1455	BR1919-2N *3HA-pch2-SV40*^{NLS}	This work
DP1456	BR1919-2N *zip1Δ::LEU2 3HA-pch2-SV40*^{NLS}	This work
DP1500	DP421 *zip1Δ::LYS2 HOP1/HOP1-mCherry::natMX4*	This work
DP1508	BR1919-2N *GFP-PCH2*	This work
DP1509	BR1919-2N *GFP-PCH2 zip1Δ::LEU2*	This work
DP1569	DP421 *ndt80Δ::kanMX3 3HA-pch2-ntd3A*	This work
DP1570	DP421 *zip1Δ::LEU2 ndt80Δ::kanMX3 3HA-pch2-ntd3A*	This work
DP1586	BR1919-2N *orc1-3mAID::hphNT* P_{HOP1}*-OsTIR1::URA3 zip1Δ::LEU2 pch2Δ::TRP1*	This work

Table S3. Plasmids

Plasmid name	Vector	Relevant parts	Source
pMK200	pRS306	*URA3* P_{ADH1}-*OsTIR1*	(Nishimura and Kanemaki 2014)
pSS75	pRS314	*TRP1 CEN6 3HA-PCH2*	PSS Lab
pSS338	pRS314	*TRP1 CEN6 3HA-pch2-nlsΔ*	This work
pSS343	YEp351	*LEU2 2μ ZIP1*	Roeder Lab
pSS346	pRS306	*URA3* P_{HOP1}-*OsTIR1*	This work
pSS358	pRS314	*TRP1 CEN6 3HA-pch2-ntd6A*	This work
pSS362	pRS314	*TRP1 CEN6 3HA-pch2-intΔ*	This work
pSS363	pRS314	*TRP1 CEN6 3HA-pch2-ntd2A*	This work
pSS364	pRS314	*TRP1 CEN6 3HA-pch2-ntd3A*	This work
pSS393	pRS314	*TRP1 CEN6* P_{HOP1}-*GFP-PCH2*	This work
pSS396	pRS314	*TRP1 CEN6* P_{HOP1}-*GFP-pch2-nlsΔ*	This work
pSS397	pRS314	*TRP1 CEN6* P_{HOP1}-*GFP-pch2-SV40*^{NLS}	This work

Table S4. Primary antibodies

Antibody	Host and type	Application* (Dilution)	Source / Reference
Hop1 (5C12E8)	Mouse monoclonal	WB (1:2000)	This work
Hop1	Rabbit polyclonal	IF (1:400)	(Smith and Roeder 1997)
Hop1-T318-P	Rabbit polyclonal	WB (1:1000)	(Penedos, *et al.* 2015)
H3-T11-P	Rabbit polyclonal	WB (1:2000)	Abcam ab5168
PGK (22C5D8)	Mouse monoclonal	WB (1:5000)	Molecular Probes 459250
Pch2	Rabbit polyclonal	WB (1:2000) IF (1:325)	This work
Nsr1 (31C4)	Mouse monoclonal	IF (1:150)	ThermoFisher MA1-10030
Nsr1 (2.3 b)	Mouse monoclonal	IF (1:20)	M. Snyder
HA (12CA5)	Mouse monoclonal	WB (1:2000) IF (1:200)	Roche 11 666 606 001
Zip1	Rabbit polyclonal	WB (1:2000) IF (1:200)	(Sym, *et al.* 1993)
mAID (1E4)	Mouse monoclonal	WB (1:400)	MBL M214-3
H4-K16ac	Rabbit polyclonal	IF (1:200)	Millipore 07-329

*WB, western blot; IF, immunofluorescence

Supplemental References

Kawakami H, Ohashi E, Kanamoto S, Tsurimoto T, Katayama T (2015) Specific binding of eukaryotic ORC to DNA replication origins depends on highly conserved basic residues. Sci Rep 5: 14929.

Kelley LA, Mezulis S, Yates CM, Wass MN, Sternberg MJ (2015) The Phyre2 web portal for protein modeling, prediction and analysis. Nat Protoc 10: 845-858.

Nishimura K, Kanemaki MT (2014) Rapid Depletion of Budding Yeast Proteins via the Fusion of an Auxin-Inducible Degron (AID). Curr Protoc Cell Biol 64: 20 29 21-16.

Penedos A, Johnson AL, Strong E, Goldman AS, Carballo JA, Cha RS (2015) Essential and Checkpoint Functions of Budding Yeast ATM and ATR during Meiotic Prophase Are Facilitated by Differential Phosphorylation of a Meiotic Adaptor Protein, Hop1. PLoS One 10: e0134297.

Smith AV, Roeder GS (1997) The yeast Red1 protein localizes to the cores of meiotic chromosomes. J Cell Biol 136: 957-967.

Sym M, Engebrecht JA, Roeder GS (1993) ZIP1 is a synaptonemal complex protein required for meiotic chromosome synapsis. Cell 72: 365-378.

CONCLUSIONES

1. El motivo básico KRK dentro del extremo N-terminal de Pch2 es necesario para su función en el *checkpoint* meiótico, así como para su localización en el nucleolo, su asociación con proteínas del complejo sinaptonémico y su correcta distribución entre los distintos compartimentos celulares.

2. El motivo básico del NTD de Pch2 no actúa, al menos solamente, como una simple NLS puesto que la sustitución de dicho motivo por la NLS canónica del virus SV40 es capaz de redirigir a Pch2 al núcleo, pero sin recuperar la localización correcta en el nucleolo ni la funcionalidad del *checkpoint*.

3. El intrón de Pch2 no tiene relevancia funcional en el *checkpoint* ni en la localización de la proteína.

4. Orc1 y Pch2 colocalizan en el nucleolo, siendo Orc1 necesario para la localización de Pch2 en esta región, pero no para la asociación de Pch2 con proteínas del complejo sinaptonémico (Zip1).

5. La activación del *checkpoint* de recombinación meiótica no se ve afectada por la ausencia de Orc1 ni, por tanto, por la falta de localización nucleolar de Pch2

CONCLUSIONS

1. The basic-rich KRK motif in the Pch2 N-terminal domain is required for meiotic checkpoint function as well as for Pch2's nucleolar localization, association to SC components and proper subcellular distribution.

2. The basic-rich motif in the NTD of Pch2 is not simply acting as an NLS sequence given that the substitution of this motif for the canonical NLS from SV40 is capable of bringing Pch2 back to the nucleus, but it does not restore its normal nucleolar distribution or its checkpoint function.

3. The *PCH2* intron is neither relevant for the meiotic checkpoint nor for Pch2 chromosomal localization.

4. Orc1 and Pch2 colocalize in the nucleolar region, being Orc1 required for Pch2 localization in this region, but not for Pch2 association with SC proteins (Zip1).

5. Activation of the meiotic recombination checkpoint is not affected by the absence of Orc1, and hence, of nucleolar Pch2.

Anexo

ANEXO: "*The meiosis-specific AAA+ ATPase Pch2 implements the chromosome-synapsis checkpoint response from outside the nucleus*"

GRAPHICAL ABSTRACT

	Pch2 localization		
Genotype	**Nucleolus**	**Cytoplasm**	**Checkpoint function**
zip1Δ	+	+	+
zip1Δ orc1-3mAID	-	+	+
zip1Δ OE-PCH2	+	+	+
zip1Δ NES-PCH2	-	+	+
zip1Δ NLS-PCH2	+	-	-

Cytoplasmic localization of Pch2 correlates with checkpoint activity

The meiosis-specific AAA+ ATPase Pch2 implements the chromosome-synapsis checkpoint response from outside the nucleus

Esther Herruzo[1] and Pedro A. San-Segundo[1]

[1] Instituto de Biología Funcional y Genómica (IBFG). Consejo Superior de Investigaciones Científicas (CSIC) and University of Salamanca. 37007-Salamanca, Spain.

INTRODUCTION

Using chromosome spreading, we have previously described that Pch2 is not recruited to the nucleolus (rDNA) in the absence of Orc1 and, consistent with that, Hop1 is not excluded from that region. However, the *zip1Δ*-triggered meiotic recombination checkpoint is fully functional in this situation, demonstrating that Pch2 nucleolar localization is dispensable for the checkpoint (Herruzo et al., 2019).

In the *zip1Δ* mutant lacking Orc1, Pch2 is not detected whatsoever associated to meiotic chromosomes, but the meiotic checkpoint is still functional. This observation raises the possibility of a chromatin/chromosome-independent fraction of Pch2 that may sustain the checkpoint response. Therefore, to elucidate where the Pch2 population that is relevant for checkpoint function localizes to, we explored Pch2 subcellular localization in whole meiotic cells in different conditions.

RESULTS

Pch2 localizes to the cytoplasm in the absence of Orc1, but the *zip1Δ*-induced checkpoint remains active

To explore Pch2 subcellular distribution in *zip1Δ orc1-3mAID* whole meiotic cells we integrated the P_{HOP1}-*GFP-PCH2* construct previously described (Herruzo et al., 2019) into the genome of *zip1Δ orc1-3mAID*. We first checked that the GFP-Pch2 protein is completely functional, as evidenced by the tight sporulation block of the *zip1Δ* P_{HOP1}-*GFP-PCH2* strain, similar to that of *zip1Δ* (Figure 1A). Consistent with our previous results (Herruzo et al., 2019), we confirmed that the checkpoint remains fully functional in the *zip1Δ orc1-3mAID* P_{HOP1}-*GFP-PCH2* strain, as manifested by high levels of Hop1 phosphorylation when Orc1 is depleted, also comparable to those of *zip1Δ* (Figure 1B).

Next, we analyzed GFP-Pch2 and Hop1-mCherry subcellular distribution by fluorescence microscopy in live meiotic cells. In the *zip1Δ* mutant, GFP-Pch2 localized to a discrete region at one side of the nucleus that does not overlap with Hop1-mCherry. According with the well-characterized Pch2 localization on *zip1Δ* chromosome spreads (Herruzo et al., 2016, 2019) this discrete region must correspond to the nucleolus. In addition, GFP-Pch2 was also detected in the cytoplasm, displaying a diffuse homogenous signal (Figure 1C). In contrast, and consistent with the lack of Pch2 nucleolar localization upon Orc1 depletion observed by immunofluorescence of chromosome

spreads (Herruzo et al., 2019), GFP-Pch2 exclusively localized to the cytoplasm in *zip1Δ orc1-3mAID* cells (Figure 1C). Quantification of the ratio between nuclear (including nucleolus) and cytoplasmic GFP signal confirmed the cytoplasmic accumulation of Pch2 in the absence of Orc1 (Figure 1D). Importantly, despite the altered subcellular distribution, GFP-Pch2 global levels were unaltered when Orc1 was depleted (Figure 1B). Since the checkpoint remains completely active in the *zip1Δ orc1-3mAID* mutant (Herruzo et al., 2019; Figure 1B) these results suggest that the cytoplasmic population of Pch2 is relevant to promote Hop1-Mek1 activation.

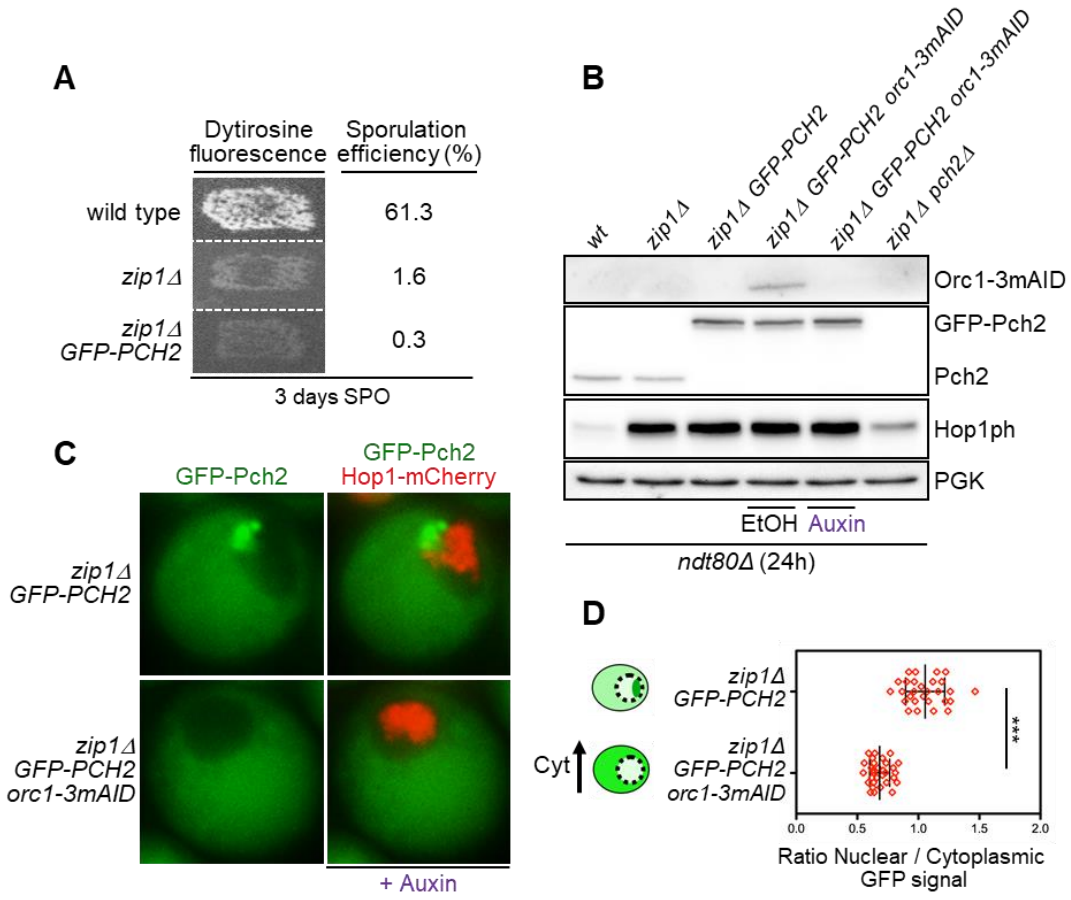

Figure 1. The absence of Orc1 leads to cytoplasmic accumulation of Pch2 and the checkpoint remains active. **A)** Functional analysis of the GFP-tagged version of *PCH2*. Dytirosine fluorescence, as an indicator of sporulation, and sporulation efficiency were examined after 3 days of sporulation on plates. Strains are DP421 (wild type), DP422 (*zip1Δ*) and DP1621 (*zip1Δ GFP-PCH2*). **B)** Western blot analysis of Orc1-3mAID production, detected with an anti-mAID antibody, GFP-Pch2 and Pch2, detected with an anti-Pch2 antibody, and Hop1-T318 phosphorylation (Hop1ph). PGK was used as loading control. Strains are DP424 (wild type), DP428 (*zip1Δ*), DP1640 (*zip1Δ GFP-PCH2*), DP1630 (*zip1Δ orc1-3mAID GFP-PCH2*) and DP881 (*zip1Δ pch2Δ*). All strains are in a *ndt80Δ* background. EtOH or auxin (500 µM) was added to *orc1-3mAID* cultures at 12h. Samples were collected at 24 h after meiotic induction. **C)** Fluorescence microscopy analysis of GFP-Pch2 (green) and Hop1-mCherry (red) distribution in whole meiotic cells 16 h after meiotic induction. Representative cells are shown. **D)** Quantification of the ratio between the nuclear (including the nucleolar) and cytoplasmic GFP fluorescent signal. The cartoon illustrates the subcellular localization of GFP-Pch2 in the different conditions. The strains in **C** and **D** are DP1636 (*zip1Δ GFP-PCH2*) and DP1633 (*zip1Δ orc1-3mAID GFP-PCH2*). Auxin (500 µM) was added to the *orc1-3mAID* culture 12 hours after meiotic induction.

GFP-PCH2 overexpression leads to cytoplasmic aggregates that retain checkpoint function

To rule out the possibility of the existence of an undetectable fraction of GFP-Pch2 present in the nucleus of *zip1Δ* cells that might still be responsible for the checkpoint, we overexpressed the P_{HOP1}-*GFP-PCH2* construct from a high-copy plasmid (*OE- GFP-PCH2*) (Figure 2A). Western blot analysis showed that strong overproduction of GFP-Pch2 was achieved (Figure 2B).

We next analyzed GFP-Pch2 localization in meiotic chromosome spreads of *zip1Δ*. We found that despite the high levels of the protein, GFP-Pch2 chromatin association was not incremented and it was only detected associated to the nucleolus (Figure 2C).

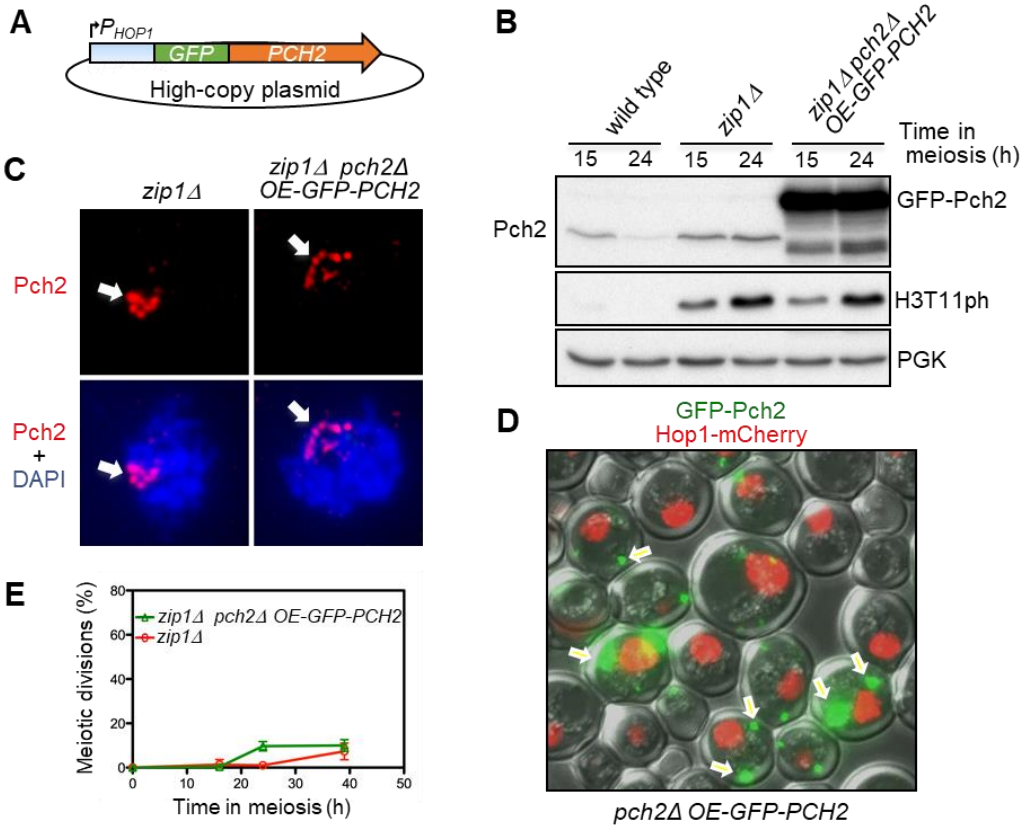

Figure 2. ***GFP-PCH2*** **overexpression leads to cytoplasmic aggregates and the checkpoint is active. A)** Schematic representation of the P_{HOP1}-*GFP-PCH2* construct in the pSS367 high-copy plasmid. **B)** Western blot analysis of GFP-Pch2 and Pch2 (detected with an anti-Pch2 antibody), and H3T11 phosphorylation as an indicator of Mek1 activation. PGK was used as loading control. Strains are DP421 (wild type) and DP422 (*zip1Δ)* transformed with the empty vector (pRS426) and DP1029 (*zip1Δ pch2Δ)* transformed with pSS367 (P_{HOP1}-*GFP-PCH2*). **C)** Immunofluorescence of meiotic chromosome spreads stained with an anti-Pch2 antibody to detect Pch2 and GFP-Pch2 (red) and DAPI (blue). Representative nuclei are shown. Samples were prepared at 15 h in meiosis. Arrows point to the rDNA region. Strains are DP422 transformed with the empty vector (pRS426) and DP1029 (*zip1Δ pch2Δ)* transformed with pSS367 (*OE-GFP-PCH2*). **D)** Fluorescence microscopy image showing GFP-Pch2 (green) and Hop1-mCherry (red) localization in whole meiotic cells. The overlay with differential interference contrast (DIC) images is also shown. Strain is DP1501 (*pch2Δ*) transformed with pSS367 (*OE-GFP-PCH2*). **E)** Time course analysis of meiotic divisions; the percentage of cells containing two or more nuclei is represented. Error bars: SD; n=3.

To investigate where the excess of the GFP-Pch2 protein localizes to, we analyzed its distribution in whole meiotic prophase cells. We observed that GFP-Pch2 was not notably detected in the nucleolus as it normally is (see Figure 1C above). In contrast, GFP-Pch2 formed conspicuous aggregates in the cytoplasm (Figure 2D, arrows).

We next explored checkpoint functionality in this condition where strong overproduction leads to GFP-Pch2 altered distribution. To this end, we monitored the kinetics of meiotic divisions (Figure 2E) and the phosphorylation status of H3T11 as a readout of Mek1 kinase activity; that is, of checkpoint activation (Figure 2B). We found that the checkpoint is functional in *zip1Δ pch2Δ* cells overexpressing *GFP-PCH2*, as manifested by the noticeable meiotic arrest and the high levels of H3T11ph, similar to those of *zip1Δ* (Figures 2E and 2B, respectively).

These observations reinforce the notion that points to the cytoplasmic pool of Pch2 as the relevant population for the checkpoint function. First, the association of GFP-Pch2 to the chromosomes remains undetectable despite the significant increase in protein levels, arguing against a technical detection issue. Second, high levels of GFP-Pch2 result in the formation of aberrant cytoplasmic aggregates compared to the normal diffuse localization; however, despite this altered distribution, the presence of Pch2 in the cytoplasm is capable of sustaining checkpoint activity.

Influence on checkpoint function of forced Pch2 nuclear export and import

To further analyze how Pch2 subcellular distribution impacts on checkpoint function we fused a Nuclear Export Signal (NES) or a Nuclear Localization Signal (NLS) to Pch2 to force its localization outside or inside the nucleus, respectively. Canonical NES and NLS sequences were inserted between the *GFP* and *PCH2* coding sequences in centromeric plasmids containing the P_{HOP1}-*GFP-PCH2* construction (see Materials and Methods for details). These plasmids were transformed into *zip1Δ* or *zip1Δ pch2Δ* strains also harboring *HOP1-mCherry* in heterozygosis as a marker both for the nucleus and for meiotic prophase stage. Live meiotic cells were analyzed by fluorescence microscopy to examine Pch2 and Hop1 localization. As controls, we used the *zip1Δ pch2Δ* strains transformed with either the empty vector or with the plasmid expressing wild-type *GFP-PCH2*. We found that, unlike the wild-type GFP-Pch2 protein, the GFP-NES-Pch2 version did not localize to the nucleolus and accumulated in the cytoplasm (Figure 3A and 3B). In contrast, GFP-NLS-Pch2 strongly accumulated in the nucleolus and also showed a diffuse pan-nuclear signal (Figure 3A and 3B).

To analyze how these variations in Pch2 distribution affect the meiotic checkpoint we quantified sporulation efficiency as a readout for checkpoint activity. The *zip1Δ* mutant showed a tight sporulation block resulting from checkpoint activation; this meiotic arrest was suppressed in the checkpoint-deficient *zip1Δ pch2Δ* double mutant transformed with the empty vector that displayed wild-type sporulation levels (Figure 3C). As expected, sporulation efficiency was strongly reduced in the *zip1Δ pch2Δ* strain expressing the wild-type *GFP-PCH2* from the centromeric plasmid, consistent with restored checkpoint function. Note that the meiotic block was not completely reestablished due

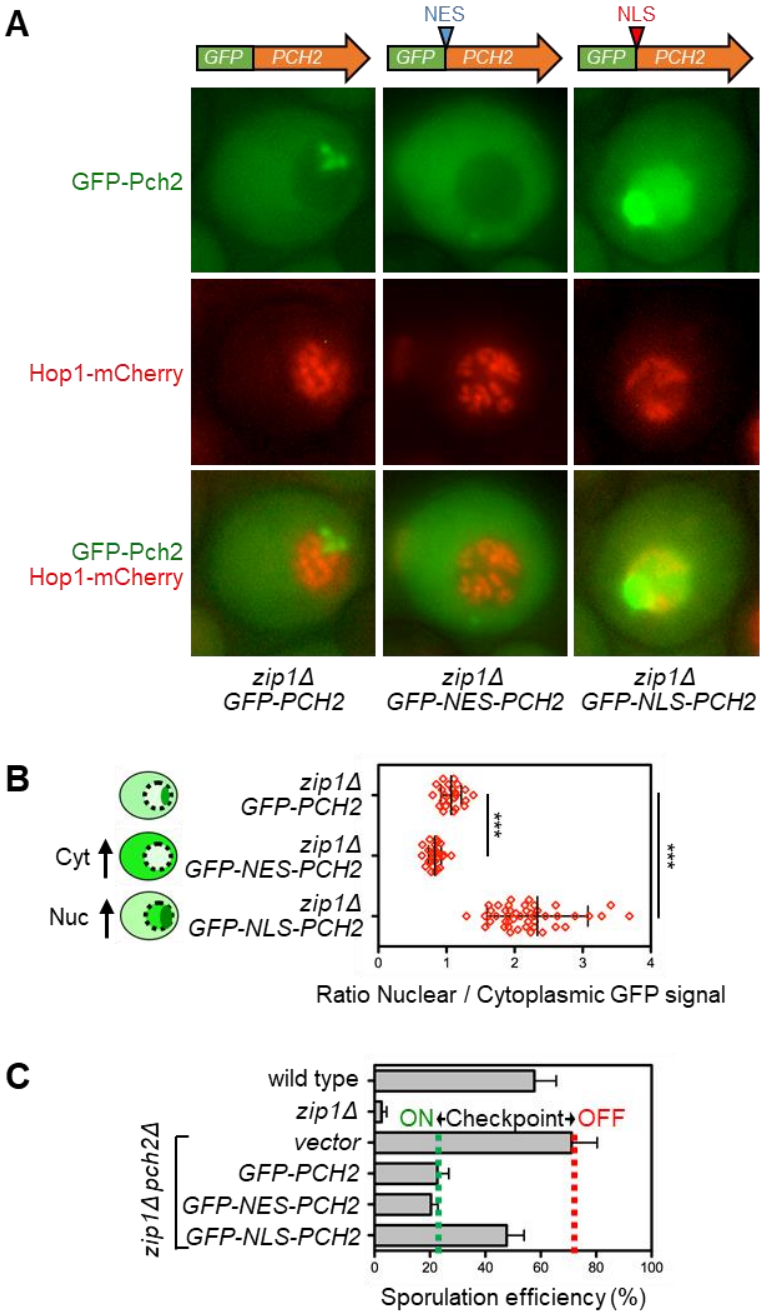

Figure 3. Pch2 subcellular distribution impacts on checkpoint function. A) Fluorescence microscopy analysis of GFP-Pch2, GFP-NES-Pch2 or GFP-NLS-Pch2 (green) and Hop1-mCherry (red) distribution in whole meiotic cells 15 h after meiotic induction. Representative cells are shown. **B)** Quantification of the ratio of nuclear (including nucleolar) to cytoplasmic GFP fluorescent signal. The cartoon illustrates the subcellular localization of the different versions of GFP-Pch2. Strains in **A** and **B** are DP1500 (*zip1Δ)* transformed with pSS393 (*GFP-PCH2)*, pSS408 *(GFP-NES-PCH2)* and pSS421 (*GFP-NLS-PCH2*) plasmids. **C)** Quantification of sporulation efficiency after 3 days on SPO plates. At least 300 cells were scored from each strain. Error bars: SD; n=3. The green and red dotted lines mark the range of full checkpoint function and full checkpoint defect, respectively, in this assay. Strains are DP421 (wild type*)* and DP422 (*zip1Δ*) transformed with the empty vector (pRS314), and DP1405 (*zip1Δ pch2Δ*) transformed with the empty vector (pRS314) or the pSS393 (*GFP-PCH2)*, pSS408 *(GFP-NES-PCH2)* and pSS421 (*GFP-NLS-PCH2*) centromeric plasmids.

to plasmid-loss events; see Herruzo et al., 2019 for explanation. Notably the presence of *GFP-NES-PCH2* also reduced sporulation in *zip1Δ pch2Δ* to similar levels as the wild-type *GFP-PCH2* did (Figure 3C) indicating that the checkpoint is fully active. In contrast, the sporulation efficiency was considerably increased in the *zip1Δ pch2Δ* strain transformed with the plasmid expressing *GFP-NLS-PCH2* (Figure 3C) indicating that the checkpoint is, at least partially, defective.

Thus, when Pch2 distribution is biased to the nucleus/nucleolus (GFP-NLS-Pch2), checkpoint function is impaired and, by the contrary, when Pch2 accumulates in the cytoplasm (GFP-NES-Pch2), checkpoint function is maintained.

DISCUSSION

In this work we have explored the functional contribution of Pch2 subcellular distribution to the meiotic recombination checkpoint triggered by synapsis defects. Our results show a strong correlation between checkpoint activation and Pch2 cytoplasmic localization, suggesting that the cytoplasmic pool of Pch2, but not the nuclear/nucleolar population, is responsible for promoting the meiotic checkpoint response.

We have previously demonstrated that the critical function of Pch2 is to promote Hop1-T318 phosphorylation at unsynapsed chromosome axes to sustain Mek1 activation and the subsequent checkpoint responses (Herruzo et al., 2016). How can Pch2 from the cytoplasm control the phosphorylation of Hop1 on chromosomes? Based on the observations described here, we hypothesize that the cytoplasmic pool of Pch2 could use its ATPase activity to modify a cytoplasmic factor required for Hop1 phosphorylation altering its conformation, as AAA+ ATPases usually do (Puchades et al., 2019). This conformational change may involve the exposition of a masked NLS (or the interaction with another NLS-containing protein) allowing its transport throughout the nuclear pore to promote Hop1 phosphorylation and its association to meiotic chromosomes (Figure 4).

Future experiments will be aimed to identify Pch2 cytoplasmic interactors, which will help us to elucidate the mechanism by which Pch2 from the cytoplasm promotes Hop1 phosphorylation on chromosomes.

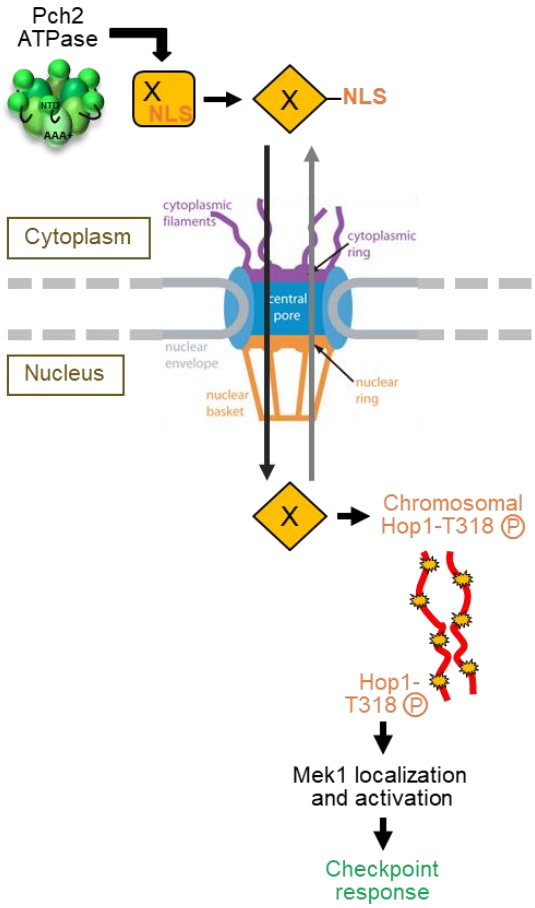

Figure 4. Working model for the possible role of the cytoplasmic Pch2 in the meiotic recombination checkpoint. See text for details.

MATERIALS AND METHODS

Yeast strains

The genotypes of yeast strains are listed in Supplementary Table S1. All strains are in BR1919 background (Rockmill and Roeder, 1990). Gene deletions and *orc1-3mAID* constructs were previously described (Herruzo *et al*., 2016, 2019; Cavero *et al*., 2016). The P_{HOP1}-*GFP-PCH2* construct was introduced into the genomic locus of *PCH2* using the *delitto perfetto* technique (Stuckey *et al*., 2011). Basically, a PCR fragment containing the *HOP1* promoter followed by *GFP* inserted at the second codon of *PCH2* separated by a five Gly-Ala repeats linker was transformed into a strain carrying the CORE cassette close to the 5' end of *PCH2*. Correct 5-FOA-resistant clones containing the construct inserted were checked by PCR and verified by sequencing.

Plasmids

The plasmids used are listed in Supplementary Table S2. The pSS367 plasmid overexpressing P_{HOP1}-*GFP-PCH2* was constructed by amplifying the *PCH2* ORF from pSS361 carrying a *PCH2* allele lacking the intron sequence, using oligos PCH2-NotI and PCH2-SphI and cloning it into *Not*I-*Sph*I sites of pSS248, a high-copy plasmid containing GFP under the *HOP1* promoter (González-Arranz et al., 2018). The pSS393 centromeric plasmid expressing P_{HOP1}-*GFP-PCH2* was previously described (Herruzo et al., 2019). The pSS408 and pSS421 plasmids driving the production of P_{HOP1}-*GFP-NES-PCH2* and P_{HOP1}-*GFP-NLS-PCH2*, respectively, were derived from pSS393. An approximately 350 bp *PCH2* fragment was amplified from pSS393 with oligos encoding the NES (LALKLAGLDI) or NLS (PKKKRKV) sequences, digested with *Not*I-*Bam*HI and cloned into the same sites of pSS393.

Other techniques

Meiotic time courses, western blotting, cytology, sporulation efficiency, dytirosine assay and statistics were performed essentially as described in Herruzo *et al*., 2019. The antibodies used for western blotting and immunofluorescence of chromosome spreads are listed in Supplementary Table S3.

REFERENCES

Cavero, S., Herruzo, E., Ontoso, D., and San-Segundo, P.A. (2016). Impact of histone H4K16 acetylation on the meiotic recombination checkpoint in *Saccharomyces cerevisiae*. *Microbial Cell*, *3*(12), 606-620.

González-Arranz, S., Cavero, S., Morillo-Huesca, M., Andújar, E., Pérez-Alegre, M., Prado, F., and San-Segundo, P.A. (2018). Functional impact of the H2A.Z histone variant during meiosis in *Saccharomyces cerevisiae*. *Genetics*, *209*(4), 997-1015.

Herruzo, E., Ontoso, D., González-Arranz, S., Cavero, S., Lechuga, A., and San-Segundo, P.A. (2016). The Pch2 AAA ATPase promotes phosphorylation of the Hop1 meiotic checkpoint adaptor in response to synaptonemal complex defects. *Nucleic Acids Research*, *44*(16), 7722-7741.

Herruzo, E., Santos, B., Freire, R., Carballo, J. A., and San-Segundo, P.A. (2019). Characterization of Pch2 localization determinants reveals a nucleolar-independent role in the meiotic recombination checkpoint. *Chromosoma*, 1-20.

Puchades, C., Sandate, C. R., and Lander, G. C. (2019). The molecular principles governing the activity and functional diversity of AAA proteins. *Nature Reviews Molecular Cell Biology*, 1-16.

Rockmill, B., and Roeder, G.S. (1990). Meiosis in asynaptic yeast. *Genetics*, *126*(3), 563-574.

Stuckey, S., Mukherjee, K., and Storici, F. (2011). In vivo site-specific mutagenesis and gene collage using the delitto perfetto system in yeast *Saccharomyces cerevisiae*. *Methods in Molecular Biology*, *745*(745), 173-191.

SUPPLEMENTAL DATA

Table S1. *Saccharomyces cerevisiae* strains

Strain	Genotype*	Source
BR1919-2N	*MAT*a/*MAT*α *leu2-3,112 his4-260 thr1-4 trp1-289 ura3-1 ade2-1*	Roeder Lab
DP421	BR1919-2N *lys2ΔNheI*	PSS Lab
DP422	DP421 *zip1Δ::LYS2*	PSS Lab
DP424	DP421 *ndt80::LEU2*	PSS Lab
DP428	DP421 *zip1Δ::LYS2 ndt80::LEU2*	PSS Lab
DP881	DP421 *zip1Δ::LYS2 pch2Δ::TRP1 ndt80Δ::LEU2*	PSS Lab
DP1029	DP421 *zip1Δ::LYS2 pch2Δ::TRP1*	PSS Lab
DP1500	DP421 *zip1Δ::LYS2 HOP1/HOP1-mCherry::natMX4*	PSS Lab
DP1501	DP421 *pch2Δ::TRP1 HOP1/HOP1-mCherry::natMX4*	This work
DP1621	BR1919-2N *zip1Δ::LEU2* P_{HOP1}*-GFP-PCH2*	This work
DP1630	BR1919-2N *orc1-3mAID::hphNT* P_{HOP1}*-OsTIR1::URA3 zip1Δ::LEU2* P_{HOP1}*-GFP-PCH2 ndt80Δ::kanMX3*	This work
DP1633	BR1919-2N *orc1-3mAID::hphNT* P_{HOP1}*-OsTIR1::URA3 zip1Δ::LEU2* P_{HOP1}*-GFP-PCH2 HOP1/HOP1-mCherry::natMX4*	This work
DP1636	BR1919-2N *zip1Δ::LEU2* P_{HOP1}*-GFP-PCH2 HOP1/HOP1-mCherry::natMX4*	This work
DP1640	DP421/BR1919-2N *zip1Δ::LEU2* P_{HOP1}*-GFP-PCH2 ndt80Δ::kanMX3*	This work

*****All strains were homozygous for the markers, except when indicated

Table S2. Plasmids

Plasmid name	Vector	Relevant parts	Source
pSS367	pYES2	*URA3 2μ* P_{HOP1}*-GFP-PCH2*	This work
pSS393	pRS314	*TRIP1 CEN6* P_{HOP1}*-GFP-PCH2*	(Herruzo *et al*., 2019)
pSS408	pRS314	*TRIP1 CEN6* P_{HOP1}*-GFP-NES-PCH2*	This work
pSS421	pRS314	*TRIP1 CEN6* P_{HOP1}*-GFP-NLS-PCH2*	This work

Table S3. Primary antibodies

Antibody	Host and type	Application* (Dilution)	Source / Reference
Hop1-T318-P	Rabbit polyclonal	WB (1:1000)	(Penedos *et al*., 2015)
H3-T11-P	Rabbit polyclonal	WB (1:2000)	Abcam ab5168
PGK (22C5D8)	Mouse monoclonal	WB (1:5000)	Molecular Probes 459250
Pch2	Rabbit polyclonal	WB (1:2000) IF (1:325)	(Herruzo *et al*., 2019)
mAID (1E4)	Mouse monoclonal	WB (1:400)	MBL M214-3

*WB, western blot; IF, immunofluorescence

Supplemental References

Penedos A, Johnson AL, Strong E, Goldman AS, Carballo JA, Cha RS (2015) Essential and Checkpoint Functions of Budding Yeast ATM and ATR during Meiotic Prophase Are Facilitated by Differential Phosphorylation of a Meiotic Adaptor Protein, Hop1. *PLoS ONE* 10(7): e0134297.

Herruzo, E., Santos, B., Freire, R., Carballo, J.A. and San-Segundo, P.A. (2019) Characterization of Pch2 localization determinants reveals a nucleolar-independent role in the meiotic recombination checkpoint. *Chromosoma,* 1-20.

CONCLUSIONES

1. La población citoplásmica de Pch2 puede ser relevante para promover la respuesta del *checkpoint* meiótico.

CONCLUSIONS

1. The cytoplasmic population of Pch2 could be relevant to promote the meiotic checkpoint response.

Artículo

4

RESUMEN

Las modificaciones epigenéticas están emergiendo como reguladores importantes del genoma. Sin embargo, los mecanismos por los que regulan procesos específicos durante la meiosis no se conocen bien. La metilación de H3K79 mediada por la histona metil-transferasa Dot1 está involucrada en el mantenimiento de la estabilidad genómica en varios organismos. En *S. cerevisiae*, Dot1 modula la respuesta del *checkpoint* meiótico inducido por defectos en sinapsis y/o recombinación promoviendo la activación de Hop1 y por tanto de Mek1, así como su incorporación en los ejes de los cromosomas sin sinapsis, al menos en parte, regulando la localización de Pch2. Sin embargo, se desconoce cómo esta proteína regula la meiosis en metazoos. Aquí describimos los efectos de la reducción de H3K79me3 mediante el análisis de mutantes *dot-1.1* o *zfp-1* en la meiosis de *Caenorhabditis elegans.* Así, hemos observado un aumento de letalidad embrionaria y esterilidad en los mutantes *dot-1.1*, lo que sugiere defectos en la meiosis. Mostramos que DOT-1.1 desempeña un papel en la regulación del apareamiento, sinapsis y recombinación en gusanos. Además, demostramos que H3K79me3 es un regulador importante del *checkpoint* de sinapsis. En resumen, nuestros resultados desvelan que la regulación de H3K79me juega un papel importante en la coordinación de los eventos meióticos en *C. elegans*.

GRAPHICAL ABSTRACT

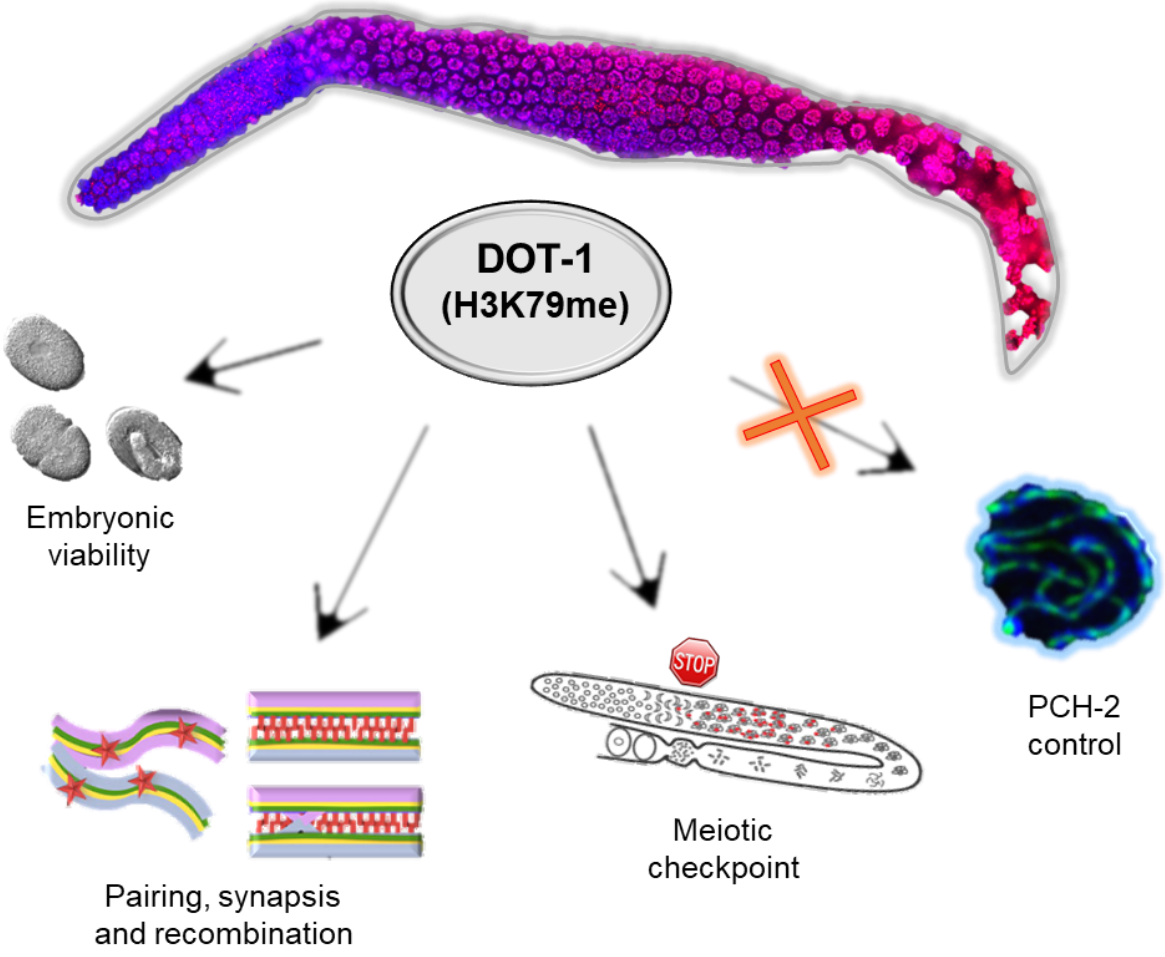

Role of DOT-1.1-dependent H3K79 methylation during meiosis in *C. elegans*

Laura I. Lascarez-Lagunas [*,1], Esther Herruzo [†,1], Alla Grishok[‡,§] Pedro A. San-Segundo[†], and Mónica P. Colaiácovo[*,2]

[*]Department of Genetics, Harvard Medical School, Boston, MA 02115; U.S.A.

[†]Instituto de Biología Funcional y Genómica. Consejo Superior de Investigaciones Científicas and University of Salamanca, 37007 Salamanca, Spain.

[‡]Department of Biochemistry, Boston University School of Medicine, Boston, Massachusetts 02118, USA

[§]Genome Science Institute, Boston University School of Medicine, Boston, Massachusetts 02118, USA

[1]These authors contributed equally to this work.

[2]**Correspondence:** mcolaiacovo@genetics.med.harvard.edu; Phone: (617) 432-6543; Fax:617-432-7663.

Keywords: DOT-1.1; DOT1L; H3K79; germline; meiosis; *C. elegans*; DSB repair; PCH-2; synaptonemal complex, checkpoint.

ABSTRACT

Epigenetic modifiers are emerging as important regulators of the genome. However, how they regulate specific processes during meiosis is not well understood. Methylation of H3K79 by the histone methyltransferase Dot1 has been shown to be involved in the maintenance of genomic stability in various organisms. In *S. cerevisiae*, Dot1 modulates the meiotic checkpoint response triggered by synapsis and/or recombination defects by promoting Mek1-dependent Hop1 activation and distribution along unsynapsed meiotic chromosomes, at least in part, by regulating Pch2 localization. However, how this epigenetic modification regulates meiosis in metazoans is unknown. Here, we describe the effects of H3K79me3 depletion via analysis of *dot-1.1* or *zfp-1* mutants during meiosis in *Caenorhabditis elegans*. We observed an increase in sterility and embryonic lethality in *dot-1.1* mutants suggesting meiotic dysfunction. We show that *dot-1.1* plays a role in the regulation of pairing, synapsis and recombination in the worm. Furthermore, we demonstrate that H3K79me3 is an important regulator of mechanisms surveillling chromosome synapsis during meiosis. In sum, our results reveal that regulation of H3K79me plays an important role in coordinating events during meiosis in *C. elegans.*

INTRODUCTION

Meiosis is an essential cell division program for all sexually reproducing organisms. It halves the genome's content by following one round of DNA replication with two successive rounds of cell division, meiosis I and II, to generate haploid gametes (i.e. sperm and oocytes). A series of well-orchestrated events ensure accurate homologous chromosome segregation at meiosis I while preserving sister chromatid associations until meiosis II (Baudat *et al.* 2013). Namely, homologs have to pair, synapse and recombine. Errors in any of these processes can lead to the formation of aneuploid gametes, which

in humans can result in birth defects such as Down syndrome, miscarriages and infertility (Hassold and Hunt 2001). While many of the proteins required for achieving homologous pairing, synapsis and recombination are known, far less is understood about how dynamic changes in the chromatin landscape affect these processes during meiosis.

Alterations in the chromatin landscape are mediated in part by post-translational modification of histones which form octamers wrapped around DNA (H3/H4 heterotetramer and two H2A/H2B dimers) to form the building blocks of chromatin, the nucleosomes (Van Holde *et al.* 1980; Luger *et al.* 1997; Kornberg and Lorch 1999; Zhang and Dent 2005). Post-translational modifications of histones play an important role in the establishment and maintenance of gene expression, and covalent histone modifications influence chromatin structure and function directly or indirectly through the recruitment of effector proteins to specific chromatin domains (Strahl and Allis 2000; Martin and Zhang 2005; Kouzarides 2007).

One of these histone modifications is the methylation of H3K79 (hereafter H3K79me) by the histone methyltransferase Dot1 which has been reported to be involved in the maintenance of genomic stability in various organisms (Wood *et al.* 2005; Mohan *et al.* 2010b; Nguyen and Zhang 2011). Dot1 is a methyltransferase that catalyzes mono-, di- and trimethylation of histone H3K79 (Ng *et al.* 2002; Frederiks *et al.* 2008). A demethylase for this histone mark has not been identified so far. Dot1 is an evolutionarily conserved protein that regulates diverse cellular processes, such as development, reprogramming, differentiation, and proliferation (Mohan *et al.* 2010a; Ontoso *et al.* 2013; Cecere *et al.* 2013; Kim *et al.* 2014). During meiosis in yeast, Dot1 modulates the meiotic checkpoint response induced in the *zip1Δ* mutant lacking a major component of the central region of the synaptonemal complex (SC). Dot1 promotes Mek1-dependent Hop1 activation and distribution along unsynapsed meiotic chromosomes. Several lines of evidence suggest that Dot1 regulates this checkpoint, at least in part, by defining Pch2 chromosomal distribution (San-Segundo and Roeder 2000; Ontoso *et al.* 2013). In mammals, defects on DOT1L (Dot1 (yeast) -Like) enzyme function are related to mixed lineage leukemia (MLL) (Nguyen and Zhang 2011). The *C. elegans* genome encodes five putative methyltransferases of the Dot1 family (Feng *et al.* 2002), among which DOT-1.1 has been shown, through computational and experimental analysis, to be the homolog of mammalian DOT1L (Cecere *et al.* 2013; Esse *et al.* 2019). Although cytological analyses of DOT1L and H3K79me distribution in mouse spermatocytes are suggestive of a functional implication for this histone modification in mammalian meiosis (Ontoso et al., 2014) the roles of DOT-1.1 and regulation of H3K79 methylation during meiosis had not been previously directly examined in a metazoan.

Despite its importance, the impact of the chromatin environment during meiotic progression has been poorly studied. Here we describe the roles of *dot-1.1* and H3K79me3 in the germline of *C. elegans*. Analysis of *dot-1.1* mutants revealed that DOT-1.1 regulates the levels of H3K79me3 in the germline and is required for normal brood size and embryonic viability. We also show that *dot-1.1* mutants exhibit impaired homologous pairing, chromosome synapsis and

recombination. Importantly, *dot-1.1* is implicated in the activation/establishment of the synapsis checkpoint in the worm in a PCH-2 localization independent manner.

MATERIAL AND METHODS

Genetics

C. elegans strains were cultured at 20°C under standard conditions as described in (Brenner 1974). The N2 Bristol strain was used as the wild-type background. The following mutations and chromosome rearrangements were used: linkage group I (LG1) *dot-1.1[knu337-(pNU1092-KO loxP::hygR::loxP)]*, *rad-54(ok615)*, *hT2*[*bli-4*(*e937*) *let-?*(*q782*) *qIs48*] (I,III); LGII *pch-2(tm1458)*; LGIII, *zfp-1(gk960739)*; LGIV, *ced-3(n1286)*, *nt1[unc-?n754]let-?gls50)(IV;V)*; LGV, *syp-1(me17)*. Full genotypes for combinatorial mutants used in this study are listed in Supplementary Table S1. *zfp-1(gk960739)III* and *dot-1.1[knu337-(pNU1092-KO loxP::hygR::loxP)]I; ced-3(n1286)IV* mutants were obtained from Alla Grishok's laboratory. These lines were back crossed at least six times.

Scoring embryonic lethality, sterility and males

Age-matched (24 hours post-L4 stage) individual hermaphrodites were placed into regular NGM plates to score the embryonic lethality, sterility and percentage of males among their progeny. Worms were moved every 24 hours to new NGM plates (this was done for four consecutive days). The total number of fertilized eggs laid, hatched, and the number of progeny that reached adulthood were scored.

Cytological Analysis

Whole mount preparation of dissected gonads and immunostainings were performed as in (MacQueen and Villeneuve 2001) with some modifications. Briefly, gonads from hermaphrodites 24h post-L4 larval stage were dissected and fixed with 1% of formaldehyde for 5 minutes, freeze-cracked and post-fixed in ice-cold 100% methanol for 1 minute followed by blocking with 1% BSA for 1 hour. Gonads for RAD-51 immunostaining were dissected and then freeze-cracked and fixed in 4% formaldehyde for 30 minutes. The following primary antibodies were used at the indicated dilutions: rabbit α-phospho HIM-8/ZIMs (1:1000, (Kim *et al.* 2015)) rabbit α-PCH-2 (1:500, (Deshong *et al.* 2014)), rabbit α-H3K79me3 (1:500, Abcam Ab2621), rabbit α-RAD-51 (1:10000, Novus Biological (SDI) 29480002), goat α-SYP-1 (1:3000, (Nadarajan *et al.* 2017)), rabbit α-HIM-8 (1:500, Novus Biological (SDI), guinea pig α-HTP-3 (1:500, (Goodyer *et al.* 2008)), rabbit anti-RAD-51 (1:10,000; Catalog #29480002; Novus Biologicals). The following secondary antibodies were purchased from Jackson ImmunoResearch Laboratories (West Grove, PA) and used at the following dilutions: α-rabbit Cy-3 (1:200), α-guinea pig Cy-5 (1:100), α-goat Alexa 488 (1:500), α-rabbit Alexa 488 (1:500), and α-guinea pig Alexa 488 (1:500). DAPI was used to counterstain DNA. Vectashield from Vector Laboratories (Burlingame, CA) was used as a mounting media and anti-fading agent.

To perform the quantitative analysis of pHIM-8/ZIMs foci the average number of foci for all seven zones composing the germline was measured. Between 4 and 6 gonads were scored for each genotype (Supplemental File S1).

To evaluate oocytes at diakinesis whole worms were Carnoy's fixed and then stained with DAPI as in (Villeneuve 1994). Images were taken from the diakinesis oocyte more proximal to the spermatheca (-1 oocyte).

Imaging was performed using an IX-70 microscope (Olympus) with a cooled CCD camera (model CH350; Roper Scientific) controlled by the DeltaVision system (Applied Precision). Images were collected using 100x objective with or without auxiliary magnification (1.5) and Z-stacks were set at 0.2 μm thickness intervals. Image deconvolution was done using SoftWoRX 3.3.6 program (Applied Precision) and processed with Fiji ImageJ (Schindelin *et al.* 2012; Schneider *et al.* 2012).

Time course analysis for RAD-51 foci

Quantitative analysis of RAD-51 foci for all seven zones composing the germline was performed as in (Colaiácovo *et al.* 2003). The average number of nuclei scored per zone (n) from 4 to 6 gonads for each genotype ± standard deviation is shown in Supplemental File S1. Statistical comparisons were performed using the two-tailed Mann-Whitney test, 95% C.I. (Supplemental File S2).

Germ cell apoptosis

Acridine orange (AO) staining of apoptotic germ cells in wild type (N2), *zfp-1*, *syp-1 and pch-2* alleles as well as in the corresponding double and triple mutants was performed as in (Craig *et al.* 2012). Briefly, apoptotic germ cell corpses were scored in the germlines of adult hermaphrodites, analyzed 24 hours post-L4 stage following incubation with Acridine Orange (AO) for 2 hours at room temperature. The germlines of a minimum of 27 worms from at least two independent biological repeats were scored for each genotype. Apoptotic germ cell corpses were visualized using a Leica DM5000B fluorescence microscope. Statistical analysis was done using an unpaired two-tailed Mann-Whitney test with 95% C.I. (Supplemental Table 3).

RESULTS

dot-1.1 mutant worms exhibit sterility, increased embryonic lethality and altered germline chromosome morphogenesis

To determine the role of DOT-1.1 during meiotic prophase all of our analyses were done using a *dot.1.1(knu339);ced-3(n1286)* double mutant, since it was demonstrated that *dot-1.1* null mutants do not survive due to massive apoptosis which can be circumvented with a mutation in *ced-3* that encodes for a homolog of mammalian caspase-3 (Esse *et al.* 2019). We assessed whether *dot-1.1;ced-3* mutants exhibit impaired chromosome segregation by scoring the number of eggs laid (brood size), embryonic lethality (Emb), and incidence of males (Him) among the surviving progeny. A 35% reduction in the mean numbers of eggs laid on plates, which is indicative of increased sterility, was observed in *dot-1.1;ced-3* mutant worms compared to wild type, but not in the *ced-3* mutant alone (Figure 1A). We also observed significantly increased embryonic lethality in *dot-1.1;ced-3* mutants compared to wild type (Figure 1A) (17.8% and 1%, respectively, $P<0.0001$ by the two-tailed Mann-Whitney test, C.I. 95%). A less significant increase in embryonic lethality was also observed in *ced-3* single mutants compared to wild type (6.2% and 1%, respectively, $P<0.05$),

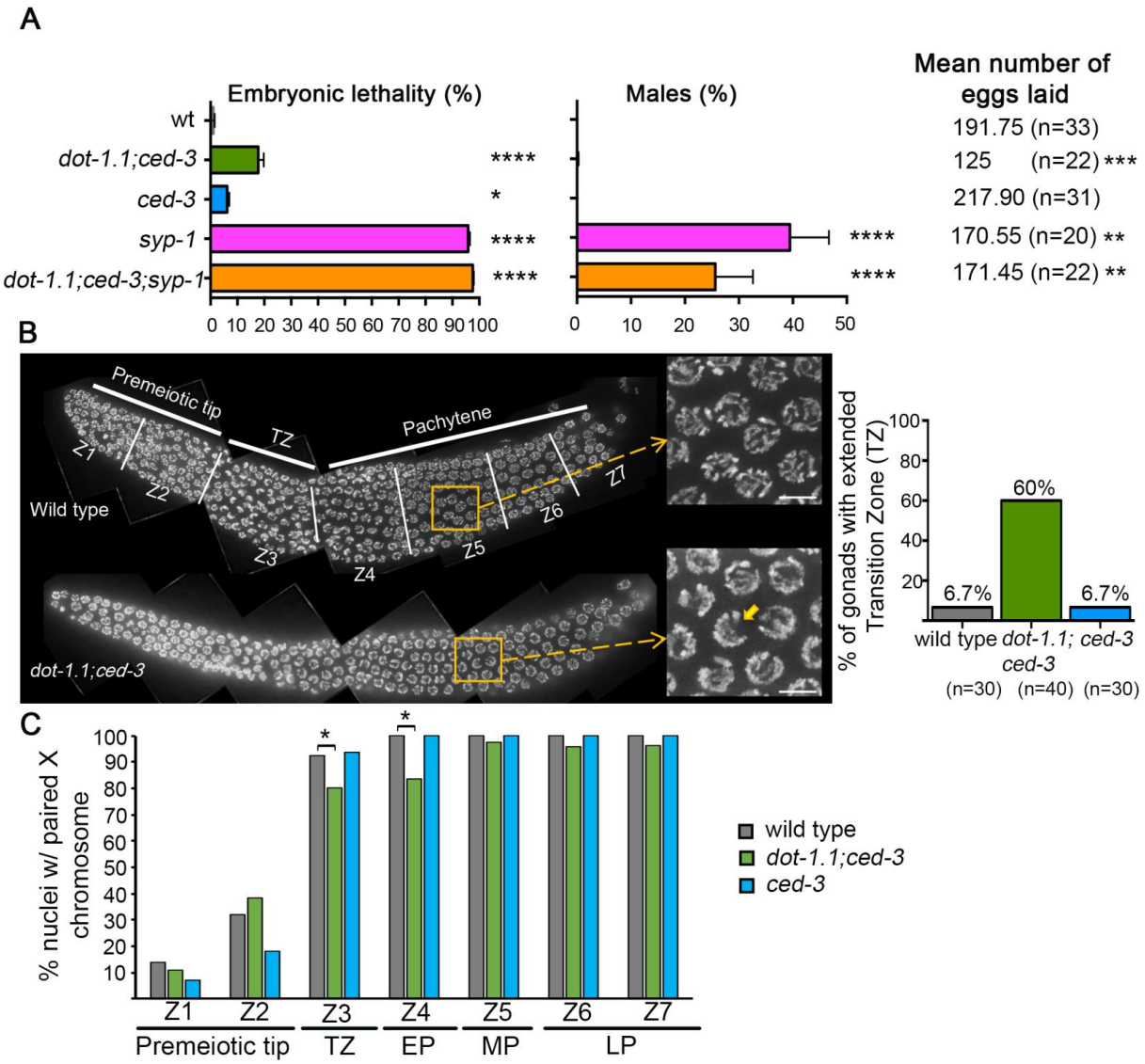

Figure 1. *dot-1.1* mutant worms exhibit increased embryonic lethality, sterility and defects in chromosomal organization in the germline. (A) Embryonic lethality, incidence of males and the number of eggs laid (brood size) are shown for the indicated backgrounds and compared to wild type. Error bars represent SEM. *P<0.05, **P<0.01,***P<0.001 and ****P<0.0001 by the two-tailed Mann-Whitney test, 95% C.I. n = number of individual worms analyzed. **(B)** Left, high-resolution images of whole mounted gonads stained with DAPI from wild type and *dot-1.1;ced-3* mutant animals oriented from left to right. The different stages of meiotic prophase are indicated above the gonads and the seven equally-sized zones scored (Z1-Z7) are delimited by vertical white lines. Nuclei in Z1 and Z2 are undergoing mitosis. They enter meiosis at Z3 when they enter the transition zone, which corresponds to the leptotene/zygotene stages. Nuclei then proceed through pachytene (Z4-Z7). Insets show the presence of transition zone-like nuclei in mid-pachytene for *dot-1.1;ced-3* mutant worms indicating the presence of lagging leptotene/zygotene nuclei. Right, histogram indicates percentage of gonads exhibiting nuclei with chromatin in a leptotene/zygotene-like organization in the pachytene zone (n = number of gonads examined for each genotype). Scale bars, 2μM. **(C)** Histogram representing the percentage of nuclei with paired HIM-8 signals scored at different zones along the germline in wild type, *dot-1.1;ced-3* and *ced-3.* The X chromosomes were scored as paired when the two HIM-8 signals were ≤ 0.75 μm apart from each other. Data was obtained from 4 to 6 independent biological repeats for wild type (n=30), *dot-1.1;ced-3* (n=40) and *ced-3* (n=30). n= number of gonads scored. * P<0.05.

however, there is a significant difference between the embryonic lethality observed in *dot-1.1;ced-3* and the *ced-3* single mutant (17.8% and 6.2%, respectively, P<0.001), which suggests that most of the increase in chromosome missegregation results from the *dot-1.1* mutation itself. We did not find high incidence of males in *dot-1.1* mutants (Figure 1A).

To explore whether the increased sterility and embryonic lethaliy are due, at least in part, to defects during meiosis we examined DAPI-stained gonads from wild type, *dot-1.1;ced-3* and *ced-3* mutant worms. In the *C. elegans* germline, nuclei are organized in a spatial-temporal gradient thereby facilitating the identification of alterations in chromosome organization at specific meiotic stages (Lui and Colaiácovo 2013). We observed an increase in the number of gonads with nuclei with chromatin in a leptone/zygotene-like organization (crescent shape configuration) at the zone corresponding to the pachytene stage in *dot-1.1;ced-3* mutants compared with either wild type or *ced-3* alone revealing an extended transition zone in the absence of *dot-1.1* (Figure 1B). Taken together, these data suggest that DOT-1.1 is required for normal meiotic chromosome morphogenesis and chromosome segregation.

DOT-1.1 is required for normal progression of homologous pairing and SC assembly and preferentially affects the X chromosome

To determine the role of DOT-1.1 during meiosis we analyzed homologous pairing, synapsis and recombination in the hermaphrodite germline. We divided germlines into seven zones of equal size and evaluated the levels of homolog pairing for the pairing center end (a *cis*-acting region implicated in homolog recognition) of the X-chromosome as visualized by localization of the zinc finger protein HIM-8 to that region (Phillips *et al.* 2005). X chromosome pairing was assessed by the presence of closely juxtaposed HIM-8 foci less then 0.75 □m apart. In wild-type and *ced-3* hermaphrodites, X chromosome pairing was observed initiating at the leptotene/zygotene stage of meiosis (zone 3; Figure 1B-C) (there is a background level of association between homologs in the pre-meiotic tip, as previously reported; (Phillips *et al.* 2005). By early pachytene (zone 4; Figure 1B-C), X chromosome homologous pairing was detected in nearly 100 percent of nuclei. In contrast, in *dot-1.1;ced-3* hermaphrodites, we observed a delay in pairing as shown by the lower levels of nuclei with paired HIM-8 signal starting at transition zone and persisting into early pachytene (zones 3 through 4, Figure 1C; P<0.05, Fisher's exact test). However, between 95% to 97% of nuclei exhibited paired X chromosomes from mid to late pachytene (zones 5 through 7) which was not significantly different from wild-type worms. Nevertheless, there were a few nuclei exhibiting unpaired HIM-8 signal until zone 7 in *dot-1.1;ced-3* mutants.

The persistence of nuclei with a leptotene/zygotene-like chromatin organization at the zone corresponding to the pachytene stage and the delay in chromosome pairing have been previously associated with defects in SC formation (MacQueen *et al.* 2002). To examine SC assembly we co-stained whole-mounted gonads from wild type, *dot-1.1;ced-3* and *ced-3* mutants with antibodies against HTP-3, a lateral element component

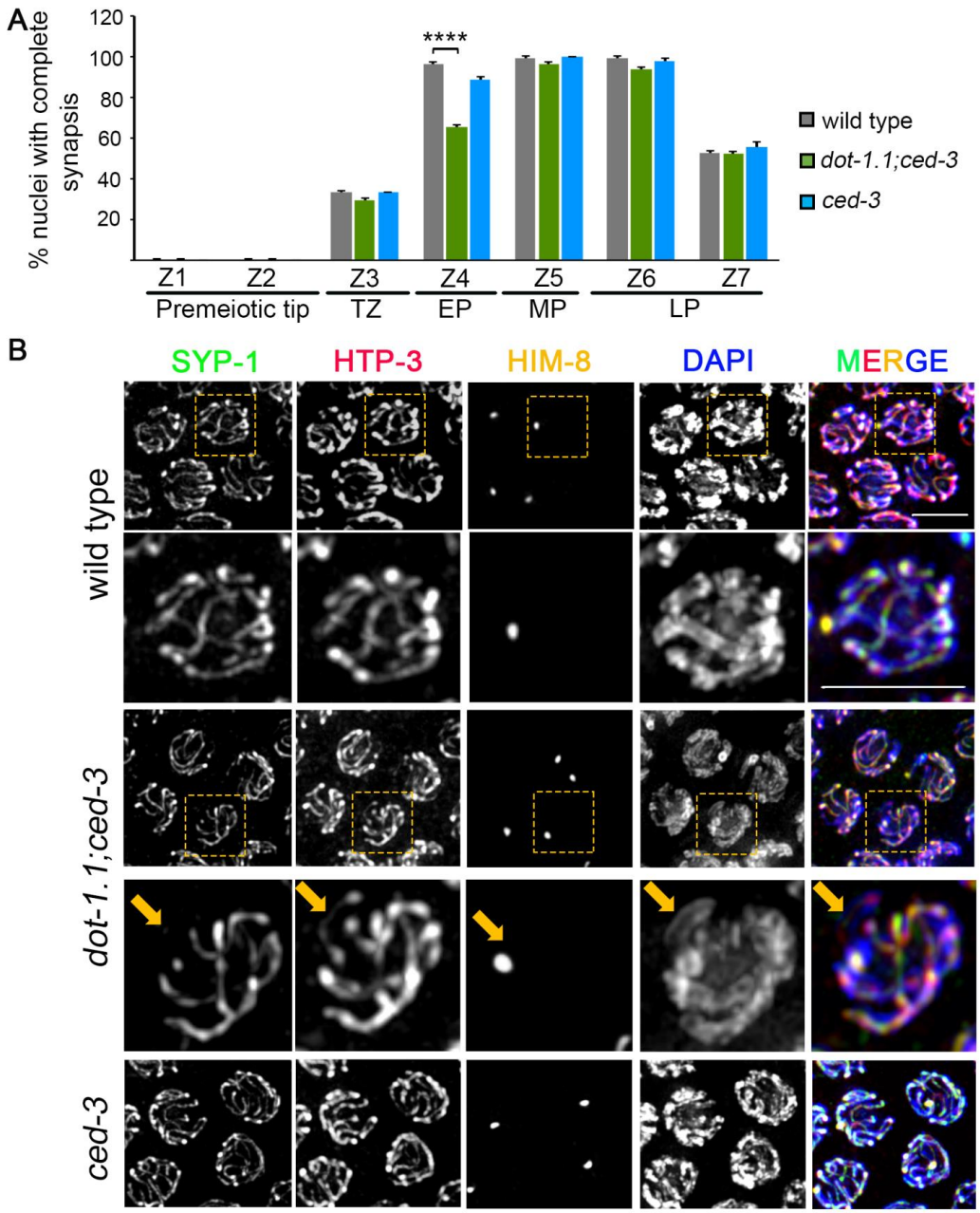

Figure 2. SYP-1 loading is affected in *dot-1.1* mutants. (A) Histogram representing the percentage of nuclei that exhibit complete synapsis as a function of meiotic progression in wild-type, *dot-1.1;ced-3* and *ced-3* mutant worms. Nuclei showing complete overlapping signal of the lateral element component HTP-3 and the central region component SYP-1 were considered as nuclei with complete synapsis. **(B)** High-resolution images of pachytene nuclei co-immunostained with SYP-1 (green), HTP-3 (red), HIM-8 (yellow) and DAPI (blue). Images show independent channels and merge. Unlike wild-type and *ced-3* mutant worms, some nuclei in *dot-1.1;ced-3* mutants exhibited DAPI-stained regions lacking SYP-1 signal at the pachytene stage (9.8%, 41/419). 24.4 % (10/41) of these nuclei did not show HTP-3 signal and in 61% (25/41) the unsynapsed chromosome corresponded to the X chromosome as indicated by presence of HIM-8 signal (arrow). Between 5 to seven gonads from three biological repeats were scored for wild type (n=312), *dot-1.1;ced-3* (n=419) and *ced-3* (n=320); n=number of nuclei scored. Higher magnification images for wild type and *dot-1.1;ced-3* are shown under the corresponding panel. Scale bars, 5 μm.

of the SC (MacQueen *et al.* 2005; Goodyer *et al.* 2008), and SYP-1, a central region component of the SC (MacQueen *et al.* 2002). We observed normal nuclei in which the SC is fully formed as shown by co-localization of HTP-3 and SYP-1 between all chromosome pairs. However, we also found nuclei with incomplete synapsis where stretches of HTP-3 were detected without SYP-1 signal, suggesting normal axis morphogenesis, but impaired assembly of SC central region components, as well as nuclei lacking both HTP-3 and SYP-1 signal, indicating a defect at the level of axis morphogenesis (Figure 2B). We calculated the percentage of nuclei with complete synapsis as a function of meiotic progression. In wild-type worms, initiation of SC assembly, defined by the presence of short patches of central region components on chromosomes with lateral element proteins fully loaded throughout the full length of the chromosomes, was first observed at transition zone (zone 3), and 96% of nuclei had completed SC assembly by early pachytene (zone 4). *dot-1;ced-3* worms also initiated SC assembly at transition zone, but only 65% of nuclei had completed SC assembly by early pachytene indicating a delay in SC assembly compared to wild type (P<0.0001, Fisher's exact test) (Figure 2A). Such defect seems to be specific to *dot-1.1* since we did not observe it in a *ced-3* single mutant. We observed similar levels of SC disassembly between wild type and *dot-1.1;ced-3* mutant worms (Figure 2A; zone 7). More detailed analysis showed that in *dot-1.1;ced-3* mutant animals 10% of the nuclei in mid to late pachytene (zones 5 and 6) did not have SYP-1 signal in at least one chromosome compared to 0.64% and 0.63% observed in wild type and *ced-3* single mutant, respectively (n=419, 312 and 320 nuclei analyzed, respectively). From those, 24.4% (15/41) also lacked HTP-3 signal explaining the absence of SYP-1 since proper assembly of the SC depends on the normal formation of axes (Goodyer *et al.* 2008). The remaining nuclei (26/41), lacked SYP-1 signal although HTP-3 signal was not altered (Figure 2B) suggesting that DOT-1.1 is implicated in the regulation of SYP-1 loading itself. Furthermore, since we observed that the absence of SYP-1 was mainly restricted to one chromosome in each nucleus and we had evidence of a delay in X chromosome pairing (Figure 1C) we used HIM-8 as a marker to evaluate whether the X chromosome was the chromosome primarily affected by lack of DOT-1.1 function. Using a triple co-immunostaining for SYP-1, HTP-3 and HIM-8 we observed that 61% of the chromosomes without SYP-1 signal (25/41) were positive for HIM-8, which means that the X chromosome is more dependent on DOT-1.1 for SYP-1 loading (Figure 2B).

DNA double-strand break formation is impaired in *dot-1.1* mutant

Since impaired homologous pairing and SC assembly can be linked with defects in meiotic recombination we assessed meiotic DSB repair progression by quantifying the levels of RAD-51 foci on immunostained whole-mounted gonads in wild type and *dot-1.1;ced-3* mutants (Figure 3). RAD51 binds to 3' ssDNA ends at resected DSBs to promote strand invasion/exchange during DSB repair (Sung 1994) and in *C. elegans*, RAD-51 foci on chromosomes indicate sites undergoing DSB repair (Colaiácovo *et al.* 2003). We scored the number of RAD-51

foci per nucleus throughout the germline. In wild-type and *ced-3* mutant gonads, low levels of RAD-51 foci were observed at the premeiotic tip where nuclei are undergoing mitosis (zones 1-2). RAD-51 foci levels start to increase upon entrance into meiosis at transition zone (zone 3), peak by mid-pachytene (zone 5) and then decrease by late pachytene (zones 6 and 7) as DSB repair is completed (Figures 3A and 3B). In contrast, *dot-1.1;ced-3* mutants showed significantly lower levels of RAD-51 foci in meiotic nuclei (zones 3-7). The lower levels of RAD-51 foci in *dot-1.1;ced-3* mutants could either be due to a reduction in the levels of DSB formation or to a faster turnover/repair of DSBs. To distinguish between these possibilities, we assayed RAD-51 foci in *rad-54*

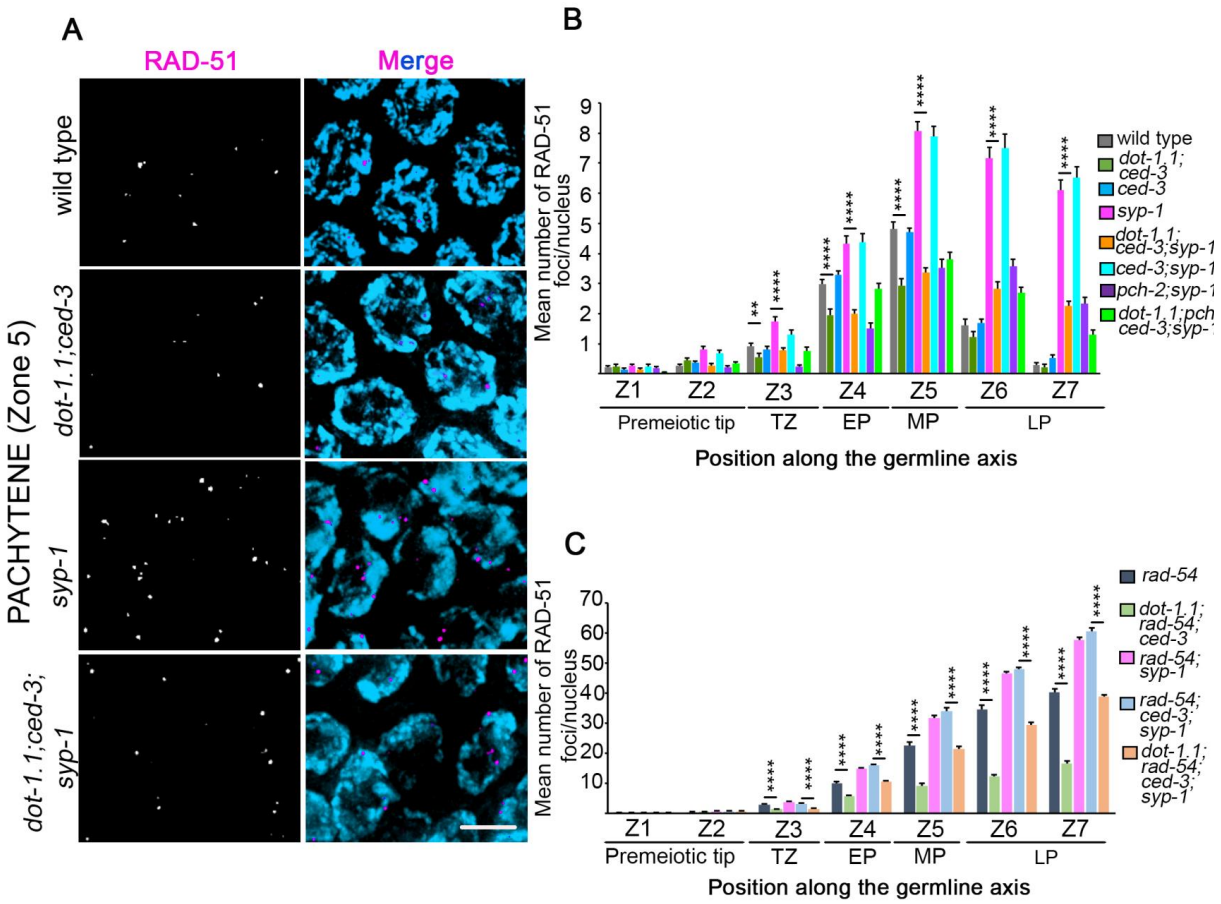

Figure 3. DSB formation is altered in *dot-1.1* mutant worms. (A) High-resolution images representative of mid-pachytene nuclei (zone 5) immunostained for RAD-51 (magenta) and co-stained with DAPI (blue). Scale bar, 5 μm. **(B)** Histogram shows the mean number of RAD-51 foci/nucleus (y-axis) scored along each zone in the germlines (x-axis) of the indicated genotypes. Between 4 and 6 gonads were scored per genotype. A significant decrease in levels of RAD-51 foci were observed for zones 4 to 7 in *dot-1.1;ced-3* germlines compared to wild-type and in *dot-1.1;ced-3;syp-1* germlines compared to *syp-1*. Error bars represent SEM from technical repeats for each of two to three biological replicates (*P<0.05, ****P<0.0001 by the two-tailed Mann-Whitney test, 95% C.I.). **(C)** Histogram shows the mean number of RAD-51 foci/nucleus for each zone along the germlines of *rad-54* combinatorial mutants. Decreased levels of DBSs for *dot-1.1;rad-54;ced-3* compared to *rad-54* and for *dot-1.1;rad-54;ced-3;syp-1* compared to rad-54;ced-3;syp-1 were observed beginning in early pachytene (zone 4) and persisting until late pachytene (zone 7). Error bars represent SEM for technical repeats from two biological repeats (****P<0.0001 by the two-tailed Mann-Whitney test, 95% C.I.).

and *dot-1.1;rad-54;ced-3* triple mutants (Figure 3C) given that a mutation in *rad-54* prevents the removal of RAD-51 from repair intermediates and stalls the progression of meiotic recombination, essentially "trapping" DSB-bound RAD-51 and allowing for quantification of the total number of DSBs. *dot-1.1;rad-54;ced-3* showed a significant decrease in the levels of RAD-51 foci in the leptotene/zygotene, early, mid- and late-pachytene stages compared to *rad-54* single mutant (zones 3, 4, 5, 6 and 7, respectively; P<0.0001; Figure 3C) suggesting that DOT-1.1 may regulate DSB formation. Raw data for *rad-51* foci quantification are included in Supplemental file S1 and all the statistics comparisons in Supplemental file S2.

Levels of CO formation are altered in *dot-1.1* mutants

To determine whether *dot-1.1* is required for normal crossover formation we used ZHP-3 as a marker to quantify the number of sites designated to be repaired as crossovers (COs) in wild type, *dot-1.1;ced-3* and *ced-3* mutants (Figure 4A). The number and distribution of COs along each pair of homologous chromosomes are tightly regulated throughout species (Baudat *et al.* 2013). This is particularly evident in *C.elegans* where only one CO occurs per homolog pair (Meneely *et al.* 2002). In wild-type and *ced-3* worms, a mean of 6 ZHP-3 foci per nucleus was observed by late pachytene, corresponding to one ZHP-3 focus for each of the six pairs of homologs. However, a mean of 6.6 ZHP-3 foci was detected in *dot-1.1;ced-3* germlines (Figure 4A). Since there are fewer DSBs formed in *dot-1.1;ced-3* mutants, this suggests that CO interference is altered in the absence of DOT-1.1.

To further investigate chiasma formation in *dot-1.1* mutants we scored the numbers of DAPI-stained bodies observed in -1 oocytes at diakinesis (the most proximal oocyte to the spermatheca) in wild-type, *ced-3* and *dot-1.1;ced-3* worms (Figure 4B). While 100% of -1 oocytes in wild type and *ced-3* mutant worms contained 6 DAPI bodies (bivalents), consistent with 6 pairs of attached homologs, only 87.4% of oocytes in *dot-1.1;ced-3* worms exhibited six DAPI bodies with 6.3% each carrying 5 and 7 DAPI-stained bodies, respectively. The presence of 5 DAPI-stained bodies suggests potential end-to-end chromosome fusions or aggregates while 7 DAPI stained bodies suggest the presence of 5 bivalents and two univalents, potentially corresponding to the X chromosome which our analysis suggests is more affected in the *dot-1.1* mutant. Careful examination of chromosome morphology revealed significantly elevated levels of -1 oocytes with aberrant chromosome condensation in *dot-1.1;ced-3* worms (P<0.0001; Fisher's exact test). Furthermore, albeit not statistically significant, *dot-1.1* chromosomes exhibited a range of defects which included the presence of fragments, frayed chromosomes and aggregates (Figure 4C).

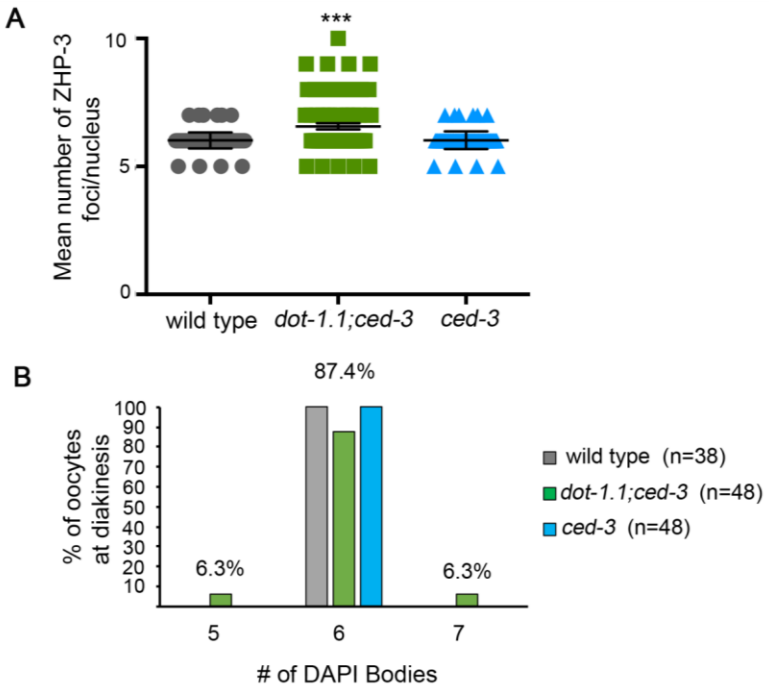

C

Chromosome morphology defects at diakinesis	-1 oocyte (%) Decond.	Fragments	Frayed	Aggreg.	n=
Wild type	0	0	2.63	0	38
dot-1.1;ced-3	25	4.16	6.25	6.25	48
ced-3	6.25	0	4.2	0	48

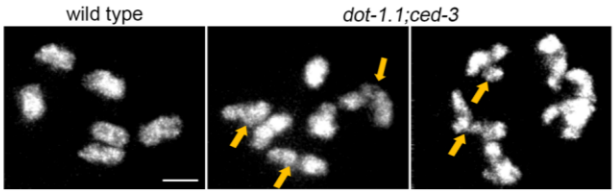

Figure 4. Altered crossover formation in *dot-1.1* mutants leads to bivalent morphogenesis defects. (A) Histogram shows the mean number of ZHP-3 foci scored for each genotype. Foci were quantified in late pachytene when six ZHP-3 foci per nucleus are clearly detected in wild type representing six COs (one per homolog pair). The number of nuclei scored for wild type, *dot-1.1;ced-3* and *ced-3* were n = 104, 76 and 83, respectively (from at least 5 gonads each from two biological repeats). Error bars represent SD (***P<0.001 by the two-tailed Mann-Whitney test, 95% C.I.). **(B)** Quantification of the number of DAPI-stained bodies observed in the -1 oocytes for the indicated genotypes. Wild-type and *ced-3* worms show 6 DAPI bodies which correspond to 6 pair of homologs. In contrast, oocytes with either 5 or 7 DAPI bodies were detected in *dot-1.1;ced-3* mutant worms. The number of nuclei scored for wild-type, *dot-1.1;ced-* and *ced-3* were n = 38, 48 and 48, respectively from three biological repeats. **(C)** Top, table shows the quantification of the percentage of -1 oocytes at diakinesis displaying each one of the indicated defects in chromosome morphology. n=number of -1 oocytes scored. Decond.= decondensation. Aggreg.= aggregates. Bottom, representative high-resolution images of DAPI-stained bodies observed in -1 oocytes at diakinesis exhibiting either normal morphology (wild-type) or defects including evidence of aggregates, chromosome fragments and frayed chromosomes (arrows) in *dot-1.1;ced-3* mutants. Scoring was done for three biological repeats. Scale bar, 2 μm.

dot-1.1 regulates a meiosis checkpoint in worms

Dot1 and its homologs appear to be solely responsible for H3K79 methylation since knockout of Dot1 in yeast, flies, and mice result in complete loss of H3K79 methylation (van Leeuwen *et al.* 2002; Shanower *et al.* 2005; Jones *et al.* 2008). The yeast protein Dot1 and its human homolog, DOT1L, are able to catalyze mono-, di-, and trimethylation in a non processive manner (Min *et al.* 2003; Frederiks *et al.* 2008). In *C. elegans*, levels of H3K79me2 are almost absent in whole worm extracts from L3 stage *dot-1.1;ced-3* mutants (Esse *et al.* 2019) and H3K79me3 signal is lost in the germline of *dot-1.1* mutant adult worms (Figure S1).

To explore the possibility that H3K79me is required for a meiotic checkpoint in worms, as observed in *S. cerevisiae* (San-Segundo and Roeder 2000; Ontoso *et al.* 2013), we examined germ cell apoptosis levels by acridine orange staining. Since *dot-1.1* must be combined with a *ced-3* mutation to maintain viability, we are unable to score germ cell apoptosis in this background lacking a caspase, so instead we examined this in a *zfp-1* mutant. The *zfp-1* gene is the worm homolog of the MLL fusion partner, acute lymphoblastic leukemia 1-fused gene from chromosome 10 (AF10). ZFP-1 has been shown to interact directly with DOT-1.1 modulating histone methyltransferase activity (Cecere *et al.* 2013). In agreement with this, we observed a decrease in H3K79me3 signal in the gonads of *zfp-1* mutant worms (Figure S1). In order to trigger the synapsis checkpoint in worms, we used the *syp-1* mutant that lacks SC formation and has been previously shown to exhibit checkpoint-dependent elevated germ cell apoptosis (MacQueen and Villeneuve 2001). As a control, we also analyzed the *pch-2* mutant implicated in the checkpoint that monitors synapsis in *C. elegans* (Bhalla and Dernburg 2005). Thus, we examined the levels of germ cell apoptosis in *syp-1*, *pch-2* and *zfp-1* single mutants as well as the combination of double and triple mutants. As expected, germ cell apoptosis was dramatically increased in *syp-1* compared to the wild type (Figure 5A) and also, as previously described, this enhanced apoptosis was reduced in the checkpoint-defective *syp-1;pch-2* double mutant (Bhalla and Dernburg 2005), thus validating this assay to monitor checkpoint activity. Interestingly, like *syp-1;pch-2*, the *syp-1;zfp-1* double mutant also displayed significantly decreased levels of apoptotic corpses compared to *syp-1* (Figure 5A), suggesting that the reduced H3K79me3 observed in the absence of ZFP-1 leads to impaired synapsis checkpoint function. Although apoptotic levels were slightly increased in the *zfp-1* single mutant, they were similar to those in *pch-2*, *zfp-1;pch-2* and *zfp-1;pch-2;syp-1* mutants, suggesting that the small increase in germ cell apoptosis observed in the *zfp-1* single mutant does not result from activation of the PCH-2-dependent checkpoint. Thus, these results suggest that regulation of H3K79me3 levels is important for the surveillance mechanism that monitors proper synapsis in *C. elegans*.

Additionally, quantification of the levels of RAD-51 foci, revealed that, like *pch-2*, mutation of *dot-1.1* also alters the number of RAD-51 foci in a *syp-1* mutant background (Figure 3B). In a *syp-1* mutant, lacking the

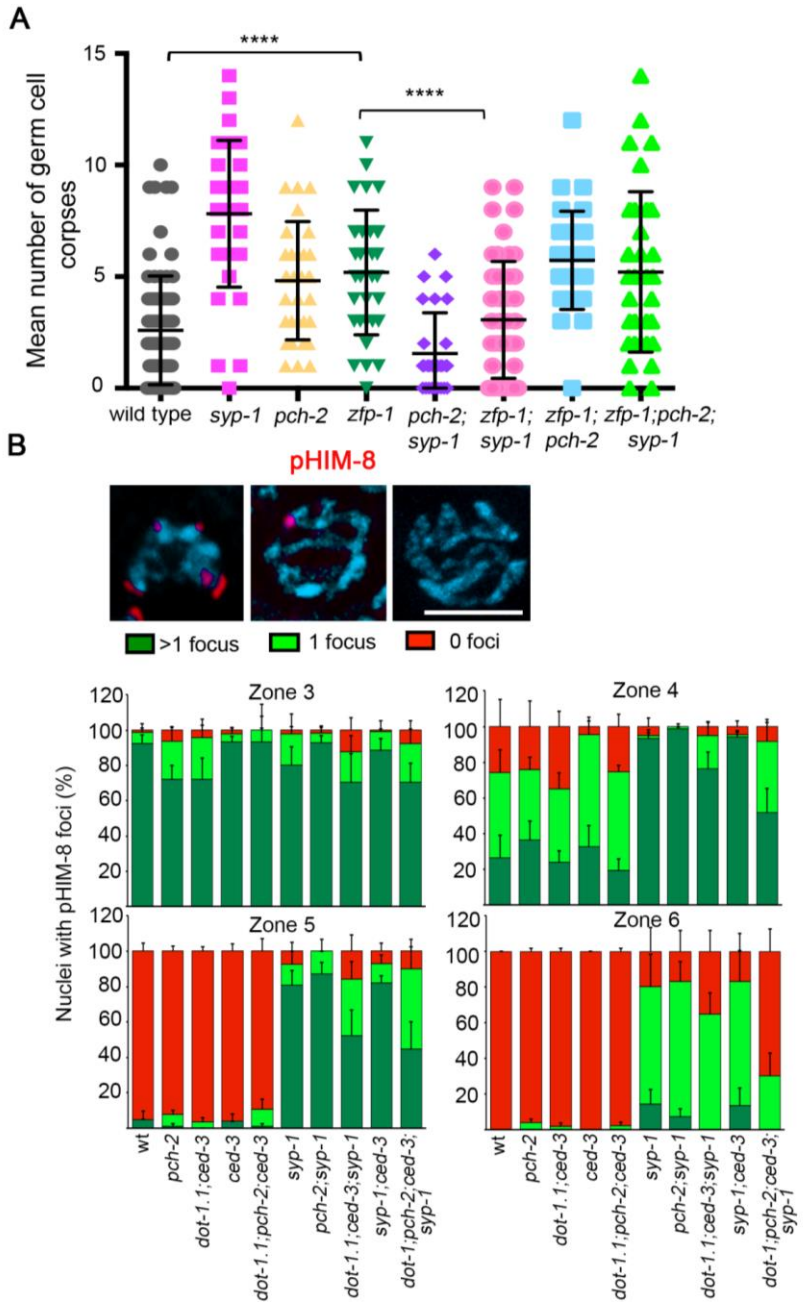

Figure 5. *dot-1.1* is required for the synapsis checkpoint. (A) Scatter plot showing the distribution of germ cell corpses in hermaphrodites from the indicated genotypes. Bars indicate mean ± SD. Levels of germ cell corpses in *syp-1* mutant worms were significantly higher than those observed in wild-type worms however such increase is no longer observed in a *zfp-1;syp-1* double mutant (****P<0.0001 by the two-tailed Mann-Whitney test, 95% C.I.). A minimum of 27 gonads per genotype were scored from two to three biological repeats. **(B)** Top, high magnification images of representative nuclei showing the different categories of phosho-HIM-8 (pHIM8) foci scored (>1 focus corresponds to zone 3, 1 focus corresponds to zone 4 and 0 foci corresponds to zone 5). Scale bar, 5 μm. Bottom, histogram representing the percentage of nuclei with >1, 1 or 0 pHIM-8 foci. In wild-type worms most of the nuclei show more than 1 focus in zone 3, even distribution of >1 and 1 focus in zone 4 and mostly 0 foci reaching zone 5. Germline nuclei in *syp-1* mutant worms never show 100% of 0 foci per nuclei; however, germline nuclei in *dot-1.1;ced-3;syp-1* show an increase in the percentage of nuclei exhibiting 0 foci in mid- to late pachytene (zones 5 and 6). The zone quantified is indicated on top of each graph. 4 to 6 gonads from two biological repeats were analyzed. Average % ± SEM are shown.

central region of the SC, the number of RAD-51 foci is drastically increased and persists for longer due to an inability to repair DSBs from a homologous partner since homologs are not stably held together in the absence of the SC (Colaiácovo *et al.* 2003). However in the *dot-1.1;ced-3;syp-1* triple mutant, the mean number of RAD-51 foci decreased significantly starting from zone 3 (Figure 3B), suggesting that a fraction of DSBs are repaired in *syp-1* when the synapsis checkpoint is abrogated. Nevertheless, the reduction in the levels of RAD-51 foci in the absence of DOT-1.1 also comes in part from a reduction in the total number of DSBs generated (Figure 3C).

As another approach to investigate the possible role of H3K79me in the synapsis checkpoint, we monitored CHK-2 activity in *syp-1* and *syp-1;dot-1.1* mutants. In yeast, it is known that Dot1 affects activity of Mek1 (the CHK-2 ortholog) (Ontoso *et al.* 2013), so we explored whether this mechanism is conserved in worms. As a proxy for CHK-2 activity we used the phosphorylation status of HIM-8, which is CHK-2-dependent (Kim *et al.* 2015). We measured CHK-2 activity by quantifying the fraction of nuclei with 1 focus, >1 foci or 0 foci for phosphorylated HIM-8 (pHIM-8) in leptotene/zygotene (zone 3) and pachytene stages of meiosis (zones 4 to 6) (Figure 5B). The distribution of pHIM-8 in the germline of *dot-1.1* mutants was similar to wild-type, with predominantly 0 foci observed by mid-pachytene when homologs are fully paired and synapsed and pHIM-8 is no longer observed (Figure 5B). As previously described, we observed that CHK-2 activity was prolonged in the *syp-1* mutant in response to synapsis failure (Kim *et al.* 2015), and we found that this striking extension was slightly reduced in *dot-1.1;syp-1* double mutants, supporting a possible role for DOT-1-dependent H3K79 methylation in the *C. elegans* meiotic checkpoint sensing chromosome synapsis (zones 4-6, Figure 5B).

Finally, in yeast, it has been proposed that Dot1 modulates the meiotic checkpoint response in part by regulating Pch2 localization. In the yeast *zip1Δ dot1Δ* double mutant, the nucleolar confinement of Pch2 is lost correlating with defective checkpoint response (Ontoso *et al.* 2013).To analyze whether *C. elegans* uses a similar mechanism we evaluated PCH-2 localization in *dot-1.1*, *syp-1* and *dot-1.1;syp-1* mutants. As previously shown, PCH-2 is present in germline nuclei prior to the transition zone and is no longer detected by late pachytene (Deshong *et al.* 2014) (Figure 6). In *dot-1.1;ced-3* worms the distribution of PCH-2 is indistinguishable from wild-type (Figure 6), which suggests that H3K79me does not regulate PCH-2 localization to the SC under normal conditions. Like in yeast, synapsis is required for PCH-2 localization to the SC, since PCH-2 localization is completely lost from chromosomes in *syp-1* mutants (Deshong *et al.* 2014) (Figure 6). However, unlike yeast, PCH-2 localization to the rDNA is not observed in *C. elegans* and analysis of PCH-2 in the *dot-1.1;syp-1* mutant background did not show alteration of the diffuse PCH-2 distribution. Thus, *pch-2* and *dot-1.1* may be working in different pathways to promote a chromosome synapsis checkpoint in *C. elegans*. Consistent with this notion, a *dot-1.1;pch-2;ced-3;syp-1* quadruple mutant exhibited a decrease in the number of nuclei with

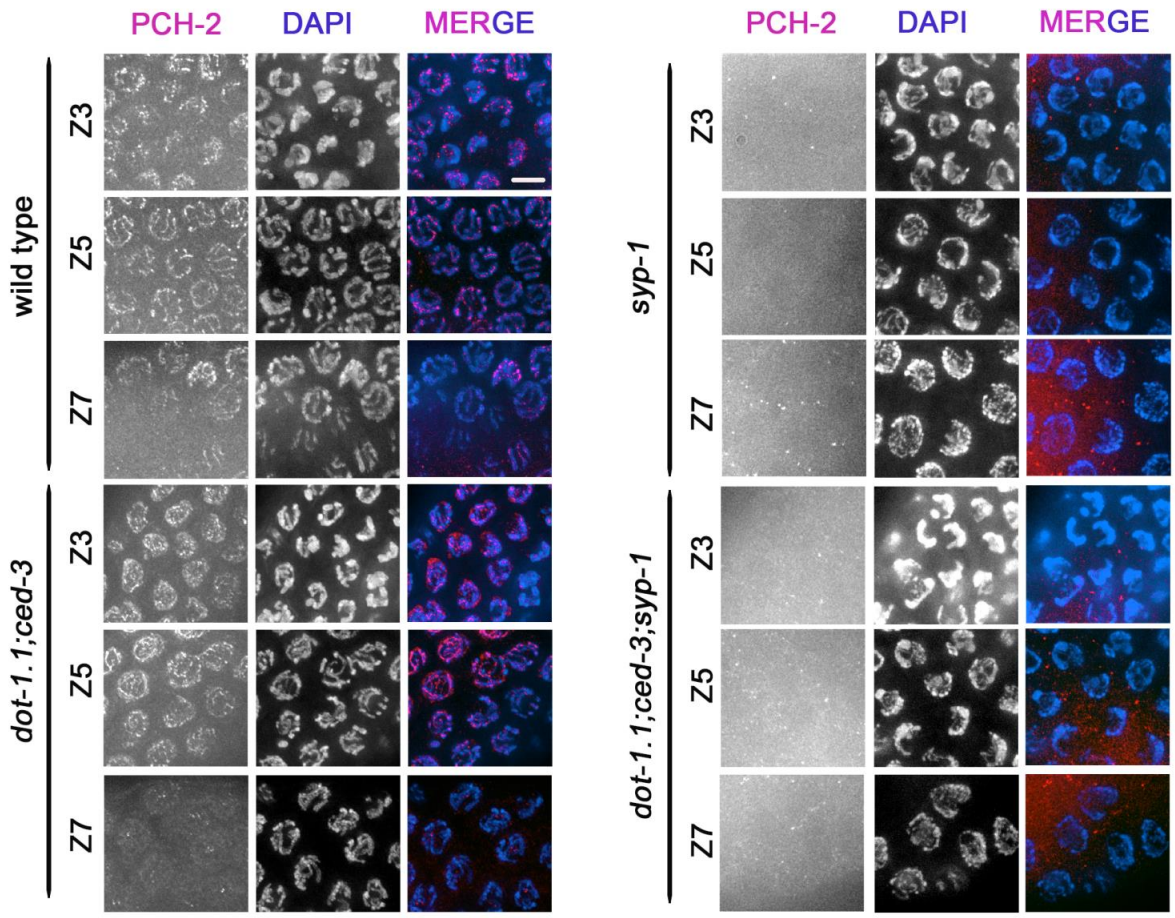

Figure 6. H3K79me3 does not regulate PCH-2 localization in *C. elegans*. High resolution images of gonads from indicated backgrounds co-immunostained with PCH-2 (red) and DAPI (blue). Images show independent channels and merge. The zones of the gonad showed were selected to indicate meiotic distribution of PCH-2. In wild type worms as in *dot-1.1;ced-3* mutant worms PCH-2 is expressed in transition zone (Z3). Once meiosis initiates and chromosomes are synapsed, PCH-2 localizes to the SC until mid-pachytene (zone 5) the signal get lost by late pachytene (Z7). Scale bar, 5 μm.

aberrant CHK-2 activity compared to that of *dot-1;ced-3;syp-1* and *pch-2;syp-1* double mutants (zone 6, Figure 5B).

DISCUSSION

Possible causes of embryonic lethality and increased chromosome non-disjunction in *dot-1.1* mutants

The decreased brood size and increased embryonic lethality observed in the *dot-1.1* mutant can be due in part to defects during meiosis leading to errors in chromosome segregation and the consequent formation of aneuploid gametes as has been previously shown in *C. elegans* (Hodgkin *et al.* 1979; Gartner *et al.* 2000). Besides problems with chromosome segregation, embryonic lethality can result from problems in early embryo development. We cannot discard the possibility that the embryonic lethality observed in *dot-1.1* mutants is the consequence of early developmental problems as it has been demonstrated in mice and flies. Specifically, germline knockout of mDOT1L results in lethality by embryonic day 10.5 (E10.5) dur-

ing organogenesis of the cardiovascular system (Jones et al. 2008). Furthermore, Grappa, the homolog of DOT1L in *Drosophila*, plays an important role in regulating transcription of developmental genes. In general, DOT1L has been implicated in regulating gene expression due to its activity as a methyltransferase. Nevertheless, although Dot1/DOT1L-dependent H3K79me preferentially occurs at actively transcribed ORFs, there are only few cases where Dot1/DOT1L has been casually linked to transcription regulation (Vlaming and van Leeuween 2016). Studies in *C. elegans* suggest that DOT-1/H3K79 methylation may promote RNA polymerase pausing (Cecere *et al.* 2013). Here, we showed that H3K79me3 levels decrease in the germline of *dot-1* mutant worms so it is likely that *dot-1.1* is regulating gene expression levels in the germline. Although DOT1L is the only H3K79 methyltransferase in mammals and H3K79 methylation is present on actively transcribed genes, inhibition of DOT1L methyltransferase activity does not result in dramatic changes in gene expression in cultured cells (Zhu *et al.* 2018). However, expression of specific genes, such as HOXA9 and MEIS1, is strongly dependent on DOT1L specially in leukemias induced by MLL-fusion proteins (Okada *et al.* 2005). So embryonic lethality and reduction in brood size could be related to the direct regulation of specific gene transcription. Moreover, particular defects observed with chromosome morphology in oocytes at diakinesis suggest specific gene expression regulation by *dot-1.1*. Specifically, problems at the level of chromosome compaction (Figure 4) can result from the direct regulation of genes such as *arf-1.2* (ortholog of human ARF1, ADP ribosylation factor 1) and *rnr-2* (orholog of human RRM2, ribonucleotide reductase regulatory subunit M2) which have been described as potential targets of *dot-1.1* and implicated in oocyte chromatin condensation (Green *et al.* 2011; Cecere *et al.* 2013). Thus, the reduction of H3K79me increased the occurrence of chromosomal abnormalities, which is consistent with the increased sterility and embryonic lethality, revealing significant defects in genomic stability.

Decreased DSB formation and CO designation levels in *dot-1.1* suggest alterations in chromosome structure

Our experiments showed a reduction in the levels of DSB formation and deregulation of CO formation (Figures 3 and 4) in the *dot-1.1* mutant worms, which may be directly related to the observed decrease in the levels of H3K79me3 in this mutant (Figure S1). Numerous enzymes have been shown to catalyze post-translational modifications of core histone proteins, and each of these modifications has profound impacts on overall chromatin organization (Jenuwein and Allis 2001; Turner 2002). Moreover, the organization of large-scale chromatin architecture in prophase I meiocytes has been attributed to a role in the global modulation of meiotic recombination and CO frequency (Heng *et al.* 1996; Kauppi *et al.* 2011; Gruhn *et al.* 2013). One key piece of evidence to substantiate this model is that the frequency of MLH1 foci, a CO marker, is more closely associated with the length of the SC than DSB marker frequency (Baier *et al.* 2014). Therefore, the relation between chromatin modifications and the lengths of the chromosome axes as well as of the chromatin loops

is essential to the establishment of chromosome structure and regulation of gene expression. In *C. elegans*, elongation of chromosome axes in condensin mutants showed that perturbations to chromosome structure influence the position and frequency of DSBs in the genome and, hence, of COs (Mets and Meyer 2009). Thus a potential explanation for CO deregulation in the *dot-1.1* mutant is the alteration of chromatin landscape derived from the depletion of H3K79me3 with potential implications in the deregulation of either chromatin loops or chromosome axes. Another non-mutually exclusive possibility is the regulation by *dot-1.1* of specific genes involved in either DSB formation and/or CO designation. Regulation of *spo-11* expression, the gene encoding for the topoisomerase-like factor that catalyzes meiotic DSBs (Dernburg *et al.* 1998), is not likely since in *dot-1.1* mutants we did not see the 12 univalents at diakinesis normally associated with the complete lack of DSB formation and subsequent CO formation. However, we cannot rule out the possibility that *dot-1.1* regulates the expression of other genes modulating DSB formation.

H3K79me3 regulates a meiotic checkpoint in *C. elegans*

Proper chromosome segregation relies on the accurate interaction between homologous chromosomes, including synapsis and recombination. During meiosis in *C. elegans*, checkpoints are set in place to monitor pairing, synapsis and recombination. Here we showed evidence that a meiotic checkpoint surveilling synapsis is misregulated in *dot-1.1* mutants. We suggest that such misregulation is directly connected to the decrease in H3K79me3 levels observed in *dot-1.1* germline as has been probed in yeast where the status of H3K79 methylation modulates the meiotic recombination checkpoint, with the H3K79me3 form being the most relevant to sustain the checkpoint response (Ontoso *et al.* 2013). Unlike yeast, where Dot1 protein is dispensable in otherwise unperturbed meiosis, we found that in *C. elegans* it has a role in the regulation of key meiotic processes: pairing, synapsis and recombination. This is closer to the general effects observed for *dot1* mutants in evolutionarily higher organisms, suggesting that H3K79me function has evolved in metazoans. We show evidence that CHK-2 activity (measured by pHIM-8) is reduced in synapsis-defective mutants when they are in combination with a *dot-1.1* mutation. CHK-2 is essential for DSB formation and acts as a master regulator that governs pairing, synapsis, and recombination during meiotic prophase (MacQueen and Villeneuve 2001). Thus, the reduced number of DSBs in *syp-1;dot-1.1* worms may stem from impaired CHK-2 activity. *dot-1.1* checkpoint regulation seems to be independent of axes proteins since HORMA domain protein HTP-3 is mostly not affected in *dot-1.1* mutants. However, it remains to be determined if *dot-1.1* directly regulates the expression/activity of *chk-2*.

The defects in chromosome synapsis and the generation of aneuploid gametes (Figures 1 and 6) are still manifested in the *dot-1.1;syp-1* double mutant despite the kinetics of meiotic progression being partially rescued in this background (Figure 5). Therefore, relief of the meiotic block by the *dot-1.1* mutation is not due to suppression of the defects that trigger checkpoint-induced arrest, but rather due to disruption of the

checkpoint *per se* as has been proposed in yeast (San-Segundo and Roeder 2000; Ontoso *et al.* 2013). The mechanism by which H3K79me, a constitutive histone mark, is regulating the checkpoint activation needs to be clarified. Like in *syp-1* worms, in yeast *zip1Δ* mutants lacking the central region of the SC, Pch2 is lost from chromosomes, but unlike worms, Pch2 remains associated to the unsynapsed nucleolar rDNA array in *zip1Δ* (San Segundo and Roeder 1999; Herruzo *et al.* 2016). In the checkpoint-defective yeast *zip1Δ dot1Δ* mutant, Pch2 is not retained in the nucleolus and Pch2 distributes throughout chromatin leading to the proposal that regulation of Pch2 nucleolar localization by Dot1 is important for checkpoint function (San-Segundo and Roeder 2000; Ontoso *et al.* 2013). However, more recent studies have demonstrated that the Pch2 protein also localizes in the cytoplasm of yeast cells, and that the presence of Pch2 in the nucleolus is actually dispensable for checkpoint function (Herruzo *et al*. 2019). In *syp-1* worms, PCH-2 is not detected associated to the chromatin (Deshong *et al.* 2014) (Figure 6), but the synapsis checkpoint is active (Bhalla and Dernburg 2005) (Figure 5A). All these observations raise the question, both in yeast and *C. elegans*, of where the Pch2 protein relevant for the checkpoint localizes to. Thus, it is conceivable that the impact of DOT-1 in the synapsis checkpoint may not be directly linked to PCH-2 chromosomal distribution. It is possible that DOT-1.1 is acting through a mechanism more similar to the one proposed in mammals for DNA damage checkpoint activation; it has been proposed that chromatin remodeling in the vicinity of DNA lesions may locally expose histone marks (i.e., H3K79me, H4K20me) supporting the recruitment of DNA damage checkpoint adaptors to activate the checkpoint (Huyen *et al.* 2004; Botuyan *et al.* 2006) so when the mark is not present the recruitment of proteins is not activated and the checkpoint activation is abrogated.

ACKNOWLEDGEMENTS

We thank members of the Colaiácovo laboratory for discussions. E.H. and P.S-S. specially thank José Pérez-Martín for generously allowing us to use the “worm” equipment. This work was supported by a CONACYT-Mexico (No. 275396) postdoctoral fellowship to L.I.L.-L, a National Institutes of Health grant R01GM105853 to M.P.C., a FPU (No. 1502035) predoctoral fellowship to E.H., and a grant RTI2018-099055-B-I00 to P.S.-S. from Ministry of Science, Innovation and Universities of Spain.

REFERENCES

Baier B., P. Hunt, K. W. Broman, and T. Hassold, 2014 Variation in Genome-Wide Levels of Meiotic Recombination Is Established at the Onset of Prophase in Mammalian Males, (M. Przeworski, Ed.) PLoSGenetics 10:e1004125.https://doi.org/10.1371/journal.pgen.1004125

Baudat F., Y. Imai, and B. de Massy, 2013 Meiotic recombination in mammals: localization and regulation. Nature Reviews Genetics 14: 794–806. https://doi.org/10.1038/nrg3573

Bhalla N., and A. F. Dernburg, 2005 A Conserved Checkpoint Monitors Meiotic Chromosome Synapsis in *Caenorhabditis elegans*. 310: 5.

Botuyan M. V., J. Lee, I. M. Ward, J.-E. Kim, J. R. Thompson, *et al.*, 2006 Structural basis for the methylation state-specific recognition of histone H4-K20 by 53BP1 and Crb2 in DNA repair. Cell 127:1361–1373. https://doi.org/10.1016/j.cell.2006.10.043

Brenner S., 1974 The genetics of *Caenorhabditis elegans*. Genetics 77: 71–94.

Cecere G., S. Hoersch, M. B. Jensen, S. Dixit, and A. Grishok, 2013 The ZFP-1(AF10)/DOT-1 complex opposes H2B ubiquitination to reduce Pol

II transcription. Mol. Cell 50: 894–907. https://doi.org/10.1016/j.molcel.2013.06.002

Colaiácovo M. P., A. J. MacQueen, E. Martinez-Perez, K. McDonald, A. Adamo, *et al.*, 2003 Synaptonemal Complex Assembly in *C. elegans* Is Dispensable for Loading Strand-Exchange Proteins but Critical for Proper Completion of Recombination. Developmental Cell 5:463–474. https://doi.org/10.1016/S1534-5807(03)00232-6

Craig A. L., S. C. Moser, A. P. Bailly, and A. Gartner, 2012 Methods for studying the DNA damage response in the *Caenorhabdatis elegans* germ line. Methods Cell Biol. 107: 321–352. https://doi.org/10.1016/B978-0-12-394620-1.00011-4

Dernburg A. F., K. McDonald, G. Moulder, R. Barstead, M. Dresser, *et al.*, 1998 Meiotic Recombination in *C. elegans* Initiates by a Conserved Mechanism and Is Dispensable for Homologous Chromosome Synapsis. Cell 94: 387–398. https://doi.org/10.1016/S0092-8674(00)81481-6

Deshong A. J., A. L. Ye, P. Lamelza, and N. Bhalla, 2014 A quality control mechanism coordinates meiotic prophase events to promote crossover assurance. PLoS Genet. 10: e1004291. https://doi.org/10.1371/journal.pgen.1004291

Esse R., E. S. Gushchanskaia, A. Lord, and A. Grishok, 2019 DOT1L complex suppresses transcription from enhancer elements and ectopic RNAi in *Caenorhabditis elegans*. RNA 25: 1259–1273. https://doi.org/10.1261/rna.070292.119

Feng Q., H. Wang, H. H. Ng, H. Erdjument-Bromage, P. Tempst, *et al.*, 2002 Methylation of H3-lysine 79 is mediated by a new family of HMTases without a SET domain. Curr. Biol. 12: 1052–1058. https://doi.org/10.1016/s0960-9822(02)00901-6

Frederiks F., M. Tzouros, G. Oudgenoeg, T. van Welsem, M. Fornerod, *et al.*, 2008 Nonprocessive methylation by Dot1 leads to functional redundancy of histone H3K79 methylation states. Nat. Struct. Mol. Biol. 15: 550–557. https://doi.org/10.1038/nsmb.1432

Gartner A., S. Milstein, S. Ahmed, J. Hodgkin, and M. O. Hengartner, 2000 A conserved checkpoint pathway mediates DNA damage--induced apoptosis and cell cycle arrest in *C. elegans*. Mol. Cell 5: 435–443. https://doi.org/10.1016/s1097-2765(00)80438-4

Goodyer W., S. Kaitna, F. Couteau, J. D. Ward, S. J. Boulton, *et al.*, 2008 HTP-3 Links DSB Formation with Homolog Pairing and Crossing Over during *C. elegans* Meiosis. Developmental Cell 14: 263–274. https://doi.org/10.1016/j.devcel.2007.11.016

Green R. A., H.-L. Kao, A. Audhya, S. Arur, J. R. Mayers, *et al.*, 2011 A High-Resolution *C. elegans* Essential Gene Network Based on Phenotypic Profiling of a Complex Tissue. Cell 145: 470–482. https://doi.org/10.1016/j.cell.2011.03.037

Gruhn J. R., C. Rubio, K. W. Broman, P. A. Hunt, and T. Hassold, 2013 Cytological Studies of Human Meiosis: Sex-Specific Differences in Recombination Originate at, or Prior to, Establishment of Double-Strand Breaks, (D. S. Dawson, Ed.). PLoS ONE 8: e85075. https://doi.org/10.1371/journal.pone.0085075

Hassold T., and P. Hunt, 2001 To err (meiotically) is human: the genesis of human aneuploidy. Nature Reviews Genetics 2: 280–291. https://doi.org/10.1038/35066065

Heng H. H., J. W. Chamberlain, X. M. Shi, B. Spyropoulos, L. C. Tsui, *et al.*, 1996 Regulation of meiotic chromatin loop size by chromosomal position. Proceedings of the National Academy of Sciences 93: 2795–2800. https://doi.org/10.1073/pnas.93.7.2795.

Herruzo E., Ontoso D., González-Arranz S., Cavero S., Lechuga A., and San-Segundo P. A. (2016). The Pch2 AAA ATPase promotes phosphorylation of the Hop1 meiotic checkpoint adaptor in response to synaptonemal complex defects. Nucleic Acids Research, 44(16), 7722-7741. https://doi.org/10.1093/nar/gkw506.

Herruzo E., Santos B., Freire R., Carballo J. A., and San-Segundo P. A. (2019). Characterization of Pch2 localization determinants reveals a nucleolar-independent role in the meiotic recombination checkpoint. Chromosoma,1-20. https://doi.org/ 10.1007/s00412-019-00696-7.

Hodgkin J., H. R. Horvitz, and S. Brenner, 1979 Nondisjunction Mutants of the Nematode *Caenorhabditis elegans*. Genetics 91: 67–94.

Huyen Y., O. Zgheib, R. A. Ditullio, V. G. Gorgoulis, P. Zacharatos, *et al.*, 2004 Methylated lysine 79 of histone H3 targets 53BP1 to DNA double-strand breaks. Nature 432: 406–411. https://doi.org/10.1038/nature03114

Jenuwein T., and C. D. Allis, 2001 Translating the histone code. Science 293: 1074–1080. https://doi.org/10.1126/science.1063127

Jones B., H. Su, A. Bhat, H. Lei, J. Bajko, *et al.*, 2008 The histone H3K79 methyltransferase DOT1L is essential for mammalian development and heterochromatin structure. PLoS Genet. 4: e1000190.https://doi.org/10.1371/journal.pgen.1000190

Kauppi L., M. Barchi, F. Baudat, P. J. Romanienko, S. Keeney, *et al.*, 2011 Distinct Properties of the XY Pseudoautosomal Region Crucial for Male

Meiosis. Science 331: 916–920. https://doi.org/10.1126/science.1195774

Kim W., M. Choi, and J.-E. Kim, 2014 The histone methyltransferase Dot1/DOT1L as a critical regulator of the cell cycle. Cell Cycle 13: 726–738. https://doi.org/10.4161/cc.28104

Kim Y., N. Kostow, and A. F. Dernburg, 2015 The Chromosome Axis Mediates Feedback Control of CHK-2 to Ensure Crossover Formation in *C. elegans*. Developmental Cell 35: 247–261. https://doi.org/10.1016/j.devcel.2015.09.021

Kornberg R. D., and Y. Lorch, 1999 Twenty-Five Years of the Nucleosome, Fundamental Particle of the Eukaryote Chromosome. Cell 98: 285–294. https://doi.org/10.1016/S0092-8674(00)81958-3

Kouzarides T., 2007 Chromatin modifications and their function. Cell 128: 693–705. https://doi.org/10.1016/j.cell.2007.02.005

Leeuwen F. van, P. R. Gafken, and D. E. Gottschling, 2002 Dot1p modulates silencing in yeast by methylation of the nucleosome core. Cell 109: 745–756. https://doi.org/10.1016/s0092-8674(02)00759-6

Luger K., A. W. Mäder, R. K. Richmond, D. F. Sargent, and T. J. Richmond, 1997 Crystal structure of the nucleosome core particle at 2.8 A resolution. Nature 389: 251–260. https://doi.org/10.1038/38444

Lui D. Y., and M. P. Colaiácovo, 2013 Meiotic Development in *Caenorhabditis elegans*, pp. 133–170 in *Germ Cell Development in C. elegans*, edited by Schedl T. Springer New York, New York, NY.

MacQueen A. J., and A. M. Villeneuve, 2001 Nuclear reorganization and homologous chromosome pairing during meiotic prophase require *C. elegans* chk-2. Genes Dev. 15: 1674–1687. https://doi.org/10.1101/gad.902601

MacQueen A. J., M. P. Colaiácovo, K. McDonald, and A. M. Villeneuve, 2002 Synapsis-dependent and -independent mechanisms stabilize homolog pairing during meiotic prophase in *C. elegans*. Genes Dev. 16: 2428–2442. https://doi.org/10.1101/gad.1011602

MacQueen A. J., C. M. Phillips, N. Bhalla, P. Weiser, A. M. Villeneuve, *et al.*, 2005 Chromosome Sites Play Dual Roles to Establish Homologous Synapsis during Meiosis in *C. elegans*. Cell 123: 1037–1050. https://doi.org/10.1016/j.cell.2005.09.034

Martin C., and Y. Zhang, 2005 The diverse functions of histone lysine methylation. Nat. Rev. Mol. Cell Biol. 6: 838–849. https://doi.org/10.1038/nrm1761

Meneely P. M., A. F. Farago, and T. M. Kauffman, 2002 Crossover distribution and high interference for both the X chromosome and an autosome during oogenesis and spermatogenesis in *Caenorhabditis elegans*. Genetics 162: 1169–1177.

Mets D. G., and B. J. Meyer, 2009 Condensins Regulate Meiotic DNA Break Distribution, thus Crossover Frequency, by Controlling Chromosome Structure. Cell 139: 73–86. https://doi.org/10.1016/j.cell.2009.07.035

Min J., Q. Feng, Z. Li, Y. Zhang, and R.-M. Xu, 2003 Structure of the catalytic domain of human DOT1L, a non-SET domain nucleosomal histone methyltransferase. Cell 112: 711–723. https://doi.org/10.1016/s0092-8674(03)00114-4

Mohan M., C. Lin, E. Guest, and A. Shilatifard, 2010a Licensed to elongate: a molecular mechanism for MLL-based leukaemogenesis. Nat. Rev. Cancer 10: 721–728. https://doi.org/10.1038/nrc2915

Mohan M., H.-M. Herz, Y.-H. Takahashi, C. Lin, K. C. Lai, *et al.*, 2010b Linking H3K79 trimethylation to Wnt signaling through a novel Dot1-containing complex (DotCom). Genes Dev. 24: 574–589. https://doi.org/10.1101/gad.1898410

Nadarajan S., T. J. Lambert, E. Altendorfer, J. Gao, M. D. Blower, *et al.*, 2017 Polo-like kinase-dependent phosphorylation of the synaptonemal complex protein SYP-4 regulates double-strand break formation through a negative feedback loop. eLife 6: e23437. https://doi.org/10.7554/eLife.23437

Ng H. H., R.-M. Xu, Y. Zhang, and K. Struhl, 2002 Ubiquitination of histone H2B by Rad6 is required for efficient Dot1-mediated methylation of histone H3 lysine 79. J. Biol. Chem. 277: 34655–34657. https://doi.org/10.1074/jbc.C200433200

Nguyen A. T., and Y. Zhang, 2011 The diverse functions of Dot1 and H3K79 methylation. Genes Dev. 25: 1345–1358. https://doi.org/10.1101/gad.2057811

Okada Y., Q. Feng, Y. Lin, Q. Jiang, Y. Li, *et al.*, 2005 hDOT1L links histone methylation to leukemogenesis. Cell 121: 167–178. https://doi.org/10.1016/j.cell.2005.02.020

Ontoso D., I. Acosta, F. van Leeuwen, R. Freire, and P. A. San-Segundo, 2013 Dot1-Dependent Histone H3K79 Methylation Promotes Activation of the Mek1 Meiotic Checkpoint Effector Kinase by Regulating the Hop1 Adaptor, (M. Lichten, Ed.). PLoS Genetics 9: e1003262. https://doi.org/10.1371/journal.pgen.1003262

Ontoso D., Kauppi L., Keeney S., San-Segundo PA, 2014. Dynamics of DOT1L localization and

H3K79 methylation during meiotic prophase I in mouse spermatocytes. Chromosoma : Biology of the Nucleus, 123(1-2), 147-164. https://doi.org/10.1007/s00412-013-0438-5

Phillips C. M., C. Wong, N. Bhalla, P. M. Carlton, P. Weiser, *et al.*, 2005 HIM-8 Binds to the X Chromosome Pairing Center and Mediates Chromosome-Specific Meiotic Synapsis. Cell 123: 1051–1063. https://doi.org/10.1016/j.cell.2005.09.035.

San-Segundo PA, R. G.,. (1999). Pch2 links chromatin silencing to meiotic checkpoint control. Cell, 97(3),313-24. https://doi.org/10.1016/S0092-8674(00)80741-2

San-Segundo P. A., and G. S. Roeder, 2000 Role for the silencing protein Dot1 in meiotic checkpoint control. Mol. Biol. Cell 11: 3601–3615. https://doi.org/10.1091/mbc.11.10.3601

Schindelin J., I. Arganda-Carreras, E. Frise, V. Kaynig, M. Longair, *et al.*, 2012 Fiji: an open-source platform for biological-image analysis. Nat Methods 9: 676–682. https://doi.org/10.1038/nmeth.2019

Schneider C. A., W. S. Rasband, and K. W. Eliceiri, 2012 NIH Image to ImageJ: 25 years of image analysis. Nat Methods 9: 671–675. https://doi.org/10.1038/nmeth.2089

Shanower G. A., M. Muller, J. L. Blanton, V. Honti, H. Gyurkovics, *et al.*, 2005 Characterization of the grappa gene, the *Drosophila* histone H3 lysine 79 methyltransferase. Genetics 169: 173–184.https://doi.org/10.1534/genetics.104.033191

Strahl B. D., and C. D. Allis, 2000 The language of covalent histone modifications. Nature 403: 41–45. https://doi.org/10.1038/47412

Sung P., 1994 Catalysis of ATP-dependent homologous DNA pairing and strand exchange by yeast RAD51 protein. Science 265: 1241–1243. https://doi.org/10.1126/science.8066464

Turner B. M., 2002 Cellular memory and the histone code. Cell 111: 285–291. https://doi.org/10.1016/s0092-8674(02)01080-2

Van Holde K. E., J. R. Allen, K. Tatchell, W. O. Weischet, and D. Lohr, 1980 DNA-histone interactions in nucleosomes. Biophys. J. 32: 271–282. https://doi.org/10.1016/S0006-3495(80)84956-3

Villeneuve A. M., 1994 A cis-acting locus that promotes crossing over between X chromosomes in *Caenorhabditis elegans*. Genetics 136: 887–902.

Vlaming H. and van Leeuwen F. (2016). The upstreams and downstreams of H3K79 methylation by DOT1L. Chromosoma, *125*(4), 593-605. https://doi.org/10.1007/s00412-015-0570-5.

Wood A., J. Schneider, and A. Shilatifard, 2005 Cross-talking histones: implications for the regulation of gene expression and DNA repair. Biochem. Cell Biol. 83: 460–467. https://doi.org/10.1139/o05-116

Zhang K., and S. Y. R. Dent, 2005 Histone modifying enzymes and cancer: going beyond histones. J. Cell. Biochem. 96: 1137–1148. https://doi.org/10.1002/jcb.20615

Zhu B., S. Chen, H. Wang, C. Yin, C. Han, *et al.*, 2018 The protective role of DOT1L in UV-induced melanomagenesis. Nat Commun 9: 259. https://doi.org/10.1038/s41467-017-02687-7

SUPPLEMENTAL DATA

Table S1. *C. elegans* strains

Strain	Genotype
AGK769	*zfp-1(gk960739)III*
AV176	*syp-1(me17)V/nt1[unc-?n754]let-?gls50)(IV;V)*
COP1302	*dot-1.1[knu337-(pNU1092-KO loxP::hygR::loxP)]I;ced-3(n1286)IV*
CV345	*pch-2(tm1458)II*
CV592	*pch-2(tm1458)II; syp-1(me17)V/nt1[unc-?n754]let-?gls50)(IV;V)*
CV775	*pch-2(tm1458)II;zfp-1(gk960739)III*
CV776	*zfp-1(gk960739)III;syp-1(me17)V/nt1[unc-?n754]let-?gls50)(IV;V)*
CV777	*pch-2(tm1458)II;zfp-1(gk960739)III;syp-1(me17)V/nt1[unc-?n754]let-?gls50)(IV;V)*
CV816	*dot-1.1[knu337-(pNU1092-KO loxP::hygR::loxP)]I;pch-2(tm1458)II;ced-3(n1286)IV;syp-1(me17)V/nt1[unc-?n754]let-?gls50)(IV;V)*
CV810	*dot-1.1[knu337-(pNU1092-KO loxP::hygR::loxP)]I;pch-2(tm1458)II;ced-3(n1286)IV*
CV811	*dot-1.1[knu337-(pNU1092-KO loxP::hygR::loxP)]I;ced-3(n1286)IV;syp-1(me17)V/nt1[unc-?n754]let-?gls50)(IV;V)*
CV824	*ced-3(n1286)IV*
WS3687	*rad-54(ok615)I/hT2 [qIs48] (I;III)*
CV842	*dot-1.1[knu337-(pNU1092-KO loxP::hygR::loxP)]I;* rad-54(ok615)I/*hT2 [qIs48] (I;III); ced-3(n1286)IV*
CV843	rad-54(ok615)I/*hT2 [qIs48] (I;III); syp-1(me17)V/nt1[unc-?n754]let-?gls50)(IV;V)*
CV844	rad-54(ok615)I/*hT2 [qIs48] (I;III); ced-3(n1286)IV; syp-1(me17)V/nt1[unc-?n754]let-?gls50)(IV;V)*
CV845	*dot-1.1[knu337-(pNU1092-KO loxP::hygR::loxP)]I;* rad-54(ok615)I/*hT2 [qIs48] (I;III); ced-3(n1286)IV; ; syp-1(me17)V/nt1[unc-?n754]let-?gls50)(IV;V)*

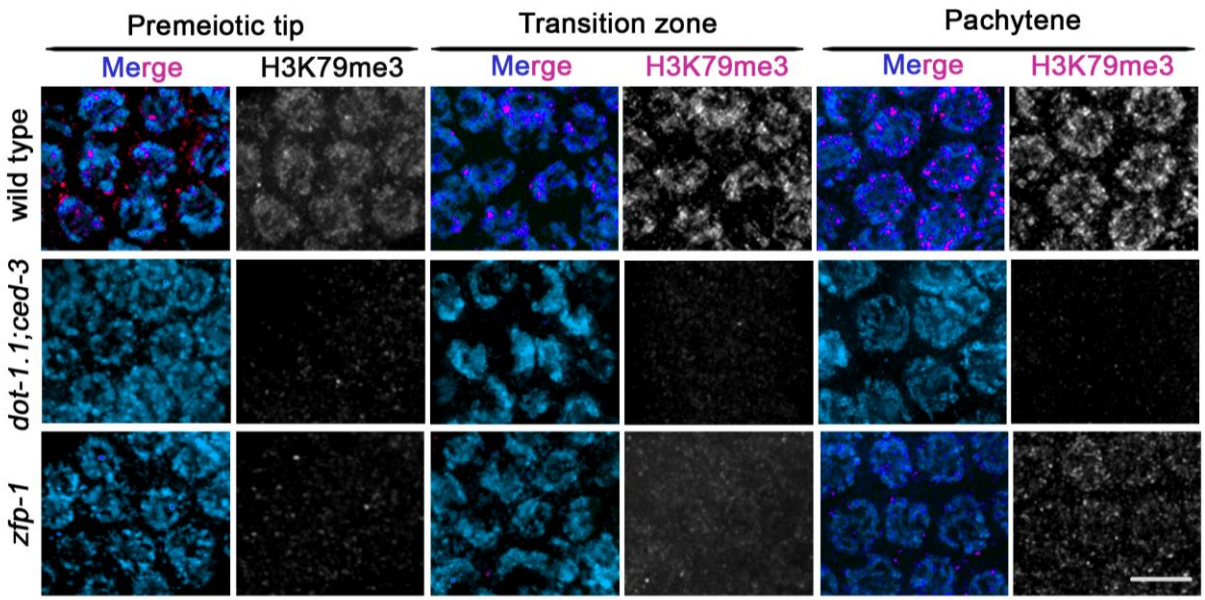

Supplemental Figure 1. (A) High resolution images of gonad nuclei from indicated backgrounds co-immunostained with H3K79me3 (magenta) and DAPI (blue). In wild-type worms H3K79me3 signal is associated with the chromatin through the entire gonad; however, in *dot-1.1;ced-3* and, less dramatically, in the *zfp-1* mutant this signal is decreased. Premeiotic tip (zone 2), transition zone (zone 3) and pahytene (zone 5) are indicated. Scale bar, 5 μm.

CONCLUSIONES

1. La regulación de H3K79me por DOT-1.1 se requiere para el correcto apareamiento, sinapsis y recombinación de los cromosomas en *C. elegans*. Por ello, niveles reducidos de H3K79me3 producen un aumento en la letalidad embrionaria y esterilidad, así como defectos en la morfología de los cromosomas en diacinesis.

2. Los niveles altos de apoptosis del mutante *syp-1* se ven reducidos en el doble mutante *zfp-1 syp-1* y la notable extensión de la actividad de CHK-2 del *syp-1* se reduce ligeramente en gusanos *dot-1.1;syp-1*. Por tanto, H3K79me3 se requiere para el *checkpoint* de sinapsis en *C. elegans.*

3. Al contrario que en *S. cerevisiae*, el papel de H3K79me en el *checkpoint* de sinapsis es independiente de PCH-2.

CONCLUSIONS

1. Regulation of H3K79me by DOT-1.1 is required for proper chromosome pairing, synapsis and recombination in *C. elegans*. Consequently, reduced levels of H3K79me3 produce an increase in embryonic viability, sterility and chromosome morphology defects in diakinesis.

2. The elevated level of apoptotic corpses in *syp-1* is reduced in the *zfp-1;syp-1* double mutant and the striking extension of CHK-2 activity in *syp-1* is slighty reduced in *dot-1.1;syp-1* worms. Thus, H3K79me is required for the synapsis checkpoint in *C. elegans.*

3. In contrast to *S. cerevisiae*, the role of H3K79me in the synapsis checkpoint is independent of PCH-2 localization.

Discusión General

Para cerrar la presente memoria hago una valoración conjunta de las principales conclusiones obtenidas a lo largo de esta tesis doctoral. Además, también propongo un modelo final que integra la actuación de Pch2 en el *checkpoint* de recombinación meiótica.

La ATPasa Pch2^{TRIP13} desempeña un papel muy importante en la meiosis. Se trata de una proteína con múltiples funciones pues, al menos en *S. cerevisiae*, participa en procesos meióticos tan diversos como son la formación de DSBs, la configuración de los ejes de los cromosomas, la regulación de los COs, el destino de la recombinación entre homólogos frente a cromátidas hermanas, la inhibición de la recombinación en el rDNA y el *checkpoint* de paquitene (Figura 3). Muchos de estos papeles se atribuyen al efecto que provoca sobre su sustrato predilecto: Hop1 (Vader 2015).

De todas estas funciones, este proyecto de tesis se centra en el papel de Pch2 en el *checkpoint* de recombinación meiótica, con el objetivo principal de profundizar en el mecanismo de acción de Pch2 en este *checkpoint* inducido por fallos en sinapsis. Para poder distinguir el papel de Pch2 en este proceso del de cualquier otra de sus funciones en una meiosis normal, empleamos el mutante *zip1Δ*. Este mutante al carecer de la región central del SC presenta fallos en sinapsis y recombinación que inducen la activación del *checkpoint*.

Así pues, comenzamos demostrando que el papel principal de Pch2 cuando existen errores en sinapsis es promover la fosforilación de Hop1 en la treonina 318 ejercida por Mec1, favoreciendo la subsiguiente fosforilación de Mek1 y la activación del bloqueo meiótico. El hecho de encontrar Hop1 como diana de la acción de Pch2 no era de extrañar, pues se conocía muy bien la acción negativa de Pch2^{TRIP13} sobre Hop1^{HORMAD1,2}, excluyendo esta proteína de los ejes de los cromosomas a medida que se va completando la sinapsis. De este modo, se impide que se formen nuevas DSBs en regiones que ya se han asociado por el SC (Roig et al., 2010; Subramanian et al., 2016). Sin embargo, aquí describimos por primera vez la acción contraria, de manera que Pch2 puede actuar también positivamente sobre Hop1 favoreciendo su fosforilación y su incorporación a los cromosomas en un mutante *zip1Δ,* es decir, en condiciones de *checkpoint* activado. Una posibilidad para entender cómo Pch2 puede ejercer acciones contrarias sobre Hop1 sería que Pch2 estuviese recibiendo señales para encender y apagar el *checkpoint*, por eso en meiosis normales excluye Hop1 y cuando el *checkpoint* está activado lo recluta. La responsable de enviar esas señales a Pch2 podría ser la quinasa Mec1, ya que Pch2 cuenta con un sitio consenso TQ potencialmente fosforilable por las quinasas sensor del *checkpoint* Mec1/Tel1. Existen evidencias que apoyarían la idea de que Pch2 puede requerir de esta modificación post-transduccional para modular su actividad. Por un lado, se ha descrito que Pch2 interacciona con el dominio BRCT de Xrs2 (Ho and Burgess, 2011) y se sabe que estos dominios interaccionan con proteínas fosforiladas (Yu et al., 2003). Por otro lado, resultados obtenidos por nosotros, no recogidos en esta memoria, muestran que la mutación de la T428 que forma parte del consenso TQ altera la respuesta del *checkpoint*, así como la distribución de Pch2 en los cromosomas meióticos.

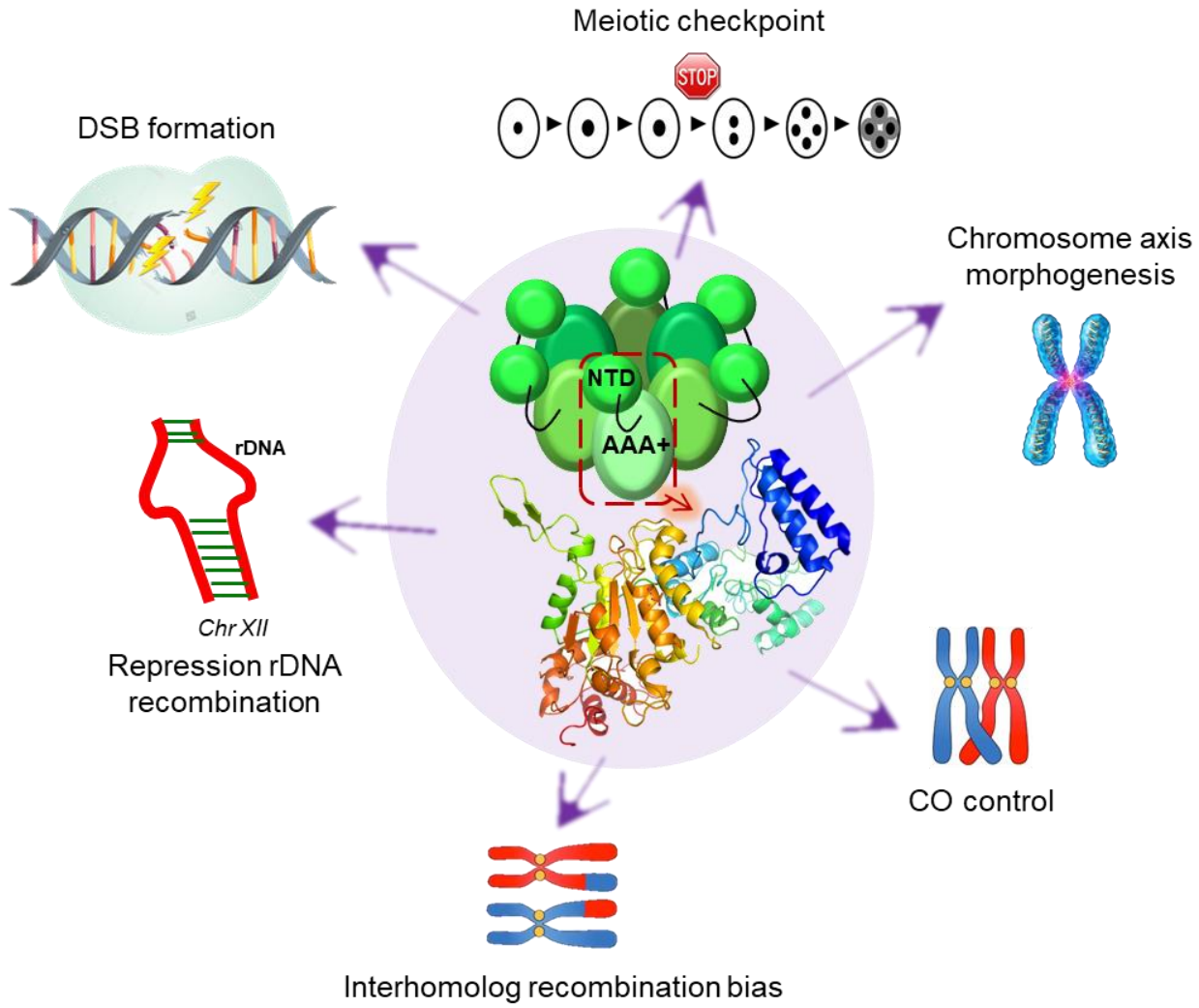

Figura 3. Funciones de Pch2 en la meiosis de *S. cerevisiae*. Pch2 participa en diversos procesos meióticos incluyendo el *checkpoint* de recombinación. Se representa la predicción de la estructura de un monómero de Pch2.

La actividad catalítica ATPasa de Pch2 es esencial para su función. Hemos demostrado que tanto la unión del ATP como la hidrólisis del ATP son necesarias para la función de Pch2 en el *checkpoint*. Además, observamos que la unión al ATP también es necesaria para su asociación a la cromatina y para la formación del complejo hexamérico.

Es bien conocido que las modificaciones post-traduccionales de las histonas regulan numerosos procesos biológicos, como la actividad transcripcional, el establecimiento de regiones de heterocromatina, la replicación, la reparación del DNA, la recombinación o el control del ciclo celular (Kouzarides 2007; Luger et al., 2012; Becker and Workman, 2013). Por lo que se refiere al *checkpoint* de recombinación meiótica, se conoce el papel de la H3K79me3 mediada por Dot1 en este mecanismo de control, siendo necesaria para la correcta localización de Pch2 en el nucleolo (Ontoso et al., 2013). Asimismo, Sir2 también participa en este proceso (San-Segundo 1999). Aquí describimos que los

niveles de H4K16ac, regulados por Sir2 y Sas2, también afectan al *checkpoint* y determinan la localización nucleolar de Pch2 debido, al menos en parte, al control de la H3K79me. Inicialmente postulamos que el impacto de ambas modificaciones de histonas en el *checkpoint* se debía a que controlan la localización de Pch2 en el nucleolo (Cavero et al., 2016). Sin embargo, al demostrar posteriormente que la población de Pch2 asociada a la cromatina no es esencial para el *checkpoint* (Herruzo et al., 2019; Anexo), planteamos la hipótesis de que Dot1 y Sir2 estén controlando también la localización de Pch2 en el citoplasma. Estudios futuros abordarán esta posibilidad.

En cuanto a otros factores que determinan la localización nucleolar de Pch2, además de los ya mencionados Sir2 y Dot1, hemos encontrado un motivo rico en aminoácidos básicos dentro del NTD de Pch2 que se requiere tanto para la localización de Pch2 en el núcleo como para su asociación al rDNA y para el *checkpoint* meiótico. La sustitución de este motivo por una NLS canónica de SV40 es capaz de dirigir la localización de Pch2 dentro del núcleo, pero no reestablece la localización nucleolar ni la funcionalidad del *checkpoint*. Estas observaciones sugieren que el motivo básico del NTD podría ser necesario para la formación del complejo hexamérico. Alternativamente, es posible que este motivo medie la interacción de Pch2 con otras proteínas a través de su NTD. De acuerdo con esta posibilidad, está descrito que el NTD de Pch2 es necesario para interaccionar con otras proteínas como Orc1 o MAD2 (Ye et al., 2017, Villar-Fernández et al., 2019). Así, pudiera serlo también para la interacción con Xrs2, una proteína con la que Pch2 colabora en la respuesta del *checkpoint* inducida por DSBs meióticas sin procesar detectadas vía Tel1 en mutantes como *sae2Δ* o *rad50S* (Ho and Burgess, 2011). Aunque la posible contribución de Xrs2 en el *checkpoint* inducido en respuesta a fallos en sinapsis (detectados vía Mec1) no está caracterizada, sí podría ser un buen candidato. Una posible hipótesis sería que Mec1 estuviese regulando por fosforilación la interacción entre Xrs2 y el NTD de Pch2, y estas dos proteínas colaborarían para promover la fosforilación de Hop1 en T318.

Por último, con el objeto de dilucidar definitivamente si existe una relación funcional entre la localización de Pch2 en el rDNA y el *checkpoint* hemos abordado en detalle el estudio de la conexión entre Pch2 y Orc1. Observamos que, tal y como se había descrito, Orc1 es necesario para reclutar a Pch2 al nucleolo (Vader et al., 2012) y comprobamos que, consecuentemente, es necesario para la exclusión de Hop1 de dicha región. Sin embargo, sorprendentemente, la función del *checkpoint* no se ve afectada por la ausencia de Orc1. Por tanto, concluimos que, contrariamente a nuestra hipótesis de partida, la localización nucleolar de Pch2 no se requiere para la funcionalidad del *checkpoint*. Estudios recientes de ChIP-seq apuntan que, además de la asociación al rDNA, Orc1 promueve la unión de Pch2 a otras regiones de la cromatina que se transcriben activamente y que no corresponden a las zonas de los ejes enriquecidas en Hop1 (Cardoso da Silva et al., 2019). Nuestros resultados implican que, ni la fracción de Pch2 nucleolar, ni ninguna otra que pudiese estar controlada por Orc1 son importantes para el *checkpoint*.

Nuestros estudios detallados de la distribución de Pch2, tanto en extensiones de cromosomas como en células intactas, han

revelado la existencia de al menos tres poblaciones de esta proteína con distintas localizaciones subcelulares: nucleolo, cromosomas y citoplasma. En el caso de condiciones de *checkpoint* activo (mutante *zip1Δ*) la localización de Pch2 se limita a nucleolo y citoplasma, ejerciendo cada población una función diferente. Así la proteína Pch2 de la fracción nucleolar, que es reclutada al nucleolo por Orc1 presumiblemente a través del NTD de Pch2, es la responsable de suprimir la recombinación en la región del rDNA, mediante la exclusión de Hop1 de dicha región. De la misma manera, la fracción de Pch2 presente en la región central del SC excluye a Hop1 de los cromosomas que han establecido la sinapsis controlando la recombinación en estas regiones. Al tratarse de una ATPasa de la familia AAA+, Pch2 es capaz de emplear la energía producida en la hidrólisis del ATP para producir cambios conformacionales en sus sustratos, promoviendo así el desensamblaje de Hop1 de los ejes cromosómicos. De hecho se han descrito interacciones *in vitro* entre Pch2 y las proteínas HORMAD (Chen et al., 2014; Ye et al., 2017). Además, nuestros estudios citológicos *in vivo* muestran que Hop1 siempre está excluido de las regiones donde hay Pch2. Sin embargo, la versión Pch2-E399Q, incapaz de hidrolizar el ATP, colocaliza con Hop1 tanto en el rDNA como en los cromosomas.

Por su parte, en el mutante *zip1Δ orc1-3mAID,* la única subpoblación de Pch2 que somos capaces de detectar es la presente en el citoplasma. Puesto que en esta situación el *checkpoint* sigue siendo completamente funcional esto implica que la fracción citoplásmica de Pch2, y no la nuclear ni nucleolar, debe ser la relevante para la respuesta de *checkpoint* frente a defectos en sinapsis (Figura 4). El uso de versiones de Pch2 en las que se altera de forma artificial su localización subcelular mediante la fusión de secuencias NES o NLS refuerzan esta misma conclusión.

Este último descubrimiento nos lleva a un escenario aún más complicado en el que Pch2 desde el citoplasma estaría promoviendo la fosforilación de Hop1 y su incorporación a los cromosomas dentro del núcleo. Por tanto, debe existir una comunicación núcleo-citoplásmica importante para el funcionamiento del *checkpoint* de recombinación meiótica que podría implicar el transporte de Pch2 del citoplasma al núcleo. De hecho, se ha descrito recientemente un papel para la nucleoporina Nup2 en la regulación de la distribución de Pch2 entre el nucléolo y los cromosomas (en cepas *ZIP1*) con el consiguiente impacto sobre Hop1 y la distribución regional de DSBs en los cromosomas (Subramanian et al., 2019). Por tanto, resultaba atractiva la hipótesis de que la nucleoporina Nup2, que forma parte de la "cesta" del poro nuclear, pudiera regular el transporte del propio Pch2 o bien el de sus posibles sustratos implicados en el *checkpoint* (Hop1, Mec1, PP4). No obstante, disponemos de resultados preliminares que indican que el *checkpoint* sigue siendo activo en el doble mutante *zip1Δ nup2Δ* (Baztán, Herruzo and San-Segundo, 2016, Trabajo de fin de Grado en realización) descartando la implicación de Nup2 en este proceso. Proponemos un modelo alternativo para el papel de Pch2 en el *checkpoint* de manera que la fracción de Pch2 presente exclusivamente en el citoplasma, mediante su actividad ATPasa, podría modificar la conformación de algún factor esencial para la fosforilación de Hop1 en

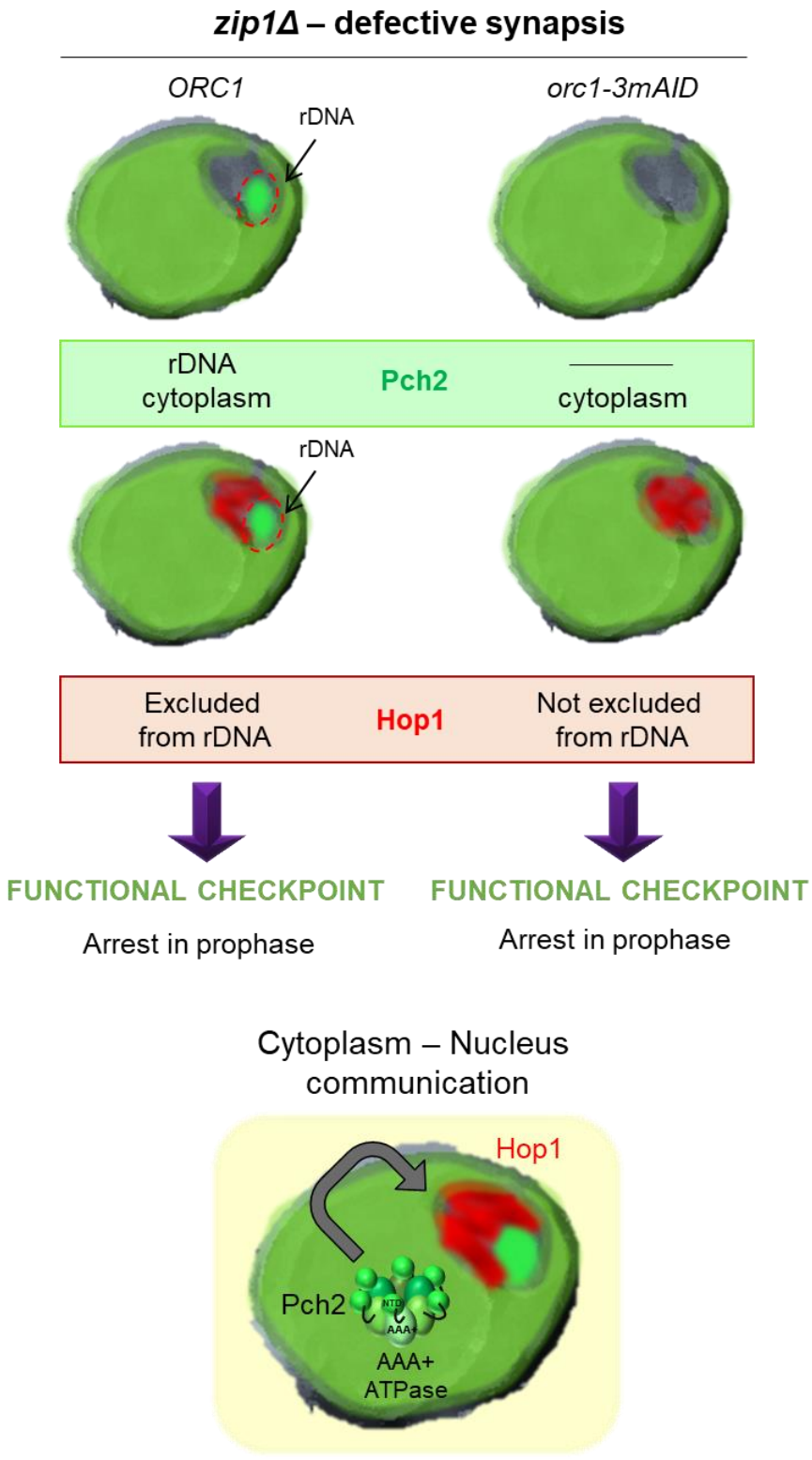

Figura 4. La fracción citoplásmica de Pch2 promueve la fosforilación de Hop1 y la activación del *checkpoint*. La función del *checkpoint* no se ve afectada por la ausencia de Orc1. Por tanto, la población nucleolar de Pch2, aunque es necesaria para excluir a Hop1 del rDNA, no es relevante para la fosforilación de Hop1 en T318 ni la activación del *checkpoint*.

T318, por ejemplo, exponiendo una posible NLS o facilitando la interacción con otras proteínas transportadoras, posibilitando su tráfico al interior del núcleo. Este factor necesario para la fosforilación de Hop1, cuyo transporte citoplasma-núcleo es controlado por Pch2, podría ser la propia quinasa Mec1, algún activador de la quinasa o bien algún inhibidor de la fosfatasa PP4. Además, debemos añadir en este escenario las proteínas modificadoras de histonas Dot1 y Sir2 que podrían estar regulando probablemente de manera indirecta, además de la población nucleolar de Pch2, también la del citoplasma (Figura 5). Estudios futuros irán dirigidos a dilucidar los mecanismos moleculares implicados en esta nueva y sorprendente situación que han abierto los resultados de esta tesis doctoral descubriendo un nivel adicional de regulación del *checkpoint* de recombinación meiótica previamente desconocido e inesperado.

La presencia de Pch2 en el nucleolo parece ser exclusiva de levaduras y no se ha encontrado en otras especies. Así, en mamíferos, nematodos y plantas se localiza asociada al SC durante la meiosis (Deshong et al., 2014; Lambing et al., 2015, Maldonado-Linares and Roig, Abstract Red Española de Meiosis). Además, en el caso de mamíferos y nematodos Pch2^{TRIP13} se ha detectado asociada a los cinétocoros, de acuerdo con su función en el *checkpoint* de ensamblaje de huso dependiente de MAD2 (Wang et al., 2014; Nelson et al., 2015). Más allá de nuestros trabajos en *S. cerevisiae*, no se ha descrito la localización de Pch2 en el citoplasma en otras especies, aunque no puede descartarse que también pueda ocurrir y no se haya detectado por cuestiones técnicas puesto que en la mayoría de los estudios citológicos de la meiosis se circunscriben al núcleo y los cromosomas. Se sabe que PCH-2 tiene un papel importante en el *checkpoint* inducido por fallos en sinapsis en *C. elegans* (mutante *syp-1*) y que, en esas condiciones, PCH-2 no se asocia a la cromatina (Deshong et al., 2014). Entonces, surge la cuestión de dónde se localiza la fracción de PCH-2 que está actuando en el *checkpoint* inducido por el mutante *syp-1*. Podría ocurrir que, al igual que en levaduras, PCH-2 esté regulando el *checkpoint* que monitoriza la sinapsis de los cromosomas desde otro compartimento celular independiente de la cromatina que podría ser el citoplasma. Nuestros estudios preliminares de inmunolocalización en gónadas de *C. elegans* parecen apoyar la posibilidad de una distribución citoplásmica de PCH-2 en el mutante *syp-1* (Lascarez-Lagunas, Herruzo, et al., 2020, en preparación).

Por otro lado, tras haber analizado el papel de la H3K79me mediada por DOT-1.1, así como haber indagado en el mecanismo del *checkpoint* meiótico en nematodos, todo apunta a que la implicación de, al menos algunas, proteínas del *checkpoint* está conservada en la evolución. Así, tal y como ocurre en *S. cerevisiae*, donde la H3K79me3 mediada por Dot1 se requiere para la fosforilación de Mek1^{CHK2} y el consiguiente bloqueo en profase cuando existen errores en sinapsis, DOT-1.1 también es una pieza clave para la meiosis de *C. elegans*. Más concretamente, podría estar desempeñando un papel importante en el *checkpoint* meiótico, afectando a la actividad de la quinasa efectora CHK-2. Sin embargo, la conservación del funcionamiento detallado de los mecanismos del *checkpoint* no parece estar tan clara. Pueden existir muchas vías adicionales con relaciones funcionales muy complicadas es-

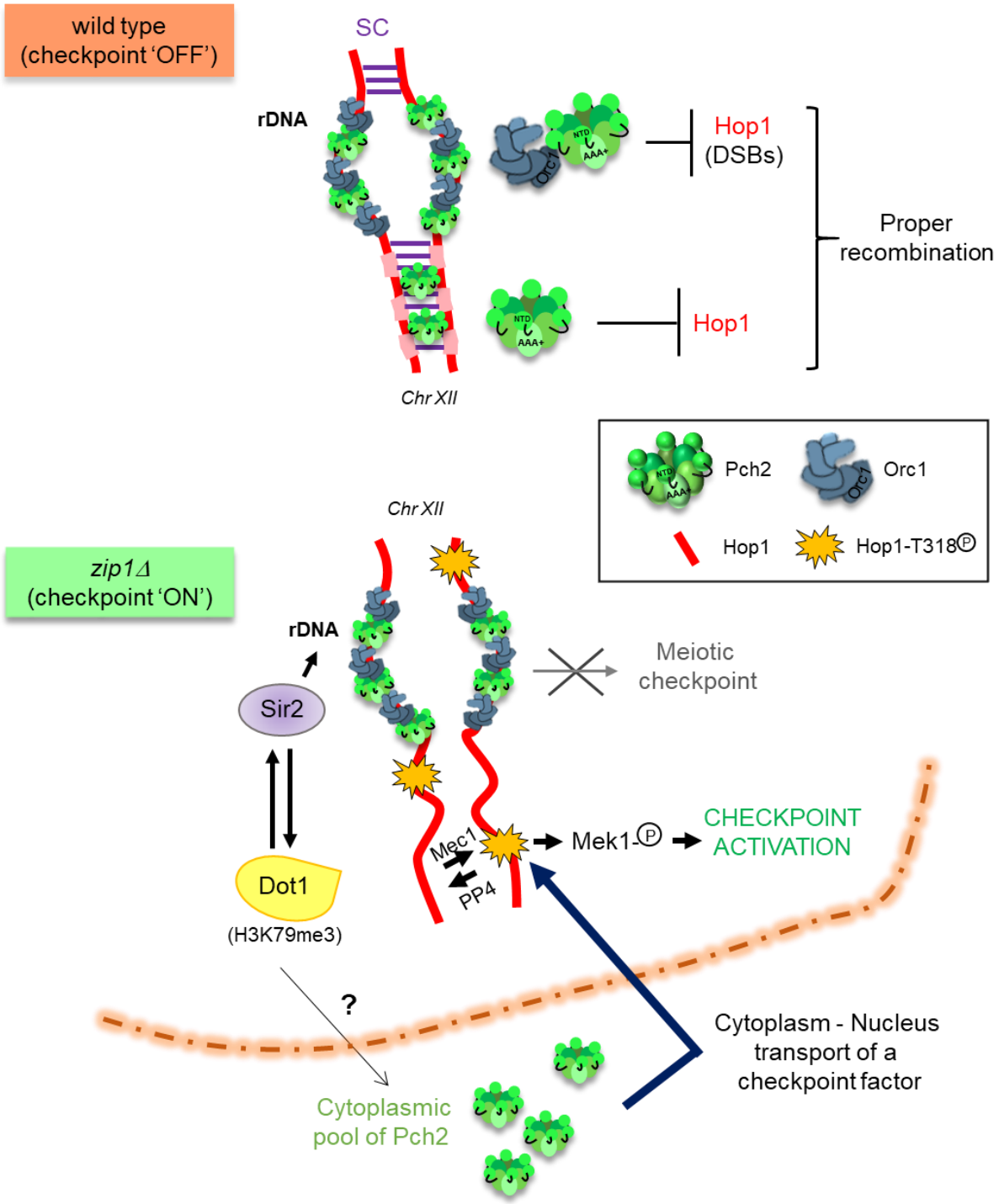

Figura 5. Modelo de acción de la ATPasa Pch2 en el *checkpoint* meiótico.

pecíficas de cada organismo. Así, aunque tanto en *S. cerevisiae* como en *C. elegans* ambas proteínas Pch2 y Dot1 participan en el *checkpoint* de recombinación meiótica, la regulación de Pch2 por Dot1 no ocurre en *C. elegans*.

En definitiva, a lo largo de esta tesis hemos ido aportando resultados que contribuyen al conocimiento del mecanismo de acción de Pch2 en el *checkpoint* meiótico pero, sobre todo, que ayudan a entender la complejidad de la red que regula la función y localización de Pch2 según las circunstancias.

Bibliografía

Acosta, I., Ontoso, D., and San-Segundo, P. A. (2011). The budding yeast polo-like kinase Cdc5 regulates the Ndt80 branch of the meiotic recombination checkpoint pathway. *Molecular Biology of the Cell, 22*(18), 3478-3490.

Alberts, B., Johnson, A., . . . Lewis, J. (2002). Meiosis. *Molecular Biology of the Cell*. 4th edition. New York: Garland Science.

Alfieri, C., Chang, L., and Barford, D. (2018). Mechanism for remodelling of the cell cycle checkpoint protein MAD2 by the ATPase TRIP13. *Nature, 559*(7713), 274.

Allers, T., and Lichten, M. (2001). Differential timing and control of noncrossover and crossover recombination during meiosis. *Cell, 106*(1), 47-57.

Bahler, J., Wyler, T., Loidl, J., and Kohli, J. (1993). Unusual nuclear structures in meiotic prophase of fission yeast: A cytological analysis. *The Journal of Cell Biology, 121*(2), 241-256.

Becker, P. B., and Workman, J. L. (2013). Nucleosome remodeling and epigenetics. *Cold Spring Harbor Perspectives in Biology, 5*(9), 10.1101/cshperspect.a017905.

Bhalla, N., and Dernburg, A. F. (2005). A conserved checkpoint monitors meiotic chromosome synapsis in *Caenorhabditis elegans*. *Science, 310*(5754), 1683-1686.

Bishop, D. K., Park, D., Xu, L., and Kleckner, N. (1992). DMC1: A meiosis-specific yeast homolog of *E. coli* recA required for recombination, synaptonemal complex formation, and cell cycle progression. *Cell, 69*(3), 439-456.

Borner, G. V., Barot, A., and Kleckner, N. (2008). Yeast Pch2 promotes domainal axis organization, timely recombination progression, and arrest of defective recombinosomes during meiosis. *Proceedings of the National Academy of Sciences of the United States of America, 105*(9), 3327-3332.

Cahoon, C. K., and Hawley, R. S. (2016). Regulating the construction and demolition of the synaptonemal complex. *Nature Structural & Molecular Biology, 23*(5), 369.

Callender, T. L., Laureau, R., Wan, L., Chen, X., Sandhu, R., Laljee, S., . . . Gaines, W. A. (2016). Mek1 down regulates Rad51 activity during yeast meiosis by phosphorylation of Hed1. *PLoS Genetics, 12*(8), e1006226.

Carballo, J. A., Johnson, A. L., Sedgwick, S. G., and Cha, R. S. (2008). Phosphorylation of the axial element protein Hop1 by Mec1/Tel1 ensures meiotic interhomolog recombination. *Cell, 132*(5), 758-770.

Cavero, S., Herruzo, E., Ontoso, D., and San-Segundo, P. A. (2016). Impact of histone H4K16 acetylation on the meiotic recombination checkpoint in *Saccharomyces cerevisiae*. *Microbial Cell, 3*(12), 606-620.

Cecere, G., Hoersch, S., Jensen, M. B., Dixit, S., and Grishok, A. (2013). The ZFP-1 (AF10)/DOT-1 complex opposes H2B ubiquitination to reduce pol II transcription. *Molecular Cell, 50*(6), 894-907.

Chakraborty, P., Pankajam, A. V., Lin, G., Dutta, A., Krishnaprasad, G. N., Tekkedil, M. M., . . . Nishant, K. T. (2017). Modulating crossover frequency and interference for obligate crossovers in *Saccharomyces cerevisiae* meiosis. *G3, 7*(5), 1511-1524.

Chen, C., Jomaa, A., Ortega, J., and Alani, E. E. (2014). Pch2 is a hexameric ring ATPase that remodels the chromosome axis protein Hop1. *Proceedings of the National Academy of Sciences of the United States of America, 111*(1), E44-53.

Chen, X., Gaglione, R., Leong, T., Bednor, L., de los Santos, T., Luk, E., . . . Hollingsworth, N. M. (2018). Mek1 coordinates meiotic progression with DNA break repair by directly phosphorylating and inhibiting the yeast pachytene exit regulator Ndt80. *PLoS Genetics, 14*(11), e1007832.

Chu, S., and Herskowitz, I. (1998). Gametogenesis in yeast is regulated by a transcriptional cascade dependent on Ndt80. *Molecular Cell, 1*(5), 685-696.

Clairmont, C. S., Sarangi, P., Ponnienselvan, K., Galli, L. D., Csete, I., Moreau, L. . . . D'Andrea, A. D. (2020). TRIP13 regulates DNA repair pathway choice through REV7 conformational change. *Nature Cell Biology, 22*(1), 87-96.

da Silva, R. C., Villar-Fernández, M. A., and Vader, G. (2019). Active transcription and Orc1 drive chromatin association of the AAA ATPase Pch2 during meiotic G2/prophase. *Biorxiv*, , 777003.

Daigle, S. R., Olhava, E. J., Therkelsen, C. A., Basavapathruni, A., Jin, L., Boriack-Sjodin, P. A., . . . Pollock, R. M. (2013). Potent inhibition of DOT1L as treatment of MLL-fusion leukemia. *Blood, 122*(6), 1017-1025.

Dang, W., Steffen, K. K., Perry, R., Dorsey, J. A., Johnson, F. B., Shilatifard, A., . . . Berger, S. L. (2009). Histone H4 lysine 16 acetylation regulates cellular lifespan. *Nature, 459*(7248), 802.

de Rooij, D. G., and de Boer, P. (2003). Specific arrests of spermatogenesis in genetically modified and mutant mice. *Cytogenetic and Genome Research, 103*(3-4), 267-276.

Deshong, A. J., Alice, L. Y., Lamelza, P., and Bhalla, N. (2014). A quality control mechanism coordinates meiotic prophase events to promote crossover assurance. *PLoS Genetics, 10*(4), e1004291.

Edelmann, W., Cohen, P. E., Kane, M., Lau, K., Morrow, B., Bennett, S., . . . Chaganti, R. (1996). Meiotic pachytene arrest in MLH1-deficient mice. *Cell, 85*(7), 1125-1134.

Eichinger, C. S., and Jentsch, S. (2010). Synaptonemal complex formation and meiotic checkpoint signaling are linked to the lateral element protein Red1. *Proceedings of the National Academy of Sciences of the United States of America, 107*(25), 11370-11375.

Farmer, S., Hong, E. E., Leung, W., Argunhan, B., Terentyev, Y., Humphryes, N., . . . Tsubouchi, H. (2012). Budding yeast Pch2, a widely conserved meiotic protein, is involved in the initiation of meiotic recombination. *PLoS One, 7*(6), e39724.

Frederiks, F., Tzouros, M., Oudgenoeg, G., Van Welsem, T., Fornerod, M., Krijgsveld, J., and Van Leeuwen, F. (2008). Nonprocessive methylation by Dot1 leads to functional redundancy of histone H3K79 methylation states. *Nature Structural & Molecular Biology, 15*(6), 550.

Gao, Jinmin, Colaiácovo,Monica P.,. (2018). Zipping and unzipping: Protein modifications regulating synaptonemal complex dynamics. *TIGS Trends in Genetics, 34*(3), 232-245.

Gartner, A., Milstein, S., Ahmed, S., Hodgkin, J., and Hengartner, M. O. (2000). A conserved checkpoint pathway mediates DNA damage–induced apoptosis and cell cycle arrest in *C. elegans*. *Molecular Cell, 5*(3), 435-443.

Geisinger, A., and Benavente, R. (2016). Mutations in genes coding for synaptonemal complex proteins and their impact on human fertility. *Cytogenetic and Genome Research, 150*(2), 77-85.

Gray, S., and Cohen, P. E. (2016). Control of meiotic crossovers: From double-strand break formation to designation. *Annual Review of Genetics, 50*, 175-210.

Hanson, P. I., and Whiteheart, S. W. (2005). AAA proteins: Have engine, will work. *Nature Reviews Molecular Cell Biology, 6*(7), 519.

Hassold, T., and Hunt, P. (2001). To err (meiotically) is human: The genesis of human aneuploidy. *Nature Reviews Genetics, 2*(4), 280.

Herruzo, E., Ontoso, D., González-Arranz, S., Cavero, S., Lechuga, A., and San-Segundo, P. A. (2016). The Pch2 AAA ATPase promotes phosphorylation of the Hop1 meiotic checkpoint adaptor in response to synaptonemal complex defects. *Nucleic Acids Research, 44*(16), 7722-7741.

Herruzo, E., Santos, B., Freire, R., Carballo, J. A., and San-Segundo, P. A. (2019). Characterization of Pch2 localization determinants reveals a nucleolar-independent role in the meiotic recombination checkpoint. *Chromosoma*, 1-20.

Ho, H., and Burgess, S. M. (2011). Pch2 acts through Xrs2 and Tel1/ATM to modulate interhomolog bias and checkpoint function during meiosis. *PLoS Genetics, 7*(11), e1002351.

Humphryes, N., Leung, W., Argunhan, B., Terentyev, Y., Dvorackova, M., and Tsubouchi, H. (2013). The Ecm11-Gmc2 complex promotes synaptonemal complex formation through assembly of transverse filaments in budding yeast. *PLoS Genetics, 9*(1), e1003194.

Jones, B., Su, H., Bhat, A., Lei, H., Bajko, J., Hevi, S., . . . Valdez, R. (2008). The histone H3K79 methyltransferase DOT1L is essential for mammalian development and heterochromatin structure. *PLoS Genetics, 4*(9), e1000190.

Joshi, N., Barot, A., Jamison, C., and Börner, G. V. (2009). Pch2 links chromosome axis remodeling at future crossover sites and crossover distribution during yeast meiosis. *PLoS Genetics, 5*(7), e1000557.

Joshi, N., Brown, M. S., Bishop, D. K., and Börner, G. V. (2015). Gradual implementation of the meiotic recombination program via checkpoint pathways controlled by global DSB levels. *Molecular Cell, 57*(5), 797-811.

Joyce EF, M. K. (2009). *Drosophila* PCH2 is required for a pachytene checkpoint that monitors double-strand-break-independent events leading to meiotic crossover formation. *Genetics, 181*(1), 39-51.

Joyce, E. F., and McKim, K. S. (2010). Chromosome axis defects induce a checkpoint-mediated delay and interchromosomal effect on crossing over during *Drosophila* meiosis. *PLoS Genetics, 6*(8), e1001059.

Keeney, S. (2001). Mechanism and control of meiotic recombination initiation. *Current Topics in Developmental Biology, 52*, 1-53.

Keeney, S., Lange, J., and Mohibullah, N. (2014). Self-organization of meiotic recombination initiation: General principles and molecular pathways. *Annual Review of Genetics, 48*, 187-214.

Kim, W., Choi, M., and Kim, J. (2014). The histone methyltransferase Dot1/DOT1L as a critical regulator of the cell cycle. *Cell Cycle, 13*(5), 726-738.

Klein, F., Mahr, P., Galova, M., Buonomo, S. B., Michaelis, C., Nairz, K., and Nasmyth, K. (1999). A central role for cohesins in sister chromatid cohesion, formation of axial elements, and recombination during yeast meiosis. *Cell, 98*(1), 91-103.

Kouzarides, T. (2007). Chromatin modifications and their function. *Cell, 128*(4), 693-705.

Lake, C. M., and Hawley, R. S. (2012). The molecular control of meiotic chromosomal behavior: Events in early meiotic prophase in *Drosophila* oocytes. *Annual Review of Physiology, 74*, 425-451.

Lambing, C., Osman, K., Nuntasoontorn, K., West, A., Higgins, J. D., Copenhaver, G. P., . . . Roitinger, E. (2015). *Arabidopsis* PCH2 mediates meiotic chromosome remodeling and maturation of crossovers. *PLoS Genetics, 11*(7), e1005372.

Leu, J., and Roeder, G. S. (1999). The pachytene checkpoint in *S. cerevisiae* depends on Swe1-mediated phosphorylation of the cyclin-dependent kinase Cdc28. *Molecular Cell, 4*(5), 805-814.

Luger, K., Dechassa, M. L., and Tremethick, D. J. (2012). New insights into nucleosome and chromatin structure: An ordered state or a disordered affair? *Nature Reviews Molecular Cell Biology, 13*(7), 436.

Lui, D. Y., and Colaiácovo, M. P. (2013). Meiotic development in *Caenorhabditis elegans*. *Germ cell development in C. elegans* (pp. 133-170) Springer.

Maldonado-Linares, A., Fuentes-Lázaro, J., Martínez-Marchal, A., Benavente, R. and Ignasi Roig. (2018). Study of TRIP13 function in the telomeres of meiotic chromosomes. Spanish Meiosis Meeting. Congreso llevado a cabo en (El Escorial) Madrid, Spain.

Marcos-Villar, L., and Nieto, A. (2019). The DOT1L inhibitor pinometostat decreases the host-response against infections: Considerations about its use in human therapy. *Scientific Reports, 9*(1), 16862-019-53239-6.

Markowitz, T. E., Suarez, D., Blitzblau, H. G., Patel, N. J., Markhard, A. L., MacQueen, A. J., and Hochwagen, A. (2017). Reduced dosage of the chromosome axis factor Red1 selectively disrupts the meiotic recombination checkpoint in *Saccharomyces cerevisiae*. *PLoS Genetics, 13*(7), e1006928.

Medhi, D., Goldman, A. S., and Lichten, M. (2016). Local chromosome context is a major determinant of crossover pathway biochemistry during budding yeast meiosis. *Elife, 5*, e19669.

Mohan, M., Herz, H. M., Takahashi, Y. H., Lin, C., Lai, K. C., Zhang, Y., . . . Shilatifard, A. (2010). Linking H3K79 trimethylation to wnt signaling through a novel Dot1-containing complex (DotCom). *Genes & Development, 24*(6), 574-589.

Nagaoka, S. I., Hassold, T. J., and Hunt, P. A. (2012). Human aneuploidy: Mechanisms and new insights into an age-old problem. *Nature Reviews Genetics, 13*(7), 493.

Nelson, C. R., Hwang, T., Chen, P. H., and Bhalla, N. (2015). TRIP13/PCH-2 promotes Mad2 localization to unattached kinetochores in the spindle checkpoint response. *The Journal of Cell Biology, 211*(3), 503-516.

Nguyen, A. T., and Zhang, Y. (2011). The diverse functions of Dot1 and H3K79 methylation. *Genes & Development, 25*(13), 1345-1358.

Niu, H., Li, X., Job, E., Park, C., Moazed, D., Gygi, S. P., and Hollingsworth, N. M. (2007). Mek1 kinase is regulated to suppress double-strand break repair between sister chromatids during budding yeast meiosis. *Molecular and Cellular Biology, 27*(15), 5456-5467.

Niu, H., Wan, L., Busygina, V., Kwon, Y., Allen, J. A., Li, X., . . . Sung, P. (2009). Regulation of meiotic recombination via Mek1-mediated Rad54 phosphorylation. *Molecular Cell, 36*(3), 393-404.

Nyberg, K. A., Michelson, R. J., Putnam, C. W., and Weinert, T. A. (2002). Toward maintaining the genome: DNA damage and replication checkpoints. *Annual Review of Genetics, 36*(1), 617-656.

Ontoso, D., Acosta, I., van Leeuwen, F., Freire, R., and San-Segundo, P. A. (2013). Dot1-dependent histone H3K79 methylation promotes activation of the Mek1 meiotic checkpoint effector kinase by regulating the Hop1 adaptor. *PLoS Genetics, 9*(1), e1003262.

Ontoso, D., Kauppi, L., Keeney, S., and San-Segundo, P. A. (2014). Dynamics of DOT1L localization and H3K79 methylation during meiotic prophase I in mouse spermatocytes. *Chromosoma, 123*(1-2), 147-164.

Pacheco, S., Marcet-Ortega, M., Lange, J., Jasin, M., Keeney, S., and Roig, I. (2015). The ATM signaling cascade promotes recombination-dependent pachytene arrest in mouse spermatocytes. *PLoS Genetics, 11*(3), e1005017.

Penedos, A., Johnson, A. L., Strong, E., Goldman, A. S., Carballo, J. A., and Cha, R. S. (2015). Essential and checkpoint functions of budding yeast ATM and ATR during meiotic prophase are facilitated by differential phosphorylation of a meiotic adaptor protein, Hop1. *PloS One, 10*(7), e0134297.

Perez-Hidalgo, L., Moreno, S., and San-Segundo, P. A. (2003). Regulation of meiotic progression by the meiosis-specific checkpoint kinase Mek1 in fission yeast. *Journal of Cell Science, 116*(Pt 2), 259-271.

Prugar, E., Burnett, C., Chen, X., and Hollingsworth, N. M. (2017). Coordination of double strand break repair and meiotic progression in yeast by a Mek1-Ndt80 negative feedback loop. *Genetics, 206*(1), 497-512.

Roig, I., Dowdle, J. A., Toth, A., de Rooij, D. G., Jasin, M., and Keeney, S. (2010). Mouse TRIP13/PCH2 is required for recombination and normal higher-order chromosome structure during meiosis. *PLoS Genetics, 6*(8), e1001062.

San-Segundo, P.A., and Clemente-Blanco, A. (2020). Resolvases, dissolvases, and helicases in homologous recombination: Clearing the road for chromosome segregation. *Genes, 11*(1), 71.

San-Segundo, P.A., and Roeder, G.S. (1999). Pch2 links chromatin silencing to meiotic checkpoint control. *Cell, 97*(3), 313-24.

San-Segundo, P.A., and Roeder, G.S. (2000). Role for the silencing protein Dot1 in meiotic checkpoint control. *Molecular Biology of the Cell, 11*(10), 3601-3615.

Schwacha, A., and Kleckner, N. (1995). Identification of double Holliday junctions as intermediates in meiotic recombination. *Cell, 83*(5), 783-791.

Schwacha, A., and Kleckner, N. (1997). Interhomolog bias during meiotic recombination: Meiotic functions promote a highly differentiated interhomolog-only pathway. *Cell, 90*(6), 1123-1135.

Smith, A. V., and Roeder, G. S. (1997). The yeast Red1 protein localizes to the cores of meiotic chromosomes. *The Journal of Cell Biology, 136*(5), 957-967.

Sourirajan, A., and Lichten, M. (2008). Polo-like kinase Cdc5 drives exit from pachytene during budding yeast meiosis. *Genes & Development, 22*(19), 2627-2632.

Stein, E. M., Garcia-Manero, G., Rizzieri, D. A., Tibes, R., Berdeja, J. G., Savona, M. R., . . . Tallman, M. S. (2018). The DOT1L inhibitor pinometostat reduces H3K79 methylation and has modest clinical activity in adult acute leukemia. *Blood, 131*(24), 2661-2669.

Subramanian, V. V., and Hochwagen, A. (2014). The meiotic checkpoint network: Step-by-step through meiotic prophase. *Cold Spring Harbor Perspectives in Biology, 6*(10), a016675.

Subramanian, V. V., MacQueen, A. J., Vader, G., Shinohara, M., Sanchez, A., Borde, V., . . . Hochwagen, A. (2016). Chromosome synapsis alleviates Mek1-dependent suppression of meiotic DNA repair. *PLoS Biology, 14*(2), e1002369.

Subramanian, V. V., Zhu, X., Markowitz, T. E., Vale-Silva, L. A., San-Segundo, P. A., Hollingsworth, N. M., . . . Hochwagen, A. (2019). Persistent DNA-break potential near telomeres increases initiation of meiotic recombination on short chromosomes. *Nature Communications, 10*(1), 970.

Sym, M., Engebrecht, J., and Roeder, G. S. (1993). ZIP1 is a synaptonemal complex protein required for meiotic chromosome synapsis. *Cell, 72*(3), 365-378.

Vader, G. (2015). $Pch2^{TRIP13}$: Controlling cell division through regulation of HORMA domains. *Chromosoma: Biology of the Nucleus, 124*(3), 333-339.

Vader, G., Blitzblau, H. G., Tame, M. A., Falk, J. E., Curtin, L., and Hochwagen, A. (2011). Protection of repetitive DNA borders from self-induced meiotic instability. *Nature, 477*(7362), 115.

Villar-Fernández, M. A., da Silva, R. C., Pan, D., Weir, E., Sarembe, A., Raina, V. B., . . . Vader, G. (2019). A meiosis-specific AAA assembly reveals repurposing of ORC during budding yeast gametogenesis. *Biorxiv*, 598128.

Voelkel-Meiman, K., Taylor, L. F., Mukherjee, P., Humphryes, N., Tsubouchi, H., and MacQueen, A. J. (2013). SUMO localizes to the central element of synaptonemal complex and is required for the full synapsis of meiotic chromosomes in budding yeast. *PLoS Genetics*, *9*(10), e1003837.

Wang, K., Sturt-Gillespie, B., Hittle, J. C., Macdonald, D., Chan, G. K., Yen, T. J., and Liu, S. T. (2014). Thyroid hormone receptor interacting protein 13 (TRIP13) AAA-ATPase is a novel mitotic checkpoint-silencing protein. *The Journal of Biological Chemistry*, *289*(34), 23928-23937.

West, A. M., Komives, E. A., and Corbett, K. D. (2017). Conformational dynamics of the Hop1 HORMA domain reveal a common mechanism with the spindle checkpoint protein Mad2. *Nucleic Acids Research*, *46*(1), 279-292.

Xu, J., Xin, S., and Du, W. (2001). *Drosophila* Chk2 is required for DNA damage-mediated cell cycle arrest and apoptosis. *FEBS Letters*, *508*(3), 394-398.

Ye, Q., Kim, D. H., Dereli, I., Rosenberg, S. C., Hagemann, G., Herzog, F., . . . Corbett, K. D. (2017). The AAA ATPase TRIP13 remodels HORMA domains through N-terminal engagement and unfolding. *The EMBO Journal*, *36*(16), 2419-2434.

Ye, Q., Rosenberg, S. C., Moeller, A., Speir, J. A., Su, T. Y., and Corbett, K. D. (2015). TRIP13 is a protein-remodeling AAA ATPase that catalyzes MAD2 conformation switching. *Elife*, *4*, e07367.

Yoshida, K., Kondoh, G., Matsuda, Y., Habu, T., Nishimune, Y., and Morita, T. (1998). The mouse RecA-like gene Dmc1 is required for homologous chromosome synapsis during meiosis. *Molecular Cell*, *1*(5), 707-718.

Yu, X., Chini, C. C., He, M., Mer, G., and Chen, J. (2003). The BRCT domain is a phospho-protein binding domain. *Science (New York, N.Y.)*, *302*(5645), 639-642.

Zanders, S., and Alani, E. (2009). The pch2Δ mutation in baker's yeast alters meiotic crossover levels and confers a defect in crossover interference. *PLoS Genetics*, *5*(7), e1000571.

Zanders, S., Sonntag Brown, M., Chen, C., and Alani, E. (2011). Pch2 modulates chromatid partner choice during meiotic double-strand break repair in *Saccharomyces cerevisiae*. *Genetics*, *188*(3), 511-21.

Apéndice

ABREVIATURAS

AAA+: ATPases associated with diverse cellular activities
AID: auxin-inducible degron
AO: acridine orange
mAID: mini-auxin-inducible degron
3mAID: 3 copies of mini-auxin-inducible degron
ATP: adenosin triphosphate
BSA: bovine serum albumin
CCD: charge-coupled device
CDK: cyclin-dependent kinase
CePch2: *Caenorhabditis elegans* Pch2
COs: crossovers
DAPI: 4', 6-diamidino-2-phenylindole
dHJ: double Holliday junction
DIC: differential interference contrast
DNA: deoxyribonucleic acid
DOI: digital object identifier
DSB: double-strand break
Emb: embryonic lethality
EP: early pachytene
GFP: green fluorescent protein
H3K79me: methylation of histone H3 at lysine 79
H3K79me1: monomethylation of histone H3 at lysine 79
H3K79me2: dimethylation of histone H3 at lysine 79
H3K79me3: trimethylation of histone H3 at lysine 79
H3T11ph: phosphorylation of histone H3 at threonine 11
H4K16ac: acetylation of histone H4 at lysine 16
HA: human influenza hemagglutinin
HATs: histone acetyltransefrases
Him: high incidence of males
Hop1-T318ph: phosphorylation of Hop1 at threonine 318
HORMAD: Hop1, Rev1 and Mad2 domain
HRP: horseradish peroxidase
HsPch2: *Homo sapiens* Pch2
IH: interhomolog
IP: immunoprecipitates
IS: intersister
ISSN: international standard serial number
LEs: lateral elements
LG: linkage group

LP: late pachytene
mDOT1L: mice DOT1L
MLL: mixed lineage leukemia
MP: mid-pachytene
MRX: Mre11-Rad50-Xrs2
NEB: New England Biolabs
NES: nuclear export signal
NGM: nematode growth media
NLS/NoLS: nuclear or nucleolar localization signal
NTD: N-terminal domain
OE: overexpression
ORC: origin recognition complex
ORF: open reading frame
PBS: phosphate buffered saline
PCR: polymerase chain reaction
PGK: phosphoglycerate kinase
PTMs: post-Translational modifications
PTS: Pch two-suppressors
PVDF: polyvinylidene difluoride
rDNA: ribosomal DNA
RFC: replication factor C
SAC: spindle assembly checkpoint
SC: synaptonemal complex
ScPch2: *Saccharomyces cerevisiae* Pch2
SD: standard desviation
SPBs: spindle pole bodies
ssDNA: single-strand DNA
SUMO: small ubiquitin-like modifier
TCA: trichloroacetic acid
TZ: transition zone
UTR: untranslated region
UV: ultraviolet
WCE: whole cell extracts
WT: wild type
YPDA: yeast extract, peptone, dextrose and adenine medium